STARS

Electronic Theses and Dissertations, 2004-2019

2006

Examining Route Diversion And Multiple Ramp Metering Strategies For Reducing Real-time Crash Risk On Urban Freeways

Vikash Gayah

University of Central Florida

STARS Citation

Showcase of Text, Archives, Research & Scholarship

EXAMINING ROUTE DIVERSION AND MULTIPLE RAMP METERING STRATEGIES
FOR REDUCING REAL-TIME CRASH RISK ON URBAN FREEWAYS

by

VIKASH V. GAYAH
B.Sc. University of Central Florida, 2005

A thesis submitted in partial fulfillment of the requirements
for the degree of Master of Science
in the Department of Civil and Environmental Engineering
in the College of Engineering and Computer Science
at the University of Central Florida
Orlando, Florida

Fall Term
2006

ABSTRACT

Recent research at the University of Central Florida addressing crashes on Interstate-4 in Orlando, Florida has led to the creation of new statistical models capable of calculating the crash risk on the freeway (Abdel-Aty et al., 2004; 2005, Pande and Abdel-Aty, 2006). These models yield the rear-end and lane-change crash risk along the freeway in real-time by using static information at various locations along the freeway as well as real-time traffic data that is obtained from the roadway. Because these models use the real-time traffic data, they are capable of calculating the respective crash risk values as the traffic flow changes along the freeway. The purpose of this study is to examine the potential of two Intelligent Transportation System strategies for reducing the crash risk along the freeway by changing the traffic flow parameters.

The two ITS measures that are examined in this research are route diversion and ramp metering. Route diversion serves to change the traffic flow by keeping some vehicles from entering the freeway at one location and diverting them to another location where they may be more efficiently inserted into the freeway traffic stream. Ramp metering alters the traffic flow by delaying vehicles at the freeway on-ramps and only allowing a certain number of vehicles to enter at a time. The two strategies were tested by simulating a 36.25 mile section of the Interstate-4 network in the PARAMICS micro-simulation software. Various implementations of route diversion and ramp metering were then tested to determine not only the effects of each strategy but also how to best apply them to an urban freeway.

Route diversion was found to decrease the overall rear-end and lane-change crash risk along the network at free-flow conditions to low levels of congestion. On average, the two crash risk measures were found to be reduced between the location where vehicles were diverted and

the location where they were reinserted back into the network. However, a crash migration phenomenon was observed at higher levels of congestion as the crash risk would be greatly increased at the location where vehicles were reinserted back onto the network. Ramp metering in the downtown area was found to be beneficial during heavy congestion. Both coordinated and uncoordinated metering algorithms showed the potential to significantly decrease the crash risk at a network wide level. When the network is loaded with 100 percent of the vehicles the uncoordinated strategy performed the best at reducing the rear-end and lane-change crash risk values. The coordinated strategy was found to perform the best from a safety and operational perspective at moderate levels of congestion. Ramp metering also showed the potential for crash migration so care must be taken when implementing this strategy to ensure that drivers at certain locations are not put at unnecessary risk. When ramp metering is applied to the entire freeway network both the rear-end and lane-change crash risk is decreased further. ALINEA is found to be the best network-wide strategy at the 100 percent loading case while a combination of Zone and ALINEA provides the best safety results at the 90 percent loading case.

It should also be noted that both route diversion and ramp metering were found to increase the overall network travel time. However, the best route diversion and ramp metering strategies were selected to ensure that the operational capabilities of the network were not sacrificed in order to increase the safety along the freeway. This was done by setting the maximum allowable travel time increase at 5% for any of the ITS strategies considered.

To my family for always believing in and encouraging me.

Without your love and support, none of this would be possible.

ACKNOWLEDGMENTS

TABLE OF CONTENTS

LIST OF FIGURES

LIST OF TABLES

LIST OF ACRONYMS/ABBREVIATIONS

AADT	Annual Average Daily Traffic
API	Application Programmer Interface
ATIS	Advanced Traveler Information Systems
CATSS	Center for Advanced Transportation Systems Simulation
DDHV	Directional Design Hourly Volume
FDOT	Florida Department of Transportation
FHWA	Federal Highway Administration
FTI	Florida Traffic Information
GUI	Graphic User Interface
HOV	High Occupancy Vehicle
INVS	In-Vehicle Navigation Systems
ITS	Intelligent Transportation Systems
LCRCI	Lane-Change Risk Change Index
OCPC	One-Car-Per-Cycle
OD	Origin-Destination
ORCI	Overall Risk Change Index
RCI	Roadway Characteristics Index
TC	Traffic-Cycle
VHT	Vehicles Hours Traveled

CHAPTER 1. INTRODUCTION

Arguably one of the most influential factors in the growth of the United States is the success of its transportation facilities. Without proper means to move goods and people across this vast land the productivity of this nation would be greatly reduced. The formation of the National System of Interstate Highways (or the Interstate system as it is commonly known) in the 1950's created an easy avenue of private transportation that can also be used to move goods and services across the nation. This sophisticated network of highways is composed of more than 46,000 miles of freeways and contains well over 15,000 interchanges (FHWA, 2006). However, one of the risks of such a sophisticated transportation system is the loss of life that occurs as people use the freeways for everyday travel. According to the Bureau of Transportation Statistics (2005) more than 42,000 died on roadways in the United States during 2003. While this number has been relatively constant for the past few years this enormous loss of life annually is an issue that is constantly being addressed by transportation engineers.

Recently, at the University of Central Florida, research was conducted to examine crashes that occur on typical urban freeways such as the Interstate system. This research developed statistical models that determined the risk of a crash occurring along Interstate-4 in Orlando, FL. These models used logistic regression to identify the crash potential for collisions (Abdel-Aty et al, 2004) along the freeway based real-time traffic conditions. Using micro-simulation, several Intelligent Transportation Systems (ITS) strategies were tested on a simulated version of the freeway to determine the effect of those strategies on the real-time crash risk. Abdel-Aty et al (2006) showed that implementing variable speed limits along the freeway is able to successfully reduce the real-time crash risk in situations at which the freeway is operating at high speeds.

Dhindsa (2005) explored the benefits of ramp metering and found it to beneficial when the freeway was operating in congested conditions. Abdel-Aty and Dhindsa (2007) also examined the coordinated use of variable speed limits and ramp metering and found that combining the two methods reduces the number of ramps required to be metered to reduce the real-time crash risk along the freeway.

The research conducted in this study expands on the previous research in many ways. First, this research uses newer crash prediction models developed by Pande and Abdel-Aty (2006). These models use neural networks to calculate the risk of both rear-end and lane-change crashes individually. They are more sophisticated than the logistic regression models used previously as they consider both real-time traffic data as well as off-line information regarding the time of day and location of ramps and curves. The crash prevention strategies that are employed in this study are tested to see which of the crash risk types are reduced, if not both. Second, this research expands on the ITS measures that were implemented previously. In this study, both ramp metering and route diversion (a type of ITS strategy that involves using Advanced Traveler Information Systems – ATIS – to give drivers real-time information about the roadway conditions so they can make better route choices) are considered. This research expounds on the ramp metering strategies that were tested by Dhindsa (2005) by comparing uncoordinated and coordinated ramp metering strategies. This research also compares the two different implementation methods of ramp metering – traffic-cycle realization and one-car-per-cycle realization. Additionally, this study uses the results from ramp metering in a localized area to make recommendations about metering ramps throughout the entire network to reduce the respective crash risk values for the entire network corridor.

Therefore, the objectives of this research are as follows:

- Examine Route Diversion and Ramp Metering to determine their affect on both the rear-end crash and lane-change crash risk

- Compare the uncoordinated ALINEA ramp metering strategy with the coordinated Zone ramp metering strategy to determine which reduces the crash risk measures with the greatest efficiency

- Compare the two implementation methods for ramp metering (traffic-cycle and one-car-per-cycle) for both the ALINEA and Zone metering algorithms to determine which combination most effectively reduces the two crash risk values across the network

- Examine the negative impacts of both crash prevention plans on the operational capabilities of the Interstate-4 system

- Make recommendations for both route diversion and ramp metering to be implemented along Interstate-4

CHAPTER 2.   LITERATURE REVIEW

2.1 Traffic Simulation

Traffic simulation is defined as the process of using a computer and various numerical techniques to model the behavior of vehicles on a transportation network. The simulation model uses numerous mathematical models that are created by transportation engineers who have studied vehicular behavior and verified that the models give an accurate representation of how drivers and vehicles behave. Individual models are created to govern specific behavioral properties of either a traffic stream or individual vehicles. For example, a simple model that is used to govern the behavior of a traffic stream is the fundamental flow-density equation which states that the flow rate is equal to the average speed multiplied by the traffic density (Roess et all, 2003). A typical model that governs the behavior of individual vehicles is a car following model. This type of model relates the distance between two successive vehicles (gap) to parameters such as the average speed of each vehicle and the current distance between them. These mathematical models use no more information than is necessary (information proven significant in the field) to output information about the transportation system. This allows the user to input the minimum amount of data in order to extract realistic results about the traffic network.

The advantages of traffic simulation are numerous. One of the main advantages to using a traffic simulation package is the ability to test multiple scenarios and alternatives and determine which one performs the best. Although no simulation will be able to determine the exact effects of any traffic management strategy, the simulation will give researchers and

engineers a better idea of what to expect with the implementation of a certain alternative in the field. By using simulation software, researchers will be able to determine the alternative that has the highest chance of providing the best results when multiple alternatives are considered. This should allow them to implement the "best" alternative with confidence. Without the simulation, engineers would be forced to use field tests to determine the outcome of a potential strategy. Field tests are extremely expensive compared to traffic simulations and require much more time and effort to implement. Although traffic simulation packages are not cheap (they usually cost in the range of a couple thousand dollars) and require many hours to build and calibrate, this pales in comparison to the cost and time required to outfit an existing roadway. Additionally, continuous field testing can instill a lack of confidence in the driving public and create confusion caused by a constantly changing environment. This can lead to the drivers shying away from the area in question or, worse, a decrease in the safety at the particular area.

Another advantage of traffic simulation is the ability to implement scenarios that simply cannot be field tested. Such an example would be the effect of widening a lane of a freeway on the traffic flow or installing a traffic signal at an intersection that is currently stop-controlled. Another example would be to test the effect of a technology that is still in the developmental stages. By using a traffic simulations researchers can gain some insight into the potential benefits and drawbacks of the new technology. Additionally, traffic simulations can be used to predict the effects of future demand scenarios on the existing transportation network and can help engineers to determine the best course of action to improve the transportation infrastructure.

2.1.1 Types of Traffic Simulation Models

There are many ways with which to classify traffic simulation models. One method is to classify the models with respect to the level of detail that the simulation software represents the traffic network. Using this criteria, there are three basic simulation types – macroscopic, mesoscopic, and microscopic. Macroscopic models are also known as low fidelity models since they describe the traffic behavior with a low level of detail. These models do not consider the movements of individual vehicles but rather focus on specific sections of the network and aggregate the traffic flow over each section. The model would not consider events such as individual lane changes but would rather assume that the vehicles are spread out across all the lanes of a roadway in a predefined distribution. Microscopic models, on the other hand, are high fidelity models in that they provide the highest level of detail. These models describe the behavior of each vehicle as it moves through the network as well as the interactions between any vehicle and the other vehicles that it encounters. Vehicles will adjust their speed, change lanes, and sometimes even change routes based on the speed and distance of nearby vehicles. Mesoscopic models are mixed fidelity models that describe the vehicles in the network at a higher level of detail than the macroscopic model but a lower level of detail than the microscopic model. For example, while microscopic models would base lane changing maneuvers on the interaction of vehicles in the traffic stream, mesoscopic models would include lane changes but instead base them on lane densities or lane speeds (Lieberman and Rathi, 1997).

In general, low fidelity models are easier to develop, execute, and maintain. However, the primary drawback to using these models for real world situations is that they are often less accurate than other model types. Higher fidelity models are by far the most accurate but they are

extremely difficult to develop since they involve many complex mathematical models that require a tremendous amount of information to accurately describe vehicular behavior. Additionally, they require a longer time investment to simulation a real life network and require a tremendous amount of computational power to run. Lastly, these models require much more time to run than macroscopic models. Whereas a macroscopic model can be run and the results reported inside of a few minutes, microscopic models could take hours or even days to get similar results.

Selecting which level of complexity is needed in a traffic simulation model then becomes very important to the situation that is being described. If a model is being built to determine flow rates on a freeway that does not have many weaving sections then a macroscopic model would probably be the best choice. However, if this same freeway has multiple weaving sections and merging areas then it is possible that the vehicular interactions at these areas would be of high importance. Additionally, if the number of lane changes that is performed in these sections is required as an output then a microscopic or mesoscopic model would be better suited to the task since the macroscopic model cannot give these results.

Another classification of traffic simulation models addresses the processes that represent variation within the models. The types of these models are either deterministic or stochastic. In deterministic models all interactions are represented by exact relationships. Stochastic models, on the other hand, include probability functions rather than exact functions to describe the vehicular relationships. For example, in deterministic models if a mean headway is specified then each vehicle would maintain that specific headway as it moves through the network. However, in stochastic models the mean headway would be defined by the user but the individual vehicular headways would follow a predefined distribution with the specified

headway as the mean. In this type of model, each vehicle would have a unique headway but the average of all vehicular headways throughout the network would be close to the specified mean headway value.

In almost all traffic simulation models time is the basic independent variable. How the simulation models time, however, is another method with which traffic simulation models can be categorized. Continuous models describe how elements in the network change continuously over time. Discrete models describe how elements change abruptly at specific instances in time. There are two different types of discrete models, discrete time and discrete event. Discrete time models split the simulation period into a number of segments or time intervals. The model updates the position, speed, and other information about each vehicle at the end of each time interval. Between these updates the speed and position are interpolated by the model. Discrete event models operate similarly but instead of segmenting the simulation period into equal time intervals, the model is segmented based on known events. An example of such an event could be when a pre-timed traffic signal changes from the green phase to the amber phase, the amber phase to the red phase, etc. While these models are more economical with respect to time they should only be used when a continuous change in the traffic flow is not expected. For continuous changes, the discrete time model gives far more accurate results.

2.1.2 Various Applications of Traffic Simulation Models

Micro-simulation, which is used in this study, has been used by numerous other researchers to predict the behavior of traffic flow. Using traffic simulation, Mahmassani and Jayakrishnan (1991) modeled route choice dynamics in the case of lane closures. Their studied proved that providing in-vehicle information to drivers increased the ability of the network to

reach a steady state condition (as opposed to a congested condition). It was also found that providing in-vehicle information to users reduced the time required for the network to achieve these steady state conditions.

An example of traffic simulation used in the industry of transportation engineering and the design process is a study performed by Korve Engineers (1996). As a part of this study the WATSIM program was used to model part of a 20 mile freeway corridor in California including SR 242, SR 4, and I-680. Future traffic demands were predicted for the years 2000, 2010, and 2020 and various alternatives were tested to determine their effect on the network. These alternatives included geometric changes, widening of roadways, HOV lanes, and ramp metering. This example showed the superiority of micro-simulation in analyzing candidate designs of large scale systems over simpler methods such as a straight-forward Highway Capacity Manual analysis.

Gardes et al (2002) used the PARAMICS micro-simulator to create a 19 mile network which simulated the I-680 freeway in San Francisco, California. The purpose of this study was to model several corridor improvement strategies that were being considered by CALTRANS (the governing body over the California freeway system). These improvements included ramp metering, auxiliary lanes, and HOV lanes. The results of this study provided CALTRANS with valuable input as to which strategies provided the best results compared to the cost of implementation.

Bertini et al (2002) used PARAMICS to model a diamond interchange at the intersection of I-5 and Wilsonville Road in Wilsonville, Oregon. Once calibrated, the model was run at different loading conditions (50%, 75%, 100%, and 125%) to examine the traffic flow through the interchange. Traffic flows, queue lengths, delays and travel times were collected and

compared with data observed in the field. The study also compared the average vehicle delay obtained by PARAMICS with the average vehicular delays that were predicted using the HCM 2000 methodology and found that they were relatively consistent.

Chu et al (2004) used PARAMICS to evaluate the potential benefit of several Intelligent Transportation Systems strategies such as local and coordinated ramp metering. A portion of the freeway network through Irvine, California was modeled and ITS techniques such as ramp metering, traveler information systems and their combinations were programmed into the simulation. This study used various measures of effectiveness such as vehicle hours traveled (VHT), the standard deviation of travel time for a particular origin-destination pair, average mainline travel speed, total on-ramp delay, and average travel time through the length of an arterial. The study found that while providing traffic information to motorists helps to relieve traffic congestion due to an incident the quickest, ramp metering fails to provide significant benefits unless paired with a traveler information strategy.

2.1.3 Applications of Traffic Simulation for Safety

Traffic simulation models have also been used to some extent in the field of traffic safety. While the safety of a freeway is not directly measurable by the simulator, researchers use surrogate measures of safety and examine how they change under different scenarios in order to indirectly measure how different traffic management strategies affect the safety of a roadway.

One such instance is the work of Drummond et al (2002) who performed a study to assess the feasibility of comparing the output of traffic simulation software to actual crash profiles to show whether there was a link between the number of crashes in a corridor and another parameter which is measurable in the simulation. Using historical traffic data from two

sites in Virginia, the study found that there was an increasing relationship between delay per mainline vehicle and stops per mainline vehicle with traffic crashes along the corridors. The researchers then used the Synchro Plus SimTraffic Software to model and make various changes to the traffic flow along the two traffic corridors. By adding signals to the modeled corridors, the researchers were able to determine the effect of the increasing signal density on the two surrogate measures of safety and, indirectly, the crash rates. This is one example of using historical data for a specific location to determine a relationship between traffic crashes and a measurable traffic parameter and then simulating the same location to test alternatives to alleviate the crashes.

Park and Yadlapati (2003) used the VISSIM program to examine the potential of variable speed limits to increase the safety of work zone areas. To capture the safety of the freeway, the researchers created an equation called the Minimum Safe Distance Equation which yields a value that shows whether or not vehicles are following at safe speeds through the work zone. The idea behind this equation is that if vehicles are following at safe speeds there will be a large enough headway between consecutive vehicles to reduce the risk of a crash (particularly read-end crashes) within the work zone area. The research found that implementing variable speed limit control strategies served to reduce the average speed variation through the work zone area which increased the safety considerably.

Another study performed by Lee et al (2004, 2005) used PARAMICS to determine the safety benefits of variable speed limits and ramp metering. Using historical loop data collected from a 10 km stretch of the Gardiner Expressway in Toronto, Canada, Lee et al (2003) developed a log-linear model that identified several real-time crash precursors. This model allowed the crash risk along the freeway to be determined in real-time. By simulating a portion of this

11

freeway and applying the model, they discovered that the individual application of variable speed limits and ramp metering successfully reduced the crash risk along the simulated freeway. However, this simulation was rather simplistic as it included only a small portion of the freeway (2.5 km) and did not use real traffic data to calibrate the simulation.

Abdel-Aty (2005) expanded on this study by simulating a much longer stretch of roadway using real traffic flow data; approximately 9 miles of Interstate-4 in Orlando, Florida was coded into the PARAMICS program. This study used a substantially more sophisticated crash prediction algorithm developed by Abdel-Aty et al (2004) with historical data taken from the same stretch of Interstate-4. In building the model, Abdel-Aty et al argued that the accuracy of a real-time crash prediction model would be increased if the model considered information from both crash cases and matched non-crash cases with similar offline factors (location, time of day, etc). Therefore, they created a matched case controlled logistic regression model that implicitly accounted for location and geometry of the freeway. In this process two separate models were created to determine the crash risk separately for the low-speed (less than 37.5 mph) and high speed (greater than 37.5 mph) flow regimes. Using this risk measure as the basis for his study, Dilmore (2005) found that the application of variable speed limits along the freeway would successfully reduce the crash risk at a particular location during the high speed scenario. During the low speed situations, variable speed limits did not have as great of an effect since speeds tended to be limited by congestion.

A study by Abdel-Aty and Dhindsa (2007) expanded on this research considerably by examining the potential benefits of both ramp metering and variable speed limits. Dhindsa used the same PARAMICS network and models as Dilmore (2005) but focused his efforts on strategies to improve the real-time crash risk during the low speed scenario. Additionally, the

12

variable speed limit methodology adopted by Dhindsa was more realistic than the implementation plan used by Dilmore and Dhindsa also tried implementing ramp metering and variable speed limit simultaneously to gauge the potential benefits. His study reached the conclusion that feedback ramp metering has significant potential to reduce the real-time crash risk during the low speed scenario. He also found that using variable speed limits on a network wide level had a significant effect of reducing the crash potential on the freeway. However, one of the main limitations in his work was that while the metering of successive ramps was attempted the metering strategy employed (ALINEA) was not a coordinated strategy. While it was found to reduce the crash risk there is the possibility that a coordinated ramp metering strategy would be able to reduce the crash risk even further. Additionally, Dhindsa only implemented ramp metering by treating the meters as traffic cycles. However, many ramp meters that are used in the United States and Europe use the one-car-per-cycle method which allows only a single vehicle to enter the freeway at a time. Lastly, Dhindsa found that when using the ALINEA strategy a higher critical occupancy value should be used for best safety benefits. However, this result is contradictory of what is expected based on the metering equation and needs to be re-examined.

2.1.4 Selecting a Traffic Simulation Software

Since the objective of this project is to determine the effects of route diversion and ramp metering on the safety of an urban freeway a microscopic simulator is deemed the most pertinent choice of simulation software. While the freeway corridor to be modeled is rather simplistic and could warrant a macroscopic model for operational studies, the purpose of the ramp metering and route diversion would be to reduce the negative effect of vehicles merging from the on-ramps to

13

disrupt the traffic stream. Since merging behavior is directly related to vehicular interaction, it is decided that the best method to capture this phenomena and the effect on the traffic safety would be through the use of a microscopic simulation software. Additionally, a stochastic software would be best used since this more accurately models the behavior of vehicles on the freeway and, additionally, a discrete time model should be used since there are no discrete events on the freeway that could be used to reduce the runtime of the simulation.

A review of the literature shows that there are a myriad of transportation simulation packages that are available. John Shaw and Do Nam (2002) worked extensively with the CORSIM 4.2 software but noted that there were some severe limitations. One of the main drawbacks of CORSIM 4.2 was a maximum of 500 nodes allowed per network. The purpose of their simulation was to model the metropolitan Milwaukee freeway system. However, creating just a single, complex interchange required the use of 430 nodes which severely limited the rest of their model. Additional problems with CORSIM included cumbersome network editing, older traffic algorithms (reflecting the fact that the original CORSIM code dated back to the 1970's), and unrealistic simulation results. They looked instead to two newer simulation packages, PARAMICS (PARAllel MICroscopic Simulation) and VISSIM. A comparison of the three microscopic simulation software packages was performed and the results are summarized below in Table 2-1. As shown, both PARAMICS and VISSIM were found to be far superior to the CORSIM package.

Table 2-1. Comparison of CORSIM, PARAMICS, and VISSIM Packages (Shaw and Nam, 2002)

Evaluation Criteria		CORSIM	PARAMICS	VISSIM
A. Model Capability				
1	Network Size Limit	★	★★★	★★★
2	Network Representation	★	★★★	★★★
3	Traffic Flow Representation	★★★	★★★	★★★
4	Detail of Output	★★	★★★	★★
5	Network Merge	★	★★★	★
6	3-D Modeling	★	★★★	★★
7	Traffic Composition	★	★★★	★★★
8	Animation	★★	★★★	★★
B. Ease of Use				
9	Input Data Requirements	★★★	★	★★
10	Network Coding / Editing	★	★★★	★★
11	Input / Output Review	★	★★★	★★
C. FSOA Application Requirements				
12	VISTA (GIS) Interface	★★★	★★★	★★
13	Economic Analysis Interface	★★	★★★	★
14	Incident Management Analysis	★	★★★	★★
15	Actuated Signal Control Devices	★	★★	★★★
16	User-Defined Traffic Control & API	★	★★★	★★★
17	Public Transportation	★	★★	★★★
D. Other				
18	Calibration Results	★★	★★★	★★
19	Program Integrity	★	★★★	★★★
20	Technical Support	★	★★	★★★
21	Documentation	★	★★	★
22	Record of Large-Scale Freeway Applications	★	★★★	★★
23	Software Cost per Copy	★★★	★	★
FINAL RATING				
★★★		4	17	9
★★		4	4	10
★		15	2	4

Boxill and Yu (2000) evaluated over 70 software packages to determine which were more suited to study Intelligent Transportation Systems (ITS) issues. Of the 76 software packages examined, the top nine were determined which included CORSIM, VISSIM, and

PARAMICS. Table 2-2 (below) shows a summary of the nine top software packages and evaluates their ability to model certain ITS features as well as other helpful properties.

Table 2-2. Comparison of Multiple Micro-simulation Packages for ITS Purposes (Boxill and Yu, 2000)

	AIMSUN 2	CONTRAM	CORFLO	CORSIM	FLEXYT II	HUTSIM	INTEGRATION	PARAMICS	VISSIM
ITS Features Modeled									
Traffic devices	X						X	X	
Traffic device functions	X						X	X	
Traffic calming					X	X	X	X	X
Driver behavior	X			X	X		X	X	
Vehicle interaction	X			X	X		X	X	
Congestion pricing						X		X	
Incident	X		X	X	X	X	X	X	X
Queue spillback	X			X	X	X	X	X	X
Ramp metering	X			X	X	X	X	X	X
Coordinated traffic signals	X	X	X	X	X	X	X	X	X
Adaptive traffic signals	X	X	X	X	X	X	X	X	X
Interface w/other ITS algorithms	X								
Network conditions		X				X		X	
Network flow pattern predictions					X	X	X	X	X
Route guidance									
Integrated simulation	X	X		X	X	X	X	X	X
Other Properties									
Runs on a PC	X	X		X	X	X	X	X	X
Graphical Network Builder	X	X			X	X			X
Graphical Presentation of Results	X	X		X	X	X	X	X	X
Well Documented	X	X	X	X	X	X	X	X	X

As shown above, PARAMICS and AIMSUN 2 appear to be the best software packages with respect to ITS features modeled as well as other properties. Although none of the software packages appear to be able to implement route guidance, PARAMICS features an Application Programmer Interface (API) that allows to user to edit select built-in functions within the

PARAMICS code that can be used to control the behavior of the vehicles. By creating an API one can change the route of a vehicle along the network while the simulation is running which effectively mimics the implementation of route guidance. Therefore, based on the studies performed by Shaw and Nam (2002) and Boxill and Yu (2000), as well as the numerous studies that have used PARAMICS in the past and have shown its reliability on freeways and urban roads, the PARAMICS software package was selected for use in this study.

2.2 Route Diversion

Most regional planning processes include a network assignment stage where vehicles are placed on a traffic network. Usually the most important factor concerning the network assignment is the travel time. Using the travel times of various links, planners are able to determine the optimal distribution of vehicles through a traffic network. However, this distribution is made under the assumption that the travel times are known to the users of the traffic network. In fact, this is rarely the case as the travel time is continually changing due to congestion, incidents, and events that cannot be fully predicted. Therefore, the actual assignment of vehicles onto a real traffic network is usually less than ideal. One method that has been proposed to alleviate this problem is to provide drivers with real-time information regarding the status of the network. Providing this information through Advanced Traveler Information Systems (ATIS) will allow users to make more informed decisions about mode and route choice which should help the traffic network achieve a state of equilibrium.

As summarized by Hall (1983), "For any given quantity of passive information there exists an ideal travel time and an actual travel time. The ideal travel time is the travel time for a traveler who chooses the best possible route using the given information, the actual travel time is

17

the travel time for actual travelers using the given information." Therefore, it can be seen that the purpose of ATIS is to reduce the gap between ideal travel times and actual travel times.

Abdel-Aty et al (1993) performed a literature review noting several important studies that were performed to assess the effect of ATIS on route choice. These studies showed, in general, that the impact of ATIS on driving behavior and route choice was significant. However, it was not clear what factors prompted drivers to change their route when not given travel information. This needs to be fully understood if researchers hope to gauge the true benefits of providing users with advanced travel information. Abdel-Aty noted that the effect of ATIS on an actual traffic network was not significant and this was mainly due to the lack of market penetration of ATIS at the time of his investigation. A later study performed by Abdel-Aty and Abdalla (2004) showed that as the level of information provided to the driver increases, the average travel time decreases. This clearly shows the effectiveness of ATIS and route diversion on travel time.

In the past few years, however, drivers have been receiving increasingly more information about the state of the traffic network than ever before. News stations provide traffic updates throughout the day that inform viewers of increasing congestion, incidents, and gives suggested alternative routes based on these situations. Radio programs offer the same advice but this is mostly heard in the car by users who have already embarked on their trip. The installation of navigation systems in vehicles, which were first used to give general directions, help to show drivers potential problems and can offer alternate routes as well. In Florida, a telephone service has been implemented that drivers can call and receive updated information about travel time and traffic incidents (511 Traveler Information Telephone Services). This information is also available on the internet (www.fl511.com). Systems such as these allow drivers to make more

informed decisions about their departure time and route choice in order to reach their destination as quickly as possible.

2.2.1 Studies on Benefits of Route Diversion

Recent advances in traffic simulation have also allowed researchers the opportunity to model some of the effects of ATIS on a traffic network. Yang and Koutsopoulos (1996) used the MITSIM program to model a segment of the A10 beltway in Amsterdam. Non-recurrent congestion was simulated by a 20 minute incident and the effect of ATIS on drivers was modeled. When 30% of the vehicles were given updated real-time traffic information, the average travel time in the network fell 2-4%. For drivers who had alternate routes available, this resulted in an 18% savings in travel time.

Chu et al (2004) performed a study in which various ITS strategies were employed to reduce incident related congestion in Irvine, California. The results showed that the most effective way to reduce incident based congestion was to provide real-time information to the users. When drivers were given information about the incident, they diverted their routes so that they would experience shorter travel times. This helped the network reach a state of equilibrium much faster than if the drivers traveled under the assumption that there was no incident.

Shah et al (2003) performed a study in the Washington, D. C. area comparing simulated travel times of network users. Paired travelers were created: one using ATIS technologies and one using a habitual route and departure time. The results showed that using ATIS significantly reduced the number of early and late arrivals of a trip. In some cases this involved users altering their departure time but it also involved drivers using an alternate route if their habitual route would cause significant delay that would reduce the chances of arriving on time. The study

19

found that the addition of ATIS also reduced trip disutility by 15%; however, no significant change in the overall travel time was found.

Work done by Oh and Jayakrishnan (2002) examined a system in which private ATIS companies could give real-time information to users currently in route. In this system, the companies would collect information from users with in-vehicle navigation systems equipped (IVNS) while also providing them with real-time traffic information. As a part of the study, the researchers also created two simulation networks to examine the ability of the IVNS to accurately describe the real-time traffic situation of the network. The two networks created were a simple traffic corridor and a model of the highway infrastructure in Anaheim, California. The simulation showed that users who were guided by ATIS information had a reduced travel time compared to non-ATIS users. However, the gap in travel time between guided and unguided vehicles decreased with the increase in market share of the IVNS. This is probably due to the fact that more vehicles having IVNS would mean fewer vehicles without. Additionally, the average travel time for all vehicles decreased significantly as the market penetration of the IVNS increased. This, once again, showed that route diversion based on information given by ATIS has a positive effect on the overall travel time of the network. However, while there have been many studies performed to describe the effectiveness of route diversion on the operational characteristics of a traffic network no studies have been found relating route diversion to improved safety conditions.

2.3 Ramp Metering

Ramp metering is becoming an increasingly popular method of relieving congestion on freeways. The idea behind ramp metering is to limit the number of vehicles that enter the

freeway to reduce the turbulence caused at on-ramps when slow moving vehicles try to enter the faster moving traffic stream. Ramp meters are basically traffic signals placed on the ramp that control when and how many vehicles enter the freeway. The earliest recorded use of ramp metering was on I-290 in Chicago, Illinois in 1963. This was rather simplistic, however, in that a police office directed traffic onto the freeway one vehicle at a time. However, the current use of ramp metering has expanded throughout the United States and the rest of the world and now involves complex algorithms that use traffic data taken from the freeway to determine how many vehicles are allowed to enter the freeway. Extensive use of ramp metering can currently be seen in the United States in Minnesota, California, New York and Washington State as well as across the world in Amsterdam, Paris, and Glasgow.

Originally, the signals that controlled ramp metering were pre-timed signals which allowed vehicles into the freeway at a controlled, but constant, rate. Now, however, actuated signals are used that take into account the conditions on the mainline when determining how much green time to allot to the meter. These strategies have two distinct types: local and coordinated. Local ramp metering takes into account the traffic conditions only near the ramp that is being metered. When using this type of strategy the metering rate of a particular ramp is independent of the rate at another ramp. Coordinated ramp metering, on the other hand, requires that the metering rate of a particular ramp to be based on traffic data from various locations within the corridor. This effectively allows the metering rate of each ramp in the corridor to be related to each other so that traffic conditions at one location could affect the metering rate of a ramp located miles away.

2.3.1 Ramp Metering Algorithms

There are many different methods that are used to determine the metering rate of the on-ramps. The demand capacity algorithm, proposed by Masher et al (1975) works by measuring the occupancy downstream from the location where the on-ramp merges onto the freeway. If this occupancy value exceeds a predetermined critical occupancy value related to congested conditions then the metering rate is set to a minimum value. In this algorithm it is undesirable to have occupancies greater than the critical occupancy since this will lead to congested conditions. If the measured occupancy is equal to less than the critical occupancy then the metering rate is set to a value that is equal to the difference between the downstream capacity and upstream volume. This is summarized below in Equation 1.

$$R = \begin{cases} \max(q_{cap} - q_{in}), & O_o \leq O_c \\ R_{\min}, & O_o > O_c \end{cases} \qquad (1)$$

Please note that in this equation R represents the metering rate, $R_{\min}$ the minimum rate, O_o the measured occupancy, O_c the critical occupancy, q_{cap} the flow rate at capacity, and q_{in} the upstream flow rate.

The percent occupancy algorithm suggested by Koble et al (1980) uses occupancy measurements upstream of the on-ramp entrance area to measure levels of congestion. In this strategy the critical occupancy is determined from historical data (Hadj-Salem et al, 1988). Equation 2 below describes the logic of this algorithm.

$$R[k] = K_1 - K_2(O_{in})[k-1] \tag{2}$$

Where $R[k]$ is the metering rate for time interval k, K_1 is the flow at capacity, K_2 is the slope of a straight line approximation of the un-congested flow portion of fundamental traffic flow diagram, and O_{in} is occupancy of the upstream detector.

These two algorithms are known as feed-forward algorithms since the metering rate at a particular time interval is independent of the rate at any previous interval. This is the major flaw in these methods as there is too much variation in successive metering rates during the application of these algorithms. Papageorgiou et al (1991) solved this by developed a feed-back algorithm that considers previous metering rates when determining the current metering rate. This method, known as ALINEA, is one of the most common ramp metering algorithms used and is based on the Proportional Integral (PI) feed-back control law. The metering rate, $R[t]$, is also a function of the difference between the measured occupancy O [t] downstream of the ramp at time t and a target set critical occupancy, O_c. K_R is a regulator parameter and δ_t is the length of interval at which each re-evaluation of the algorithm is done. The equation for ALINEA algorithm is given in Equation 3.

$$R[t] = R[t - \delta_t] + K_R(O_c - O[t]) \tag{3}$$

The ALINEA algorithm has been modified to improve its accuracy in different situations. MALINEA proposed by Oh and Sisiopiku (2001) is modified to take into account the occupancy both upstream and downstream of the on-ramp. FL-ALINEA proposed by Smaragdis and

Papageorgiou (2003) expands the application of ALINEA to use flow measurements from downstream detectors rather than occupancy measurements. UP-ALINEA (Smaragdis and Papageorgiou, 2003) uses occupancy measurement upstream of the on-ramp and estimates the downstream occupancy. This method shows good results in areas that previously used the demand capacity algorithm or the percent occupancy method. Lastly, X-ALINEA/Q (Smaragdis and Parageorgiou, 2003) modifies ALINEA to add queue control. This method accounts for queues building into the on-ramp and increases the release rate to reduce the amount of congestion on the on-ramp that spills over into surrounding surface streets. Excluding X-ALINEA/Q, these variations of ALINEA are all less efficient than the traditional ALINEA method but allow for use of the ALINEA method when certain detector information is missing. The ALINEA method has also been modified for coordinated ramp metering use. The algorithm, termed METALINE, was assessed by Papageorgiou et al (1997) and it was determined that ALINEA was not inferior to METALINE. Since ALINEA is much simpler to implement than the complex METALINE algorithm, ALINEA is preferred for use.

Another popular ramp metering algorithm is the ZONE ramp metering algorithm. In this method, which is a coordinated algorithm, the freeway is broken up into small sections 3 to 6 miles long (called zones) and all ramps within each zone are examined together (Stepanedes, 1993). Typically, the upstream area of each zone is a free flow area and the downstream area is a bottleneck section but this does not have to be the case. The objective of this method is to balance the volume of traffic entering the zone with the traffic leaving the zone. Stephanedes (1994) tested this strategy on a ring road in Minneapolis, Minnesota and found that it yielded a 31% reduction in travel time. Detailed information on the implementation of the Zone algorithm is provided in Section 3.6.2.1.

Note that there are two ways to implement any ramp metering method in the field (Papageorgiou and Kotsialos, 2002). The first, termed one-car-per-green realization, allows only one car to enter the freeway per metered traffic cycle. Therefore, the green time is fixed at a small value (between 1.3 and 2.0 seconds) to allow for a single vehicle to enter. The metering rate that is determined using the algorithms mentioned above is then enacted by altering the cycle length. A longer cycle length would be more restrictive while a shorter cycle length would allow more vehicles to enter the freeway. The second method is called the traffic-cycle realization. In this method the cycle length is held constant and the green time is altered. When this method is implemented more than one vehicle will be allowed to enter the traffic stream at a time, permitting that there is enough green time on the cycle to allow this.

2.3.2 Studies on the Benefits of Ramp Metering

There have been several field studies performed to assess the benefits of ramp metering. A study performed by Cambridge Systematics (2001) on the Zone ramp metering strategy in Minnesota determined that ramp metering saves the city over $40 million annually and increases average mainline freeway speeds from 46 mph to 53 mph. This is also noted with a reduction in the number of traffic crashes.

Papageorgiou et al (1997) also tested the benefits of ALINEA on the Boulevard Peripherique in Paris, France, as well as the A10 Motorway in Amsterdam, Netherlands. The study showed that ALINEA provided superior results and helped to reduce travel and congestion along the roadway. The study also proclaimed that ALINEA distinguished itself from other local ramp metering strategies due to its simplicity, transferability, low implementation costs, efficiency, and flexibility.

Due to public opposition to ramp metering, the Minnesota legislature passed a law in 2000 requiring ramp metering (which used the Zone algorithm) to be turned off for 8 weeks. In those eight weeks, congestion and the number of traffic crashes were shown to increase significantly. Additionally, the travel patterns of drivers changed based on the increased congestion. However, the study also showed that ramp metering increases travel time for shorter trips while decreasing travel time for longer trips (Levinson et al., 2002).

Zhang et al (2001) as part of the PATH program at the University of California used PARAMICS to compare four typical metering algorithms: ALINEA, Bottleneck, Zone, and SWARM. The results showed that all of the algorithms serve to improve the traffic flow. Additionally, none of the algorithms significantly distinguished itself in terms of operational benefits. Hasan et al (2002) used MITSIMLab to study ramp metering on the Big Dig network in Boston, Massachusetts. The study compared the local strategy ALINEA with the coordinated strategy FLOW. The results showed that although ramp metering almost always improved the mainline flow, the overall system performance was reduced when ramp metering was implemented at lower demand levels. Coordination was found to be very effective at higher demand levels and at locations with bottlenecks while the addition of queue control always served to improve the system performance.

Therefore, ramp metering has been shown to have tremendous operational benefits. Additionally, in Minnesota it was proved that removing ramp metering decreased traffic crashes by 26 percent (Cambridge Systematics, 2001). However this is not a real-time benefit of ramp metering but rather a benefit aggregated after some time. Lee et al (2006) used PARAMICS to show the real-time benefit of ramp metering on the crash potential on a freeway. However, this study considered a very small network with only a single ramp. Dhindsa (2005) expanded on

this research to include up to 7 ramps and showed that ramp metering provided good real-time safety benefits in congested conditions. However, in this study only local ramp metering was considered using the ALINEA strategy. It is likely that the use of a coordinated ramp metering strategy such as the Zone algorithm would reduce the crash risk even further during specific traffic conditions. Also, Dhindsa's study only focused on the traffic-cycle realization of ramp metering and did not consider the possibility of using the one-car-per-cycle method.

After a review of the literature it is clear that both route diversion and ramp metering have the ability to greatly improve the operational capability of a given traffic network. What is less known, however, is the real-time effects on the safety of the network. While some preliminary work has been performed with ramp metering, it is not comprehensive enough to make a formal decision about the potential of ramp metering to be a real-time crash prevention device. PARAMICS has been found to be a tool that can be accurately used to assess the effects of both route diversion and ramp metering on the safety of a typical urban freeway.

CHAPTER 3.   METHODOLOGY

3.1 PARAMICS Micro-simulator

As mentioned in Section 2.1.4, the software chosen to model the network used in this study is the PARAMICS program. PARAMICS (short for PARAllel MICroscopic Simulation) is a suite of traffic simulation software tools developed by Quadstone Limited (2002). The PARAMICS project suite consists of the Modeler, Processor, and Analyser. The Modeler is the main tool that provides a visual representation of the road network through a graphical user interface (GUI). It is in this program that the user will code the network by entering information about the network geometry and travel data. Because the program has to simulate the movements of each vehicle and update the visualization on the screen, the speed of the Modeler is directly related to the size of the network and processing power available on the computer. Once a network is coded in the Modeler, the Processor module can be used to simulate runs without the visualization option. This allows the simulation to run much faster than in the Modeler and is the most used method once the network has been coded. The Analyser module (not used in this study) allows the user to take runs that have already been completed and compare the simulation results through a GUI.

3.2 Study Area

The study area for this work was a portion of Interstate-4 that runs through Orlando, Florida. Interstate-4 generally runs in an east-west direction from Daytona Beach, Florida to Tampa, Florida, bisecting Orlando, Florida along the way. The specific area that was modeled for this study was the 36.25 mile segment that runs through the downtown Orlando metropolitan

area. Although the movements along I-4 are described as east-west, this segment actually runs north-south through the heart of the downtown area starting at S.R. 192 in the southwest and ending just north of Lake Mary Blvd in the northeast. Figure 3-1 (below) shows a map of Orlando with the Study Area highlighted. In Figure 3-1, the downtown area is outlined with a dotted line. This is the area that will be mostly affected by route diversion and ramp metering.
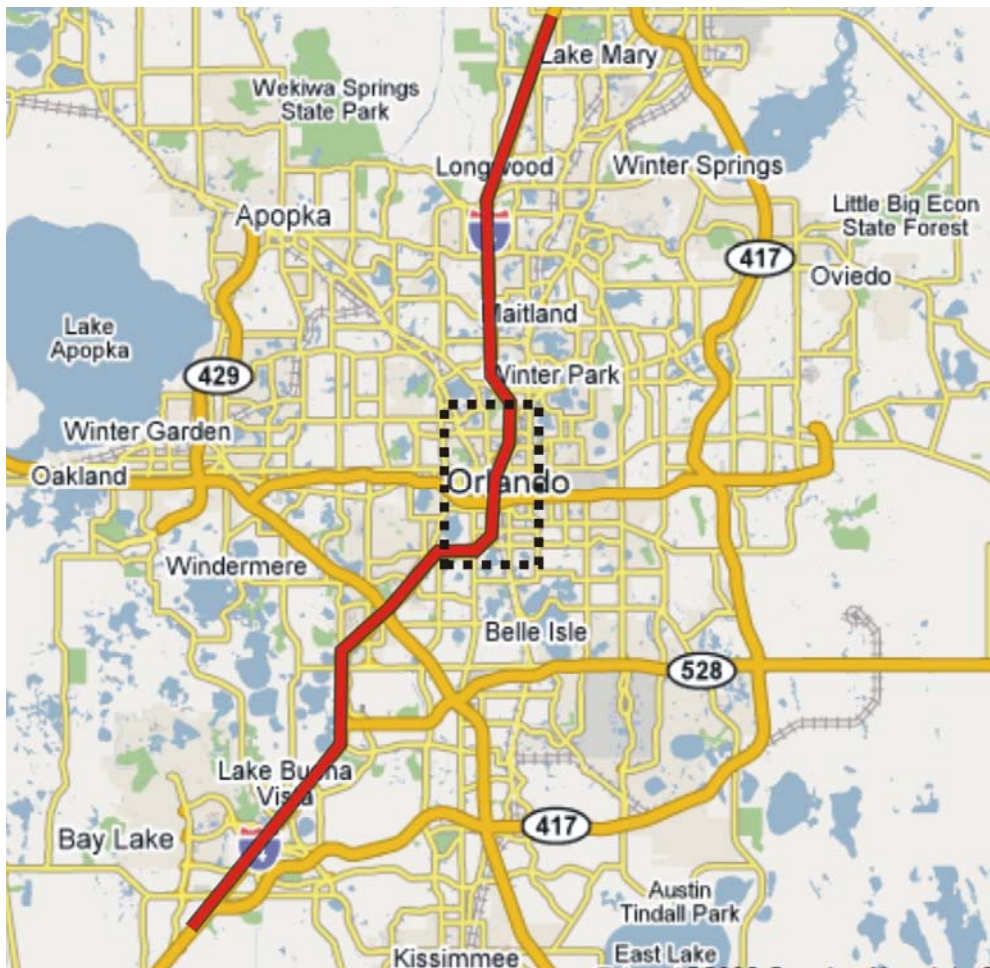
Figure 3-1. Map of Orlando Showing I-4 (Study Area)

For the majority of its length through downtown, I-4 is a 6-lane freeway (although in some areas the freeway is either 4 or 8-lanes wide) with 12-ft lanes and speed limits varying between 50 mph and 65 mph. The speed limit throughout the downtown area, the heart of the

network, is the lowest (50 mph) while the speed limit generally increases with the distance from downtown. The composite AADT as defined by the Florida Department of Transportation to give an estimate of the amount of traffic that exists on I-4 through the Orlando region is approximately 183,000 vehicles/day (FDOT, 2003). This composite AADT value is an average AADT from different locations along I-4 through Orlando.

3.3 Network Building

The following sections describe in detail the process that was completed to code the I-4 network into PARAMICS. The steps involved, in order, were:

- Overlay Generation

- Coding of Nodes and Links

- Coding of Zones and Vehicular Demand

- Coding of Loop Detectors

- Network Calibration

- Creation of Origin-Destination Matrix

- Network Validation

- Implementation of Route Diversion

- Implementation of Ramp Metering

3.3.1 Overlay Generation

In order to accurately code the freeway geometry an overlay of the roadway was needed. A previous network created by Dilmore (2005), which studied a smaller section of the same

freeway corridor, used a combination of aerial photography obtained from the Seminole County Property Appraiser's Office and the Orange County Property Appraiser's Office as the base for the overlay. This aerial photograph was also combined with AutoCad drawings obtained from the Orange County Transportation GIS department (Dilmore, 2005). A sample of this hybrid overlay is shown below in Figure 3-2.
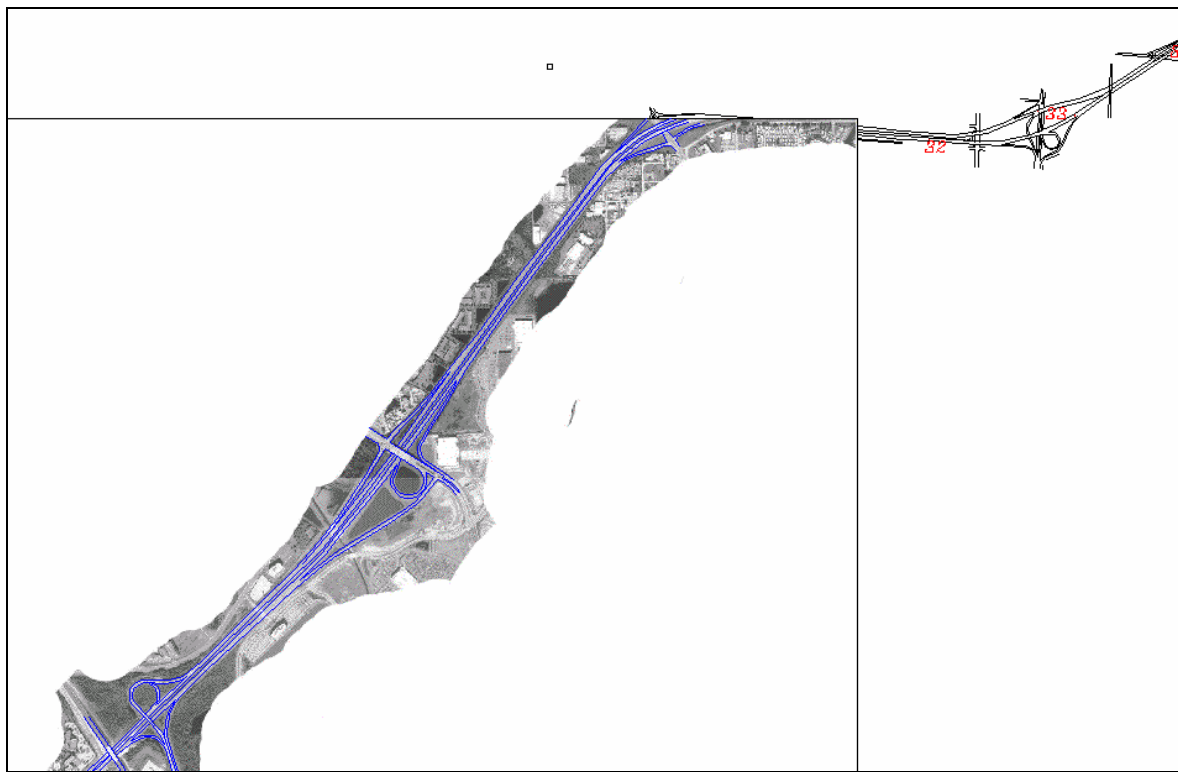
Figure 3-2. Sample of Hybrid Overlay Used by Dilmore (2005)

While this process was sufficient for the study area used by Dilmore (2005) the study area for the present research was significantly larger (36 miles compared to just 20 miles). Therefore, the remaining geometry was obtained from aerial imagery obtained from the Google Earth Aerial Mapping program. This program allows users to have free access to aerial images

of several heavily populated areas throughout the world. The aerial images in the Google Earth program available for Orlando, Florida were taken during April 2002.

Obtaining a single aerial for the entire study area was not practical as it did not have a sufficient resolution to see detailed portions of the roadway. Therefore, individual pieces of the aerial were obtained from the Google Earth program and then assembled into one master file using the Adobe Photoshop program. Great care was taken when extracting the aerials from Google Earth to ensure that the graphical scales of all individual pieces were the same. Once the entire network was captured using individual aerials, they were overlaid against the low resolution image to ensure that there were no errors with the individual components that were used and that the roadway alignment was correct.

Since PARAMICS only accepts *.dxf and *.bmp files as overlays, the master aerial was then saved as a *.bmp file for import into the simulation program. However, this file was too large to be imported directly (greater than 100 MB) so the master overlay had to be split into seven distinct segments to be imported into PARAMICS. A sample of one of the 7 segments is given below in Figure 3-3. Please note in Figure 3-3 the two sample grids that were drawn next to the aerial. Each box in the grid represented a 500 ft x 500 ft square and was used in the scaling of the aerial in PARAMICS.
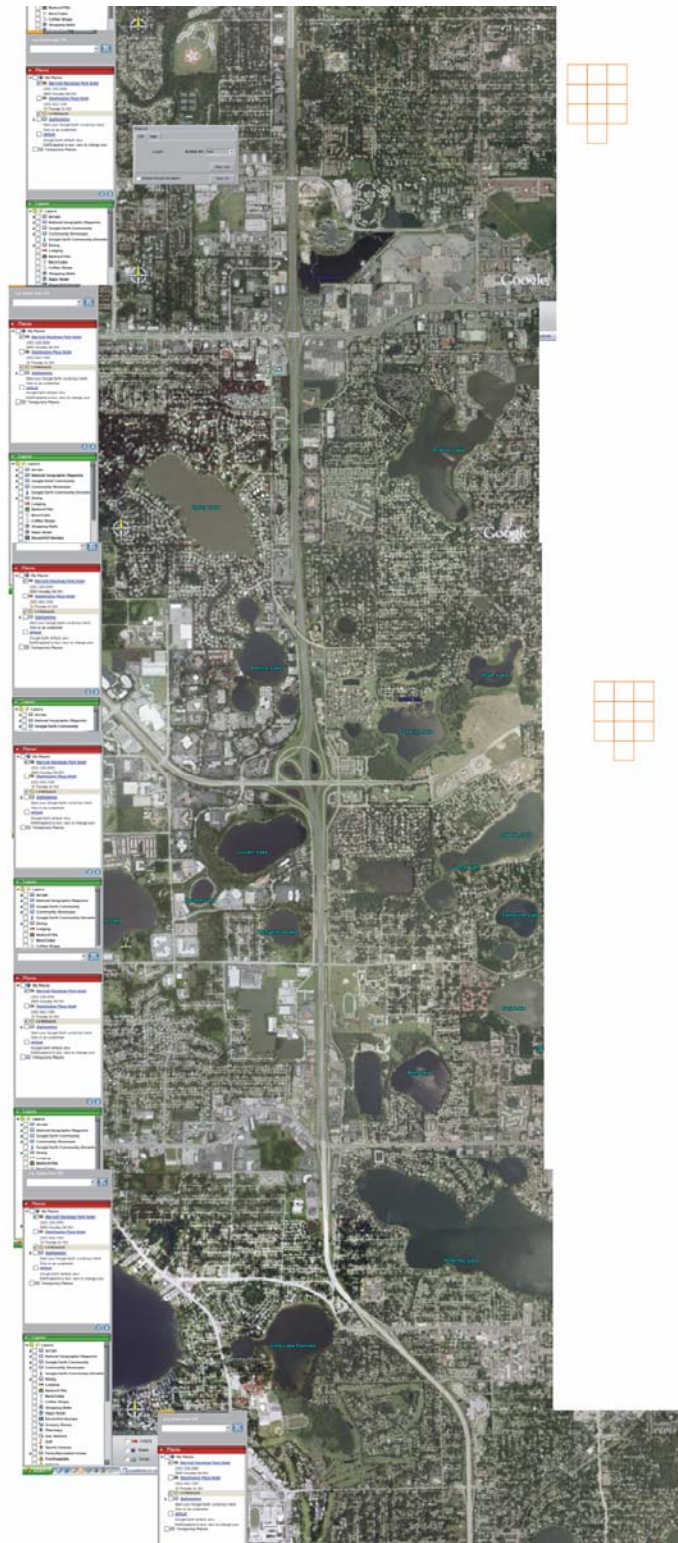
Figure 3-3. One of Seven Distinct Sections of Aerial Used in Network Construction

Once each segment was imported, it was scaled individually (using the grid boxes seen in Figure 3-3) and then reassembled in the PARAMICS program to form the master aerial. This was then checked once again with a single, low-resolution image to ensure that there were no scaling errors. Once this was completed, the next step was to draw the roadway network.

3.3.2 Two One-Way Roads vs. One Two-Way Road

It was decided at this stage to code the eastbound and westbound directions separately as two different one-way roads rather than a single, two-way roadway. This choice was made for a few different reasons. First, and more simply, the two directions had different speed limits and geometries that could only be properly modeled if the two directions were coded independently of one another.

The second reason requires a more intimate knowledge of how a network is coded in PARAMICS and how vehicles behave in the network. A PARAMICS network is a series of "links" or segments of roadway that have homogenous properties (number of lanes, speed limits, etc). Each link is defined at the extremities by two "nodes." These nodes designate the starting and ending point of a link. Therefore, changes in the roadway geometry, such as a lane addition or drop, is defined by a node which separates the two links with different properties. When a link merges with another link, such as a ramp entrance point, another node must be created to define this point. Vehicles in PARAMICS are only capable of making lane changing and routing decisions for the next two links it will encounter. If one two-way roadway is used to define the freeway, this will essentially double the number of links that will be used in either direction of freeway; the network will also have to include many extremely short links to properly place the entrance ramps. Additionally, each on-ramp is given a value for the awareness distance. This

34

awareness distance defines how far upstream of the ramp vehicles on the mainline recognize the existence of the ramp and merge left in order to allow vehicles on the ramp to merge into the traffic stream. The maximum value for the awareness distance of any ramp cannot be greater than the length of the nearest link. Therefore, having a single roadway with many shorter links would result in improper vehicular behavior at the on-ramps as there will not be sufficient gaps for vehicles to merge onto the freeway. Separating the two directions of traffic would reduce the number of short links since each direction would only have to split links for its own on-ramps or off-ramps. Lastly, when a single roadway is used the default PARAMICS options would allow vehicles traveling in the eastbound direction to exit using off-ramps in the westbound direction and vice versa. Clearly this does not occur in the field as vehicles can only use off-ramps for the particular direction of the freeway that they are using. Although this could be turned off manually by editing the junction properties, this would have to be set for every single on-ramp and off-ramp which is a very tedious process. Using two one-way roadways will counter this problem without any extra coding effort.

The only drawback to using two one-way roads to code the freeway is that it neglects the presence of "rubber-necking" or the reduction in capacity on one direction of the freeway due to situations that occur on the other direction. The rubber-necking phenomenon is especially important when incidents occur on the network as it has been proven to reduce the capacity of the freeway by as much as 12.7% (Masinick and Teng, 2004). However, for this study this effect was assumed to be negligible since no incident occurred during the simulation.

3.3.3 Building Network Nodes and Links

Once it was determined to code both directions of the freeway separately, the nodes that defined the links for each direction were coded into the simulation. A new node was created at every location where the roadway changed geometry (curved section to straight section), number of lanes, speed limits, or a ramp entered the mainline. These different nodes were then connected with links which represented the roadway that the simulated vehicles would use. Each roadway link was assigned to a category that contained information about the number of lanes and speed limit on the link. The information from the number of lanes and curvature of each link was obtained visually from the Google Earth aerial maps. The speed limit for each link was determined from the placement of speed limit signs that were found from watching a video stream of I-4 obtained from the Roadway Characteristics Information (RCI) obtained from the Mainframe Database operated by the Florida Department of Transportation (FDOT). Once the links were created, the next step was to adjust the kerb points in the links to match the real roadway geometry. Kerb points are locations on each link that define the shape of the link more specifically than simply using the nodes and curvature tools. Adjusting the kerb points is essential to ensure that the simulated vehicles move freely between links without interruption.

3.3.4 Creating Ramps

Another decision that had to be made was the coding of the individual ramps. PARAMICS includes a special function to code an on-ramp and another to code the deceleration lane that typically precedes an off-ramp. However, these two functions can only be used in specific cases which do not represent the gamut of ramp types found on I-4. Therefore, most of the ramps in the network that could use the on-ramp or slip lane function were coded using these

functions while the rest were coded as a regular merge or diverge area. Figure 3-4 shows a brief summary of when the PARAMICS on-ramp or slip lane functions were used and when the merge / diverge areas were chosen.
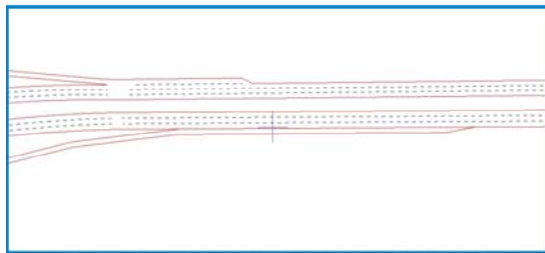
On-Ramp Using RAMP Function

Off-Ramp Using SLIP LANE

Off-Ramp Created Using DIVERGE Lane

(NOTE: SLIP LANE cannot be used since the off-ramp
is on the left hand side of the freeway)
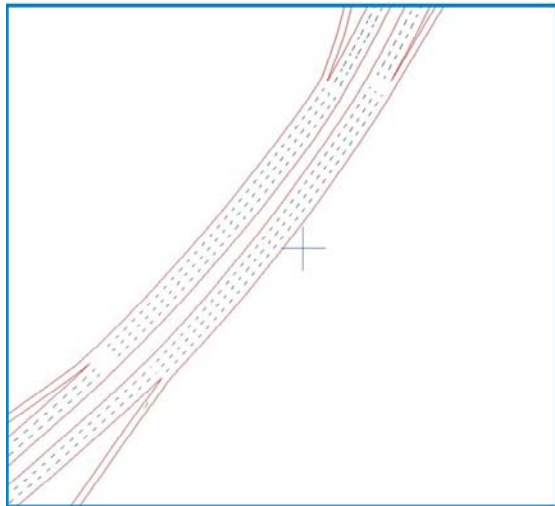
On-Ramp and Off-Ramp Pair Connected Using
Traditional MERGE / DIVERGE Lanes

(NOTE: RAMP Function or SLIP LANE cannot be used
since there is a weaving lane that connects the two ramps)
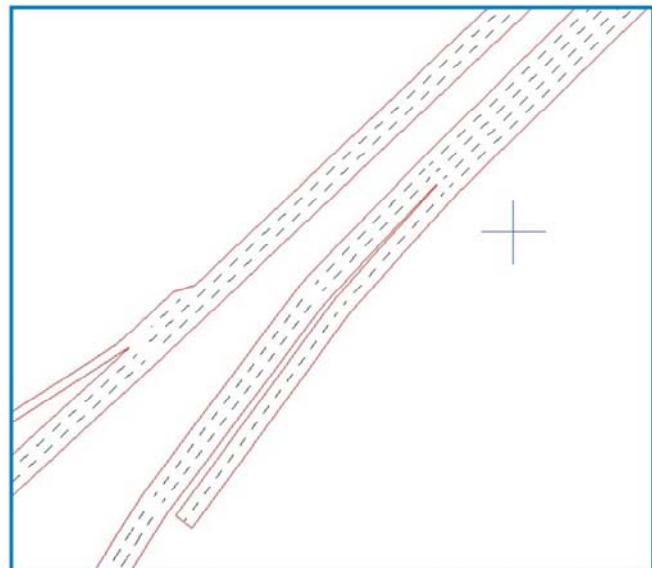
On-Ramp Created Using MERGE Lane

(NOTE: RAMP Function cannot be used since the on-ramp
is a two-lane ramp)

Figure 3-4. Types of Ramps Encountered and How They Were Coded in PARAMICS

There was one major problem that was noted concerning vehicular behavior on PARAMICS defined on-ramps. The problem was that vehicles were not merging onto the mainline freeway with regularity causing the ramp to back-up and not allowing any vehicles on the network. This was alleviated by adjusting the signpost distance for the ramp. Increasing the signpost distance for the ramp increased the awareness of the mainline vehicles to the ramp and caused the mainline vehicles to change lanes to give vehicles on the on-ramps sufficient gaps to merge onto the mainline freeway. Once the signposting distance was adjusted, merging behavior using the ramp function behaved as would be expected in the field.

3.3.5 Adding Zones and Vehicles

Once the geometry was completed, the zones that defined the origins and destinations of the network were created. For the freeway portion, defining the origins and destinations were rather simple as each on-ramp represented an origin and each off-ramp represented a destination. Once finished, vehicles were loaded artificially onto the network to test the vehicular behavior. It was noted in many places, particularly merge and diverge areas where the number of lanes changed at the end of one link and the beginning of another, that vehicles were changing lanes improperly (for example, a vehicle changing from the right-most lane directly to the left-most lane while crossing over other simulated vehicles in the process). This problem was fixed by adjusting the nextlanes function which defined which lanes were available for vehicles traveling from one link to the next on a specific lane.

3.3.6 Loop Detectors

One of the reasons that this section of freeway was chosen was because the specific section of I-4 that is used in this study contained induction loop detectors embedded in the asphalt. These loop detectors were spaced approximately every 0.5 miles apart on the roadway and gave values of the average speed, volume, and lane occupancy at 30-second intervals for the mainline freeway lanes.   Therefore, in order to make sure the data obtained from the PARAMICS network matched the real-life data obtained in the field, the detectors had to be placed in the same locations. The detector mileposts were obtained from the FDOT Roadway Characteristics Information (RCI) database and placed in the appropriate positions along the network.   After every simulation run, during the post-processing stage, the loop data was extracted from the PARAMICS data files and stored in the same format as the loop data obtained from the real I-4 roadway.

As previously mentioned, throughout the majority of the study section Interstate-4 is a 6-lane freeway. However, at some sections the roadway was widened to eight lanes. In these locations loop detectors exist in each lane but only information from three lanes is archived. These three lanes are considered to be the three "mainline" lanes. In most instances, these mainline lanes are the left-most lanes since vehicles typically enter and exit from ramps on the right-hand side of the freeway. However, on Interstate-4 there are a few locations where left-hand ramps are present. For these locations, the three mainline lanes are considered to be the right-hand most lanes. In order to simplify the network creation procedure, loop detectors in the network were built over all lanes and the mainline lane issue was resolved in the post-processing procedure.   As will be explained, the post-processing procedure involved converting the

PARAMICS output to the loop detector data format that is archived. In this process, only the mainline information will be converted to ensure that the data obtained by loop detectors in the network is equivalent to that found in the field.

<div align="center">3.4 Network Calibration and Validation</div>

Typically, the most tedious process in creating any micro-simulation network is the Calibration and Validation. The calibration procedure involves changing pre-specified model parameters that affect driving behavior of the simulated vehicles to match the driving behavior of drivers in the real network. Although the default values have been shown to approximate decent driving behavior, tweaking the parameters would more accurately represent driving behavior for the particular study area. A review of the literature shows that the values of these parameters are found by comparing the flow and travel time along the network (Bertini et al, 2002; Abdullhai et al, 2002; Trapp, 2002, and Stewart, 2001). The calibration parameters that are typically changed are mean headway and driver reaction time (Gardes et al, 2002; Abdulhai et al, 2002; Lee et al, 2004).

<div align="center">3.4.1 Previous Calibration Procedure</div>

In a previous study performed by Dhindsa (2005), a 20 mile segment of I-4 (contained within the 36 mile corridor modeled in this study) was created in PARAMICS and used to test various ITS strategies (locally coordinated ramp metering and variable speed limits). An exhaustive calibration procedure was carried out to determine the values of four calibration parameters: mean driver reaction time, mean driver headway, queuing distance, and queue speed. The mean driver reaction time refers to the time vehicles take to react to events around them

<div align="center">40</div>

such as the merging of a vehicle into its lane or the deceleration of a vehicle that it was following. The mean driver headway refers to the average time gap that vehicles try to maintain while moving through the freeway. The queue speed is the maximum speed with which queuing behavior occurs. Vehicles traveling below this speed will behave using the built-in PARAMICS queue behavior. Queuing distance is the minimum distance between two vehicles that causes queuing behavior to end. Once this distance is achieved between successive vehicles in a queue, the queuing behavior of that vehicle will end. This calibration procedure used 5-min vehicular flows as well as 5-min vehicular speeds as factors used to calibrate the network. Although the use of flows has been seen in previous studies, this was the first use of flows at such short time intervals (5-min) as well as the use of 5-min speeds.

Since the study area in the network used by Dhindsa is incorporated in the 36.25 mile network created for this study, and also because his calibration procedure is so comprehensive, the calibration parameters determined by Dhindsa to represent traffic behavior is used in this study. It is unlikely that the addition of just over 16 miles of the network would change the driver behavior significantly to alter the values of the calibration parameters that are needed to be used. The following sections will give a brief overview of some of the steps taken during the previous calibration procedure. For more information, please refer to Dhindsa (2005).

3.4.1.1 Calibration of O-D Matrix

In order to estimate the OD Matrix that would used to define vehicular demand on the network, the study by Dhindsa used traffic data obtained from the 2003 Florida Traffic Information (FTI) CD. Hourly ramp volumes were also available from the Center of Advanced Transportation Systems Simulation at the University of Central Florida.

Since the basic freeway segment contained two one-way roads, there were some simple rules that were used in the OD matrix estimation. First, all rows that held the origin data for zones on off-ramps were given a value of zero as no off-ramp could produce vehicles onto the freeway. Second, all columns that held destination data for on-ramps were treated similarly as vehicles could not end their trip (exit the freeway) at an on-ramp. Additionally, ramps from one direction of the freeway could not have trips that originated from or were destined to ramps in the other direction of the freeway. Therefore, these pairs were given a value of zero in the OD matrix. Last, all cells that represented a trip from an on-ramp that was located downstream of an off-ramp was given a value of zero since a vehicle could not travel backwards on the freeway (Dhindsa, 2005). The rest of the values of the origin-destination matrix were calculated using a simple gravity model. Using the gravity model showed some differences between the sum of the columns and the known ramp volumes at that ramp. This was corrected using the following steps:

- If the sum of a row or column is either both too high or too low the count is adjusted appropriately to change this

- When the sum of a column is too high the count is lowered

- If both the sum of a column and row value for a cell is too low the count is increased

- Steps 2 and 3 are repeated until the error is minimized

It should be noted that the previous steps were performed at all ramps excluding the East-West Expressway (S. R. 408) ramps since the majority of error was expected to be found at this location. Once the errors at the other ramps were minimized, the S. R. 408 ramps were adjusted. The final error of the OD matrix, found by comparing the simulation on-ramps and off-ramp volumes with those found in the field, was 4.10%.

<u>3.4.1.2 Calibration of Flows and Speeds</u>

  The simulation was run and the volumes on the mainline were compared to data obtained

from the loop detectors embedded in I-4. The flows in the simulation were checked against the

average flows taken from a 20-day period between September 23, 2003 to November 20, 2003

(note: only data obtained from Tuesdays, Wednesdays, and Thursdays were used). Initially, the

mainline flows were lower than what was expected by the loop data. The flows between the end

zones were increased and re-run to get a more adequate value. A sample of the comparison

between the actual flow and simulated flow on a 5-minute basis for a group of 6 stations is

shown below in Table 3-1. Note that this table does not show the best case but is just a sample

of the tables used to determine which set of calibration parameters yield the best results.

Table 3-1. Difference between 5-min flows for Simulated and Real Data from Dhindsa (2006)

5 min. Time Interval	Detector 33	Detector 34	Detector 35	Detector 36	Detector 37	Detector 38
1	69.5594	72.5338	51.8638	51.5588	129.5172	164.1730
2	46.7231	59.1504	24.9548	57.2571	128.3921	150.6219
3	20.3438	59.2487	41.9722	61.9213	120.5060	138.7657
4	20.9601	48.3512	23.5370	52.8326	102.1730	120.8567
5	-20.5063	5.0061	-18.9889	3.6741	47.3865	71.4978
6	7.1344	0.1267	-30.6444	-6.2352	48.4093	77.1837
7	-31.2777	-25.3324	-34.8509	1.8475	51.6759	73.6704
8	-27.3818	-26.5561	-49.1922	-32.1415	39.6663	78.2341
9	-75.9589	-68.6024	-85.1784	-11.0970	45.6919	48.7433
10	-84.1765	-55.1797	-43.9852	-24.4583	28.4913	62.6543
11	-82.7436	-65.7757	-61.2659	10.4417	35.9804	58.0231
12	-85.7216	-29.1626	-36.4718	17.5000	71.5478	94.7971
13	-50.3237	-20.7685	13.5167	51.7796	60.0415	61.1008
14	-6.8202	25.9179	-4.5537	12.6169	6.2121	26.1900
15	-20.5017	-15.5427	-59.3002	-6.5659	39.6744	83.0488
16	-80.5463	-49.8531	-15.6204	33.0861	44.5268	51.8855
17	-42.2757	6.3500	-2.5989	-9.7932	11.1174	35.8532
18	-36.6879	-36.5705	-48.3998	-39.7924	13.9457	47.0101
19	-105.9332	-77.9436	-44.9802	-11.4575	36.5701	81.7641
20	-103.8652	-61.0370	-41.5275	-6.0697	50.9495	102.6571
21	-57.7538	-14.9252	-8.5558	-5.0798	58.9383	93.2179
22	-62.6049	-30.1087	-18.3831	-15.0128	44.4453	100.8202
23	-12.5058	-33.5481	-33.0565	-10.7173	47.9923	87.5548
24	-40.1569	-47.8800	-28.6787	-32.1049	53.9039	118.1519
25	-19.2656	-56.0143	-27.5900	16.8254	67.9889	121.8310
26	11.0968	-5.1175	14.2253	-26.2165	41.8273	120.7842
27	-8.3443	-30.9317	-37.0866	-20.2100	52.8059	109.0692
28	-31.0426	-52.6972	-34.9500	-31.8696	76.5455	124.3371
29	14.2661	-33.0025	-24.1252	-24.1400	51.4606	96.0697
30	41.7084	-12.2174	-33.3755	-49.8579	37.5833	94.8364

Additionally, plots were made that compared the average simulated speed and the average speed from the loop detectors at 5-minuate intervals. These plots contained 10% error bars for the simulation data to show the acceptable range of speeds that the simulation data represented. An example of such a plot is shown below in Figure 3-5.
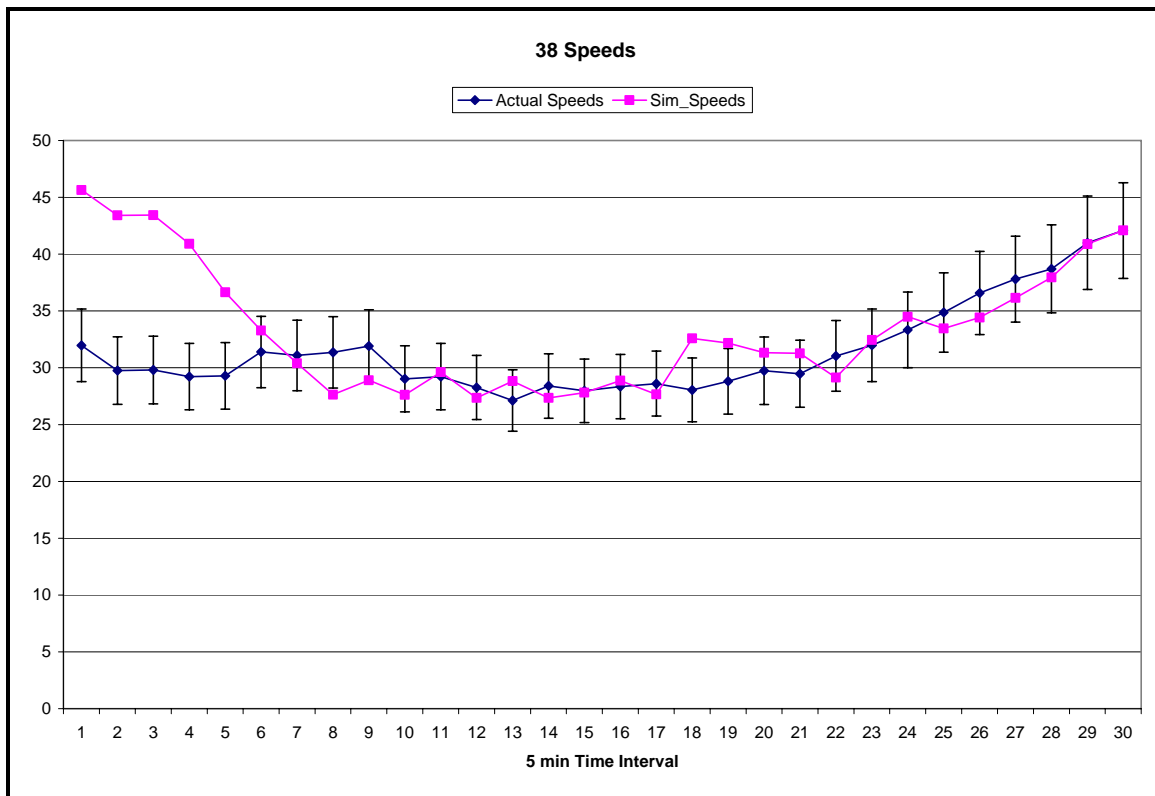
Figure 3-5. Sample Plot Showing Real Average Speeds with 10% Error Bars and Simulated Speed from Dhindsa (2006)

At this point, various values of the mean driver headway and mean driver reaction time were selected and tried to minimize the error in flows and speeds while holding the queue speed and queue distance constant at 8 mph and 9 ft, respectively. These values for queue speed and queue distance were chosen because increasing them tended to increase the persistence of queues at any location once formed.

Based on the errors in the flows and speed, the final mean headway and mean driver reaction time were chosen to be 1.00 seconds and 0.45 seconds, respectively. These values were close to previous values used on a similar project performed by Dilmore (2005) and, therefore, found to be acceptable in the calibration of driver behavior along Interstate-4 in Orlando, Florida.

45

3.4.2 Origin-Destination Matrix

As previously mentioned, these same calibration parameters from Dhindsa (2006) were used in this study since the two studies have essentially the same study area. However, since the network used in this study is larger and contains several new on-ramps and off-ramps the origin-destination matrix for this study had to be recreated.

The procedure used to create the origin-destination matrix was similar to the procedure used by Dhindsa described above in Section 3.4.1.2. Rows holding origin data for off-ramps were given a value of 0. Columns containing destination data for on-ramps were also given a value of 0. Last, values below the diagonal (which represented a vehicle traveling from an on-ramp downstream of a particular off-ramp) were given a value of 0. This minimized the number of cells that needed to be calibrated.

Using traffic data obtained from the Florida Traffic Information (FTI) 2003 CD and hourly data obtained from the Center for Advanced Transportation Systems Simulation (CATSS) as well as the origin-destination matrix that was used by Dhindsa as a starting point, the O-D matrix for this study was computed using a simple gravity model. The resulting OD matrix was then input to PARAMICS and the network checked against expected queues. From basic field observations it was noticed that there were large queues that took occurred at the downtown areas during a majority of the simulation time period. However, using the OD matrix that was created from the gravity model did not reflect this observation. Instead, vehicles tended to move freely and the queues that did form were not reoccurring queues formed by congestion but were instead short-term queues that involved 4 or 5 vehicles and dissipated very quickly. The OD matrix was then modified to include more vehicles at the Interstate-4 / S.R. 408 interchange and

at the terminus zones of the network to increase the flow and induce congestion. This resulted in the formation of queues around the Interstate-4 / S.R. 408 interchange and a traffic flow that was more consistent with the field observations that were done.

3.4.3 Network Validation

Once the OD matrix was determined, the next step was to perform a brief validation procedure to confirm that the traffic flow in the simulation closely resembled the traffic flow in the field. Field data for the validation procedure was taken from a database that contained loop detector data from Interstate-4. Loop data for a period of 20 weekdays, excluding Mondays and Fridays, were extracted from the loop detector database. The period during which data was extracted was from September 23, 2003 to November 20, 2003; this was the same time period that was used in the validation procedure in work done by Dhindsa. Please note that due to periodic loop failure data was note available for all loop stations during this time period.

Flow data from 20 selected stations were then compared against the simulated flows in the PARAMICS network. The comparison was performed by computing the GEH statistic. The GEH statistic is a measure that is essentially a modified chi-squared statistic that takes into account both the absolute and relative difference in the observed and simulated traffic data. This statistic is widely used by researchers working with PARAMICS (Oketch and Carrick, 2005). The GEH statistic is calculated at each location as follows in Equation 4.

$$GEH = \sqrt{\frac{(M-O)^2}{1/2 * (M+O)}}$$

(4)

Where M = the hourly flow rate obtained from the simulated network and O = the hourly flow rate obtained from the field. Generally, a GEH statistic less than or equal to 5 represents a good fit while a GEH statistic between 5 and 10 could still be considered good but requires further investigation. A value of the GEH greater than 10 implies that the simulated flow rate is not a good fit of the observed data.

The 20 stations for which flows were compared were selected based on the availability of the loop data and based on the need to get a good representation of the entire traffic network with a focus on the downtown area (since this area will be the area mainly affected by the route diversion and ramp metering). Simulated data was averaged for 10 PARAMICS runs and the hourly volume was determined at each station selected and then compared to the loop data that was acquired from the loop database. Table 3-2 (below) gives a summary of the 20 stations selected, the actual and simulated volumes, and the GEH statistic at each location.

Table 3-2. Comparison of Observed vs. Simulated Flow Rates

Station	Flow From Loop Data (veh/hr/lane)	Simulated Flow (veh/hr/lane)	GEH Statistic
7	932	700	8.14
18	1102	1031	2.17
19	1104	1031	2.25
20	1129	959	5.26
21	1073	954	3.76
22	1183	1006	5.35
23	934	933	0.01
24	1011	920	2.91
26	914	994	2.59
30	1380	1038	9.82
34	1317	1316	0.01
35	1304	1333	0.80
36	1331	1251	2.22
37	1342	1494	4.03
41	1550	1748	4.87
42	1535	1706	4.24
43	1870	1884	0.33
44	1520	1917	9.57
49	1840	1791	1.15
50	1849	1987	3.16
52	1532	1581	1.24
53	1549	1483	1.69
56	1495	1514	0.50
57	1411	1257	4.22
61	1389	1250	3.83

Based on this comparison, 80% of the loop stations have a GEH statistic less than 5. Additionally, the average GEH value for all stations considered is well under 5 at 3.36 and no station has a GEH statistic greater than 10. Therefore, this shows that the origin-destination matrix, which was calibrated to induce queues at the downtown locations, actually provides a good fit of the observed field data in terms of hourly volumes as well. This validates the network as providing an accurate representation of the field data and should allow conclusions to be made as the result of the implementation of various strategies to the network.

3.5 Implementation of Route Diversion

The implementation of the route diversion into the PARAMICS network was a two-fold process. First, the alternate routes that were to be simulated had to be coded onto the network. Before this was completed, the only route available to vehicles was Intersate-4. The route diversion that is used here does not allow vehicles to bypass I-4 completely. Rather, vehicles forego entering I-4 at one location and travel to a later on-ramp for entry onto I-4. The second part of implementing route diversion involved getting vehicles to use the secondary route. Left to their own network assignment models, the simulated vehicles would travel on the shortest path. On this network, this is always on I-4. Therefore, a method had to be devised to force some simulated vehicles to use the alternative routes. These two steps are further explained in the following sections.

3.5.1 Alternate Routes

When initially deciding to implement route diversion on the I-4 network the question of where to include the diversion routes arose. Since the goal of this research is to reduce the crash risk on I-4 the initial thought was to implement the route diversion in such a way that the changes in the crash risk would occur at a location of high crash risk along the freeway. However, this is all dependent upon the availability of an alternate route. Therefore, when selecting the area on the freeway to implement route diversion two factors were considered: the existence of natural diversion routes and an area known to have high risk. Previous knowledge of the area and driving experience in Orlando, Florida gives that the Interstate-4 / S. R. 408 Interchange is an area of high freeway turbulence. This turbulence is caused by the large amount of vehicles that travel from S. R. 408 (the main east-west arterial road in Orlando) to Interstate-4

(the main north-south arterial through downtown Orlando) and vice versa. During the peak periods, this large merging volume onto Interstate-4 causes considerable congestion which is known to be related to traffic incidents. Therefore, when considering diversion routes, an emphasis was placed on routes that would have an effect on the crash risk at or around this interchange.

To determine the specific routes used in the route diversion, a map of Interstate-4 was visually inspected to determine what the best feasible alternate routes would be. Alternate routes were determined to be roads that formed a practical connector between one I-4 on-ramp and another downstream on-ramp. Three specific routes were found to be suitable through the downtown I-4 area which would directly affect traffic conditions around the Interstate-4 / S. R. 408 Interchange. These routes were defined as Route Diversion 1, 2, and 3. Route 1 is shown in Figure 3-6 as DP-1A and DP-1B. Route 2 is also shown in this figure. Route 3 is shown in Figure 3-7 as DP-3A and DP-3B and is a mirror image of Route 1 which affects the westbound direction of I-4 (Route 1 affects only the eastbound direction).
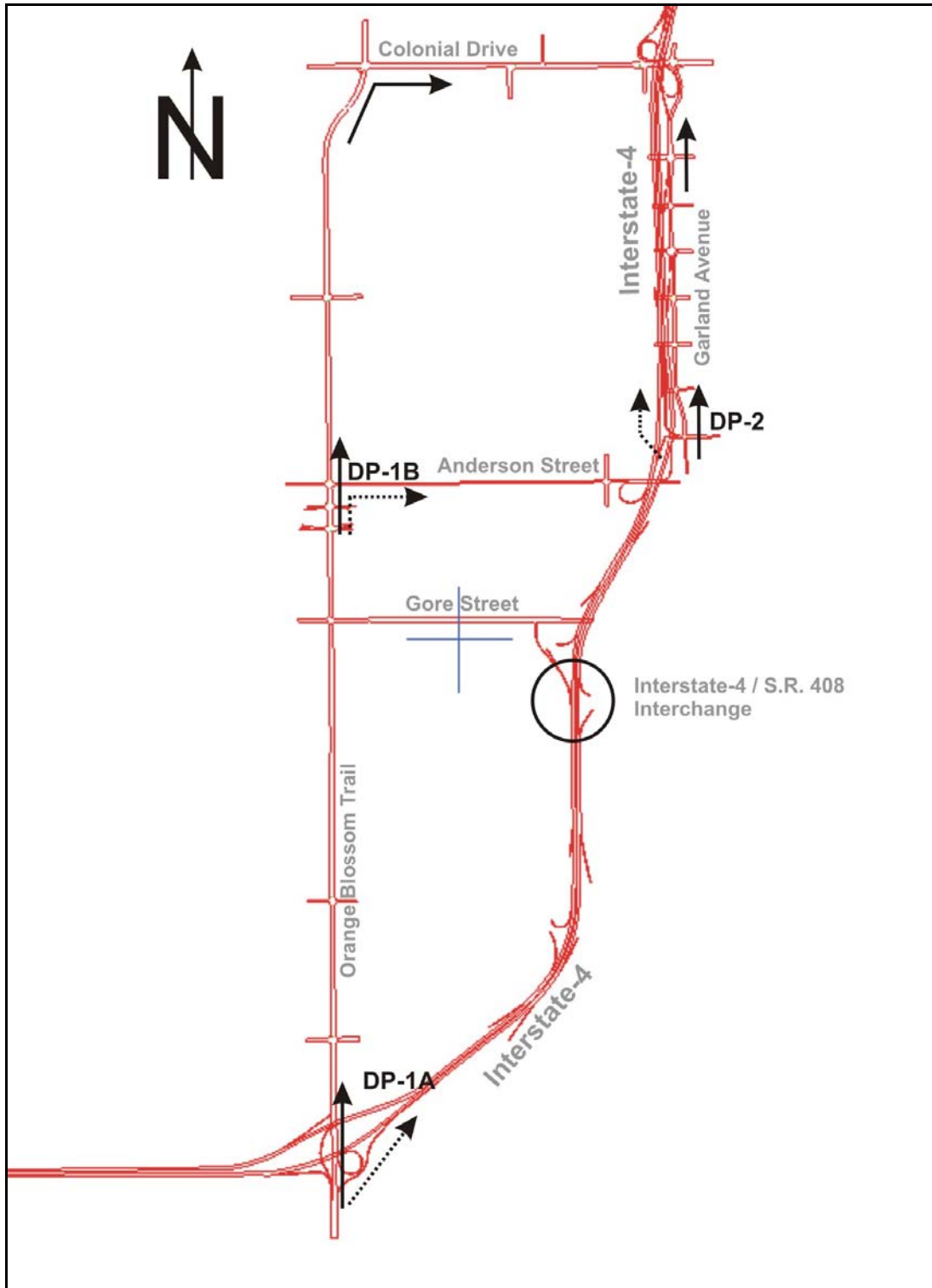
Figure 3-6. Decision Points for Eastbound Diversion Routes
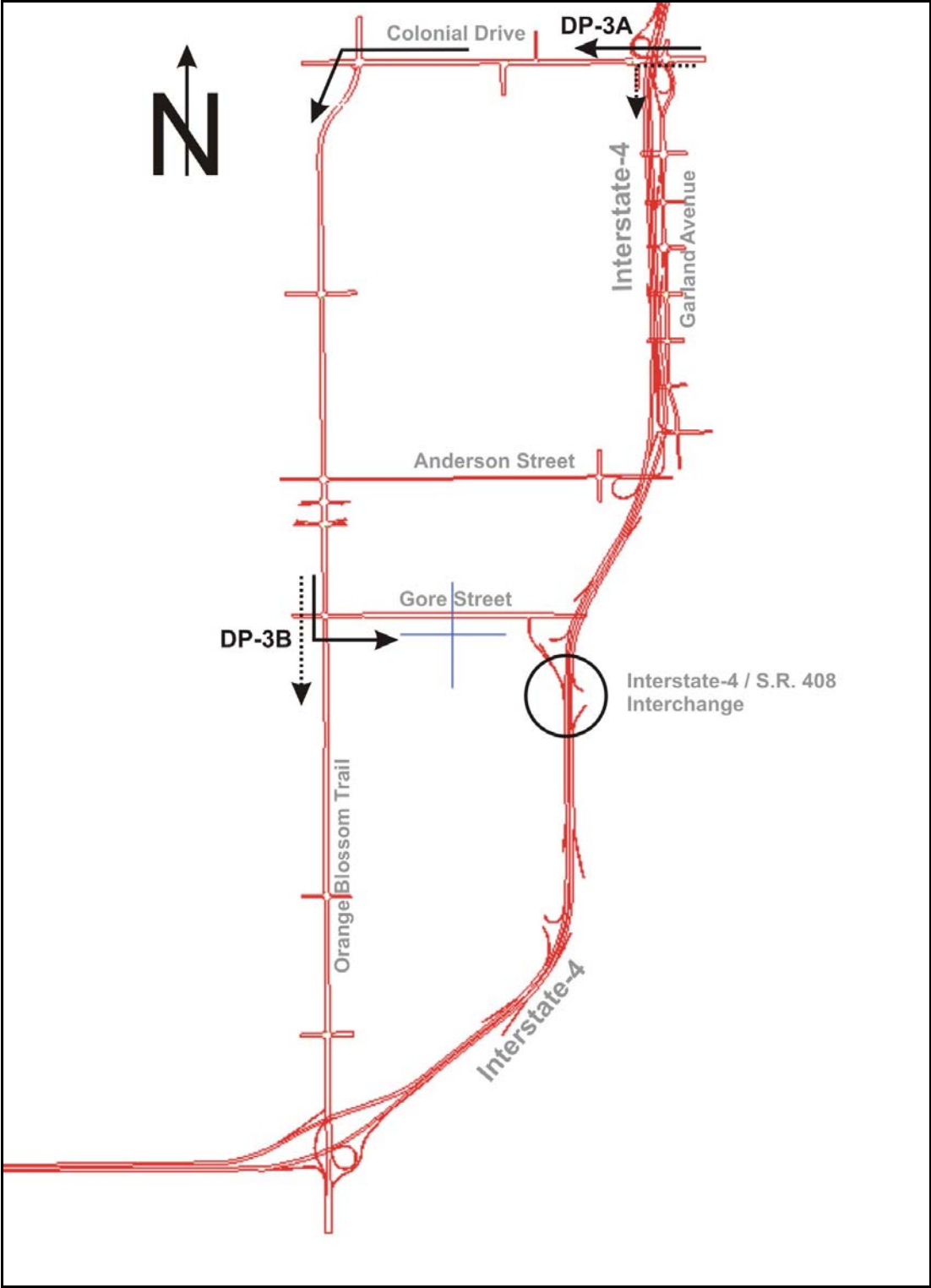
Figure 3-7. Decision Points for Westbound Diversion Routes

Each route has either one or two decision points, depending on the length of the diversion route. A decision point defines whether a vehicle enters I-4 at a particular location or continues traveling for the next convenient entrance point. The decision points are also shown in Figures 3-6 and 3-7 and are labeled as DP-1A through DP-3B. Route Diversion 1 is comprised of DP-1A and DP-1B. At DP-1A, the vehicle must choose between entering the EB direction of Interstate-4 or continue traveling north on Orange Blossom Trail to reach the next entrance point. While traveling north on Orange Blossom Trail, the vehicle will encounter another decision point, DP-1B. At DP-1B, the vehicle can decide to turn east onto Anderson Street and enter I-4 in the eastbound direction by using an on-ramp location further downstream. The alternative to this is traveling north to the intersection of OBT and Colonial Drive, traveling east on Colonial Drive and entering EB I-4 at an on-ramp located on Colonial Drive. This route would essentially divert vehicles from entering the freeway just before the Interstate-4 / S. R. 408 Interchange and have them re-enter downstream of this location.

Another choice is Route Diversion 2 which is rather short compared to the previous route. Route Diversion 2 consists of only one decision point, DP-2. At DP-2, vehicles traveling west on South Street can either enter eastbound I-4 immediately or travel north on Garland Avenue until they reach the I-4 on-ramp further downstream on Garland Avenue near Colonial Drive. This route affects the Interstate-4 / S. R. 408 by diverting vehicles that would enter the freeway just after the interchange (causing more congestion around this area) and require them to enter a little less than 1 mile downstream. By diverting vehicles in this manner the traffic volume is reduced immediate downstream of the I-4 / S. R. 408 Interchange and reintroduced onto the freeway further downstream which should reduce the potential for a bottleneck at the Interchange.

54

The previous two diversion routes described affect the eastbound travel direction of Intestate-4. The only diversion route that affects westbound travel is denoted as Route Diversion 3 (shown in Figure 3-7). Route Diversion 3 is also comprised of two unique decision points, DP-3A and DP-3B. Please note that Route Diversion 3 is approximately a mirror image of Route Diversion 1 except it affects traveling in the westbound direction on I-4 as opposed to the eastbound direction (which is affected by Route Diversion 1). At DP-3A vehicles trying to enter I-4 in the westbound direction may do so or traveling west on Colonial Drive and then south on OBT until the next decision point. At DP-3B, the shorter path for vehicles is to continue traveling south on OBT until the WB I-4 on-ramp. However, vehicles may elect to travel east on Gore Street and enter I-4 on the WB on-ramp that is located on Gore Street. Since this is a mirror of Route Diversion 1, this route would halt vehicles traveling in the westbound direction from entering before the Interstate-4 / S. R. 408 Interchange and cause them to enter just downstream of this location.

Coding the Diversion Routes onto the network required the creation of traffic signals in the PARAMICS network. The three diversion routes actually included 29 traffic signals. However, in order to reduce the amount of coding required in the creation of the network as well as to reduce the amount of traffic data needed, only 19 traffic signals from major intersections were considered. The important signals were decided based on both the size of the intersection (all of the larger intersections were included) and field observations as to which signals delayed vehicles the most along the diversion routes in order to successfully capture that added delay in this analysis. The traffic signal timing data was obtained from the Orange County Traffic Engineering Department.

The signal timing data indicated that most of the signals that were to be included in this network were actuated signals. However, in order to reduce the complexity of the PARAMICS simulation, the signals were treated as pre-timed signals. At the intersection of two major roadways (Orange Blossom Trail and Colonial Drive, for instance) the pre-timed signal timings that were used were set to maximum green time for each direction. Doing this assumed that all approaches of the intersection were saturated (or nearly so) during the peak period. Based on field observations, this was most always the case. At the intersection of a major roadway and minor roadway (Colonial Drive and Parramore Road, for example) preference in the signal timing was always given to the major roadway (Colonial Driver or Orange Blossom Trail in all cases).

Once the diversion routes were created, the next step required was to add vehicles to the diversion routes to approximate the traffic conditions that diverted vehicles would encounter on the surface streets. However, there was a question of how to approximate volumes and delays that are experienced by these vehicles. Unlike the freeway, where loop data was recorded and stored at regular intervals, there was no automatic counter in place along these roads. One idea was to use the AADT (annual average daily traffic) value and K value to approximate the DDHV (directional design hourly volume). However, there is question over the accuracy of these estimates. While they are traditionally used by traffic engineers and planners, AADT's are usually only an estimate from data taken over the course of a few days. Additionally, AADT values are not updated every year.

Therefore, the surface streets were calibrated based on previous knowledge of traffic flow on the diversion routes. The goal of this calibration became to match the long queues at intersections along Orange Blossom Trail and Colonial Drive through the downtown region that

56

is typically expected during the afternoon peak hour on any particular day. Additionally, surface streets within the downtown area (diversion route 2) were always congested during this time period.

3.5.2 Route Diversion API

As previously mentioned, there are two decision points that comprise Route Diversion 1. Each of these decision points represent a variable in the simulation in that a vehicle may either choose one of two paths to get onto I-4 from that location. However, after creating the network with the alternate routes and observing the simulation, it was seen that vehicles only took a single path to reach their final destination – the path through I-4. Therefore, a method had to be devised to force some vehicles to divert from their traditional route and to instead travel on the surface streets to re-enter I-4 downstream and, eventually, reach its destination zone.

PARAMICS allows for dealing with multiple paths between zones by the addition of dynamic traffic assignment. However, even when the dynamic traffic assignment is calibrated properly the dynamic traffic assignment method does not allow for specific user control over the amount of vehicles diverted from a particular point. Instead, each vehicle selects a path that will reduce its disutility of travel. Therefore, in order to control the amount of diversion, code had to be written to control vehicular behavior through the use of the PARAMICS Application Programmer Interface (API). The API allows a user to use C programming to write a code that will access and modify certain preexisting PARAMICS functions during the simulation run. The result of an API can be as simple as reporting the average speed at a location at regular time intervals or as involved as changing the speed limit at a particular location based on specified conditions.

In order to get vehicles to divert from their natural path, an API was written to override the preexisting route choice algorithm in select situations. Since the route choice algorithm is accessed by every vehicle on the network, special conditions had to be met before the route choice algorithm was overridden to ensure that the right vehicles were diverted. The special conditions were the origin zone of the vehicle, destination zone, and current link. The origin zone was used to ensure that only vehicles that are entering I-4 at one of the diversion locations were diverted. The destination zone was used to ensure that vehicles that were diverted to a downstream on-ramp would not overshoot their intended off-ramp and have no logical route to reach their destination once they entered I-4 downstream. Note that if diverted vehicle did overshoot its destination, the vehicle would proceed to the downstream off-ramp, circle back to the original on-ramp and enter I-4 from the original location. Lastly, the current link was specified to ensure that vehicles were only diverted when they were located on the link immediately upstream of a decision point. Not specifying this link caused vehicles to travel in a circle continuously.

Therefore, if a vehicle was traveling from a specific zone near the on-ramp of interest and its destination was at a location further downstream on I-4 than the vehicle's re-entry ramp the vehicle would only divert its route at the link preceding the on-ramp of interest. Additional code was added to control how many vehicles diverted per simulation run. This was done by specifying the percentage of vehicles that would divert at each decision point. Once each vehicle met the diversion conditions it was assigned a random number between 0 and 100. If that random number was less than the percentage of vehicles that were to be diverted, the vehicle's course was altered to use the route diversion. If not, the vehicle was left to its own route choice algorithm. Therefore, the percentage of vehicles diverting were not exact due to the random

nature of the diversion assignment but generally averaged out to the number that was specified. The code for the API is given in the Appendix.

3.6 Implementation of Ramp Metering

Because there were two types of ramp metering that were considered in this analysis, two unique methods of implementing ramp metering had to be used. In order for both methods to be implemented some changes first had to be made to the network. These changes included the lengthening of the on-ramps to include the full storage capacity since vehicles would be queued in the ramp while waiting for the meter. Additionally, traffic signals were added to the merge area on the ramp which would act as the main control (or meter) in the ramp metering process. For the ALINEA ramp metering method those were all the changes that were needed. However, for the ZONE ramp metering algorithm meters were also added to the beginning of each ramp to measure the inflow of vehicles onto the ramp.   A basic description of how each method was implemented is in PARAMICS given in the following sections.

3.6.1 ALINEA Ramp Metering

As previously mentioned in Section 2.3.1, the ALINEA ramp metering algorithm is rather simple to implement. The ALINEA algorithm calculates the metering rate for a particular freeway on-ramp by using only occupancy measurements taken from the nearest loop detector downstream of the on-ramp in question. If the occupancy is higher than a pre-determined critical value, the metering rate is reduced to allow time for the congestion to decrease before the ramp is open to free-flow.

To implement the ALINEA ramp metering algorithm special controls that are available in PARAMICS to model vehicle actuated signal controls (VA signals) were used. The VA signals allows the program to access data obtained from loop detectors in the network and, based on an algorithm coded by the user, changes the signal timing with changes in the traffic flow. Using this methodology involves the creation of two new network files called the "phases" and "plans" files. The phases file specifies which signal is to be controlled (i.e. which ramp to be metered) and what detectors are to be accessed by the metering algorithm (which are the nearest downstream loop detectors). The plans file defines the algorithm that will be used to change the signal timing. In this file the occupancy values are calculated from the loop detectors in PARAMICS and the metering rate is changed as per Equation 3. Because the ALINEA controls are the same for each ramp, the code only had to be written once and was then copied for each subsequent meter. A sample of the phases and plans files for the ALINEA control is given in the Appendix.

3.6.2 ZONE Ramp Metering

3.6.2.1 Zone Ramp Metering Algorithm

As previously mentioned in the review of current literature, the main purpose of the Zone Ramp Metering Algorithm is to balance the number of vehicles entering a freeway zone with the number of vehicles leaving. This is done by using Equation 5 given below (Bogenberger and May, 1999).

$$M + A + U \leq B + X + S \text{, where:} \tag{5}$$

M = the on-ramp flow through the metered ramps

B = the downstream bottleneck capacity (1800 - 2100 vehicles per hour per lane)

X = the sum of the measured off-ramp volumes

S = the spare capacity available on the mainline (measure of density and speed)

A = the measured upstream mainline traffic volume

U = the measured sum of the un-metered on-ramps

Looking at Equation 5, the only variable that can be altered by ramp metering is the variable M. Therefore, M is a function of the measured in-flow volume, out-flow volume and the spare capacity within the zone. For the Zone algorithm, M will be updated every time period, in this study 5 minutes, to determine the allowable flow rate of vehicles from metering ramps onto the mainline. Once M has been calculated, the metering rate of each metered on-ramp, R_n in veh/hr, is calculated by using Equation 6.

$$R_n = \frac{M * D_n}{D} \tag{6}$$

In this equation, R_n is equal to the proposed meter rate for ramp n, D_n is equal to the current flow rate of vehicles entering ramp n, and D is the total number of vehicles wishing to enter the freeway through any of the metered on-ramps in the zone. As can be seen in the equation, the equation basically assigns the total allowable inflow rate for the entire zone, M, to each of n metered ramps proportionally by the volume of vehicles that are using the ramp. Therefore, a ramp that has twice the volume of another ramp should receive twice the green time of the second ramp.

Once R_n is determined, this rate is checked against a predetermined minimum rate. If the proposed rate is less than the minimum metering rate, then the rate is set to the minimum rate. The minimum metering rate is determined based on the length of the ramp and the density of queued vehicles waiting on the on-ramp. The goal of the minimum metering rate is allow vehicles into the freeway stream after a maximum waiting time of four minutes. Therefore, calculating the minimum metering rate is done by determining the number of vehicles that can be queued in the ramp and dividing this value by four minutes. Once scaled to vehicles per hour this will yield the minimum metering rate for the ramp and would represent the rate that would allow vehicles queued on the ramp to enter the freeway after waiting for a maximum of four minutes.

3.6.2.2 Zone Algorithm in PARAMICS

Implementing the ZONE ramp metering algorithm was a considerably more difficult process than implementing the ALINEA algorithm due to the large amount of data required to calculate the respective metering rates. While the ALINEA algorithm requires just the occupancy reading from a single detector, the Zone algorithm requires that speeds, densities, and flows be known from multiple locations on the freeway mainline as well as the various on-ramps and off-ramps within the metered zone. Even more importantly, however, is the fact that the respective metering rates within a zone are all dependant on one another. If it were not for this fact, the VA built-in signal controls in PARAMICS could still be used to model the Zone algorithm although the code would be much more complicated than the code for the ALINEA algorithm.

Instead, an API was created to control the signals. Using an API is advantageous for a few reasons. For one, using an API allows the code to be written in the C-language instead of the built-in VA control language. Although the VA control language resembles C, there are some functions that are not possible using the VA control language. Because the API is written in C-code, multiple functions can be created in the API, each representing the metering of a different zone. Doing this allows the user to easily turn zones on or off depending on the control strategy being tested. This allows multiple scenarios to be tested much easier than with the VA control method which would require the creation of individual phases and plans files for each combination of control strategies that is to be tested.

3.7 Output of PARAMICS

There are two types of output from PARAMICS that will be useful to this analysis. Global output is data taken from the entire network and does not require a location to be specified in order for the data to be collected. This type of network output includes the travel time (total vehicle hours traveled – VHT), total distance traveled (total vehicle miles traveled – VMT), and total number of vehicles on the network at any point in time, among other measures. The other type of output is specific to a particular location and usually requires the inclusion of a loop detector on the network at that location. Data that can be collected from a particular detector includes flow, headway, speed, occupancy, acceleration, gap, and density (on a particular link – does not require a detector but the link must be specified).

The detectors included in the PARAMICS network were placed in the same locations as the detectors in the field so that the two sets of data could be compared. This is important because the models that will be used to define the crash risk in the simulation were created with

63

the loop data extracted directly from Intersate-4. However, PARAMICS outputs the loop detector data in a manner that is inconvenient for analysis. The loop data that is collected along I-4 is an average of the speed, flow, and occupancy on every lane at 30 second intervals. PARAMICS outputs the speed and occupancy data at every detector at every instant that a vehicle completely crosses the detector. Therefore, the PARAMICS output provides a signal line of data every time a vehicle crosses over a detector. In order for the two to be compared, the output from PARAMICS must be post-processed to convert it from the given form into the form that is available in the field. This is accomplished by using a Visual Basic macro written in Microsoft Excel. This macro essentially reads the data line by line and groups the data into 30 second time intervals and, using those groups, computes the average speed, volume, and occupancy. Once completed, the macro outputs the data in exactly the same format as that collected in the field. The only downside to the macro is the processing time. While a typical simulation run takes anywhere between 20 to 80 minutes to run in the PARAMICS Processor module, running the macro for a single set of output data takes anywhere from 1 to 6 hours depending on the processing power of the computer. Therefore, the time needed to analyze a single set of 10 runs can be as little as 12 hours to 2 or more days.

Once the output has been converted into the loop data format, there is still one more step that must take place before the crash risk (the variable of interest) can be determined. All models defining crash risk use traffic parameters that have been aggregated into 5 minute intervals. However, the output from PARAMICS (and the real loop data) is given in 30 second intervals. Therefore, another macro was written to group the 30 second data into 5 minute intervals and compute the average, standard deviation, and coefficient of variance for speed, volume, and occupancy. In order to save time, however, this macro does not convert all of the data, only the

64

specific variables that are needed in order to calculate the crash risk measure. These parameters are listed later in Sections 4.3 and 4.5. For this reason, this macro has a much shorter runtime (about 30 to 90 minutes per run) than the first macro. Therefore, a typical set of 10 runs takes about 10 hours to complete. This brings the average time to perform a group of 10 runs in PARAMICS processor batch mode, convert the data to loop data format, and pull the variables needed to compute the crash risk to about 50 hours. Note, however, that this value changes based on the processing power of the computer used to run the macro and the loading case being performed. Due to the large number of scenarios and multiple runs performed per scenario, multiple computers were used to run the macros. The runtimes for the various computers and loading scenarios ranged from 20 hours at lower loading cases (60 percent loading) with the fastest computer to about three days for higher loading cases (100 percent loading) with the slowest.

CHAPTER 4.   EXPERIMENTAL DESIGN

The purpose of the experimental design is to evaluate the effects of route diversion and compare the effects of different ramp metering strategies on the real-time safety of an urban freeway using the PARAMICS microscopic simulation program.   Although micro-simulation packages have been used extensively in studying the effects of various ITS measures on traffic flow, the use of micro-simulation in the field of traffic safety presents the challenge of how to quantify the effects of the ITS strategy.   For changes in the traffic flow, measures of effectiveness can include many simple metrics ranging from the traffic volume entering a particular roadway segment or intersection, the total travel time for all vehicles in the simulation, the density on a particular link, etc.   These quantities are directly measurable by the simulation program and are often reported automatically upon the conclusion of the simulation run.

However, there is no standard metric which provides the level of safety on a simulated traffic network.   Real networks can rely on case studies over a period of time in which the number of crashes that occur at a particular location or section of roadway is used as the variable of interest.   Even though this is essentially a flawed approach due to the random nature and human error involved in most traffic crashes, it is still the best approach transportation engineers can use when a large dataset is present.   This method allows researchers to determine the areas that are more prone to traffic collisions with respect to the rest of the traffic network.   However, it is impossible to include the occurrence of crashes on a simulated network since it is impossible for a computer to determine when and where a crash will occur.   Instead, when using simulation packages researchers look to other measurable variables that have a known relationship to traffic

66

crashes. These surrogate measures of traffic safety do not directly depend on the frequency of crashes and instead reflect the behavior of all the vehicles traveling in the traffic stream.

Some surrogate measures of safety include simple variables such as mean speed or speed variance (Gettman and Head, 2003). Other, slightly more complicated, safety measures described in this work were variables such as Time to Collision and Post Encroachment Time. However, some researchers have spent much time developing models which use these directly measurable values as inputs to describe the safety (or crash risk) on the roadway. These models would then be used to describe the level of safety on a network during the simulation. One such example, from researchers in Virginia, is an equation that compares the actual following distance of a vehicle to the recommended safe following distance (Park and Yadlapati, 2003). Another example comes from researchers at the University of Central Florida who created a measure of crash risk based on a logistic regression model developed using within stratum matched sampling and real-time traffic variables taken from loop detectors embedded in the freeway (Abdel-Aty et al, 2004). This measure was used in studies that assessed the change in the crash risk based on the implementation of variable speed limits (Dilmore, 2005) and localized ramp metering (Dhindsa, 2005).

However, one problem with using the metric described in Abdel-Aty et al (2004) is the fact that it describes the crash risk locally for each loop detector station. Therefore, this measure of crash risk is not comparable across different stations. By using these measures one cannot determine which location on the freeway has the highest risk of a collision. To overcome this, more recent research done by Pande and Abdel-Aty (2006) has created newer models to determine the real-time risk of rear-end and lane-change crashes using neural networks. These models include explicit variables to account for location (instead of implicitly accounting for

67

location) and, therefore, produce rear-end and lane-change crash risk values that are able to be compared across location. This will provide a better picture of the rear-end and lane-change crash risk along the freeway.

This study will focus on these models presented by Pande and Abdel-Aty (2006) to describe the rear-end and lane change crash risk along the Interstate-4 freeway. The following sections will provide more information about the models that are used to calculate the rear-end and lane-change crash risks as well as how the models are implemented in this study.

4.1 Clustering of Rear-End Crashes

Similar to the research that calculated the crash risk based on logistic regression models (Abdel-Aty et al, 2005) which that found that crashes occur within two separate speed conditions (high-speed and low-speed), the more recent research by Pande and Abdel-Aty (2006) has found that rear-end crashes are more accurately described as occurring within one of two distinct traffic regimes. These traffic regimes cannot be defined as simply high-speed or low-speed, however, and require loop data from multiple locations in the freeway in order to be classified. To describe these different regimes, a classification tree model was created that used freeway speeds at different locations around the station of interest as the input. The two regimes were originally defined using speed data taken from 0 to 5 minutes before the rear-end crash. However, in an effort for the final rear-end crash risk model to be used in real-time in a predictive fashion, the classification tree used to separate crashes into the two different regimes used speed data taken from 5 to 10 minutes before the crash. More information on the classification tree method can be found in Pande and Abdel-Aty (2006).

The result of the classification tree model was a set of simple if-then statements that used the speed variables to classify the data into seven distinct "leaves" on the tree. Each of these leaves had a different percentage of regime 1 crashes and regime 2 crashes and this probability was used to define the traffic conditions as either regime 1 or regime 2. If a particular leaf had a percentage of regime 1 crashes that was greater than 0.50, then that leaf was assumed to represent regime 1 conditions. Likewise, if the percentage of regime 1 crashes was less than 0.50, then the leaf was said to denote regime 2 conditions. Figure 4-1 below gives a summary of the classification tree rules as well as the associated percentages of regime 1 to regime 2 conditions for each leaf. Please note that the percentage of regime 1 crashes for a particular leaf is also known as the probability that traffic conditions belonging to regime 1. This value was given the variable name "a" and will be used as part of the surrogate measure of safety.
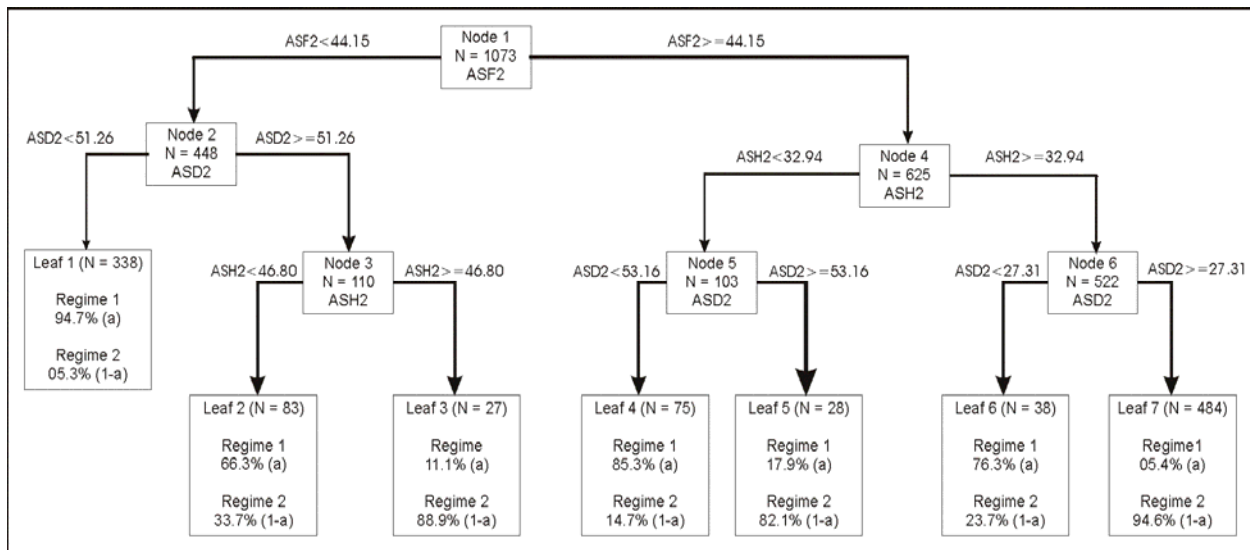
Figure 4-1. Classification Tree to Determine Regime Conditions for Traffic Data (Pande, 2005)

In order to understand the nomenclature for each variable in Figure 4-1 it is necessary to understand the format of the loop data that are used to calculate these variables. The loop data is given as the average speed, volume, and lane occupancy every 30 seconds for each of three lanes

69

on the freeway. The variables listed above are all calculated for a time period of 5 minutes. Therefore, each variable takes into account 30 data points since there are 10 observations for each of the three lanes in the 5 minute period.

The first letter(s) in each variable name describes the measure that is calculated from the 30 data points. "A" represents average, "S" represents standard deviation and "CV" represents the coefficient of variation. The coefficient of variation is defined as the standard deviation divided by the average value. The next letter refers to what measure is being computed. "O" refers to occupancy, "S" refers to speed and "V" refers to the volume. The final letter refers to which station is used to calculate this value. Figure 4-2 (below) shows how the stations are referenced by letter. Station F refers to the station of interest. Stations A through E are upstream of the station of interest while Stations G and H are downstream. Since each station is approximately 0.5 mile apart, Station D would represent the station 1 mile upstream of the station of interest. Although the classification tree in Figure 4-1 only uses variables of average speed, the other variable terms will be used in the crash risk models described in subsequent sections.
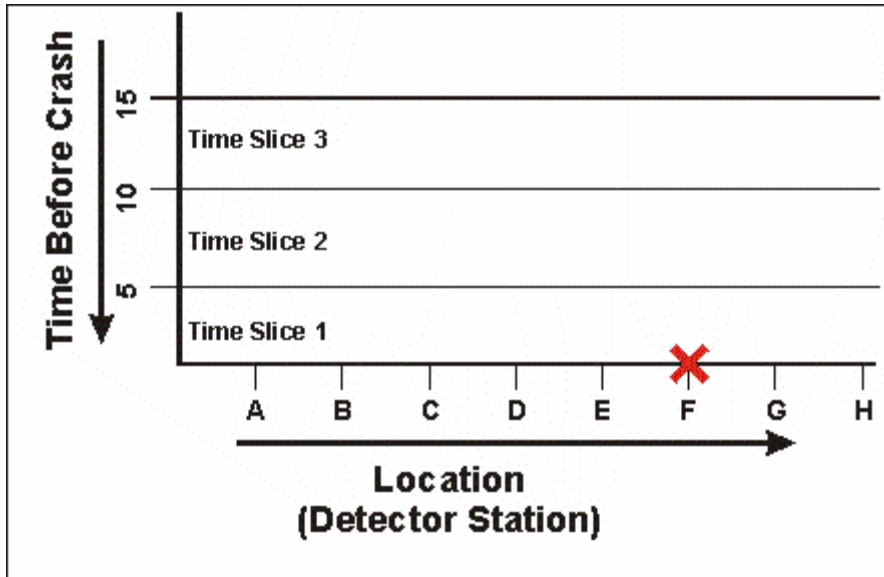
Figure 4-2. Time-Space Diagram Showing Time and Location of Interest

The final number at the end of the variable name refers to the time period over which this value is calculated. The time period used for all variables in this measure of rear-end crash risk is time period 2 which refers to the time 5 to 10 minutes before the time of interest. For reference, time period 1 refers to 0 to 5 minutes before the time of interest. Therefore, based on this coding system, the meaning of any of the loop variables above can be determined. For example, ASD2 refers to the average speed 1 mile upstream of the station of interest, 5 to 10 minutes before the time of interest. Figure 4-3 is provided to summarize the variable nomenclature.

71

SSC2

XXXX

Average or Standard Deviation (A or S) ←

Speed Volume or Occupancy (S, V or O) ←

Station D to H ←

Time Slice 1 to 4 ←
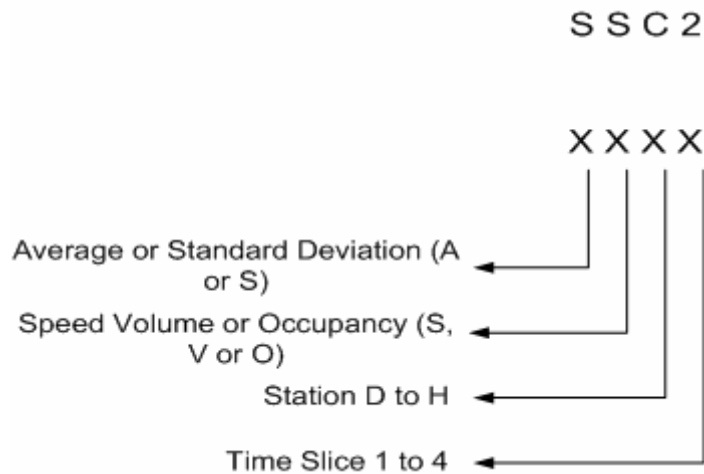
Figure 4-3. Nomenclature of Variables Describing Loop Data

As seen from Figure 4-1, regime 1 conditions are generally lower speed conditions that represent congestion on the freeway. Regime 2 conditions tend to occur at higher speeds and represent un-congested traffic flow. Also, please note that the typical value of "a" for each leaf is not close to 0.50. This shows that the classification tree does a good job of partitioning the data into one of the two traffic regime conditions.

4.2 Crash Frequencies in the Different Regime Conditions

Once the classification tree model was created, the rear-end crash data was sorted into two categories: regime 1 crashes and regime 2 crashes. It was found that 45.8% of all rear-end crashes occur during regime 1 conditions while the remaining 54.2% occurred during regime 2 conditions. Random non-crash data was then subjected to the classification tree and it was determined that regime 1 conditions were only prevalent in 6.3% of the random non-crash data while regime 2 conditions represented the remaining 93.7%. This led to the belief that regime 1 conditions were more risky since nearly 46% of the crashes occurred in situations that were only seen 6% of the time on the freeway. This shows that there is a definite difference between the

72

regime 1 and regime 2 conditions. Initial measures of effectiveness tried to capture this increase in the crash risk during regime 1 conditions.

4.3 Posterior Probability Models

Once the rear-end crashes were grouped into their respective regimes the modeling procedure began. Separate models were created to describe the crash risk in regime 1 and regime 2 conditions since it was likely that these two types of crashes would have different factors associated with the likelihood of a crash. Classification trees were used to identify factors that were significantly associated with rear-end collisions within each respective regime. Factors considered included both on-line factors (loop detector variables describing the currently conditions on the roadway) and off-line data (variables describing location and geometry along the roadway). In the first stage, only loop data taken from the station of the crash was included. However, subsequent analyses included data from three and five loop detector stations around the crash in order to see if this would improve the accuracy of the model. As will be mentioned later, adding loop data from multiple stations was required to improve the accuracy of the regime 2 model.

Once significant factors were determined, models were created using neural networks. A neural network can be described as a parallel-distributed processor that is made up of several independent processing units, or nodes. These nodes are capable of storing data and making it available for use by other nodes. The basic structure for a neural network involves an input layer of nodes, a hidden layer, and an output layer. Each node is connected to other nodes in the previous and following layer and each connection has an interconnection weight. Training the model is the performed by applying the model to a set of data using arbitrary weight values and

continually adjusting the interconnection weights in an effort to minimize the difference between the output provided by the model and the actual output. The most important factor affecting the performance of neural networks is the number of nodes that are used in the hidden layer. The modeling procedure performed by Pande and Abdel-Aty (2006) considered using between 1 and 10 nodes (in 1 node increments) in the hidden layer to determine the best case. For each trial, the output of the model was compared by using a measure to capture the accuracy of the model classification. More information on the model building procedure and the neural network architecture that was used can be found in Pande and Abdel-Aty (2006) and Pande (2005).

The final outcome of this was a model to determine the rear-end crash risk when traffic conditions are within regime 1 conditions and another to determine the crash risk in regime 2 conditions. The rear-end crash risk values that are outputted by each model are actually posterior probabilities that a crash will occur given the inputted traffic and offline factors. A posterior probability of a random event (crash) is the conditional probability of the event occurring taking into account the relevant evidence of the dataset used to create the model. Therefore, the output of the regime 1 model is analogous to the probability that a crash will occur for the inputted conditions given the data used to train the neural network model. Please note that the models describe the rear-end crash risk at a particular location and time use loop data taken 5 to 10 minutes before the particular time of interest. Therefore, if the model is fed continuously with loop data taken in real-time it will essentially describe the crash risk that should be expected on the freeway for the next 5 to 10 minutes. This allows time for crash prevention measures to be implemented if this crash risk measure is used in real-time.

The best model created to determine the posterior probability of a crash during regime 1 conditions contained the following variables:

- AOF2

- CVSF2

- SOF2

- SVF2

- base_milepost

- downstreamon

- upstreamoff

- downstreamoff

Note that the first four variables are variables derived from the loop detector data. The coding of these variables is given above in the previous section. The other four variables are categorical variables describing off-line information about the location in question. These variables describe the location and proximity of the location to ramps along the freeway. A full description of these variables is given in Table 4-1. Of the variables listed previously, the variable that most affects the Regime 1 crash risk is AOF2 (Pande, 2005). Increasing the occupancy at the location of interest serves to increase the probability that a rear-end crash risk occur.

The best regime 2 model created was much more complex. This model used data from the station of interest (Station F) as well as the stations included up to one mile upstream and one mile downstream of the station of interest. The reason for this has to do with the differences between the two traffic regimes. Regime 1 generally represents congested traffic conditions. In these situations, only the station of interest needs to be examined since the traffic flow is moving

very slowly and there is not much of a speed difference between adjacent stations. In such a case the occupancy at the station of interest becomes very important to describing the rear-end crash risk. However, if conditions are not congested (regime 2) then speeds are much higher and factors across multiple stations are needed to assess the risk of a rear-end crash. Such important factors are the speed difference between upstream and downstream locations as well as the speed variance at different stations. Therefore, more variables are needed from a larger area around the station of interest. The variables used in this model are as follows:

- ASD2
- AVD2
- ASE2
- AVE2
- SSE2
- ASF2
- AVF2
- ASG2
- SOG2
- SSG2
- SVG2
- AOH2
- ASH2
- AVH2
- crashtime

- downstreamon

- upstreamoff

- downstreamoff

- base_milepost

- stationf

The variables with the most influence on the Regime 2 crash risk are ASG2 and ASF2. These two variables are the most important because in un-congested conditions the speed differential (faster moving vehicles approaching slower moving vehicles) contributes to the chance of a rear-end crash occurring. In addition to the loop variables described previously, there are several offline variables needed to determine the crash risk. These variables are: the time (crashtime), the milepost of the location being analyzed (base_milepost), the distance from this location to the nearest upstream off-ramp (upstreamoff), nearest downstream on-ramp (downstreamon), nearest downstream off-ramp (downstreamoff), and whether or not the location being analyzed is location upstream or downstream of the nearest loop detector station (stationf). The purpose of these variables is to take into account location and geometry in the model which will allow the crash risk to be compared across locations. The coding of these variables is given below in Table 4-1. The categories that are created for each variable are not random and were obtained by Pande and Abdel-Aty (2006) based on the relationship between each variable and the binary target variable (crash or non-crash).

Table 4-1. List of Categorical Variables Used to Determine Rear-End Crash Risk

CRASHTIME
=0 if Time of crash between midnight to 12:26 AM
=1 if Time of crash between 12:26 AM to 6:46 AM
=2 if Time of crash between 6:46 AM to 7:24 PM
=3 if Time of crash between 7:24 PM to midnight

BASE_MILPOST
=0 if 0<base_milepost<=13.75
=1 if 13.75<base_milepost<=15.96
=2 if 15.96<base_milepost<=25.74
=3 if 25.74<base_milepost<=36.25

DOWNSTREAMON
=0 if nearest downstream on-ramp is located further
than 0.7743 miles
=1 if nearest downstream on-ramp is located within
0.7743 miles

DOWNSTREAMOFF
=0 if nearest downstream off-ramp is located further
than 0.6323 miles
=1 if nearest downstream off-ramp is located within
0.6323 miles

UPSTREAMOFF
=0 if nearest upstream off-ramp is located further than
0.3196 miles
=1 if nearest upstream off-ramp is located within
0.3196 miles

STATIONF
=0 if Loop detector station nearest to crash location is
located upstream
=1 if Loop detector station nearest to crash location is
located downstream

4.4 Problems with Assessing Risk Using Regime 1 and Regime 2 Models

As previously mentioned, two different models were created to assess the posterior

probability of a rear-end crash occurring within regime 1 and regime 2 conditions. However,

one of the major problems with these models it that they are not comparable to each other. The

values outputted by each model would only be comparable to values outputted by the same

model since they are not on the same scale. In other words, the risk of a regime 2 crash

occurring could be determined for two continuous time slices to compare whether or not the crash risk has increased, decreased, or remained the same. However, this assumes that the conditions for the two time slices are both regime 2 conditions. When the traffic conditions change from regime 1 to regime 2 conditions (or vice versa), the values outputted by the models cannot be used to say that the risk in regime 1 is greater or less than regime 2.

Since this shift between traffic conditions occurs mostly during specific times on the real network (only when congested conditions are formed and dissipated, i.e. the beginning and ending of the peak hour) this problem could possibly be neglected in the field since the change would occur for a more or less known period of time. However, the lack of comparability between the two models presents a problem to the simulation. The purpose of the simulation will be to test various ITS strategies and their effects on the crash risk. The strategies tested will change the rear-end crash risk by altering the traffic flow which can (and does) change the traffic conditions from regime 1 to regime 2 and vice versa. It is essential to know how changing the traffic conditions from one regime to another affects the crash risk. If the two models are not comparable, then there is no way of knowing if the implemented procedure is increasing or decreasing the risk of a rear-end crash on the freeway. Therefore, some method must be used to transform the output of the two models into a single measure that can be used to assess the crash risk. Details about the methods considered a given in the following sections.

4.4.1 Method 1

The first method that was considered to make the output of the two models comparable to each other was to apply a scale factor to the value outputted by one of the models and then compare this to the second model. To determine the value of the scale factor, the probability of

observing a crash in each particular traffic condition as well as the probability of observing each particular traffic condition in the field was considered. In general, it was seen that 46% of the rear-end crashes occur during Regime 1 conditions while the remaining 54% occur during Regime 2 conditions. However, using randomly collected traffic data it was observe that Regime 1 conditions are only persistent 6% of the time while Regime 2 conditions are more prevalent and occur in 94% of all traffic cases. Using ratios, Regime 1 conditions are about 13.65 times more risky (on average) than Regime 2 conditions ([0.46 / 0.06] / [0.54 / 0.94]). Therefore, the initial idea was to multiply the Regime 1 risk (R1) by 13.65 and compare it with the Regime 2 risk (R2). Using this method, Equation 7 was used to describe the crash risk:

$$Risk\_1 = \begin{cases} 13.65 * R1 & regime\ 1\ Conditions \\ R2 & regime\ 2\ Conditions \end{cases} \tag{7}$$

The initial thought was that using such a large number would greatly undervalue the importance of the Regime 2 risk. This could have been the case if the output from the models were actual probabilities of crash occurrence within each of the regime. However, the actual output is posterior probabilities which are relative measures of the crash risk and not actual probabilities of crash occurrence. In actuality, using a scale factor of 13.65 did not undervalue the importance of the Regime 2 risk at all due to the scale of the Regime 2 risk vs. the Regime 1 risk. When the values that were outputted by the two models for 10 simulations runs were compared, it was seen that the range of the values outputted by the regime 1 model was extremely different from the range of values outputted by the regime 2 model. Figures 4-4 and 4-5 (below) show the distribution of the outputs from the two models for random traffic

conditions. As can be seen, the output of the regime 1 model lies between 0.0 and 0.015 while the output of the regime 2 model lies between 0.0 and 0.60 making them incomparable to each other.
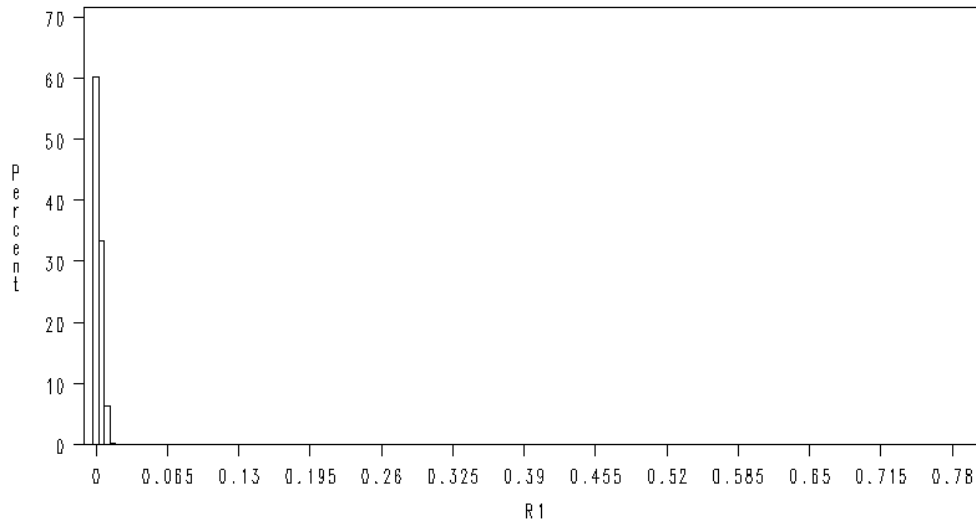
Figure 4-4. Distribution of Regime 1 Model Output
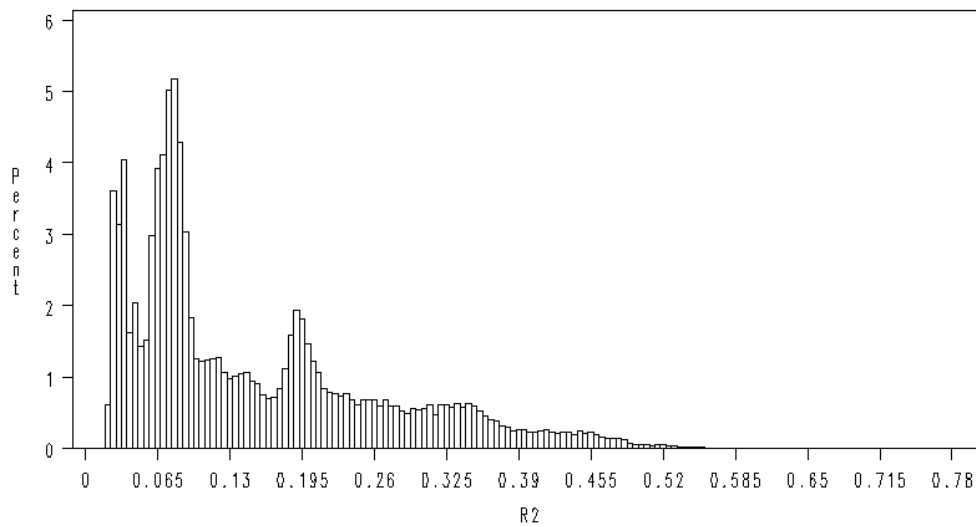
Figure 4-5. Distribution of Regime 2 Model Output

Therefore, applying a scaling factor of 13.65 would only increase the range of the regime 1 risk values to between 0.0 and 0.218. This range is still much smaller than the range of values outputted by the regime 2 model which would mean that regime 2 conditions are more risky than regime 1 conditions. However, since 46% of the crashes occur within regime 1 conditions (6% of the traffic flow) it is expected that the regime 1 risk value would be higher than the regime 2 risk value.

The range of the regime 1 conditions could be artificially increased by applying a larger scale factor. However, the problem still remains of which number to use as the scale factor. Applying too large of a scale factor would overemphasize the importance of the regime 1 risk while applying scale factor that is too small would emphasize the importance of the regime 2 risk. In either case, no other scaling factor is justifiable and since the value of the scale factor is essential to the calculation of the crash risk this method was abandoned.

4.4.2 Method 2

Since such a large number of crashes (46%) occurred during regime 1 conditions, which were typically rare (6% of all non-crash cases), the next method of assessing the rear-end crash risk considered treating all regime 1 conditions as equally risky. This method would assign a single value of the crash risk during regime 1 conditions to represent regime 1 conditions since it would be assumed that all regime 1 conditions are equally undesirable. One problem with this method lies with what value of risk should be assigned to regime 1 conditions. In general, the value of regime 1 risk that is to be selected needs to be higher than any regime 2 risk value (since regime 1 conditions have been shown to be more dangerous than regime 2 conditions). Since the range of regime 2 risk values is between 0.0 and 1.0, selecting a value of 1.0 (upper-bound on the

82

posterior probability) seems the most appropriate. Therefore, the measure called Risk_2 was created (Equation 8).

$$Risk\_2 = \begin{cases} 1 & regime\ 1\ Conditions \\ R2 & regime\ 2\ Conditions \end{cases} \qquad (8)$$

Using this measure would ensure that the regime 1 risk is higher than the regime 2 risk at all times. Therefore, if a crash prevention plan is implemented and the conditions change from regime 1 to regime 2, the risk will always be reduced. However, if the resulting regime 2 risk turns out to be a high value, like 0.91, it would ensure that the improvement that was made is not overestimated.

Note that the value of regime 1 risk chosen should not be influenced by the value of the regime 2 crash-risk value. It was proposed that the equivalent regime 2 rear-end crash risk of regime 1 conditions be equal to the maximum of the rear-end risk during regime 2 conditions. However, this option was ruled out as the maximum would vary for different test cases, loading cases, and starting value seeds. Using 1.0 is independent of the regime 2 risk. It should also be noted that using the value 1.0 does not imply that regime 1 conditions will ALWAYS lead to a crash. Since the probabilities that are determined by the model are posterior probabilities, the value outputted by the crash prediction models give a measure of the crash likelihood – not the probability that it will occur. Therefore, using a value of 1.0 for regime 1 conditions merely implies that regime 1 conditions are always worse from a crash standpoint than regime 2 conditions.

The main problem with this method is that it inherently treats all regime 1 conditions as the same. This essentially ignores the output of the regime 1 crash risk model which has proved that there were indeed different levels of crash risk within the regime 1 conditions. Since the output of the regime 1 crash risk model shows that there is a definite variation in the crash risk during regime 1 conditions, treating all regime 1 conditions as having equal crash risk would be an incorrect assumption. Additionally, this method assumes that regime 1 conditions are ALWAYS more likely to have a crash than regime 2 conditions, regardless of the exact traffic conditions. While it is expected that regime 1 conditions would be more risky on average, it is an incorrect assumption to assume that the lowest regime 1 crash risk value is more risky than the highest regime 2 crash risk value. For these reasons, this method was abandoned.

4.4.3 Method 3

The next method that was tried considered standardizing the output of the two models in order to normalize the scales of the models. A simple standardization procedure that can be used to force the mean of a distribution to be equal to zero and the standard deviation to equal one is to subtract the actual mean from each value and divide this by the actual standard deviation. This is given in Equation 9.

$$Norm\_Risk = \frac{Risk - \overline{Risk}}{\sigma_{Risk}} \tag{9}$$

Using this equation, the risk output from the regime 1 and the regime 2 models were standardized so that they were on the same scale. However, there is still the problem of how to

84

determine the standard deviation and mean of each model's output. The mean and standard deviation of the regime 1 risk could be calculated from traffic situations that are in regime 1 only or all random traffic situations, regardless of if they are regime 1 or regime 2. A case can be made to use both methods to calculate the mean and standard deviation of the crash risk. Therefore, both methods were initially used in different forms to assess the crash risk. The standardized output from the models using only the respective traffic conditions (using only regime 1 conditions to determine the regime 1 risk) is denoted as the first normalized risk (N1) while the standardized output using all random traffic situations is denoted as the second normalized risk (N2). Therefore, the normalized risk values for each model will be denoted as follows: [normalization method]_[risk model]. For example, N1_R1 would represent the output of the regime 1 model normalized using the first method.

The scales of both the R1 and R2 when standardized by the two normalization methods are presented below in Figures 4-6 through 4-9. Please note that the scales of the standardized risk values are now approximately equal.
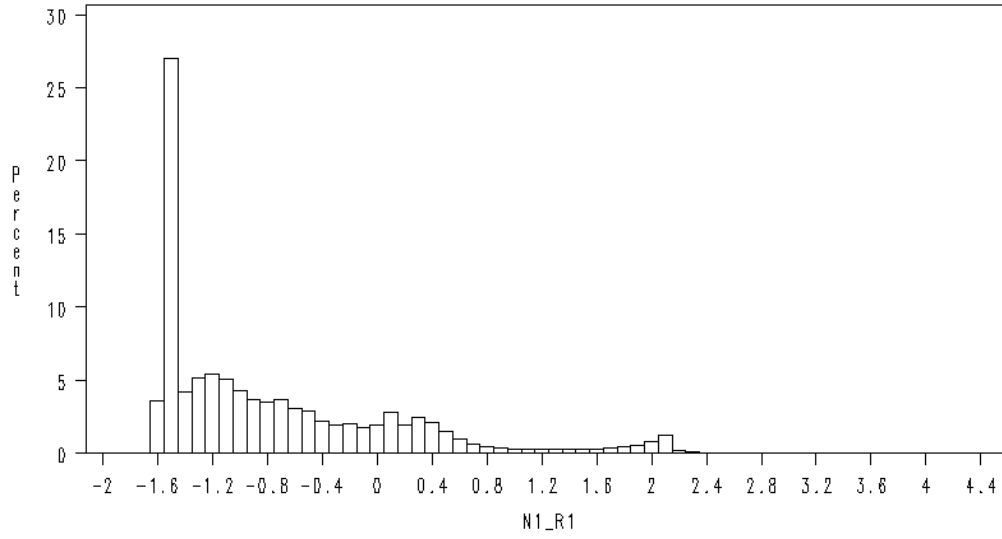
Figure 4-6. Regime 1 Model Normalized by First Method
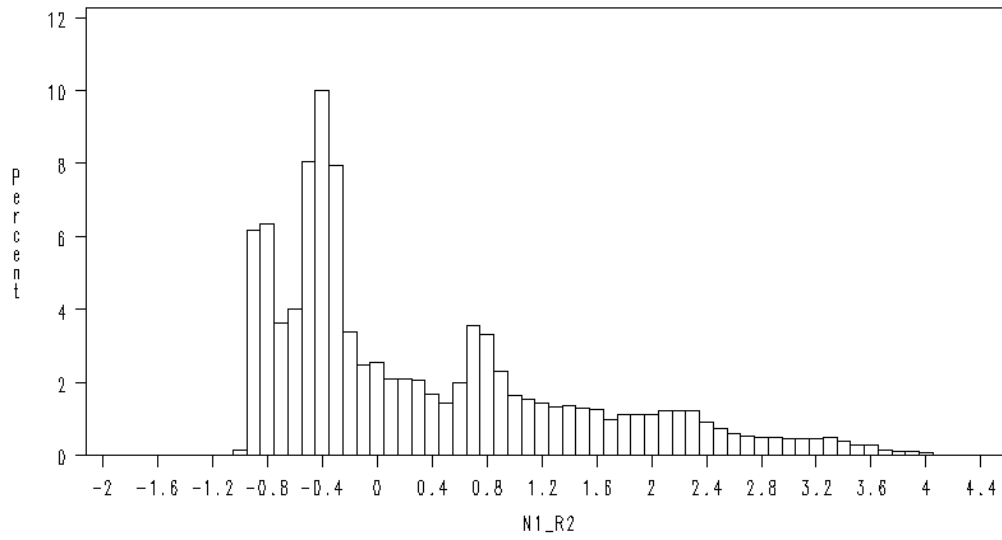
Figure 4-7. Regime 2 Model Normalized by First Method

86
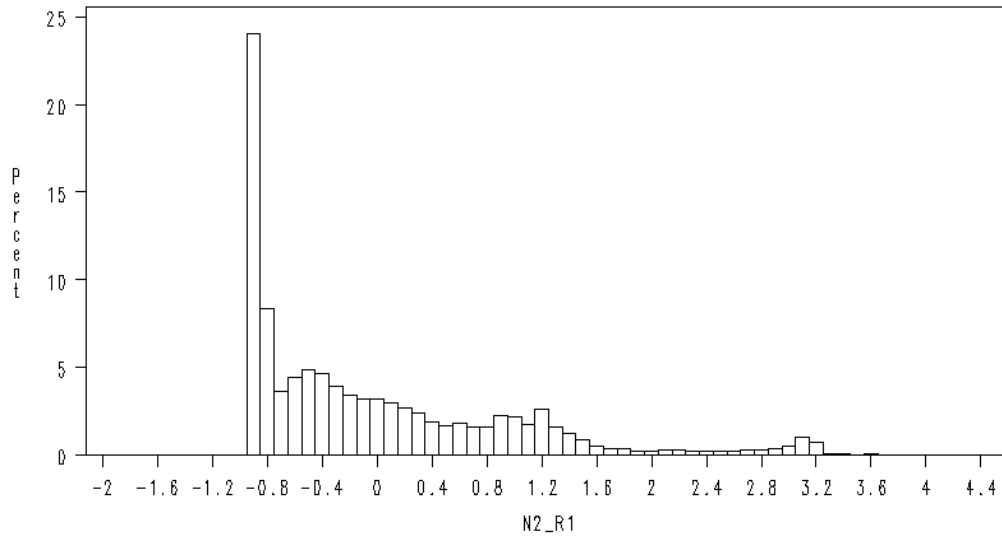
Figure 4-8. Regime 1 Model Normalized by Second Method
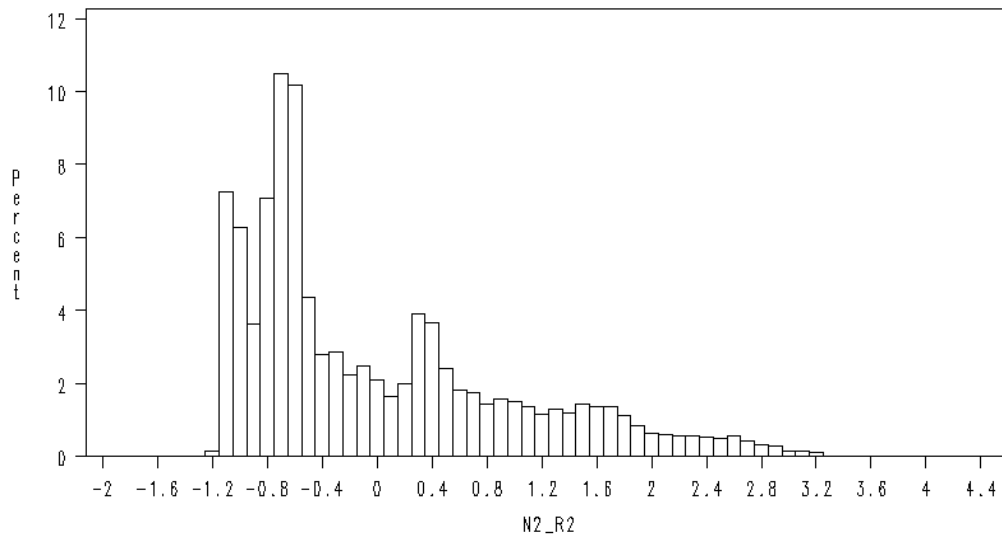
Figure 4-9. Regime 2 Model Normalized by Second Method

Now that there are two standardized risk variables for each model, the next step is to determine a single metric of the crash risk at a certain location and time. One method is to use the normalized risk of a respective regime condition if the traffic conditions fall into that regime.

In this case, the first normalization method would be used since the traffic conditions are already known to be of that regime. Therefore, the equation for Risk_3A is given in Equation 10.

$$Risk\_3A = \begin{cases} N1\_R1 & regime\ 1\ Conditions \\ N1\_R2 & regime\ 2\ Conditions \end{cases} \tag{10}$$

However, this assumes that regime 1 and regime 2 conditions (which are based on the classification tree model described in Figure 4-1) are absolute. In reality, after the classification tree is applied, the result is a probability that the traffic conditions are regime 1 conditions or regime 2 conditions; this probability is labeled as the value a or 1-a, respectively, in Figure 4-1. Therefore, combining this probability into the risk equation would make the measure of crash risk more accurate. Since the output of the regime 1 and regime 2 models are posterior probabilities (the probability of having a regime 1 or regime 2 crash given those conditions), it would make sense to compute a weighted average of the normalized regime 1 risk and the normalized regime 2 risk based on the probability of the traffic conditions being regime 1 or regime 2. Therefore, risk metrics 3B and 3C are defined in Equations 11 and 12, respectively.

$$Risk\_3B = a * (N1\_R1) + (1 - a) * (N1\_R2) \tag{11}$$

$$Risk\_3C = a * (N2\_R1) + (1 - a) * (N2\_R2) \tag{12}$$

Where a = the probability that the traffic conditions are regime 1 conditions and $1 - a$ is the probability that the traffic conditions belong in regime 2. N1_R1, N1_R2, N2_R1, and N2_R2 have been previously defined as the risk models from regime 1 or 2 normalized by the

first or second method. These risk measures (Risk_3B and Risk_3C) are essentially weighted averages of the normalized output from the regime 1 and regime 2 models using the probability that the traffic conditions belong to that specific traffic regime as the weighting factor.

If the probability of a particular traffic condition belonging to regime 1 or regime 2 is used then the second method of crash risk normalization is more applicable since this recognizes that the regime conditions are not absolute. Therefore, Risk_3C is more justified than Risk_3B from a theoretical standpoint. This makes sense since using the weighted average risk measure inherently assumes that the regime of the traffic conditions is not an absolute value but a probability. The first method of normalization (used in Risk_3B) assumes (by normalizing based on values only from within the corresponding regime) that the regime is absolute and, therefore, is not as appropriate as Risk_3C. However, both measures will be compared to determine the final, best metric.

4.4.4 Comparison of Risk Methods

The first step taken to compare the usefulness of the three different risk measures is to compare them visually by graphing the measures for the same situation. Once graphed, the individual values can be compared against one another as well as against what is expected in that situation to determine which measure best represents the data. This was done for different situations to see how the metrics change for different traffic conditions. Figures 4-10 to 4-16 show a plot of the three measures in question (Risk_3A, Risk_3B, and Risk_3C) for various situations. In addition, a line is shown on the plot (regime) that shows whether or not the traffic conditions are of regime 1 or regime 2 to compare the crash risk values between regime 1 and regime 2 conditions.
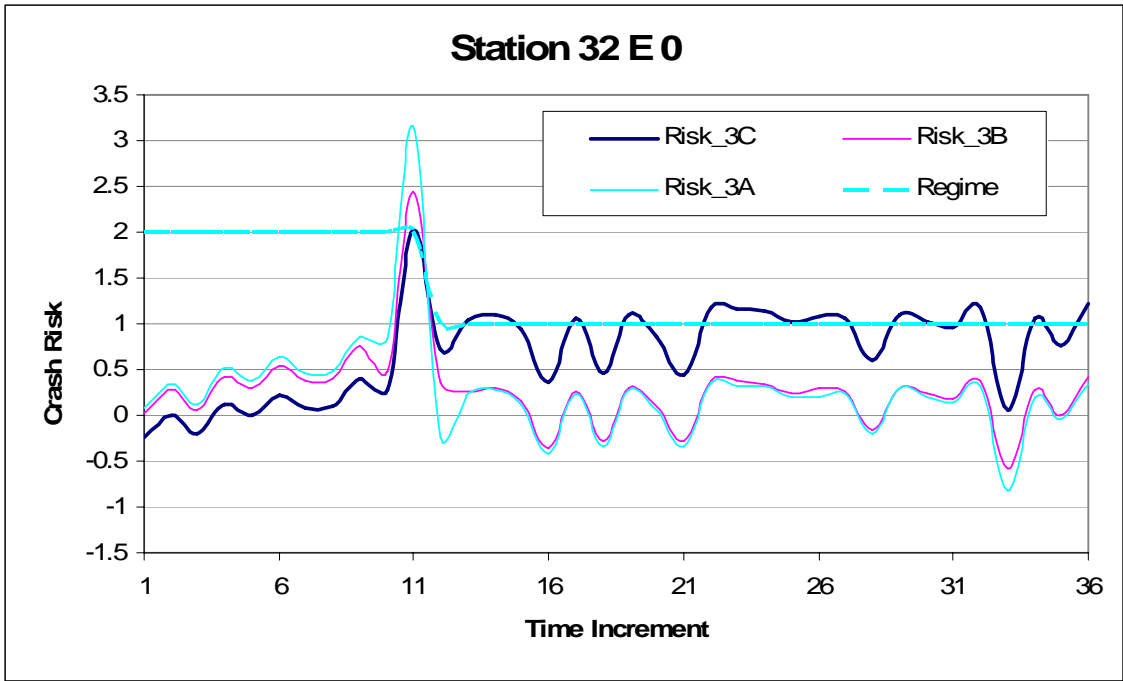
Figure 4-10. Graph of Crash Risk Values at Station 32 E 0
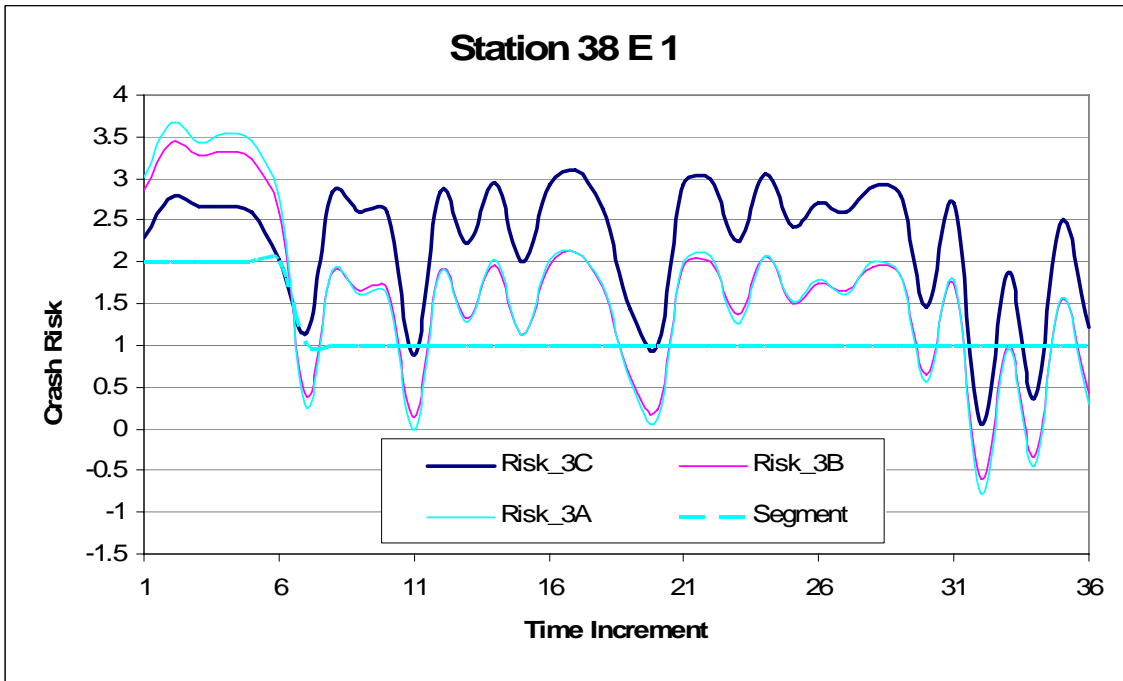
Figure 4-11. Graph of Crash Risk Values at Station 38 E 1
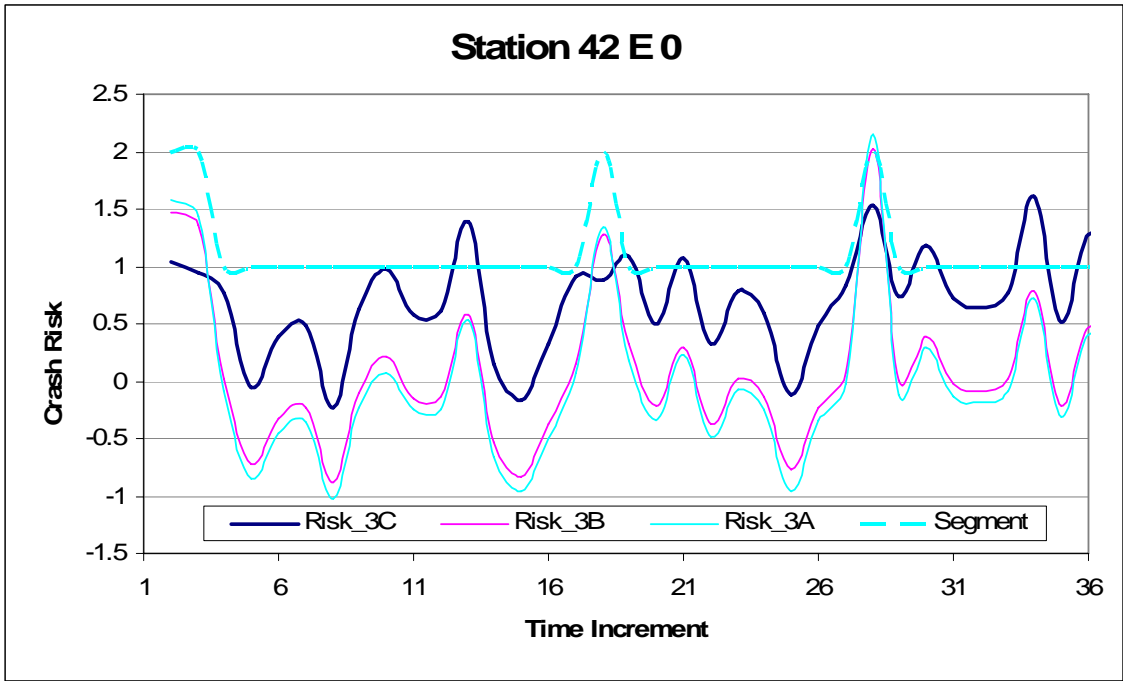
Figure 4-12. Graph of Crash Risk Values at Station 42 E 0
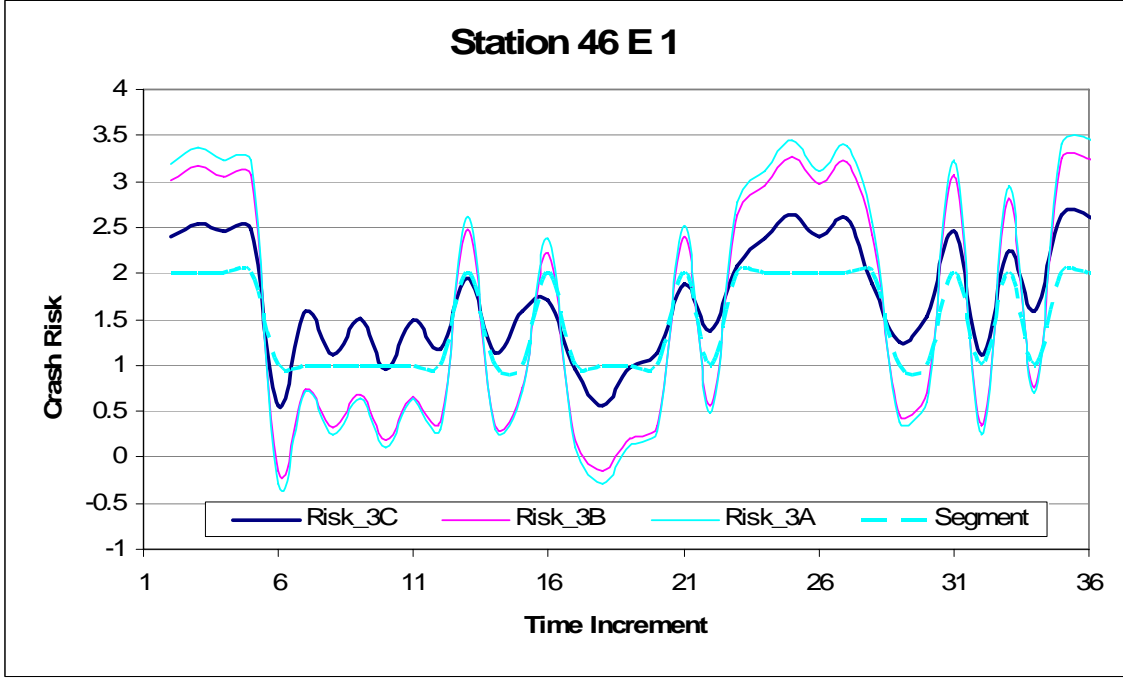
Figure 4-13. Graph of Crash Risk Values at Station 46 E 1
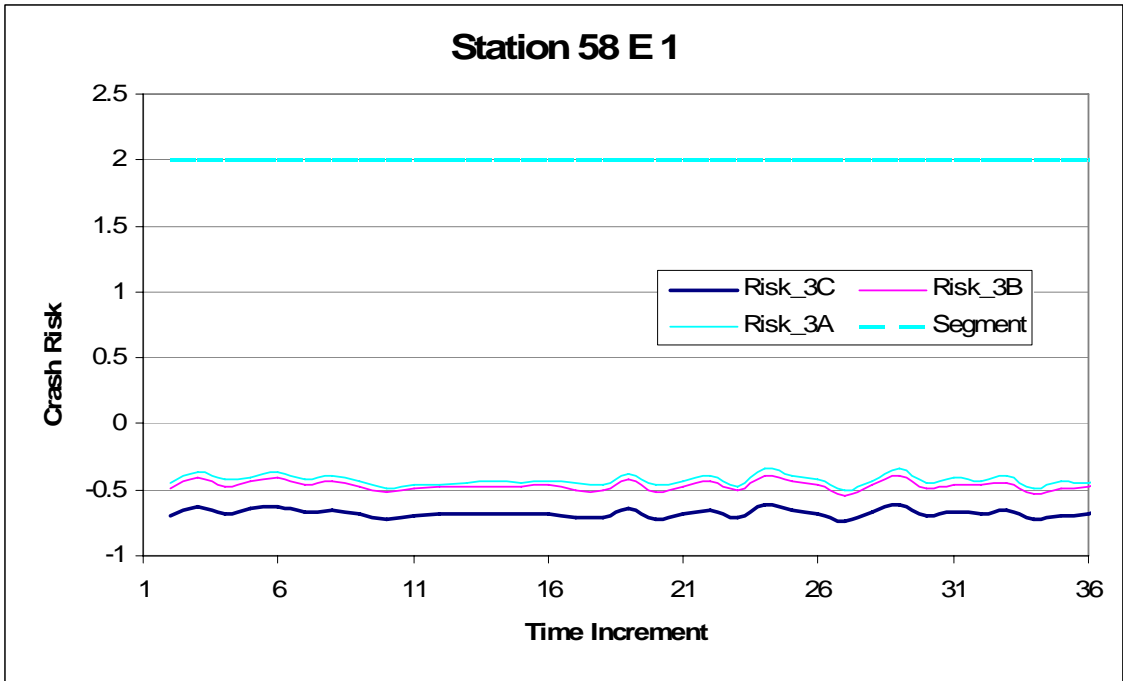
Figure 4-14. Graph of Crash Risk Values at Station 58 E 1
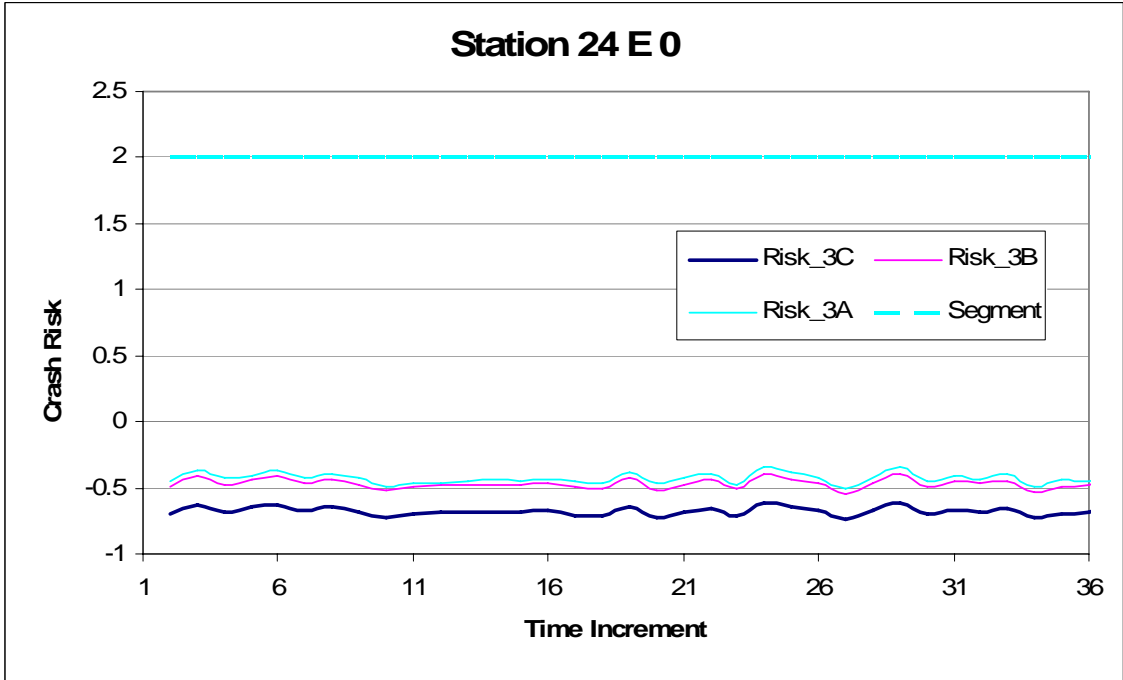
Figure 4-15. Graph of Crash Risk Values at Station 24 E 0

From Figures 4-10 to 4-16, it is seen that the values of Risk_3A and Risk_3B seem to be nearly equivalent. Judging by the equations that define Risk_3A and Risk_3B this only occurs when the value of "a" is close to 0 or 1 (which is most often the case as seen in Figure 4-1). Looking at the trend of values of each risk measure, the average risk values for Risk_3A and Risk_3B are lower when the traffic conditions are regime 1 compared to when traffic conditions are in regime 2. This is the opposite of what is expected to occur. This trend is also apparent at times for Risk_3C. However, there is an important difference in the measure Risk 3A, Risk_3B, and Risk_3C. As shown in the plot of the crash risks at nearly all stations provided, the value of Risk_3C is almost always lower than the value of Risk_3B / Risk_3A during regime 2 conditions and higher during regime 1 conditions. This means that Risk_3C gives higher values during regime 1 conditions and lower values during regime 2 conditions, which is what is expected. Therefore, Risk_3C shows potential to be used as the rear-end crash risk measure.

However, there is still the issue of whether or not Risk_3C provides higher risk values (on average) during regime 1 conditions compared to regime 2 conditions. To test whether or not this is true, the correlation of the risk values is computed with Risk_2 and the regime conditions. The correlation coefficient will give an indication of whether or not two separate measures have the same general trend. Comparing the correlation of Risk_3C with Risk_2 (which has a maximum risk value of 1 during ALL regime 1 conditions) will show whether or not the values of Risk_3C are higher during regime 1 conditions than regime 2 conditions. The correlation matrix between all 5 risk measures and the regime of the traffic conditions are shown below in Table 4-2.

Table 4-2. Correlation of Various Risk Metrics and Regime Conditions

	risk_1	risk_2	risk_3a	risk_3b	risk_3c	regime
risk_1	1.0000	-0.0102	0.9333	0.9071	0.6655	0.2206
risk_2	-0.0102	1.0000	0.2005	0.2903	0.6501	-0.9761
risk_3a	0.9333	0.2005	1.0000	0.9874	0.8599	-0.0142
risk_3b	0.9071	0.2903	0.9874	1.0000	0.9019	-0.1059
risk_3c	0.6655	0.6501	0.8599	0.9019	1.0000	-0.5114
regime	0.2206	-0.9761	-0.0142	-0.1059	-0.5114	1.0000

As shown in Table 4-2, the correlation between Risk_2 and Risk_3C is very high (0.65005) compared to the correlation of Risk_2 with Risk_3A (0.2005) and Risk_3B (0.2903). Additionally, the correlation between Risk_3C and the regime conditions is also high (-0.51140) compared to the correlation of the regime conditions and Risk_3A (-0.0142) and Risk_3B (-0.1059). This implies that Risk_3C shows more clearly a higher value of crash risk for segment 1 conditions. Only Risk_2 has a higher correlation with the regime conditions (-0.9761) and that occurs because for this measure all regime 1 conditions are artificially given the highest value of risk (1.0). Therefore, Risk_3C provides not only the best measure from a practical perspective, but Risk_3C also describes the higher risk during regime 1 conditions better from a statistical perspective as well. Therefore, the measure of rear-end crash risk that will be used for this study will be computed using the method described above for Risk_3C.

4.5 Lane-Change Crash Risk

As previously mentioned, Pande and Abdel-Aty (2006) also created a model to assess the lane changing crash risk along Interstate-4. For this model a lane change crash was assumed to

be all sideswipe crashes and also the angle crashes that occurred on the left most and center lanes along the freeway since these crashes are typically associated with lane changing maneuvers. Lane-changing crashes were not found to occur within different traffic regimes and, therefore, one model was sufficient to assess the lane-change risk for all situations encountered. This makes the lane-change crash risk measure extremely easy to use as no process is needed to relate different risk values (since there is only one model). However, the output of the lane-change crash risk model was normalized by subtracting the mean and dividing by the standard deviation in order to equate the scales of the rear-end and lane-change crash risk. The mean of this new lane-change crash risk measure is now equal to 0.0 and the standard deviation equal to 1.0.

Because lane-changing behavior is dependant upon the traffic characteristics in individual lanes of the freeway, some of the variables used considered occupancy in individual lanes in addition to variables aggregated over the three lanes like in the rear-end model case. Classification trees were used to determine variables that are significantly related to lane changing crashes and a neural network approach was used to create the model. The following variables were found significant to the prediction of lane changing crash risk:

- ASW2

- ASU2

- AOW2

- ADALOU2

- SVW2

- SSW2

The nomenclature used to describe the variables is the same as previously mentioned except for two important differences. First, the variable ADALOU2 is a unique variable that

takes into account the difference in occupancy between adjacent lanes. This variable can be described as in Equation 13.

$$ADALOU2 = \frac{1}{10}\sum_{t=1}^{10} |LO - CO| + |CO - RO| \qquad (13)$$

In this equation LO, CO, and RO represent the lane occupancy in the left, center, and right lane, respectively. The second difference between the naming of the variables in the rear-end models and the lane changing models is the variable that represents the station name. In the lane changing models the station name is represented by U or W which represents the station upstream or downstream of the location of interest, respectively.

4.6 Travel Time

In addition to the measures of rear-end and lane-change crash risk, the travel time will be considered in examining the effects of the various test scenarios performed in this study. The travel time is an important measure to consider due to the potential negative impacts of route diversion and ramp metering on the operational capabilities on the network. Diverting vehicles from entering Interstate-4 at one location and moving them to another downstream location will increase the volume of vehicles using the surface streets. This would not only increase the travel time of the diverted vehicles but the vehicles currently on the surface streets would experience additional delays due to the added volume on the network. Ramp metering will also directly affect travel time by delaying vehicles on the on-ramps before they are allowed to enter the freeway. The travel time that will be used as a measure of effectiveness in this study is the

overall network travel time. This value is given as a standard parameter in the PARAMICS program and is computed by summing the individual travel times for all vehicles on the network. A change in this value will indicate the effects of the ITS strategy on the overall network performance. For this reason, even a modest increase in the travel time of 10% is significant since this would mean that the average travel time for ALL vehicles is increased by this amount. In selecting the best metering algorithm, while preference will be given to strategies that most effectively reduce the crash risk along the freeway, travel time will also be used to determine which strategies are feasible to implement. For this study the maximum allowable increase in the network-wide travel time for any of the scenarios was set at 5%. This is a small enough value that it will not significantly hinder the network users and can be sacrificed to improve the overall safety of the freeway.

4.7 Network Loading Scenarios

During the peak period, the downtown area of Interstate-4 usually operates at a Level of Service F. The simulation represents this as heavy congestion is present during a majority of the simulation runtime in the downtown area. However, this study wishes to test the ITS alternatives at various levels of congestion on the freeway that occurs throughout a typical day. This is desired as implementing route diversion and ramp metering may yield different results at the different loading cases. Therefore, four loading scenarios have been created for testing of the ITS alternatives. These loading scenarios are as follows: 100% loading (heavy congestion), 90% loading (typical congestion), 80% loading (approaching congestion), and 60% loading (free flow conditions). The 90% loading condition is what can be expected on a typical day on I-4 during the peak hour. The 100% loading condition is an extreme condition that occurs when the travel

demand peaks at the same time. Since there are 4 different loading scenarios in this study, the network loading will be the first variable tested in the experimental design for both route diversion and ramp metering.

4.8 Route Diversion Scenarios

The purpose of the first half of the experimental design is to examine the feasibility of route diversion as a real-time crash risk prevention strategy. Additionally, the experimental design is meant to determine the best diversion strategy given the specific diversion routes that are being used. The two unique diversion routes presented in this study are Diversion Route 1 and Diversion Route 2.

4.8.1 Route Diversion 1

The first diversion route has two decision points. The initial decision point (DP-1A) will determine the number of vehicles that divert from their initial ramp entrance. The second decision point will determine which entrance the diverted vehicles will use to re-enter the freeway. Vehicles that do not use the second diversion (DP-1B) will enter the freeway 2 miles downstream of their initial entrance location and enter the freeway on Anderson St. If DP-1B is used, however, these vehicles will enter the freeway 1 mile further downstream at Colonial Drive which increases the length that vehicles were diverted by 50% (see Figure 3-6). Please note that the secondary decision point is contingent upon the first. Only vehicles that have diverted at DP-1A will be available to divert at DP-1B. Therefore, diverting 50% of the vehicles at DP-1B when 60% of the vehicles were diverted initially (% 1A) will result in 30% of the vehicles using the nearer re-entry location and 30% of the vehicles traveling to the further re-entry location.

The variables that will be used in the experimental design to test the feasibility of Route Diversion 1 are: the percentage of vehicles diverted at DP-1A (% 1A), the percentage of vehicles diverted at DP-1B (% 1B), and the network loading. Figure 4-16 represents the levels of each variable that were used in the experimental design. For this study, a factorial design was employed which examined every variable combination in order to determine the best case and trends within each variable. The individual test cases created by the factorial design are shown below in Table 4-3.

Factor 1: Network Loading	**Factor 2:** Percent of Vehicles Diverted from DP-1A	**Factor 3:** Percent of Vehicles Diverted from DP-1B
• 60 Percent • 80 Percent • 90 Percent • 100 Percent	• 20 Percent • 40 Percent • 60 Percent • 80 Percent • 100 Percent	• 0 Percent • 50 Percent • 100 Percent
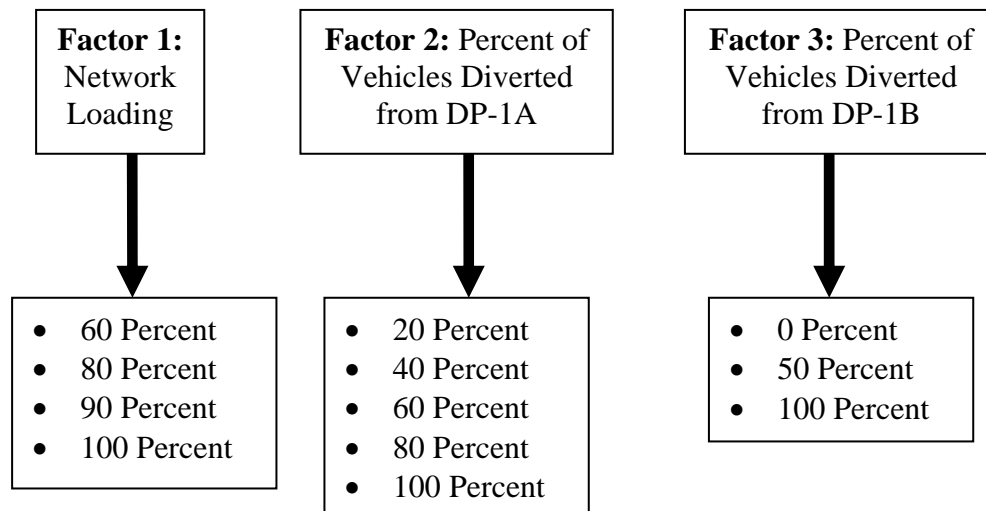
Figure 4-16. Factorial Design for Route Diversion 1

Table 4-3. Test Cases for Route Diversion 1

Case Number	Percent Loading	Percent Vehicles Diverted From DP-1A	Percent Vehicles Diverted From DP-1B
1	60	20	0
2	60	40	0
3	60	60	0
4	60	80	0
5	60	100	0
6	60	20	50
7	60	40	50
8	60	60	50
9	60	80	50
10	60	100	50
11	60	20	100
12	60	40	100
13	60	60	100
14	60	80	100
15	60	100	100
16	80	20	0
17	80	40	0
18	80	60	0
19	80	80	0
20	80	100	0
21	80	20	50
22	80	40	50
23	80	60	50
24	80	80	50
25	80	100	50
26	80	20	100
27	80	40	100
28	80	60	100
29	80	80	100
30	80	100	100
31	90	20	0
32	90	40	0
33	90	60	0
34	90	80	0
35	90	100	0
36	90	20	50
37	90	40	50
38	90	60	50
39	90	80	50
40	90	100	50
41	90	20	100

Case Number	Percent Loading	Percent Vehicles Diverted From DP-1A	Percent Vehicles Diverted From DP-1B
42	90	40	100
43	90	60	100
44	90	80	100
45	90	100	100
46	100	20	0
47	100	40	0
48	100	60	0
49	100	80	0
50	100	100	0
51	100	20	50
52	100	40	50
53	100	60	50
54	100	80	50
55	100	100	50
56	100	20	100
57	100	40	100
58	100	60	100
59	100	80	100
60	100	100	100

4.8.2 Route Diversion 2

A similar factorial experimental design was used to examine the effects of Diversion Route 2. As shown in Figure 3-6, this diversion route is much smaller than the previous route. Diverted vehicles will travel less than 1 mile on the surface streets before re-entering the freeway at Colonial Drive. Because there is only one re-entry location for these diverted vehicles, route diversion 2 contains only a single decision point (DP-2) which controls the number of vehicles that are diverted. This is shown visually in Figure 3-6. Note from this figure that the area of the freeway affected by route diversion 2 is encompassed in the latter half of route diversion 1.

The two variables considered in this section of the experimental design were the network loading and the percentage of vehicles diverted at DP-2. The levels of the factorial design are presented below in Figure 4-17. The individual test cases are also given in Table 4-4.

Factor 1: Network Loading	Factor 2: Percent of Vehicles Diverted from DP-2

- 60 Percent
- 80 Percent
- 90 Percent
- 100 Percent

- 20 Percent
- 40 Percent
- 60 Percent
- 80 Percent
- 100 Percent
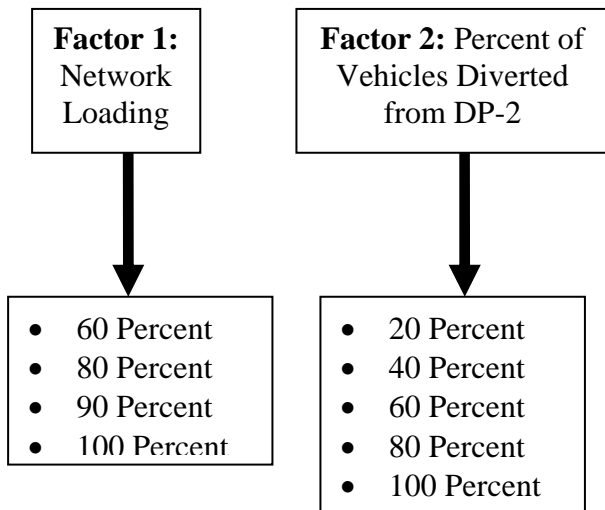
Figure 4-17. Factorial Design for Route Diversion 2

Table 4-4. Test Cases for Route Diversion 2

Case Number	Percent Loading	Percent Vehicles Diverted From DP-2
61	60	20
62	60	40
63	60	60
64	60	80
65	60	100
66	80	20
67	80	40
68	80	60
69	80	80
70	80	100
71	90	20
72	90	40
73	90	60
74	90	80
75	90	100
76	100	20
77	100	40
78	100	60
79	100	80
80	100	100

4.9 Ramp Metering Scenarios

The purpose of the second half of the experimental design is to find the best ramp metering strategy to reduce the crash risk through the downtown Orlando portion of the network. The experimental design will compare the feasibility of using the ALINEA ramp metering strategy and the Zone Algorithm against the no metering case and against each other (Section 4.9.2.1). Additionally, the experimental design will also compare the effectiveness of both the Zone and ALINEA algorithm using the traffic cycle realization and the one-car-per-cycle realization (Section 4.9.2.2). However, the first portion of the experimental design will be completed to confirm the best operational parameters for the ALINEA strategy.

4.9.1 Calibration of ALINEA Parameters

Previous work has been done to examine the effects of using the ALINEA ramp metering strategy to reduce the real-time crash risk on a freeway (Lee et al, 2006; Dhindsa, 2005). However, the calibration parameters for the ALINEA algorithm, such as the critical occupancy and cycle length, differ between the study performed by Dhindsa (2005) and what is expected in the field. Dhindsa (2005) found that using a higher critical occupancy (which would make the algorithm less restrictive) increased the safety benefits which does not make sense as allowing more vehicles onto the network should increase the crash risk. Therefore, a portion of the experimental design must be dedicated to determining the calibration parameters for the ALINEA network. As seen in the ALINEA equation (Equation 3) the following parameters can be altered when using ALINEA: the regulator parameter (K_R) and the critical occupancy (o_c). Additionally, when the traffic-cycle realization is used the cycle length becomes another

103

important factor. Previous work by Dhindsa (2005) as well as studies performed to optimize the operational capabilities of ALINEA (Papageorgiou et al, 1997) has found that the optimal value of the regulator parameter is 70 veh/hr. However, various different cycle lengths and critical occupancy values have been used.

The first portion of the experimental design will implement ALINEA and the traffic-cycle realization using different cycle lengths and critical occupancies to determine the best combination to use to compare against the Zone algorithm. A factorial design was again chosen to test three values of cycle length (30, 45, and 60 seconds) as well as three values of the critical occupancy (0.17, 0.20, and 0.23). The last factor in the factorial design was the network loading level. Since the purpose of ramp metering is to alleviate and eliminate congestion (Jin and Zhang, 2001), it is impractical to implement ramp metering in non-congested situations. Therefore, only two loading levels were deemed appropriate for this analysis – the 90 percent loading and 100 percent loading scenarios. The 60 percent loading and 80 percent loading scenarios were briefly examined outside the experimental design but were found to show no significant crash risk changes as a result of ramp metering. The individual cases in the experimental design are shown below in Table 4-5.

Table 4-5. Test Cases for ALINEA Parameters

Case Number	Percent Loading	Cycle Length	Critical Occupancy
81	100	30	0.17
82	100	30	0.20
83	100	30	0.23
84	100	45	0.17
85	100	45	0.20
86	100	45	0.23
87	100	60	0.17
88	100	60	0.20
89	100	60	0.23
90	90	30	0.17
91	90	30	0.20
92	90	30	0.23
93	90	45	0.17
94	90	45	0.20
95	90	45	0.23
96	90	60	0.17
97	90	60	0.20
98	90	60	0.23

The section of freeway that is metered using ALINEA for this portion of the experimental design is the area immediately upstream of the Interstate-4 / S. R. 408 Interchange. This section includes 3 ramps that are metered and denoted in Figure 4-18 (Section 4.9.3) as Zone 1. Note that even though the ramps are designated as Zone 1 this does not mean that the Zone algorithm is used or the metering algorithm is coordinated. This just means that the ramps that make up Zone 1 will be metered individually in this portion of the experimental design.

4.9.2 Comparison of Ramp Metering Strategies

4.9.2.1 Differences in Zone and ALINEA Algorithms

The ALINEA and Zone ramp metering algorithms were described in detail in Sections 2.3.1 and 3.6.2.1, respectively.   The major differences between the two algorithms are summarized below.

- The ALINEA algorithm considers only the occupancy on the freeway in order to determine the metering rate at a particular ramp. However, the Zone algorithm considers traffic volumes (at on-ramps, off-ramps, and entry and exit points to the zone in question), speeds, and densities. Therefore, the Zone algorithm is more complex and requires more information to be implemented but uses a more complete picture of the traffic flow to determine the metering rate.

- The Zone algorithm requires that the ramps in the freeway be grouped into zones or groups of ramps that will be metered together. This again increases the complexity of the algorithm as a single ramp cannot be metered by itself. However, the ALINEA algorithm can meter single ramps as well as consecutive ramps with ease.

- The ALINEA algorithm is not coordinated and only considers loop information from the nearest detector in order to meter a particular ramp. The algorithm cannot "look ahead" at traffic conditions upstream or downstream to see how to best change the metering rate. On the other hand, the Zone algorithm considers traffic information for the entire zone in order meter any particular ramp.   Therefore, this method is more suited to handle situations with large areas of congestion as the algorithm will recognize these areas and account for it by lowering the metering rate.

- The ALINEA algorithm does not take into account the traffic demand at any on-ramp. Therefore, when using ALINEA a ramp that has a high traffic demand could have a more restrictive metering rate than another ramp that few vehicles use. This would result in unnecessary delays and queues as vehicles that need to enter the freeway are not able to while excessive green time is allowed for ramps that have no traffic demand. This unnecessary restrictiveness actually causes the ALINEA algorithm to perform better from an operational standpoint since fewer vehicles are allowed onto the freeway. The Zone algorithm, on the other hand, accounts for on-ramp demand and proportionally allows for green time based on how many vehicles at each ramp need to enter the freeway.

- Because ALINEA meters ramps individually this algorithm performs better when there is localized congestion. When localized congestion is present, the metering rate near the ramp in question it reduced to allow the congested conditions to dissipate. The Zone algorithm cannot handle these situations as well since the localized congestion at one detector would be just a small part of the larger zone.

Looking at the various differences between the two metering algorithms there is no clear "best" strategy for reducing the rear-end and lane-change crash risk. Each algorithm has its own unique advantages and disadvantages. Therefore, in order to determine which algorithm provides the best safety results they must be compared in the last part of the experimental design to determine the overall best ramp metering strategy.

4.9.2.2 Differences in Traffic-Cycle and One-Car-Per-Cycle Realizations

Both the ALINEA and Zone ramp metering algorithms yield the metering rate in veh/hr for each of the on-ramps that are being metered. Once the metering rate is known, however, the

traffic signals that control the ramp must then reflect that particular metering rate. As mentioned by Papageorgiou et al (1997), there are two methods of implementing the ramp metering strategy – the traffic-cycle realization and the one-car-per-cycle realization.

In the traffic-cycle realization method, after the final metering rate values ($R[t]$ for ALINEA and R_n for Zone) are assigned, the rates must be converted to green time for the ramp meter. The meters used in this study assume a cycle length between 30 and 60 seconds. Assuming a saturation flow rate of the meter of 1900 vehicles per hour (Highway Capacity Manual, 2000), Equation 14 converts the flow rate into green time for the meter (assuming lost time is equal to extension of effective green time). Using this method allows vehicles to enter the freeway in platoons. The average size of the platoon that is allowed to enter the freeway is determined by the cycle length. For equal metering rates, a longer cycle length would mean that larger platoons are allowed to enter the freeway.

$$Green = \frac{rate * cycle\_length}{1900} \qquad (14)$$

For the one-car-per-cycle method, the implementation is slightly different. Once the metering rate is determined, the average cycle length is calculated assuming that only a single vehicle enters the freeway per cycle. From this cycle length, the red-time is determined by assuming a constant green-time for each cycle (2 seconds, enough for one vehicle to utilize the phase). The cycle lengths used range from 2.1 seconds (1714 veh/hr) to a maximum cycle length defined for each ramp that is metered. This maximum cycle length is calculated by determining the minimum metering rate for the respective ramp by using the method mentioned in Section

3.6.2.1 which sets the minimum metering rate to keep average vehicular delay at on-ramps to 4 minutes. When this method is used, platoons of vehicles are prohibited from entering the freeway at once. This reduces the amount of turbulence to the mainline traffic flow caused by vehicles entering the traffic stream from the on-ramps since only one vehicle would have to merge into the traffic stream at a time. However, the drawback to this strategy is reduced operational capabilities as vehicles are delayed at the ramp meters for a longer amount of time. Additionally, when this method is used at less restrictive metering rates vehicles (smaller cycle lengths) vehicles will have extremely small delays at the meters and will enter the freeway almost as quickly as they arrived at the ramp). In other words, the meter will essential not do anything during these situations.

4.9.3 Ramp Metering Scenarios

The major variable in the implementation of the Zone ramp metering algorithm is the zone that is chosen to be metered. Once the zone is chosen, there are no major algorithm variables that can be used to alter the effectiveness of the metering strategy. However, since the traffic-cycle realization is being applied the optimal cycle length is still a factor that needs to be determined. The experimental design will therefore include the varying cycle lengths and three different zones that have been created to explore the effectiveness of the Zone algorithm in downtown Orlando. The three chosen zones are shown in a schematic drawing presented in Figure 4-18.
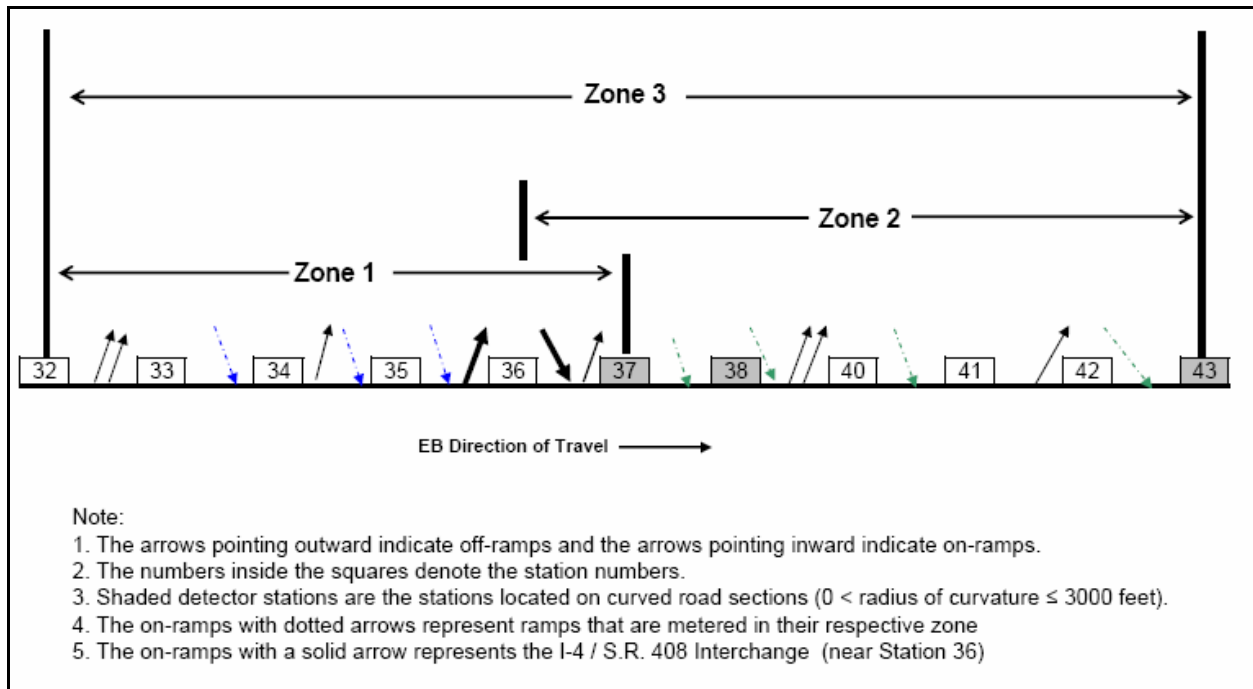
Figure 4-18. Zones Metered for Ramp Metering Strategies

The zones were chosen with the objective of reducing the crash risk in the downtown area around the Interstate-4 / S. R. 408 Interchange. The ramp leading from S. R. 408 to Interstate-4 (located between stations 36 and 37) is included as a non-metered ramp due to the large volumes that use this interchange. Each of the three zones includes this interchange so that the large in-flow volume from this interchange factors into the metering algorithm. The first zone is located just upstream of the interchange and includes the three ramps upstream. The second zone extends downstream from the interchange to incorporate the ramps four downstream. The third zone is the largest zone that incorporates most of the downtown area and is a union of zones 1 and 2.

In the experimental design, each zone was metered using both the Zone and ALINEA algorithms. Although the ALINEA strategy is a localized strategy, the same zones could be metered using ALINEA by simply metering the ramps that encompass the zone individually.

110

For the ALINEA algorithm the calibration parameters from Section 4.9.1 (Table 4-5) were used and the ramps involved in the zone were metered in an uncoordinated fashion. For the Zone algorithm with the traffic-cycle realization, each zone was metered three times with varying cycle lengths. This was done to determine if the cycle length was an important variable in the traffic-cycle realization of the Zone algorithm. Additionally, each zone was metered with the ALINEA and Zone algorithms using the one-car-per-cycle (OCPC) method of allowing vehicles onto the mainline. The full experimental design is listed below. Note this is basically another factorial design with 4 factors. The factors are: loading (90 or 100 percent), Zone (1, 2, or 3), Algorithm (Zone or ALINEA), and cycle properties (30 second, 45 second, 60 second, one-car-per-cycle). However, there is a partial factor in the experimental design as the ALINEA algorithm will only be run with the best cycle length (from Section 4.9.1) and the one-car-per-cycle length.

Table 4-6. Test Cases for Zone and ALINEA Ramp Metering

Case Number	Percent Loading	Metered Zone	Algorithm	Cycle Length
99	100	1	Zone	30
100	100	1	Zone	45
101	100	1	Zone	60
102	100	1	ALINEA	BEST
103	100	1	Zone	OCPC
104	100	1	ALINEA	OCPC
105	100	2	Zone	30
106	100	2	Zone	45
107	100	2	Zone	60
108	100	2	ALINEA	BEST
109	100	2	Zone	OCPC
110	100	2	ALINEA	OCPC
111	100	3	Zone	30
112	100	3	Zone	45
113	100	3	Zone	60
114	100	3	ALINEA	BEST
115	100	3	Zone	OCPC
116	100	3	ALINEA	OCPC
117	90	1	Zone	30
118	90	1	Zone	45
119	90	1	Zone	60
120	90	1	ALINEA	BEST
121	90	1	Zone	OCPC
122	90	1	ALINEA	OCPC
123	90	2	Zone	30
124	90	2	Zone	45
125	90	2	Zone	60
126	90	2	ALINEA	BEST
127	90	2	Zone	OCPC
128	90	2	ALINEA	OCPC
129	90	3	Zone	30
130	90	3	Zone	45
131	90	3	Zone	60
132	90	3	ALINEA	BEST
133	90	3	Zone	OCPC
134	90	3	ALINEA	OCPC

4.10 Number of Simulation Runs

Due to the stochastic nature of the PARAMICS micro-simulation there is a fair amount of variation in-between runs of a specific testing alternative. This variation occurs because each run that is performed is unique. A random number generator is used to assign individual headways, trip departure times, minimum gap acceptance values, etc. for individual vehicles in the network in stochastic fashion. For each run a different random number seed is used which defines the rest of the random numbers used by PARAMICS. Therefore, if two runs are performed with the same seed value the results from PARAMICS will be identical for the two runs. In this study, multiple runs of different seed values were used to ensure that the results that were determined were based on the tested strategy and not an isolated event resulting from behavior due to a particular seed value. Because of this a large number of runs needed to be performed in order to reduce the variation in the crash risk to acceptable levels.

A good rule of thumb in simulation is that a minimum of 30 runs should be performed for each case in order to have a statistically sound experimental design. This requires no calculation of the amount of variation within the data as this number of runs is assumed to be large enough to account for the simulation variance. However, performing this many runs would require an enormous amount of processing time (especially for the macros that are used to summarize the data). Therefore, another method has been used to help reduce the number of runs to be performed. In this method, a group of runs (10 for this study) is performed for all cases. Once completed, the variation of within runs is determined. Using Equation 15 the number of required runs is calculated based on the variation observed in the initial group of runs.

113

$$N \approx \left(KS \Big/ E \right)^2 \qquad\qquad\qquad (15)$$

In this equation, N represents the number of runs required, K is a statistical factor related to the confidence level that is required (K = 1.645 for the 90% confidence level which is used in this study), S is the standard deviation of the data in question, and E is the error that is allowable for the runs. For this study, S was calculated by examining the average crash risk at a particular station across the 10 initial runs. A separate N value was calculated for every station within a group of runs. The station that yielded the highest N value was used to determine the number of runs required for that particular group of test runs. The allowable error was assumed to be 0.100 for the rear-end crash risk; note the rear-end crash risk was used as it generally had more variation than the lane-change crash risk. The value of 0.100 is equivalent to about 2% of the range of the rear-end crash risk values that were observed (-1.0, 3.5).

In all cases, scenarios performed at the 60 percent loading scenario required no further runs to be performed. The majority of other scenarios also required no further runs to be performed. For those test cases that did require additional runs the maximum number that was needed to be done for any particular test case was a total of 20. Note that this is significantly less than 30 runs that are typically used to ensure a good experimental design.

CHAPTER 5.   RESULTS

5.1 Analyzing Simulation Runs

Values of the rear-end and lane-change crash risk were calculated at every time period and location for each of the individual runs performed for each test case using the aforementioned crash risk models. Although a statistically sufficient number of runs were performed for each test case described in Section 4.10, there still is a fair amount of variation of the rear-end and lane-change for a particular time and location between the individual runs of a particular test case. This variation occurs due to the random, stochastic nature of the simulation program and is reflected equally in the field due to the random fluctuations in traffic flow over multiple days. An example of this variation is shown in Figure 5-1 which is a plot of the rear-end crash risk values vs. time for each run at a particular station of a particular scenario (case 25) in the experimental design. Note that the rear-end crash risk values plotted in all subsequent sections is the Risk_3C that is defined in Equation 12. The scale of the rear-end and lane-change crash risk is between -1.0 and 3.5. This occurs because the probabilities obtained from the neural network models are normalized by subtracting the mean and dividing by the standard deviation. Therefore, these crash risk values should be used to compare the risk at different times and locations. A crash risk value of 0.0 would represent crash risk conditions that are equal to the mean crash risk that is experienced while a higher value would show the crash risk is higher than the mean risk of the freeway corridor.

Crash Risk vs. Time (Station 40 E 0)
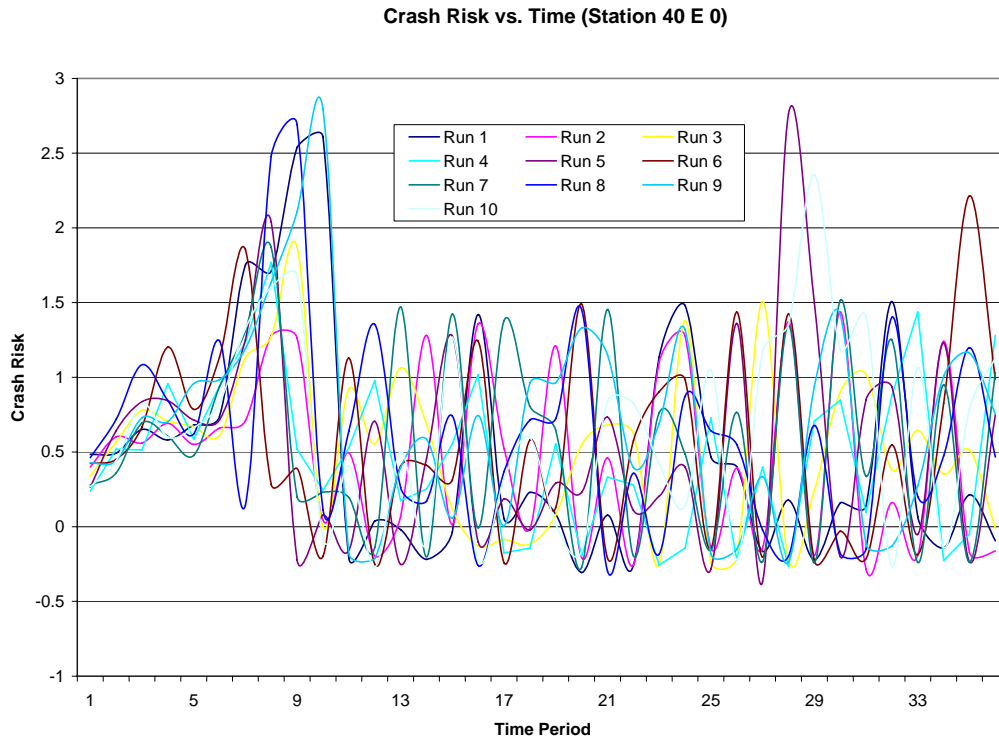
Figure 5-1. Plot of Crash Risk vs. Time at Station 40 E 0 for All Runs in Test Case 25

If the individual crash risk curves for each run were used to compare two different test cases even more crash risk vs. time curves would be required on a single plot than shown on Figure 5-1. If ten runs were performed for each of the two test cases this would mean that 20 curves would be required on a single plot to compare two alternatives. Visually comparing the change in crash risk in this manner would be difficult due to the large number of curves on the plot. Deciphering which of the test cases has a higher or lower crash risk would also be equally challenging. Additionally, these plots would be unreadable due to the large number of curves and would not provide any insights into the trends of the ITS strategies on the different crash risk values along the network corridor. In an effort to eliminate this problem, a single crash risk profile was created for each test scenario for both the rear-end and lane-change crash risk. This

116

single rear-end crash risk profile has a value of the rear-end (or lane-change) crash risk at every station and time that is equal to the average of the rear-end crash risk values at the respective station and time over the number of simulation runs performed at that particular scenario. Equation 16 (below) shows how this average crash risk profile is calculated.

$$(Risk\_profile)_{tl} = \frac{1}{N} \sum_{r=1}^{N} (Risk)_{trl}$$
(16)

Where: $(Risk)_{trl}$ = the crash risk for time t, run r, and location l for particular test case scenario

N = the number of runs required for the particular test case scenario

$(Risk\_profile)_{tl}$ = the crash risk averaged over the number of runs for each location l and time t

Using a single crash risk curve for each scenario is ideal for two main reasons. First, comparing the crash risk between two scenarios would be much simpler since only two lines would have to be compared with each other. Second, averaging the rear-end crash risk over multiple runs should inherently account for the natural variation that occurs due to the different simulation seed values that were used. Comparing this to the field, this should account for that natural fluctuation in speed and flow that are observed over a particular location at the same time on multiple days. A plot of the average rear-end crash risk profile for the scenario shown in Figure 5-1 is given below in Figure 5-2 to show the result of this process.
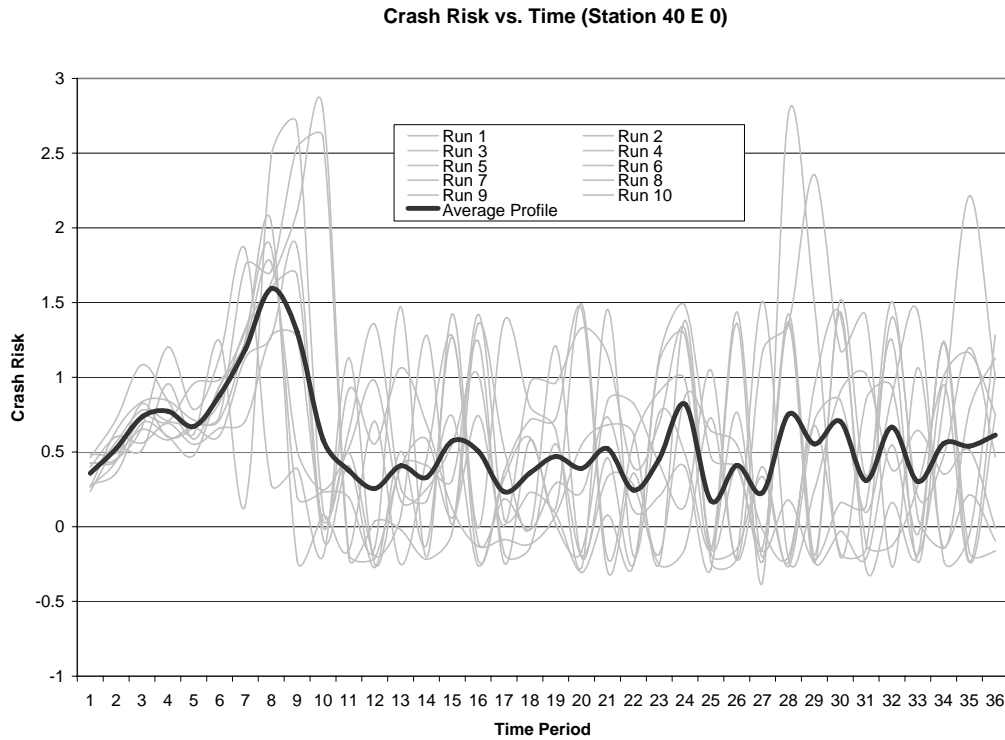
Figure 5-2. Average Crash Risk Profiles Station 40 E 0 for Test Case 25

To compare the change in the crash risk for the various route diversion and ramp metering strategies, two types of graphical comparisons were created. These two methods compare the crash risk across space (location of loop detector stations) and time, respectively. To compare the average crash risk versus location, the average risk at each station was found by computing the average of the crash risk values at individual time periods throughout the 3 hour simulation. Since the both the rear-end and lane-change crash risk are calculated every 5 minutes, this resulted in each station having 36 distinct crash risk values per 3 hour period. The calculation of the average crash risk value for each location is shown more clearly in Equation 17.

$$(Average\_Risk)_l = \frac{1}{T}\sum_{t=1}^{T}(Risk\_profile)_{tl} \tag{17}$$

Where: $(Risk\_profile)_{tl}$ = the crash risk averaged over the number of runs for each location l and time t

T = the total number of time periods that the risk is calculated during the simulation (T = 36 as there are 36 5-minute periods in the 3 hour simulation time)

$(Average\_Risk)_l$ = the crash risk averaged by both time and number of simulation runs at location l

This process was completed for the rear-end crash risk as well as the lane-change crash risk. A typical profile of the rear-end crash risk (for the base case of the 60 percent loading scenario) is shown in Figure 5-3.

Average Crash Risk vs. Location
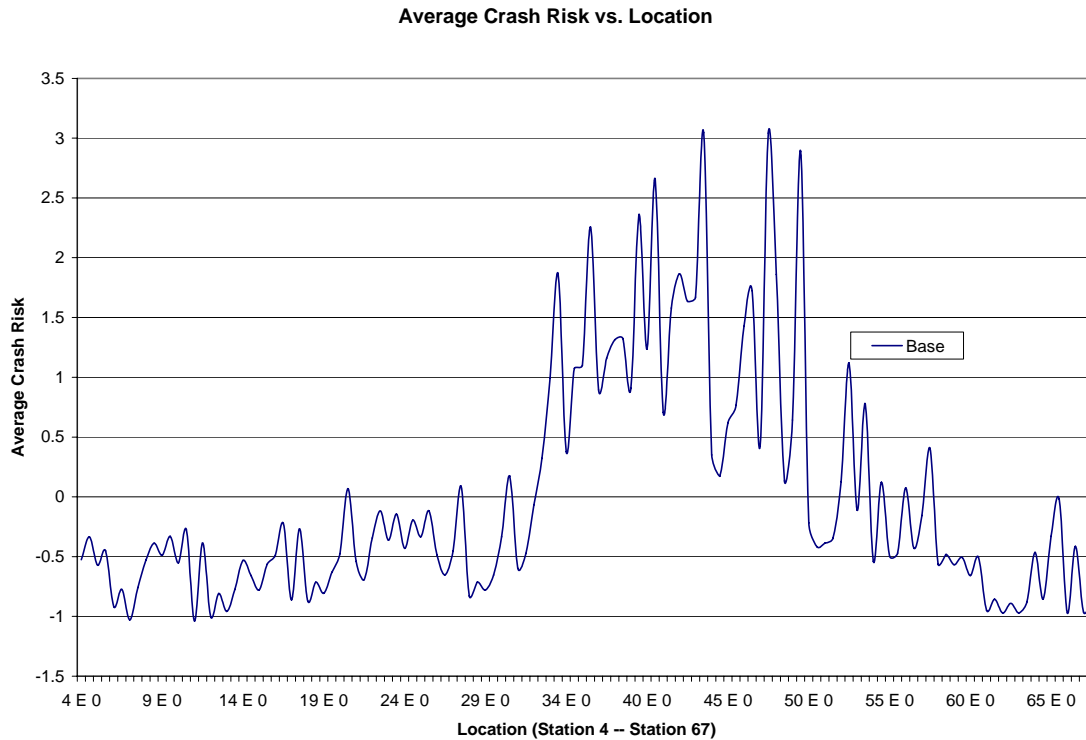
Figure 5-3. Plot of Average Crash Risk vs. Location for 60 Percent Base Scenario

Please note that for each loop detector station two crash risk values are calculated. The first value is calculated for the area immediately upstream of the loop detector station while the second value describes the crash risk downstream of the detector station. In order to denote crash risk both upstream and downstream of each detector the flowing naming convention was adopted. The first number identifies the loop detector station, the following letter represents the direction of the freeway being considered (this study focuses solely on the eastbound direction of travel so this letter is always E) and the last number represents whether the area is upstream or downstream of the loop detector station. The number 0 represents an upstream area while 1 represents a downstream area. Therefore, the location named 42 E 0 represents the area upstream of loop detector station 42 in the eastbound direction. The various plots of the crash

120

risk given do not include the label for the downstream crash risk value due to the limited space on the plots but it should be noted that this value has been calculated and is included on all plots. Also, please note that Station 39 does not exist. Therefore, all plots show Station 38 immediately followed by Station 40.

As shown in Figure 5-3, the plot of average rear-end crash risk versus location shows numerous peaks and valleys where the rear-end crash risk increases or decreases suddenly. The sudden changes in the crash risk value over locations are caused by both the different traffic conditions at the various locations as well as the presence of on-ramps and off-ramps along the freeway. As previously mentioned in Chapter 4, the rear-end and lane-change crash risk values are based on both on-line loop detector data and off-line information about the geometry of the freeway. The occurrence of these ramps greatly affects the value of the crash risk. Therefore, at a particular station the value of the crash risk for the upstream area and downstream area could differ greatly solely because a nearby ramp even though the loop detector data for that single location is identical.

Another type of plot that can be examined is the crash risk vs. time for a particular station. This graph will be used to ensure that the application of a particular crash prevention strategy reduces the crash risk over all (or most) time periods. A sample plot is given below in Figure 5-4 for the base case during the 90 percent loading scenario. As shown below in Figure 4, the rear-end crash risk is calculated every 5-minutes for the length of the 3-hour simulation run. The peaks and valleys in this plot are due solely to the interaction vehicles on the network since the location (in this example, Station 42 E 1) is constant.

Crash Risk vs. Time (Station 42 E 1)
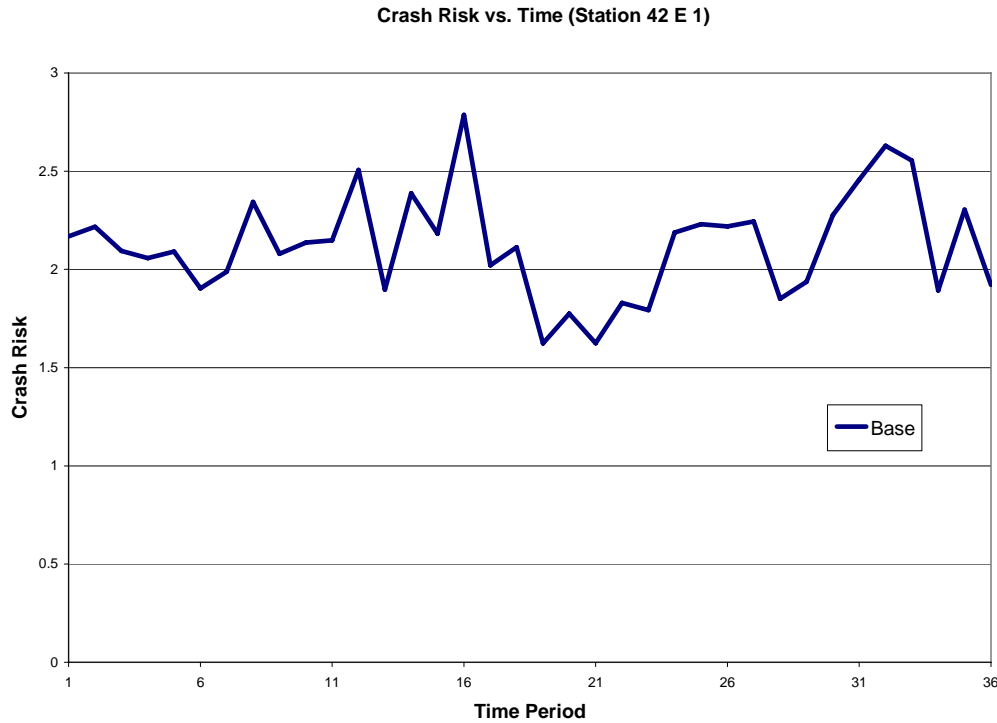
Figure 5-4. Plot of Crash Risk vs. Time for Station 42 E 1 at 90 Percent Base Case

The first type of plot (risk vs. location) will allow for the identification of areas that were affected by the various diversion and metering strategies that will be employed. Once discovered, the value of the change in risk over those individual areas can be determined by comparing the average risk value for that area for the base and test cases. Once this change in risk value is determined, the statistical significance of the change in risk will be calculated using a traditional two sample t-test. The t-test will show whether the change in rear-end or lane-change crash risk is based on the implementation of the crash prevention strategy (it is statistically significant) or random simulation error (not statistically significant).

In addition to quantifying the risk changes at particular locations the overall change in the both the rear-end and lane-change crash risk was calculated throughout the length of the network. This measure, hereafter named the Overall Risk Change Index (ORCI) for the rear-end

crash risk and the Lane-Change Risk Change Index (LCRCI) for the lane-change crash risk, is calculated by summing the differences in the average crash risk between the base case and test case for stations that exhibit a crash risk change. This value will include stations that show both a positive and negative change in the respective crash risk values. Therefore, the values of the ORCI or LCRCI can be either positive or negative which would show an overall improvement or deterioration in the crash risk, respectively. These values can then be used to compare various strategies across a single loading condition to determine which strategy more effectively reduces the respective crash risks. The result is that the strategy with the highest ORCI or LCRCI will yield the greatest overall improvement in rear-end crash risk or lane-change crash risk, respectively, over the study area.

Please note that the percent change in the risk is NOT calculated for the rear-end crash risk. The reason for this is because since the range of the risk values is (-1.5, 3.5) there is a chance that the average risk could be 0.0 for certain stations. This will lead to deceiving results as the percent change would be deceptively high for a station (or group of stations) whose average rear-end crash risk value is about equal to 0.0. When compared to another group of stations, the group with the average rear-end crash risk nearer to 0.0 will always have a much higher percent change in risk even if the change is miniscule. Therefore, in order to avoid this problem, the absolute difference in the rear-end crash risk will be determined and used to compare stations. Since the range of the lane-change crash risk is always greater than zero (0.02 to 0.06) the percent change in the crash risk is a meaningful value.

5.2 Analysis of Route Diversion

5.2.1 First Diversion Route

As previously mentioned in Section 4.8.1, using the 1st diversion route a vehicle can be diverted either 2 or 3 miles downstream of its initial entry ramp at Orange Blossom Trail. This on-ramp typically has a very high volume of about 1020 veh/hr in the peak hour (100 percent loading scenario).   Therefore, it is expected that the effects of route diversion would be readily seen since such a large volume of vehicles can be diverted. Note that the nearer re-entry ramp typical has a volume of about 300 veh/hr while the further re-entry ramp has a much higher volume of about 970 veh/hr. Therefore, diverting too many vehicles to the further on-ramp would increase the volume beyond capacity and would lead to the deterioration of traffic operations on the ramp and surrounding surface streets.

5.2.1.1 60 Percent Loading Scenario

As previously mentioned in the Experimental Design (Section 4.8.1), there were 15 different route diversion cases that were run at the 60 percent loading case. The 15 cases were designed to test the effect of the total amount of vehicles diverted (controlled by DP-1A) as well as where the vehicles are diverted to (controlled by DP-1B). Figure 5-5 shows the average rear-end crash risk vs. location plot for the base case and cases 1 to 5 of the experimental design. Test cases 1 to 5 all have in common that 0% of the diverted vehicles are re-diverted at DP-1B which means that all the diverted vehicles re-enter I-4 at the nearer re-entry location. The cases differ in the percentage of vehicles initially diverted at DP-1A. For example, the line with

reference 20% (1A) means that this line shows the crash risk curve when 20% of the vehicles are diverted from decision point DP-1A.

Average Rear-End Crash Risk vs. Location
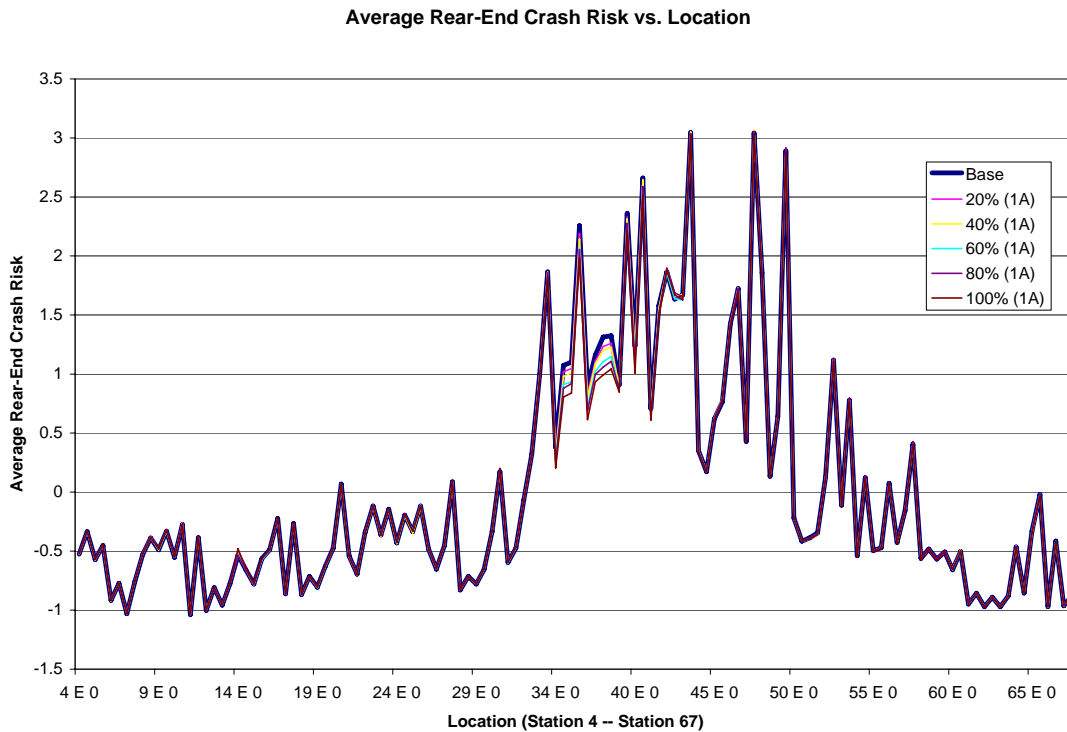
Figure 5-5. Average Rear-End Crash Risk vs. Location for Cases 1 to 5

As shown in Figure 5-5, the area over which the average rear-end crash risk is different for the test cases is rather small compared to the overall network. This makes sense since the route diversion occurs in a localized area and, therefore, should only affect the rear-end crash risk for a very short portion of the freeway. For Diversion Route 1, when vehicles forego the secondary diversion at DP-1B they are diverted from entering just before Station 34 and are instead enter the freeway at Station 38. In Figure 5-5, it appears that this area is encompassed within the area that shows a change in the rear-end crash risk along the freeway. In order to

125

better interpret this plot it is advantageous to zoom in on the portion that shows change in the rear-end crash risk due to the route diversion strategies. This plot is given below in Figure 5-6.

Average Rear-End Crash Risk vs. Location
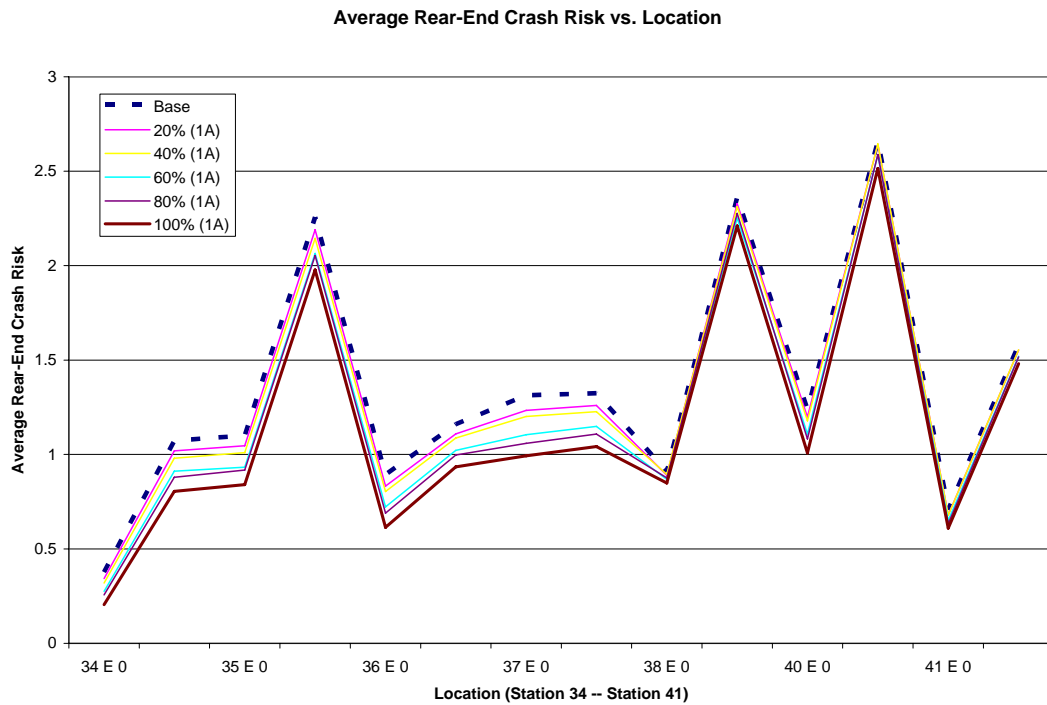
Figure 5-6. Average Rear-End Crash Risk vs. Location for Cases 1 to 5 - Magnified

As shown in Figure 5-6 (above), upon magnification of Figure 5-5 it can be seen that there is indeed a difference between the average rear-end crash risks for the different scenarios. This change in risk occurs between Stations 34 and 41, although the crash risk changes between Stations 39 and 41 are very small. Each line in the plot represents a different percentage of the vehicles diverted (% 1A) from the initial entry location on I-4. As expected, the value of the rear-end crash risk decreases proportionally with the number of vehicles that are diverted. When only 20% of the vehicles are diverted the change is minimal while there is considerable change when 100% of the vehicles are diverted from the ramp. The average rear-end crash risk for each

of the test cases along with the base case is given in Table 5-1. This table also includes the difference in the crash risk between the base case and each of the subsequent test cases. Each of the test cases is described by the case number as well as the type of diversion that was implemented. For example, test case 1 is also denoted as 20% 1A, 0% 1B. This means that for test case 1, 20% of the vehicles were diverted at the initial diversion location (DP-1A) and 0% of the vehicles were diverted at the secondary position (DP-1B).

Table 5-1. Summary of Average Rear-End Crash Risk Change for Cases 1 to 5

	Test Case ID					
	Base	**Case 1**	**Case 2**	**Case 3**	**Case 4**	**Case 5**
	---	**20% 1A** **0% 1B**	**40% 1A** **0% 1B**	**60% 1A** **0% 1B**	**80% 1A** **0% 1B**	**100% 1A** **0% 1B**
Average Crash Risk (Stations 34 to 41)	1.3538	1.3088	1.2880	1.2261	1.2095	1.1486
Crash Risk Benefit	---	0.0450	0.0658	0.1277	0.1444	0.2053
T-Statistic (Benefit Significance)	---	3.7444	5.4070	9.3844	13.3827	18.7122
ORCI	---	0.6305	0.9213	1.7876	2.0213	2.8737

Please note that the amount of change has been calculated as the difference between the average risk values for the base case and scenario case for all stations that show a significant change in risk (Stations 34 to 41). What is also interesting to note is that there is a direct relationship between the amount of vehicles that are diverted and the change in the risk value. In Figure 5-6, this is shown by the fact that the amount of decrease in the rear-end crash risk at each station increases with the number of vehicles that are diverted (% 1A).

Also shown in Table 5-1 is the t-statistic comparing the change in risk between each test case and the base case versus the value zero. This value must be compared to the critical t-statistic value in order to determine whether or not the change in the crash risk is statistically significant. The critical value for a t-test given 18 degrees of freedom and a 90% confidence

127

level is found to be 1.7341. Since the calculated t-statistic for all levels of diversion are greater than this value, the average decrease in the rear-end crash risk for each level of diversion is shown to be statistically significant. This means that diverting any amount of vehicles at the 60 percent loading case will provide significant reductions in the rear-end crash risk between Stations 34 and 41. Additionally, Table 5-1 shows that the average overall reduction in the rear-end crash risk increases with the amount of vehicles that are diverted from DP-1A. This is also reflected in the value of the ORCI which increases with the number of vehicles that have been diverted. As previously mentioned, the ORCI value is calculated by summing the change in the crash risk for all the locations that exhibit a rear-end crash risk difference between the base case and test case.

A similar process has been carried out for cases 6 to 10 (in which 50% of the vehicles are diverted at DP-1B and, therefore, use the further re-entry location while the remaining 50% of the vehicles use the nearer re-entry location) and cases 11 to 15 (in which 100% of the vehicles are diverted at DP-1B and use the further re-entry location). The results of these analyses are presented below in Tables 5-2 and 5-3, respectively.

Table 5-2. Summary of Average Rear-End Crash Risk Change for Cases 6 to 10

	Test Case ID					
	Base	Case 6	Case 7	Case 8	Case 9	Case 10
	---	20% 1A 50% 1B	40% 1A 50% 1B	60% 1A 50% 1B	80% 1A 50% 1B	100% 1A 50% 1B
Average Crash Risk (Stations 34 to 41)	1.354	1.325	1.266	1.217	1.172	1.124
Crash Risk Benefit	---	0.028	0.088	0.136	0.182	0.230
T-Statistic (Benefit Significance)	---	2.567	6.596	13.024	11.852	19.130
ORCI	---	0.397	1.232	1.910	2.550	3.224

Table 5-3. Summary of Average Rear-End Crash Risk Change for Cases 11 to 15

		Test Case ID				
	Base	Case 11	Case 12	Case 13	Case 14	Case 15
	---	20% 1A 100% 1B	40% 1A 10% 1B	60% 1A 100% 1B	80% 1A 100% 1B	100% 1A 100% 1B
Average Crash Risk (Stations 34 to 41)	1.354	1.324	1.261	1.205	1.155	1.092
Crash Risk Benefit	---	0.030	0.093	0.149	0.198	0.262
T-Statistic (Significant of Change)	---	2.165	6.561	9.725	13.506	20.068
ORCI	---	0.418	1.299	2.085	2.777	3.666

Tables 5-2 and 5-3 show trends in the results that are similar to those presented in Table 5-1. The average change in rear-end crash risk for the cases where 50% of the vehicles are diverted at DP-1B (Table 5-2) and the cases where 100% of the vehicles are diverted at DP-1B (Table 5-3) are statistically significant for all levels of diversion. Additionally, the trend that diverting more vehicles leads to a greater reduction in the rear-end crash risk holds for these two groups of cases as well. This means that regardless of where the vehicles are diverted there will always be a safety benefit if vehicles are diverted during the 60 percent loading scenario. However, this still leaves the question of which diversion route is more preferable. When considering Tables 5-1, 5-2, and 5-3 simultaneously, it can bee seen that 1) the safety benefit increases with an increase in the number of vehicles that are diverted and 2) the safety benefit increases with an increase in the number of vehicles diverted to the further re-entry area. This trend can be proved by fitting a simple linear regression equation to determine the value of the ORCI based on the values of % 1A and % 1B. The results of the linear regression analysis, presented in Table 5-4 below, show that both the percentage of vehicles diverted initially (% 1A) and the percentage of vehicles using the secondary diversion (% 1B) are significant to the measurement of safety (ORCI). Additionally, both have a positive coefficient which states the

more vehicles diverted and the more vehicles diverted to the farther re-entry location, the higher

the value of ORCI which means an improved rear-end crash risk situation.

Table 5-4. Linear Regression Analysis for ORCI in Test Cases 1 to 15 (60 Percent Loading)

Parameter	Estimate	Standard Error	t Value	Pr > |t|
Intercept	-0.4016	0.1271	-3.16	0.0082
% 1A	0.0342	0.0017	20.16	<.0001
% 1B	0.0040	0.0012	3.42	0.0051

Please note from Tables 5-1, 5-2, and 5-3 that the area that is affected by the route

diversion during this specific loading condition is the same regardless of the level of % 1B (the

percentage of vehicles using the secondary diversion). This shows that, at the 60 percent loading

scenario, diverting vehicles further downstream has no significant impact on the location of rear-

end crash risk changes along the network for this specific diversion route. Figure 5-7 shows the

location of the rear-end crash risk change along the network graphically for the various levels of

% 1B tested. In this figure, the vertical axis represents location along the freeway with vehicles

traveling downwards. The horizontal axis represents the different values of % 1B tested.

Lighter shaded areas represent locations which realize a decrease in the rear-end crash risk with

respect to the specific implementation of route diversion while darker shaded areas represent

locations that realize an increase in the crash risk. Note that there is no increase in the crash risk

during the 60 percent loading scenarios; therefore no dark areas are shown. Medium shades

represent locations that exhibit no change in the crash risk due to route diversion. These shades

can be seen upstream and downstream of Stations 34 and 41, respectively, in Figure 5-7. The

location at which vehicles are initially diverted from is denoted as a solid horizontal line. The

locations where vehicles are diverted to are denoted as dashed horizontal lines. The nearer re-

entry location is used only in the 0% 1B and 50% 1B case and the further re-entry location is

only used in the 50% 1B and 100% 1B case. Note the 50% 1B case has two dotted lines showing the two re-entry locations that are used in this scenario. This figure will be used to compare with the results realized at higher loading levels.
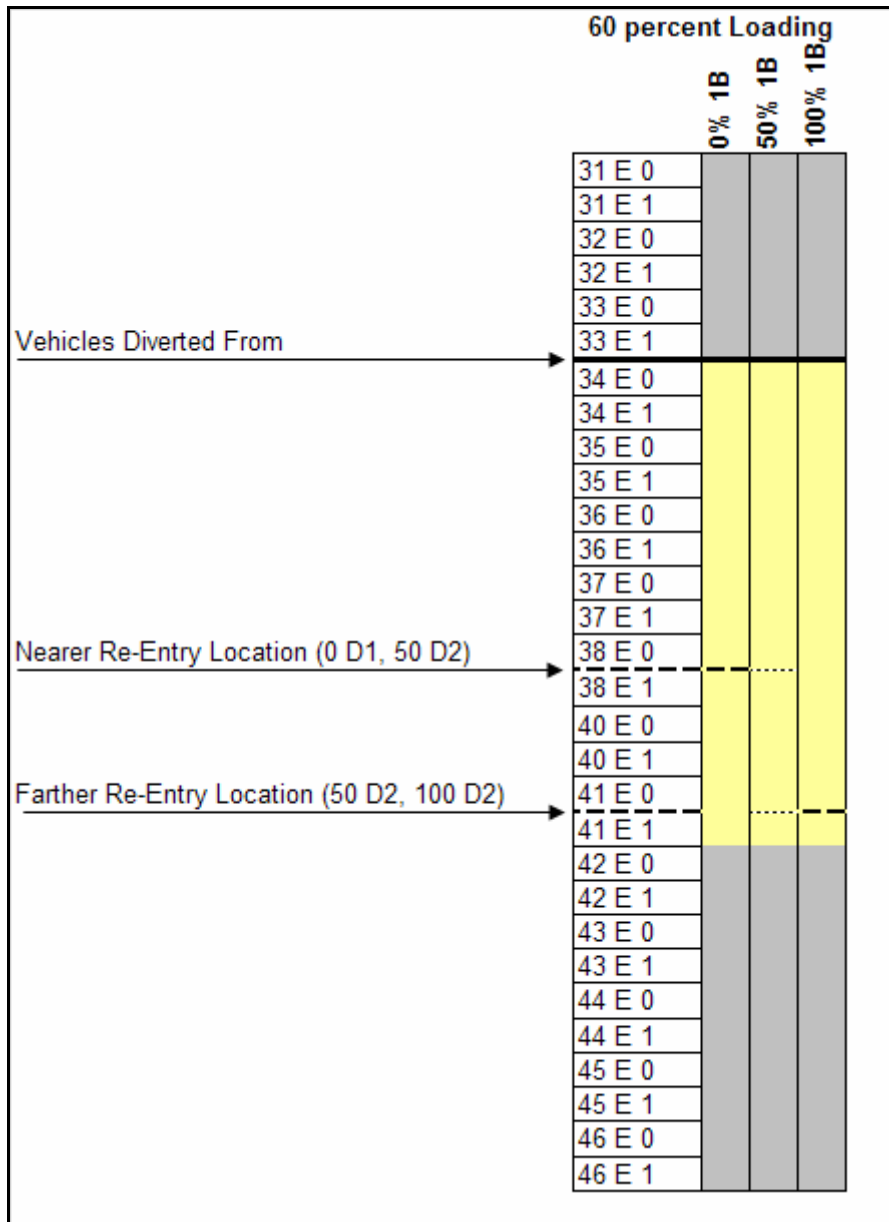
Figure 5-7. Locations Affected by Route Diversion at 60 Percent Loading Scenario

In addition to comparing the average crash risk between the base case and test cases, it is also important to look at the range of the average crash risk values for each run within a particular test case. The size of this range will show how reliable the change in crash risk is for any particular case. Figure 5-8 shows the best test case found for the 60 percent loading scenario (case 15) compared to the base case. In addition, the average crash risk range is given as a 95% confidence interval of the average rear-end crash value based on the individual simulation runs for test case 15. As shown in Figure 5-8, the range given by the 95% confidence interval is very small. Therefore, implementing route diversion in this manner should not induce any particularly high rear-end crash risk values compared to the average.

Average Crash Risk Vs. Location
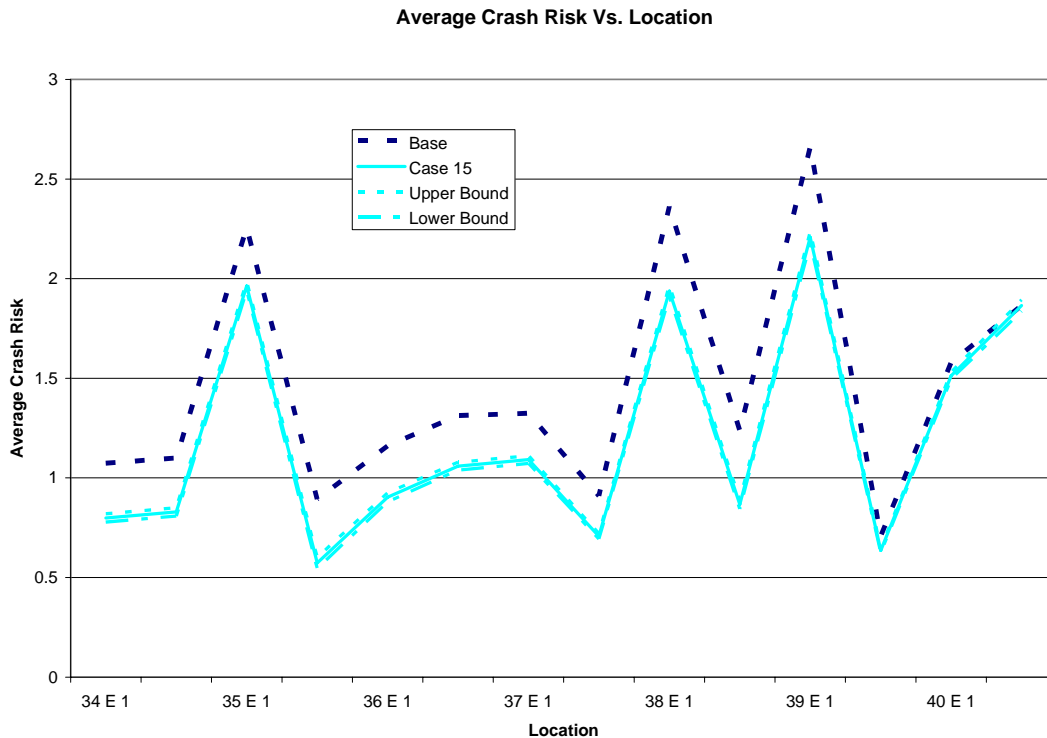
Figure 5-8. Range of Rear-End Crash Risk Values for Case 15

In addition to the average crash risk at every location, it is important to look at the crash risk over time at every location to ensure that the crash risk is reduced in real-time. A typical plot of the rear-end crash risk vs. time is provided below in Figure 5-9 for case 15. As shown, the rear-end crash risk is decreased for every time step during the simulation. This shows the real-time benefit in addition to the overall benefit provided in the previous figures.

Rear-End Crash Risk vs. Time (Station 37 0)
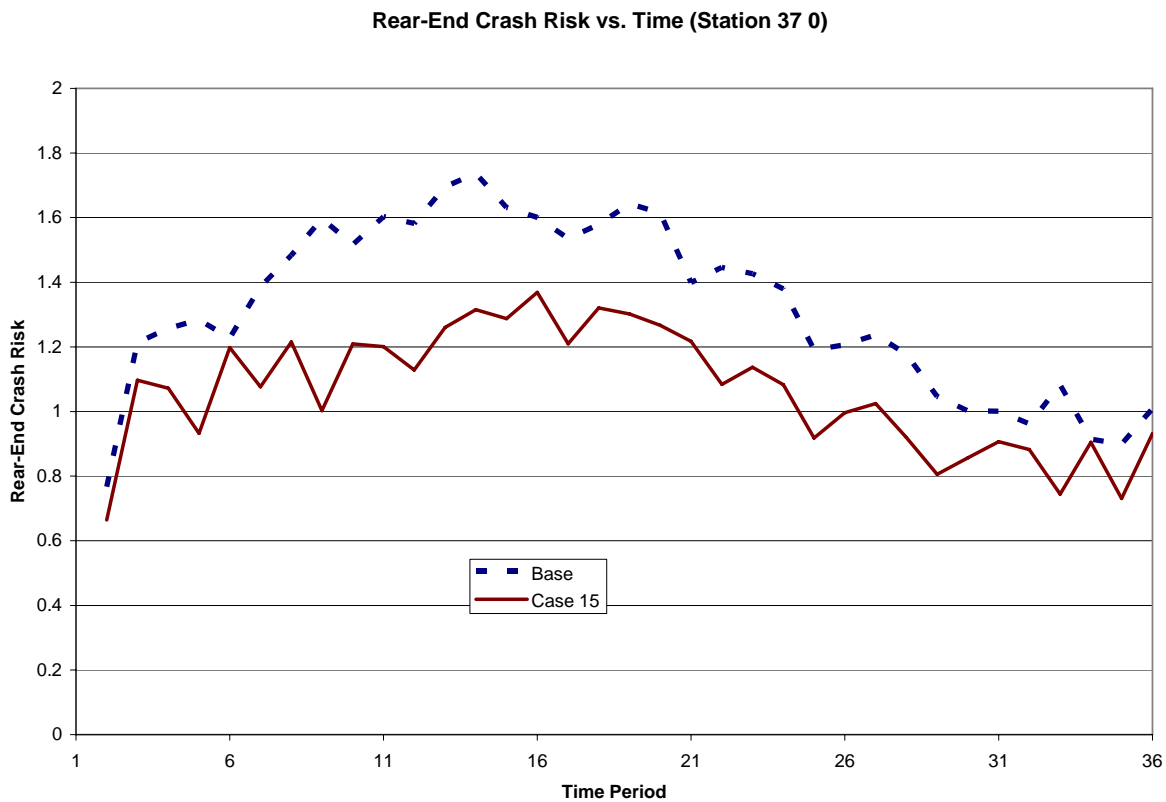
Figure 5-9.   Rear-End Crash Risk vs. Time for Case 15 (Station 37 E 0)

The lane-change risk was also taken into account for these test cases. Figure 5-10 shows the lane change crash risk vs. location for the length of the simulation corridor for experimental cases 1 to 5.

133
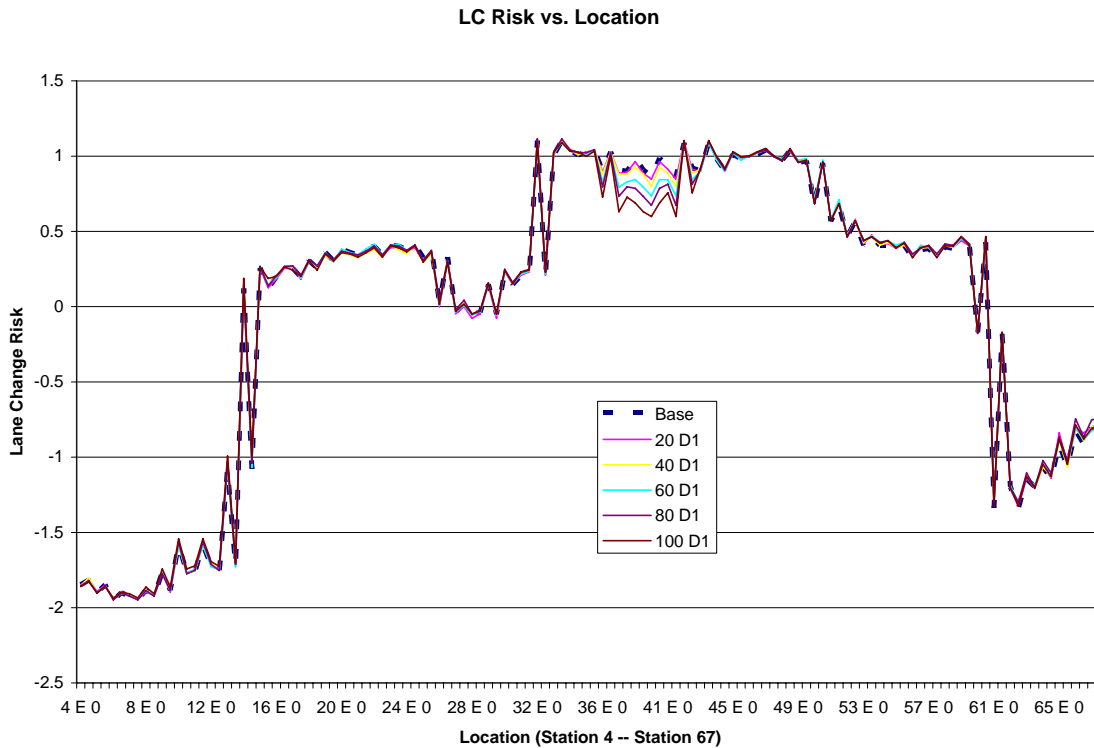
LC Risk vs. Location

Figure 5-10. Average Lane-Change Crash Risk vs. Location for Cases 1 to 5 (20 % 1A to 100 % 1A, 0 % 1B)

This plot looks very similar to the corresponding rear-end crash plot for these test cases (Figure 5-5). As noticed, only a small area of the freeway is affected by the implementation of route diversion with respect to the lane-change crash risk. This area is magnified in Figure 5-11.
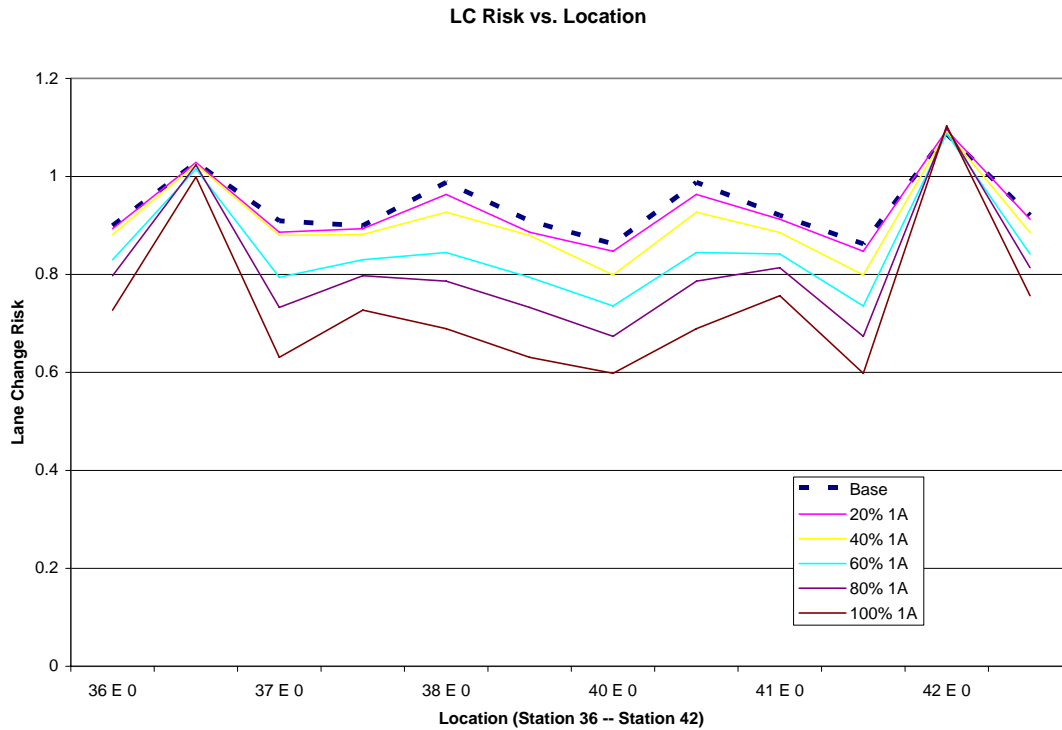
LC Risk vs. Location

Figure 5-11. Average Lane-Change Crash Risk vs. Location for Cases 1 to 5 - Magnified

Figure 5-11 shows the same gradual trend in the reduction of the lane change crash risk as the number the diverted vehicles increase that was seen in the plot for the rear-end crash risk. Table 5-5 is a numeric summary of the change of the lane change crash risk with the number of vehicles that are diverted for test cases 1 to 5. The values of % 1A and % 1B shown in this table are defined the same as given in Tables 5-1, 5-2, and 5-3 regarding the rear-end crash risk. A measure similar to the ORCI is calculated to quantify the benefits of each test case using the lane-change risk value. This is called the Lane Change Risk Change Index (LCRCI). Note also that the crash risk benefit is calculated as a percentage for the lane change crash risk. This is allowed since the range of the lane change crash risk value does not include 0.0. Additionally, please note that the values of the LCRCI are very small compared to the ORCI. This is due to

135

the scale of the lane changing risk which is only 0.02 to 0.06 while the rear-end crash risk value

has a scale of about -1 to 3.5.

Table 5-5. Summary of Average Lane-Change Crash Risk Change for Cases 1 to 5

	Test Case ID					
	Base	Case 1	Case 2	Case 3	Case 4	Case 5
	---	20% 1A 0% 1B	40% 1A 0% 1B	60% 1A 0% 1B	80% 1A 0% 1B	100% 1A 0% 1B
Average Crash Risk (Stations 36 to 42)	0.9395	0.9274	0.9050	0.8495	0.8108	0.7421
Crash Risk Benefit	---	0.0121	0.0345	0.0900	0.1287	0.1974
T-Statistic (Benefit Significance)	---	1.7950	4.8340	10.7082	14.6298	27.4801
LCRCI	---	0.1453	0.4137	1.0798	1.5440	2.3687

The numeric summary for the 50% 1B cases and 100% 1B cases are given in Tables 5-6

and 5-7, respectively.

Table 5-6. Summary of Average Lane-Change Crash Risk Change for Cases 6 to 10

	Test Case ID					
	Base	Case 6	Case 7	Case 8	Case 9	Case 10
	---	20% 1A 50% 1B	40% 1A 50% 1B	60% 1A 50% 1B	80% 1A 50% 1B	100% 1A 50% 1B
Average Crash Risk (Stations 36 to 42)	0.9395	0.9266	0.9075	0.8676	0.8289	0.7720
Crash Risk Benefit	---	0.0129	0.0320	0.0719	0.1106	0.1675
T-Statistic (Benefit Significance)	---	1.5796	3.5120	11.4692	13.7860	18.1482
LCRCI	---	0.1549	0.3844	0.8631	1.3271	2.0104

Table 5-7. Summary of Average Lane-Change Crash Risk Change for Cases 11 to 15

	Test Case ID					
	Base	Case 11	Case 12	Case 13	Case 14	Case 15
	---	20% 1A 100% 1B	40% 1A 100% 1B	60% 1A 100% 1B	80% 1A 100% 1B	100% 1A 100% 1B
Average Crash Risk (Stations 36 to 42)	0.9395	0.9252	0.9059	0.8686	0.8400	0.7928
Crash Risk Benefit	---	0.0143	0.0336	0.0709	0.0995	0.1467
T-Statistic (Benefit Significance)	---	2.1469	4.5328	8.2624	13.6808	18.2020
LCRCI	---	0.1713	0.4029	0.8503	1.1939	1.7599

For all cases (1 to 15) the general trend is that the crash risk benefits increase as the number of vehicles diverted increases. The change in the crash risk is also statistically significant in all cases which shows that the impact is statistically sound. What is interesting, however, is that the greatest benefit in the lane change crash risk is realized when vehicles are diverted to the nearer re-entry location (0% 1B). This opposes what is seen for the rear-end crash risk value which is minimized when vehicles are diverted further away. This is shown more clearly in the linear regression equation that is fit for this data which relates the LCRCI with % 1A and % 1B (percent of vehicles diverted at the respective diversion location). As shown in Table 5-8, the positive coefficient of the % 1A variable indicates that the LCRCI increases with the percentage of vehicles that are diverted while the negative coefficient of the % 1B variable means that the overall lane-change crash risk decreases as vehicles are diverted further downstream. One of the reasons for this could be the fact that the further re-entry location has a much higher original on-ramp volume than the nearer re-entry location. Therefore, diverting vehicles to the further re-entry location will increase the occupancy of the right most lane in the loop detectors near the on-ramp. Increasing this occupancy increases the

lane-change crash risk since the occupancy in each individual lane is an important factor in the model.

Table 5-8. Linear Regression Analysis for LCRCI in Test Cases 1 to 15 (60 Percent Loading)

Parameter	Estimate	Standard Error	t Value	Pr > |t|
Intercept	-0.3246	0.1089	-2.98	0.0115
% 1A	0.0237	0.0015	16.26	<.0001
% 1B	-0.0023	0.0010	-2.33	0.0383

5.2.1.1.1 Travel Time Analysis

Based on crash risk (rear-end and lane-change) results it is easy to say that if route diversion is being used then 100% of the vehicles should always be diverted (100% 1A) since this produces the maximum benefit in the crash risk index. However, there is an added negative effect to implementing route diversion. As vehicles are diverted from the freeway to the surface streets it is expected that the travel time would be greater as 1) vehicles would have to travel a further distance to re-enter Interstate-4, 2) the speed limit is much lower on the surface streets than the freeway, and 3) the additional traffic volume and presence of signals along the surface streets would increase congestion and cause more delays. Therefore, in addition to a plot of the change in crash risk for each test scenario, a plot of the average travel time versus the percentage of vehicles diverted has been created for cases 1 to 15 and is shown below in Figure 5-12. As can be seen, the data has been fit to three quadratic regression curves – one for each level of % 1B – to help explain the results. The R^2 values for the 0% 1B, 50% 1B, and 100% 1B curves are 0.9695, 0.8539, and 0.9189, respectively, which shows that the models provide a good fit of the data. The curves have been created to see if the change in the travel time can be predicted with a reasonable accuracy at other diversion levels. If the curve has a good fit, this will help to

determine the maximum amount of diversion that is allowed without an unreasonable increase in the overall network travel time.

Travel Time vs. Percent Vehicles Diverted from DP-1A
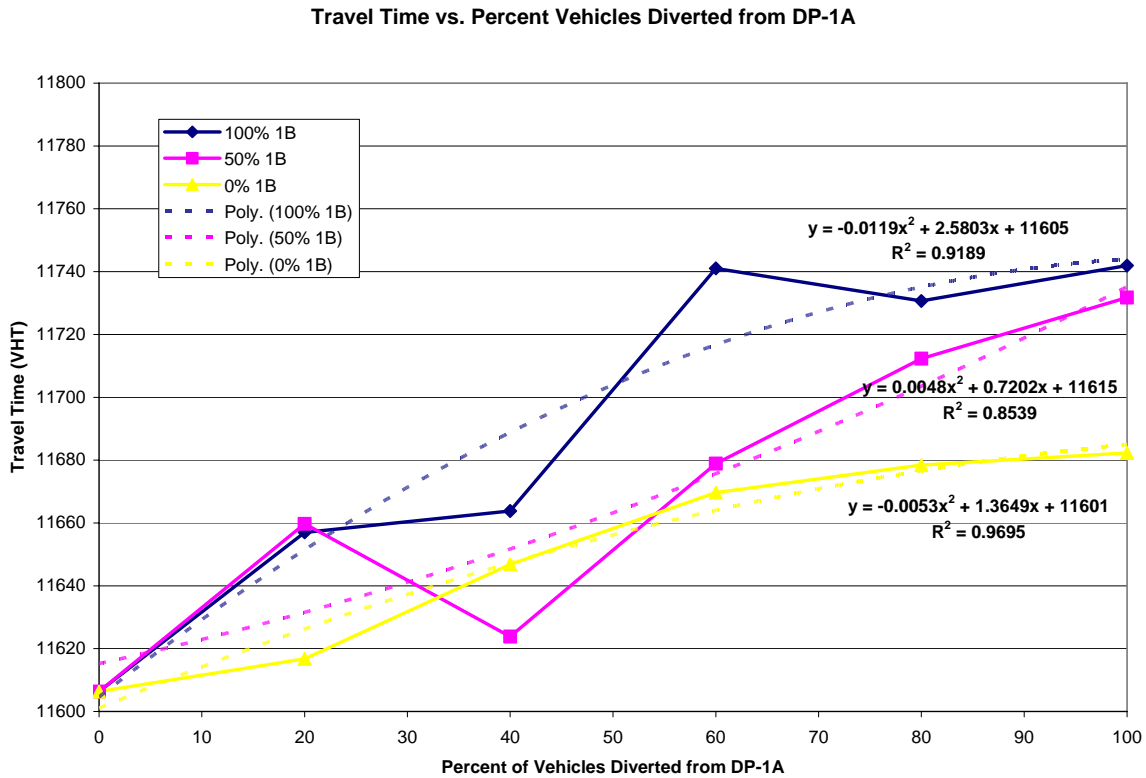
Figure 5-12. Travel Time Plot for Cases 1 to 15

As shown in the plot, the travel time and the number of vehicles that are diverted have a direct relationship. However, the maximum increase in the travel time – realized by diverting 100% of the vehicles from % 1A – is only 1.2%. Since this is a rather small increase it is safe to conclude that at the 60 percent loading scenario the maximum number of vehicles should be diverted to help reduce the crash risk the most. Please note that this travel time increase includes the change in travel time for the freeway traffic as well as traffic on the surface streets which increases due to the route diversion.

139

5.2.1.2 80 Percent Loading Scenario

A similar analysis was performed for test cases 16 to 30 in the experiment design. These test cases contained the same diversion parameters (% 1A and % 1B) as cases 1 to 15 except considered the 80 percent loading scenario instead of the 60 percent loading scenario. However, there were two important differences between the scenarios performed at 60 percent loading and those performed at 80 percent loading. First, both a decrease and increase in the rear-end crash risk was noted due to the implementation of route diversion. This is significant as it shows that there is the potential for crash migration – the decreasing of rear-end crash risk at one location coupled with a simultaneous increase in rear-end crash risk at another location – due to the 1st diversion route. The second important difference is that the stations affected by the route diversion were different depending on the amount of vehicles using the secondary diversion. This is an important point as it shows that in addition to examining the magnitude of the risk change (whether positive or negative) the location of the risk change must also be assessed. The magnified plots of the average rear-end crash risk vs. location for the cases 16 to 20 (0% of vehicles using DP-1B) is presented in Figure 5-13. The plots for cases 21 to 25 (50% of the vehicles using DP-1B) and cases 26 to 30 (100% of the vehicles using DP-1B) were very similar to Figure 5-13 and are not shown.

Average Rear-End Crash Risk vs. Location
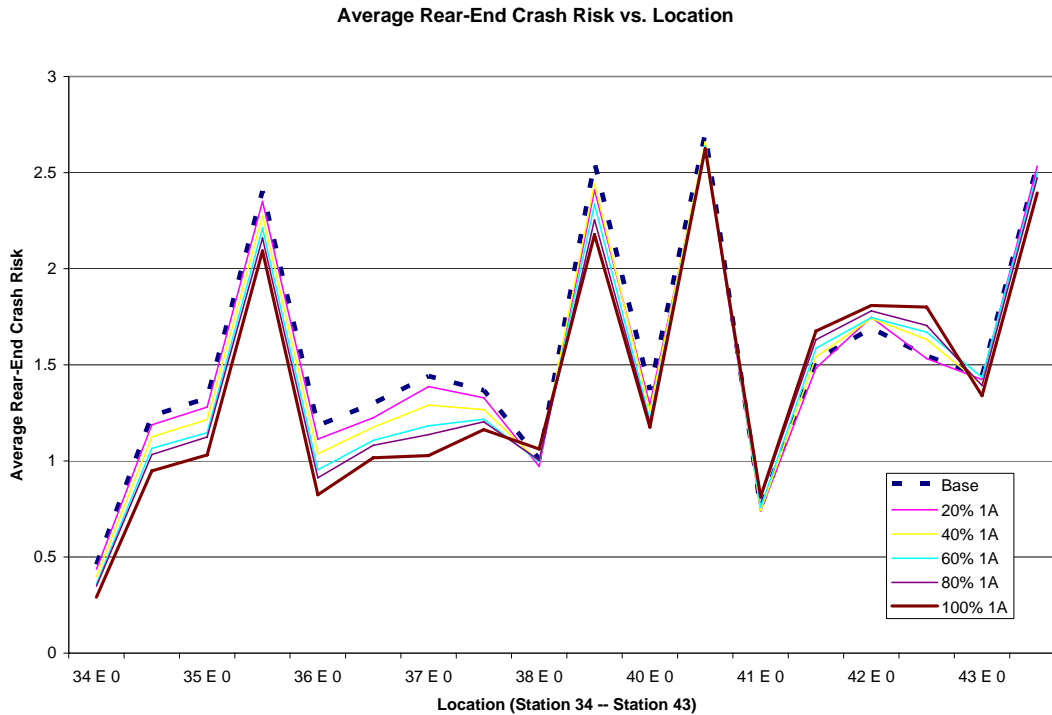
Figure 5-13. Average Rear-End Crash Risk vs. Location for Cases 16 to 20

As noted in Figure 5-13 during the 80 percent loading case, using diversion route 1 causes a decrease in the rear-end crash risk starting near the location that vehicles are diverted from. Near the area where vehicles are diverted to (Station 38, nearer re-entry point, and Station 41, farther re-entry location), however, an increase in the rear-end crash risk is noted. This is caused by the increase in the number of vehicles entering the freeway at this ramp location combined with the higher traffic volume that is currently on the freeway at that point. The added inflow on the ramp will increase the congestion in that area enough to increase the rear-end crash risk in this location. Directly downstream of this area exists a short length of freeway at which the rear-end crash risk was reduced. This is most likely a result of the added congestion upstream, at the re-entry location. The added congestion creates a small bottleneck and immediately downstream of this bottleneck free-flow conditions persist which yields a slightly

141

reduced rear-end crash risk versus the base case. However, this area is rather small and the effect is shown as not statistically significant in most cases. Also worth noting from Figure 5-13 is the fact that at most stations there is a direct relationship between the number of vehicles diverted and the change in the risk. Diverting 20% of the vehicles will reduce the risk less at a station of reduced risk than diverting 40% of the vehicles. This trend continues for all levels of diversion at the 80 percent loading scenario.

Figure 5-14 was created to show the locations affected by route diversion along the freeway graphically. This figure is similar to Figure 5-7 created for the 60 percent loading scenario. In Figure 5-14, the lighter colored areas represent stations that experienced a decrease in the rear-end crash risk due to route diversion while the darker areas represent areas that experienced an increase in the rear-end crash risk. Medium shades are used to represent areas that experienced no significant change in the rear-end crash risk due to the route diversion. The results of this figure are very interesting. First, the crash migration effect, described above, occurs directly downstream of the re-entry ramps in all cases. This is probably caused by the added inflow of vehicles at these ramps which increase the traffic flow and, therefore, induce short-term congestion. Second, the further vehicles are diverted from the original location, the further the effects of the route diversion on the rear-end crash risk. This result is expected since it makes sense that by diverting vehicles further away, the rear-end crash risk will be affected for a longer distance. What is also interesting is the fact that diverting vehicles further away appears to increase the overall safety benefit of the network. As shown in Figure 5-16, the further vehicles are diverted away from the original ramp location, the smaller the area of negative safety benefit on the freeway. One reason for this could be the fact that if diverted vehicles have to travel farther to reach the re-entry location, there is a greater chance of platoons of diverted

vehicles being separated by traffic signals and other vehicles on the surface streets. Therefore, they will enter the freeway in a more staggered arrival pattern which would affect the mainline flow in a less obtrusive manner. Vehicles diverted to the closer re-entry location have a greater probability of re-entering the freeway as a platoon which causes longer queues in the PARAMICS simulation.
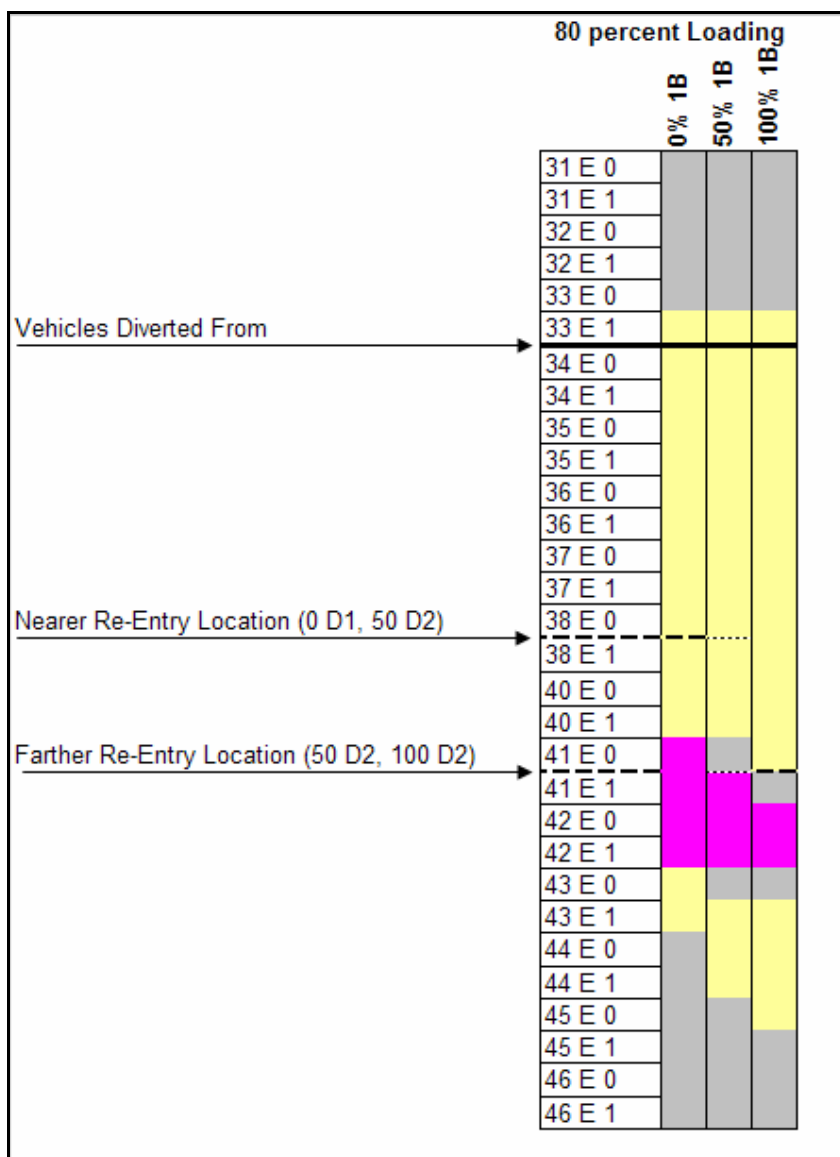
Figure 5-14. Locations Affected by Route Diversion at 80 Percent Loading Scenario

The average rear-end crash risk change over the different areas presented above in Figure 16 are given below in a Tables 5-9, 5-10, and 5-11 for the 0% 1B, 50% 1B, and 100% 1B cases, respectively. Instead of calculating the change in crash risk for a single area along the freeway, as was done for the cases performed at 60 percent loading, these tables show the crash risk for three distinct areas. This was done because, as mentioned previously, at 80 percent loading the route diversion caused three distinct areas of rear-end crash risk change – two areas with decreased risk and one area of increased risk.

Table 5-9. Summary of Average Rear-End Crash Risk Change for Cases 16 to 20

	Test Case ID					
	Base	Case 16	Case 17	Case 18	Case 19	Case 20
	---	20% 1A 0% 1B	40% 1A 0% 1B	60% 1A 0% 1B	80% 1A 0% 1B	100% 1A 0% 1B
Average Crash Risk (Stations 33 to 40)	1.561	1.504	1.466	1.410	1.383	1.332
Crash Risk Benefit	---	0.057	0.095	0.151	0.178	0.229
T-Statistic (Benefit Significance)	---	4.359	9.296	13.882	14.136	19.894
Average Crash Risk (Stations 41 to 42)	1.380	1.376	1.414	1.440	1.514	1.525
Crash Risk Benefit	---	0.004	-0.034	-0.060	-0.135	-0.145
T-Statistic (Benefit Significance)	---	0.106	1.099	2.096	3.548	4.113
Average Crash Risk (Station 43)	1.993	1.979	1.937	1.967	1.933	1.867
Crash Risk Benefit	---	0.015	0.056	0.027	0.061	0.127
T-Statistic (Benefit Significance)	---	0.264	1.302	0.569	1.266	2.690
ORCI	---	0.788	1.211	1.779	1.893	2.651

Table 5-10. Summary of Average Rear-End Crash Risk Change for Cases 21 to 25

	Test Case ID					
	Base	**Case 21**	**Case 22**	**Case 23**	**Case 24**	**Case 25**
		20% 1A	**40% 1A**	**60% 1A**	**80% 1A**	**100% 1A**
	---	**50% 1B**	**50% 1B**	**50% 1B**	**50% 1B**	**50% 1B**
Average Crash Risk (Stations 33 to 40)	1.561	1.504	1.463	1.409	1.355	1.291
Crash Risk Benefit	---	0.057	0.098	0.152	0.206	0.270
T-Statistic (Benefit Significance)	---	4.431	8.304	12.956	15.193	23.837
Average Crash Risk (Stations 41 to 42)	1.588	1.616	1.646	1.650	1.666	1.709
Crash Risk Benefit	---	-0.028	-0.058	-0.062	-0.079	-0.121
T-Statistic (Benefit Significance)	---	0.627	1.268	1.446	2.006	3.786
Average Crash Risk (Stations 43 to 44)	1.193	1.191	1.169	1.155	1.136	1.111
Crash Risk Benefit	---	0.002	0.024	0.037	0.056	0.081
T-Statistic (Benefit Significance)	---	0.035	0.449	0.707	1.012	1.479
ORCI	---	0.666	1.173	1.901	2.613	3.391

Table 5-11. Summary of Average Rear-End Crash Risk Change for Cases 26 to 30

		Test Case ID				
	Base	Case 26	Case 27	Case 28	Case 29	Case 30
		20% 1A	40% 1A	60% 1A	80% 1A	100% 1A
	---	100% 1B	100% 1B	100% 1B	100% 1B	100% 1B
Average Crash Risk (Stations 33 to 40)	1.503	1.445	1.402	1.353	1.295	1.229
Crash Risk Benefit	---	0.058	0.101	0.151	0.209	0.275
T-Statistic (Benefit Significance)	---	5.454	10.030	13.431	18.700	26.401
Average Crash Risk (Station 42)	1.618	1.622	1.675	1.700	1.693	1.775
Crash Risk Benefit	---	-0.003	-0.057	-0.082	-0.075	-0.157
T-Statistic (Benefit Significance)	---	0.060	1.088	1.593	1.258	3.324
Average Crash Risk (Stations 43 to 45)	1.112	1.091	1.091	1.093	1.029	0.977
Crash Risk Benefit	---	0.022	0.021	0.020	0.083	0.135
T-Statistic (Benefit Significance)	---	0.461	0.530	0.427	1.805	2.902
ORCI	---	0.899	1.390	2.026	3.105	4.069

The results show that increasing the percentage of vehicles that are diverted (increasing % 1A) increases the safety benefit in the upstream locations (near the initial diversion location) and increases the rear-end crash risk at the re-entry location. Additionally, diverting vehicles farther away from the original entry point increases the overall safety on the freeway. This is seen by the increasing ORCI values at the same level of diversion (% 1A) for increasing levels of % 1B. A simple linear regression analysis was performed again to confirm these results. The results (given below) show that the values of % 1A and % 1B are both statistically related to the value of ORCI.

Table 5-12. Linear Regression Analysis for ORCI in Test Cases 16 to 30 (80 Percent Loading)

Parameter	Estimate	Standard Error	t Value	Pr > |t|
Intercept	-0.2818	0.1918	-1.47	0.1676
% 1A	0.0323	0.0026	12.58	<.0001
% 1B	0.0063	0.0018	3.57	0.0039

Once again a plot was created to analyze the best case found above (case 30) with respect to the variation within the individual runs. This plot is given below in Figure 5-15. As shown in this figure, the range of the average rear-end crash risk values is relatively small for most of the locations that show a crash risk change. However, between Stations 41 to 44 there is fair amount of variation which shows that the average crash-risk value might be slightly higher or lower than the average. However, this change is not that great compared to the base case and should not be considered significant.
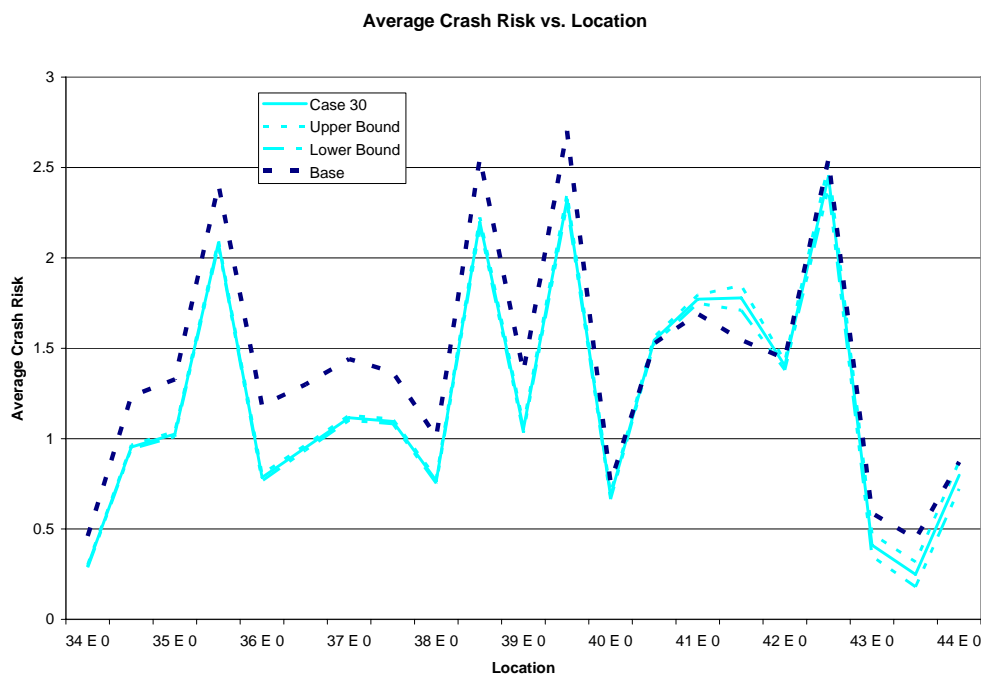
Figure 5-15. Range of Rear-End Crash Risk Values for Case 30

147

Plots were also created to analyze the effect of the route diversion on the lane-change crash risk at the 80 percent loading scenario. These plots are provided below in Figures 5-16, 5-17, and 5-18 for cases 16 to 20, 21 to 25, and 26 to 30, respectively. As shown in those Figures, the lane-change crash risk only differed between stations 36 to 42.
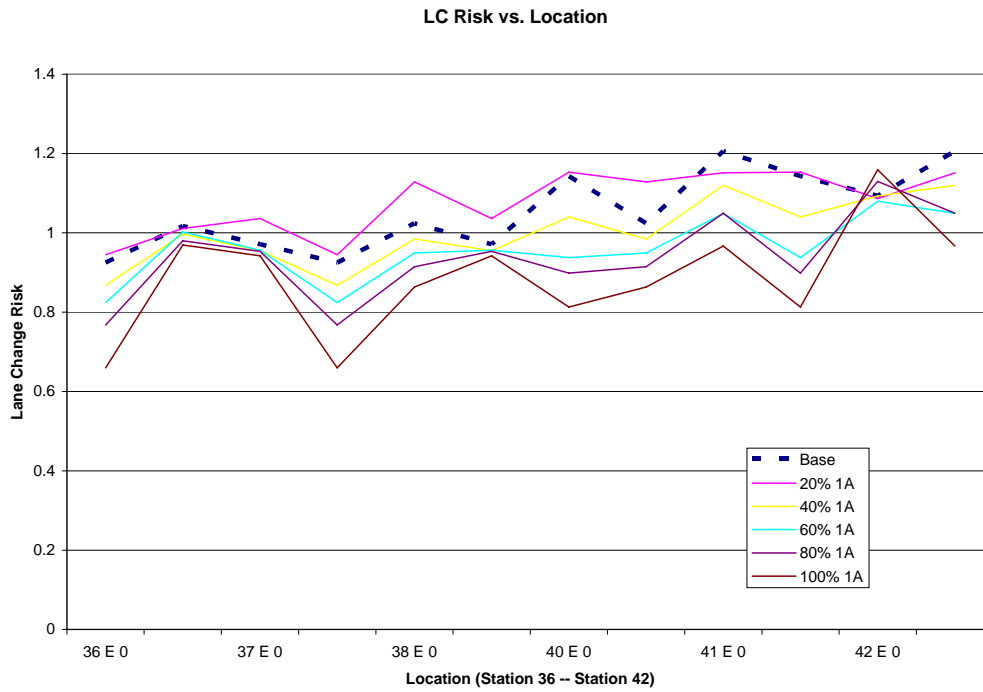
Figure 5-16. Average Lane-Change Crash Risk vs. Location for Cases 16 to 20

148
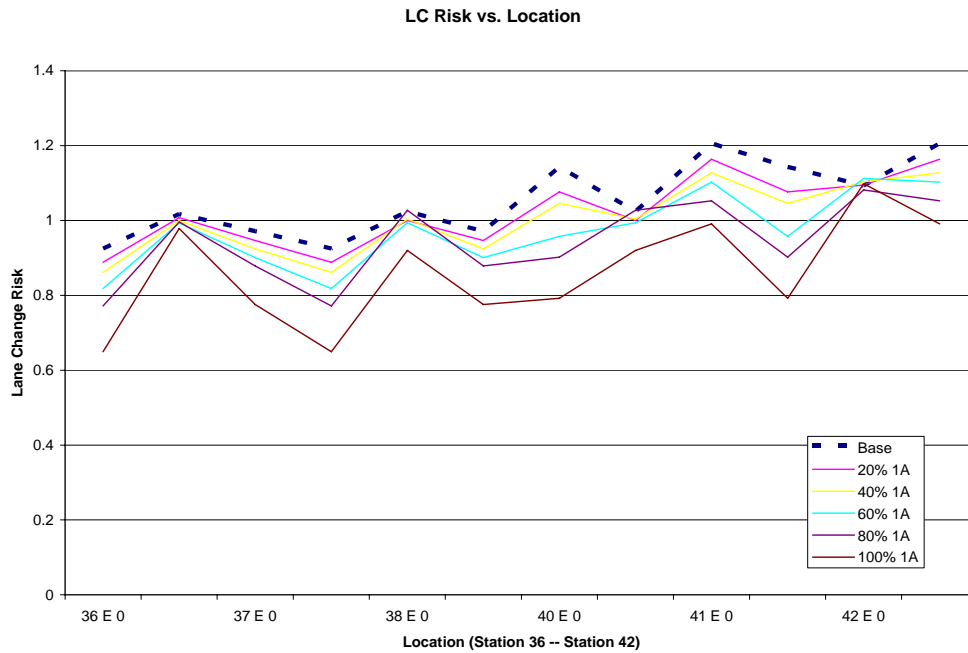
LC Risk vs. Location

Figure 5-17. Average Lane-Change Crash Risk vs. Location for Cases 21 to 25
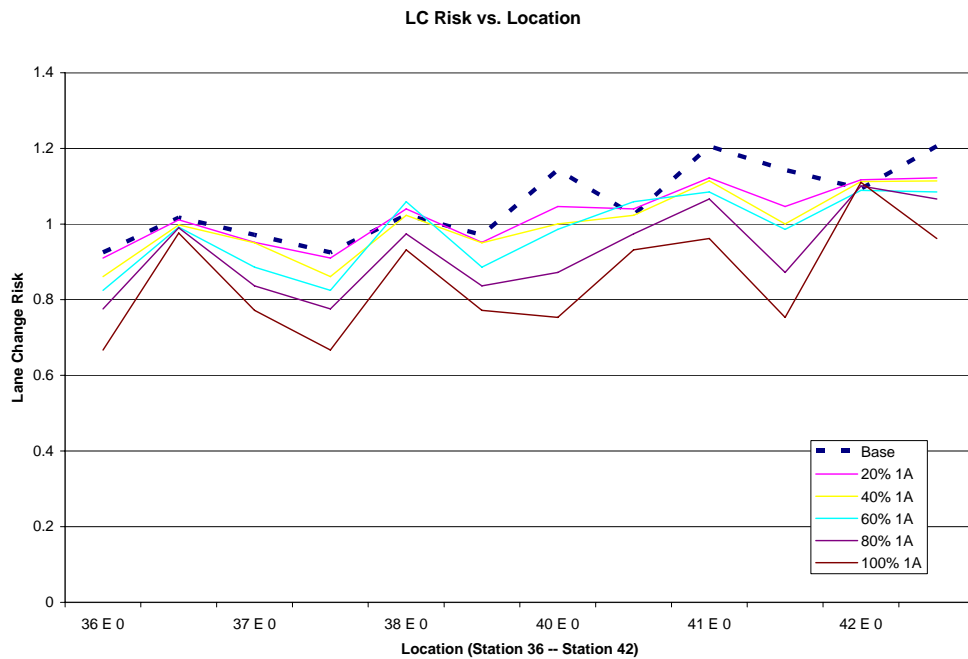
LC Risk vs. Location

Figure 5-18. Average Lane-Change Crash Risk vs. Location for Cases 26 to 30

As shown in these plots, the lane-change crash risk decreases gradually with the number of vehicles that are diverted. Except for the few locations when there is no change between the base case and test cases (Station 36 E 1, for example) the change is logical in that the 20% 1A case has a higher risk than the 40% 1A case which, in turn, has a higher crash risk than the 60% 1A case and so on. The numerical summary of this risk value at the 80 percent loading case is given below in Tables 5-13, 5-14, and 5-15.

Table 5-13. Summary of Average Lane-Change Crash Risk Change for Cases 16 to 20

	Test Case ID					
	Base	Case 16	Case 17	Case 18	Case 19	Case 20
	---	20% 1A 0% 1B	40% 1A 0% 1B	60% 1A 0% 1B	80% 1A 0% 1B	100% 1A 0% 1B
Average Crash Risk (Stations 36 to 42)	1.0541	1.0771	1.0021	0.9596	0.9398	0.8848
Crash Risk Benefit	---	-0.0230	0.0520	0.0945	0.1143	0.1693
T-Statistic (Benefit Significance)	---	0.5500	2.1193	4.2403	4.5826	7.3334
LCRCI	---	-0.2765	0.6240	1.1340	1.3718	2.0311

Table 5-14. Summary of Average Lane-Change Crash Risk Change for Cases 21 to 25

	Test Case ID					
	Base	Case 21	Case 22	Case 23	Case 24	Case 25
	---	20% 1A 50% 1B	40% 1A 50% 1B	60% 1A 50% 1B	80% 1A 50% 1B	100% 1A 50% 1B
Average Crash Risk (Stations 36 to 42)	1.0541	1.0209	1.0023	0.9710	0.9450	0.8610
Crash Risk Benefit	---	0.0331	0.0518	0.0831	0.1091	0.1931
T-Statistic (Benefit Significance)	---	1.2178	1.8977	3.1574	2.8484	7.7045
LCRCI	---	0.3977	0.6216	0.9969	1.3087	2.3167

Table 5-15. Summary of Average Lane-Change Crash Risk Change for Cases 26 to 30

	Test Case ID					
	Base	Case 26	Case 27	Case 28	Case 29	Case 30
	---	20% 1A 100% 1B	40% 1A 100% 1B	60% 1A 100% 1B	80% 1A 100% 1B	100% 1A 100% 1B
Average Crash Risk (Stations 36 to 42)	1.0541	1.0224	1.0007	0.9802	0.9284	0.8547
Crash Risk Benefit	---	0.0317	0.0534	0.0739	0.1257	0.1994
T-Statistic (Benefit Significance)	---	1.2799	1.9297	2.0889	5.3954	9.6223
LCRCI	---	0.3809	0.6411	0.8872	1.5085	2.3923

As shown in the Tables and linear regression equation (Table 5-16), the general trend of the LCRCI at the 80 percent loading case is to increase with higher values of % 1A and % 1B. This is contrary to what was observed at the 60 percent loading case but since the parameter estimate for % 1B is insignificant (p > 0.05) it can be assumed that there is no real difference in the lane change risk change index for different levels of % 1B. A comparison of the tables shows that this makes sense since there is no definitive pattern of the LCRCI values compared to various levels of % 1B.

Table 5-16. Linear Regression Analysis for LCRCI in Test Cases 16 to 30 (80 Percent Loading)

Parameter	Estimate	Standard Error	t Value	Pr > |t|
Intercept	-0.4814	0.1479	-3.25	0.0069
% 1A	0.0246	0.0020	12.46	<.0001
% 1B	0.001851	0.001369	1.35	0.2013

5.2.1.2.1 Travel Time Analysis

Once again a travel time analysis was performed to ensure that the change in travel time due to route diversion is reasonable. Figure 5-19 shows the plot that was created to examine this. Quadratic equations were fit for the 0 % 1B, 50 % 1B, and 100 % 1B cases. The latter two

equations have reasonable R^2 values. However, for the 0 % 1B cases a quadratic equation does not provide a good fit for the data as its R^2 value was extremely low at 0.1423. However, as shown in Figure 5-19, since the travel time does not change very much for this level of % 1B this should be okay since the expected travel time at the various diversion levels does not change much compared to the base case.

Travel Time vs. Percent Vehicles Diverted from DP-1A

$y = 0.1137x^2 - 3.4982x + 16413$
$R^2 = 0.957$

$y = -0.0055x^2 + 2.544x + 16388$
$R^2 = 0.8045$

$y = 0.0295x^2 - 2.336x + 16481$
$R^2 = 0.1423$
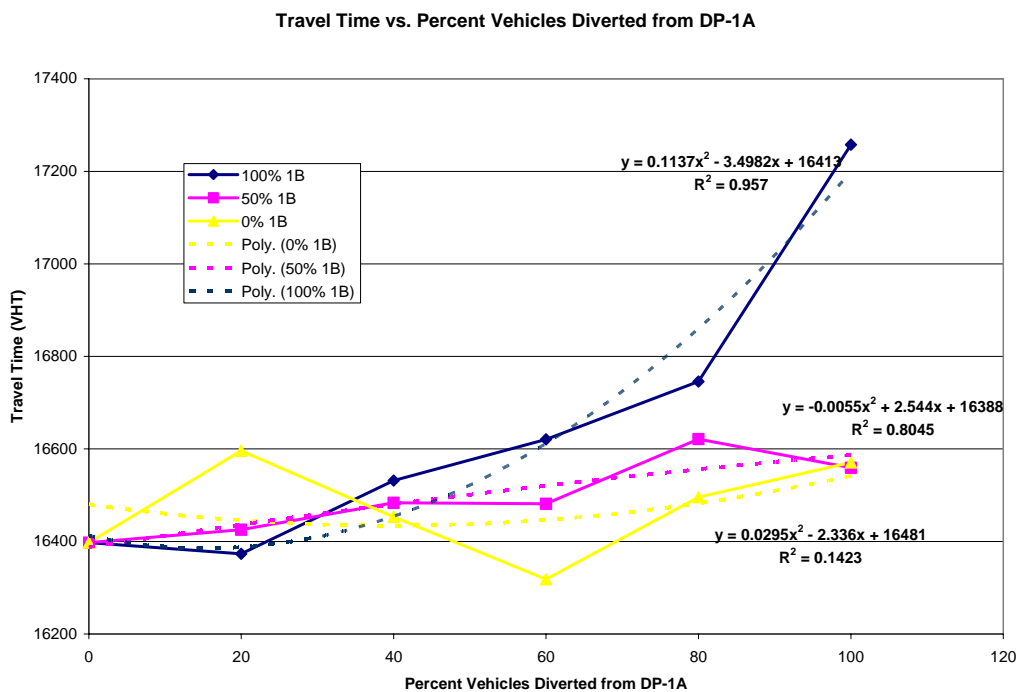
Figure 5-19. Travel Time Plot for Cases 16 to 30

The largest increase in travel time due to route diversion is 5.2%. This occurs when 100 percent of the vehicles are diverted to the further re-entry location. Since this is close to 5%, the target that is deemed reasonable, it can be concluded that diverting the maximum number of vehicles can be diverted at the 80 percent loading case would results in the maximum amount of risk without significantly increasing the travel time.

152

5.2.1.3 90 Percent Loading Scenario

Cases 31 to 45 all test the 1st diversion route during the 90 percent loading scenario. There are a few differences in the results between the cases run at the 80 percent loading scenario and the 90 percent loading scenario. The first major difference is that the area of the freeway that is affected by route diversion is significantly increased. This is caused primarily because of the high traffic volume that is present at this loading scenario. Since the network is at typical levels of congestion during this scenario, diverting some of the vehicles serves to reduce the severity of some of the long queues that form during congestion. This essential causes the traffic conditions to change from regime 1 to regime 2 which is the reason the rear-end crash risk models for regime 1 and 2 had to be normalized and combined into a single crash risk metric. The second difference is that the statistical significance of the crash risk increase near the re-entry areas is much greater than at the previous loading scenario. This means that diverted vehicles cause a much more significant increase in the crash risk than seen previously and the effects of crash migration are more apparent.

Figures 5-20 and 5-21 show the plot of the average rear-end crash risk vs. location for cases 31 to 35 in the experimental design. Note that two figures are needed to show the larger area that is affected by route diversion at this level of loading.

Crash Rear-End Risk vs. Location
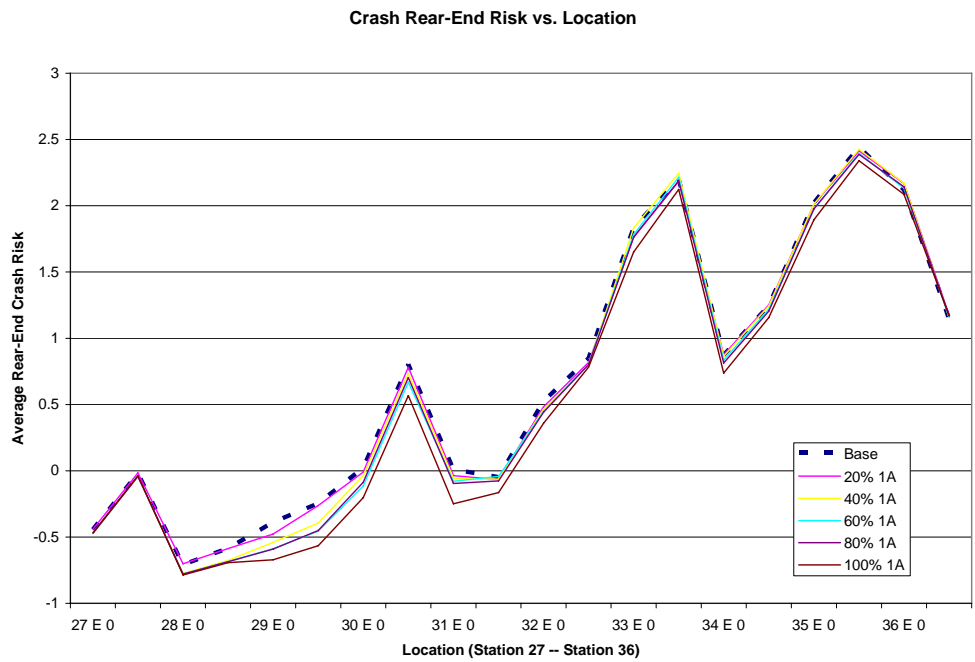
Figure 5-20. Average Rear-End Crash Risk vs. Location for Cases 31 to 35

Crash Rear-End Risk vs. Location
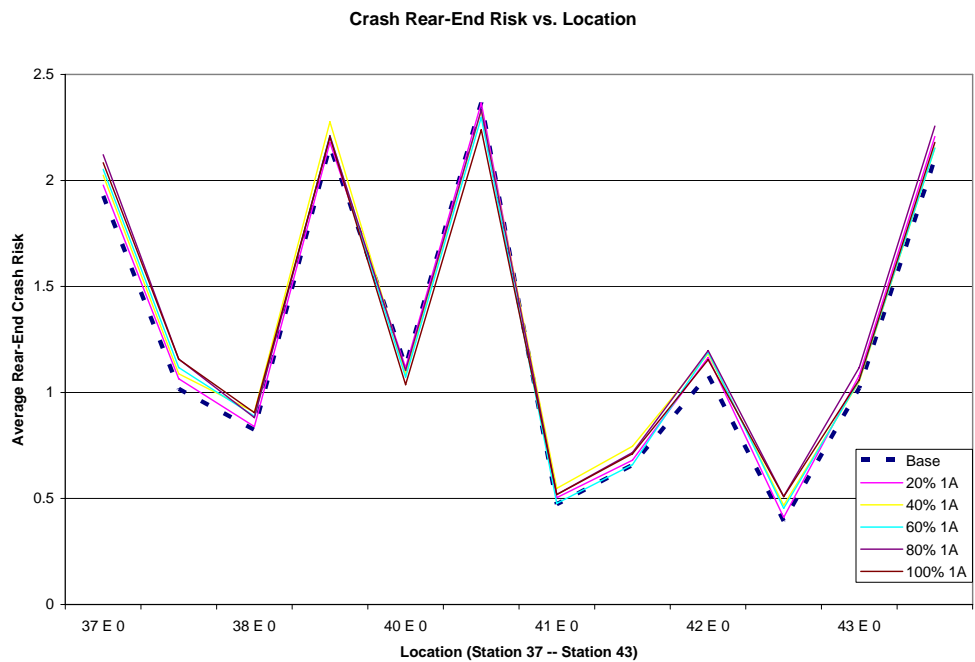
Figure 5-21. Average Rear-End Crash Risk vs. Location for Cases 31 to 35 - 2

154

The numerical summary of the change in rear-end risk realized in cases 31 to 35 is given below in Table 5-17. The changes in the rear-end crash risk for this case were contained within two distinct areas – one area with a crash risk decrease and another with a crash risk increase. The reduction in the crash risk only becomes statistically significant at the 60 percent diversion case while the increase in the crash risk is significant at diversion levels higher than 20 percent. As shown in Table 5-17, the value of ORCI does not always increase as the percentage of vehicles that are diverted from DP-1A increase. While all levels of diversion have a positive value of ORCI (which means an overall positive rear-end crash risk change) the fact that the crash risk increase at Stations 37 to 42 is statistically significant at lower levels of diversion shows that crash risk migration issue is more significant than the crash risk decrease. Therefore, there is a chance that the crash risk will be increased to unacceptably high levels at certain locations.

Table 5-17. Summary of Average Rear-End Crash Risk Change for Cases 31 to 35

	Test Case ID					
	Base	Case 31	Case 32	Case 33	Case 34	Case 35
	---	20% 1A 0% 1B	40% 1A 0% 1B	60% 1A 0% 1B	80% 1A 0% 1B	100% 1A 0% 1B
Average Crash Risk (Stations 28 to 35)	0.679	0.653	0.631	0.600	0.595	0.517
Crash Risk Benefit	---	0.026	0.048	0.079	0.084	0.162
T-Statistic (Benefit Significance)	---	0.649	1.444	2.169	2.506	4.157
Average Crash Risk (Stations 37 to 42)	1.203	1.230	1.266	1.242	1.275	1.252
Crash Risk Benefit	---	-0.027	-0.063	-0.039	-0.072	-0.049
T-Statistic (Benefit Significance)	---	1.188	2.559	1.491	2.996	1.908
ORCI	---	0.144	0.135	0.866	0.622	2.096

Similar results are seen for test cases 36 to 40 and 41 to 45. The summary of those cases are given below in Tables 5-18 and 5-19. Cases 37 and 38 show the first instances of negative ORCI values. This means that diverting vehicles in this manner decreases the overall safety along the network corridor. The cases involving diverting all vehicles to the further re-entry location (100% 1B) all show much higher decreases in the rear-end crash risk than using the nearer on-ramp exclusively or splitting the diverted vehicles between the two options.

Table 5-18. Summary of Average Rear-End Crash Risk Change for Cases 36 to 40

	Test Case ID					
	Base	Case 36	Case 37	Case 38	Case 39	Case 40
	---	20% 1A 50% 1B	40% 1A 50% 1B	60% 1A 50% 1B	80% 1A 50% 1B	100% 1A 50% 1B
Average Crash Risk (Stations 28 to 36)	0.763	0.702	0.744	0.699	0.652	0.605
Crash Risk Benefit	---	0.061	0.019	0.065	0.112	0.158
T-Statistic (Benefit Significance)	---	1.580	0.593	1.773	2.807	4.466
Average Crash Risk (Stations 37 to 43)	1.263	1.305	1.353	1.367	1.362	1.402
Crash Risk Benefit	---	-0.042	-0.090	-0.105	-0.099	-0.139
T-Statistic (Benefit Significance)	---	2.031	4.084	5.424	5.112	6.168
ORCI	---	0.535	-0.754	-0.155	0.704	1.021

Table 5-19. Summary of Average Rear-End Crash Risk Change for Cases 41 to 45

	Test Case ID					
	Base	**Case 41**	**Case 42**	**Case 43**	**Case 44**	**Case 45**
	---	**20% 1A** **100% 1B**	**40% 1A** **100% 1B**	**60% 1A** **100% 1B**	**80% 1A** **100% 1B**	**100% 1A** **100% 1B**
Average Crash Risk (Stations 28 to 37)	0.845	0.810	0.818	0.713	0.600	0.456
Crash Risk Benefit	---	0.034	0.027	0.132	0.245	0.389
T-Statistic (Benefit Significance)	---	1.087	0.716	3.821	7.632	14.207
Average Crash Risk (Stations 41 to 43)	0.955	1.032	1.009	1.041	1.055	1.131
Crash Risk Benefit	---	-0.077	-0.054	-0.086	-0.100	-0.176
T-Statistic (Benefit Significance)	---	2.571	2.175	2.850	4.122	8.164
Average Crash Risk (Stations 44 to 45)	0.914	0.940	0.952	0.915	0.868	0.777
Crash Risk Benefit	---	-0.026	-0.038	0.000	0.047	0.137
T-Statistic (Benefit Significance)	---	0.961	1.616	0.020	1.652	5.577
ORCI	---	0.113	0.070	1.995	4.188	6.746

Table 5-20. Linear Regression Analysis for ORCI in Test Cases 31 to 45 (90 Percent Loading)

Parameter	Estimate	Standard Error	t Value	Pr > |t|
Intercept	-2.1239	0.9772	-2.17	0.0505
% 1A	0.0403	0.0131	3.09	0.0094
% 1B	0.0185	0.0090	2.04	0.0635

The linear regression analysis, presented in Table 5-20, show that the ORCI values increase with increasing values of % 1A and % 1B. However, even though the fit of the data to the regression line is statistically significant the results are in question based on the inconsistencies seen in the ORCI in Tables 5-17, 5-18, and 5-19. Especially in Table 5-18 which shows that diverting 20 percent of the vehicles (20% 1A) increases the safety of the freeway while diverting 40 or 60 percent of the vehicles (40% 1A, 60% 1A) decreases the safety. The

regression parameters are also in question due to the large ORCI values of cases 44 and 45 on the model fit. These large values, 4.188 and 6.746, respectively, tend to influence the model more than the other values and therefore cause the linear regression model to be significant when values of the ORCI show otherwise. Therefore, this model should not be used to describe the data and it would appear that the application of route diversion at 90 percent loading is inconsistent at reducing the rear-end crash risk with respect to the variables % 1A and % 1B.

Figure 5-22 shows which locations the implementation of route diversion affects the rear-end crash risk at the 90 percent loading scenario. As expected when vehicles are diverted further away from the original ramp (50% 1B and 100% 1B cases) the location of rear-end crash risk change moves further downstream. The 50% 1B case affects both the nearer and further re-entry locations since vehicles are diverted to both locations.
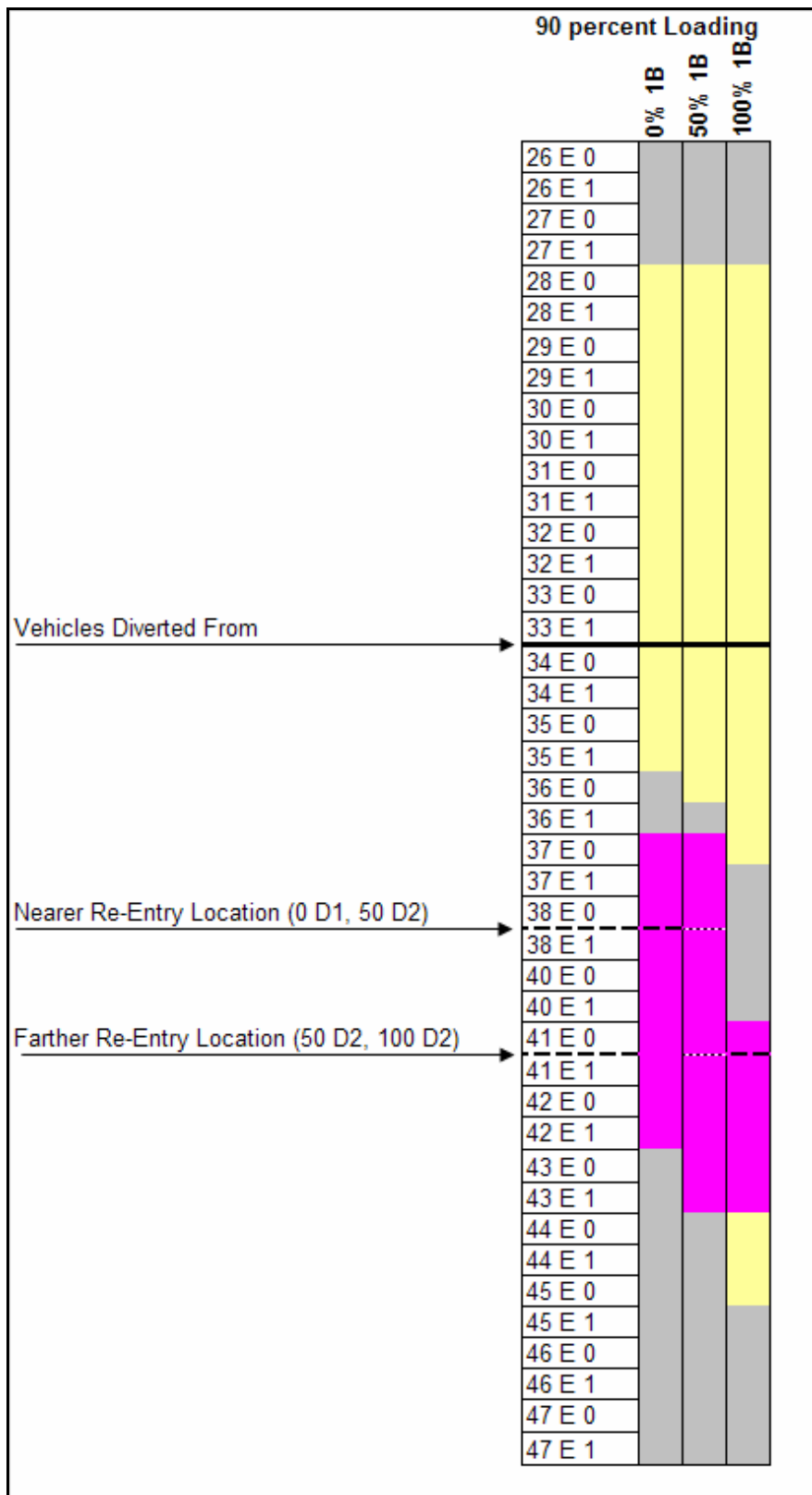
Figure 5-22. Locations Affected by Route Diversion at 90 Percent Loading Scenario

159

Figures 5-23 and 5-24 show the variation in the average rear-end crash risk vs. location. As shown, there is more variation for the best case (case 45) at the 90 percent loading scenario than the 60 or 80 percent loading scenarios. However, this variation is still rather modest and the upper bound does not deviate from the results found previously.

Average Crash Risk vs. Location
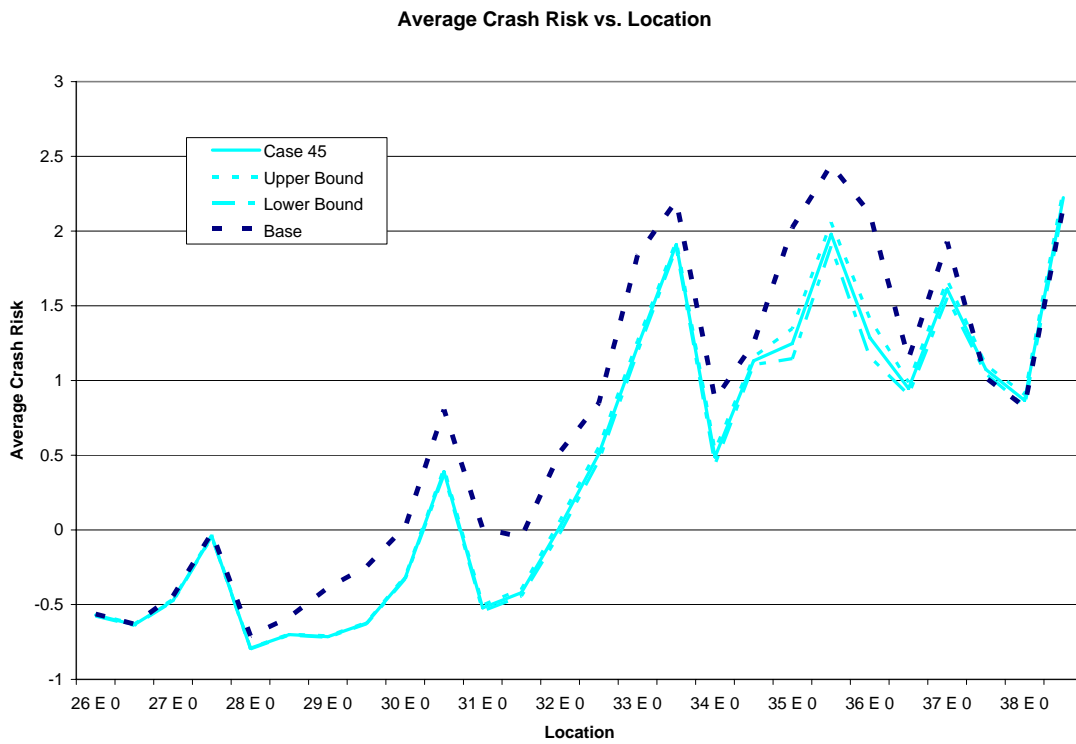
Figure 5-23. Range of Rear-End Crash Risk Values for Case 45

Average Crash Risk vs. Location
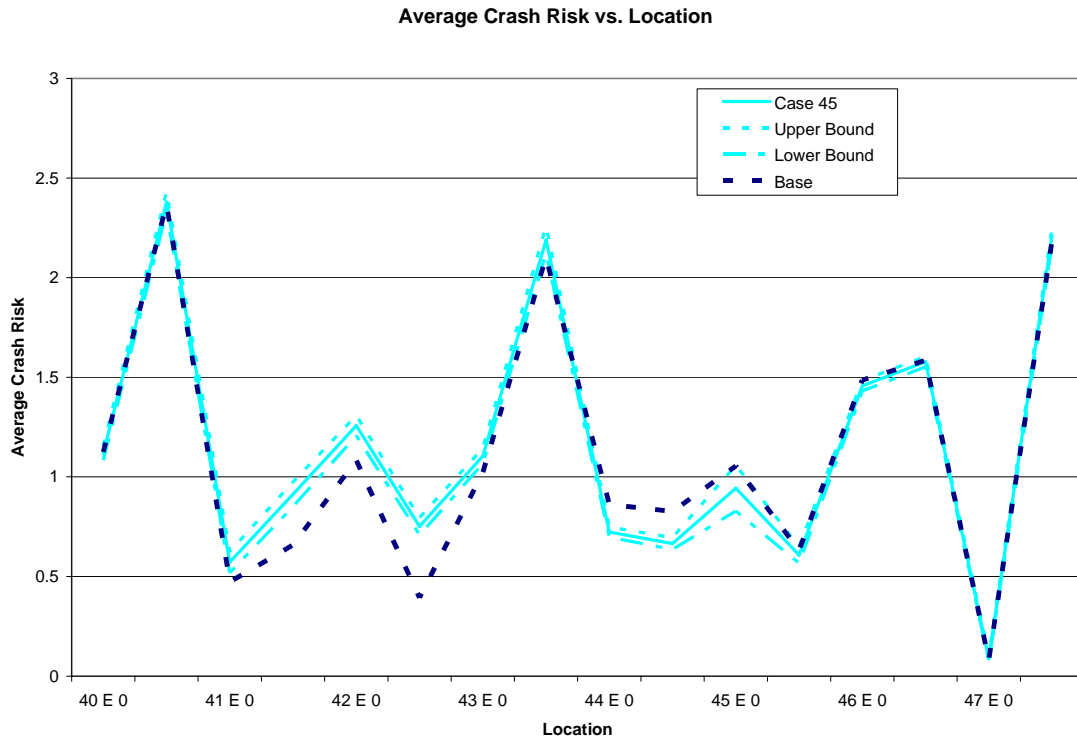
Figure 5-24. Range of Rear-End Crash Risk Values for Case 45 - 2

The effect of the route diversion on the lane-change crash risk is quite similar to the results found for the rear-end crash risk. Figure 5-25 shows a plot of the lane change crash risk for the areas affected by route diversion for cases 36 to 40. Please note in this figure the randomness of the order of LCRCI for different diversion values across different stations. There does not appear to be a pattern present for the crash risk vs. the percent of vehicles diverted like shown in the lower loading scenarios. Tables 5-21, 5-22, and 5-23 summarize the results for the lane-change crash risk for cases 36 to 40, 41 to 45, and 46 to 50, respectively. Note in Table 5-21 that diverting vehicles at the 90 percent loading scenarios almost always causes an increase in the overall lane-change crash risk along the network.

161
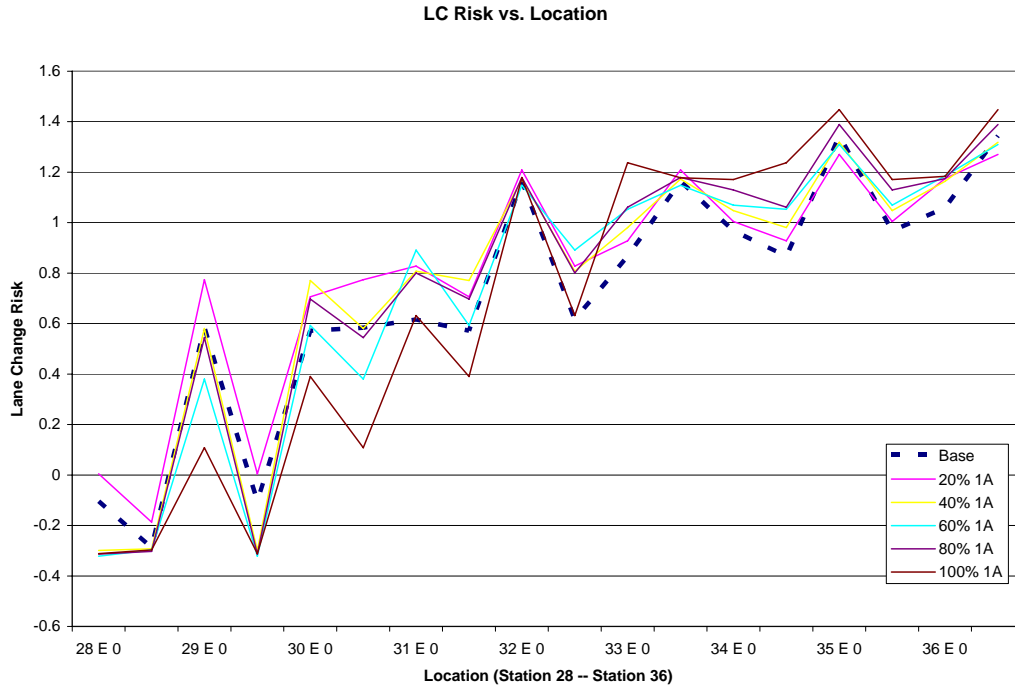
LC Risk vs. Location

Figure 5-25. Average Lane-Change Crash Risk vs. Location for Cases 31 to 35

Table 5-21. Summary of Average Lane-Change Crash Risk Change for Cases 31 to 35

	Test Case ID					
	Base	**Case 31**	**Case 32**	**Case 33**	**Case 34**	**Case 35**
	---	**20% 1A 0% 1B**	**40% 1A 0% 1B**	**60% 1A 0% 1B**	**80% 1A 0% 1B**	**100% 1A 0% 1B**
Average Crash Risk (Stations 28 to 32)	0.4212	0.5648	0.4602	0.3936	0.4333	0.2520
Crash Risk Benefit	---	-0.1437	-0.0390	0.0276	-0.0122	0.1692
T-Statistic (Benefit Significance)	---	1.3870	0.4460	0.2980	0.1240	1.6610
Average Crash Risk (Stations 33 to 36)	1.0724	1.0986	1.1287	1.1496	1.1891	1.2592
Crash Risk Benefit	---	-0.0262	-0.0563	-0.0772	-0.1166	-0.1868
T-Statistic (Benefit Significance)	---	2.0350	1.9110	5.8960	7.3830	12.5740
LCRCI	---	-1.6460	-0.8402	-0.3415	-1.0547	0.1982

162

Table 5-22. Summary of Average Lane-Change Crash Risk Change for Cases 36 to 40

	Test Case ID					
	Base	**Case 36**	**Case 37**	**Case 38**	**Case 39**	**Case 40**
	---	**20% 1A 50% 1B**	**40% 1A 50% 1B**	**60% 1A 50% 1B**	**80% 1A 50% 1B**	**100% 1A 50% 1B**
Average Crash Risk (Stations 28 to 32)	0.5822	0.4651	0.5061	0.4307	0.3400	0.2530
Crash Risk Benefit	---	0.1170	0.0761	0.1514	0.2422	0.3292
T-Statistic (Benefit Significance)	---	1.9296	1.4832	2.5668	4.1311	6.1533
Average Crash Risk (Stations 33 to 36)	1.0900	1.1096	1.1256	1.1627	1.1716	1.2311
Crash Risk Benefit	---	-0.0196	-0.0356	-0.0726	-0.0816	-0.1410
T-Statistic (Benefit Significance)	---	1.8130	2.5044	6.1690	6.6057	10.9459
LCRCI	---	1.0137	0.4761	0.9333	1.7692	2.1639

Table 5-23. Summary of Average Lane-Change Crash Risk Change for Cases 41 to 45

	Test Case ID					
	Base	**Case 41**	**Case 42**	**Case 43**	**Case 44**	**Case 45**
	---	**20% 1A 100% 1B**	**40% 1A 100% 1B**	**60% 1A 100% 1B**	**80% 1A 100% 1B**	**100% 1A 100% 1B**
Average Crash Risk (Stations 28 to 42)	0.9567	0.9210	0.9095	0.8424	0.7761	0.6796
Crash Risk Benefit	---	0.0357	0.0471	0.1143	0.1805	0.2771
T-Statistic (Benefit Significance)	---	1.5987	2.1049	4.7948	9.1894	17.0662
LCRCI	---	0.9293	1.2258	2.9725	4.6942	7.2035

Table 5-24. Linear Regression Analysis for LCRCI in Test Cases 31 to 45 (90 Percent Loading)

Parameter	Estimate	Standard Error	t Value	Pr > |t|
Intercept	-3.0662	0.7174	-4.27	0.0011
% 1A	0.0385	0.0096	4.01	0.0017
% 1B	0.0414	0.0066	6.24	<.0001

A linear regression analysis of the change in LCRCI versus the various levels of route diversion is also presented in Table 5-24. As shown in this table, the linear regression is a good

fit of the data due to the low p-values. This shows that there is a definite pattern in the LCRCI value compared to the amount of route diversion. In general, the LCRCI value increases as the number of vehicles are diverted and also increases as more vehicles re-enter the freeway further away from the initial diversion location. This conforms to the general trend that was realized at other loading cases.

5.2.1.3.1 Travel Time Analysis

The travel time plot for cases 31 to 45 are presented below in Figure 5-26. Both the 0% 1B and 100% 1B curves have well-fitting regression equations. The 50% 1B curve does not have a well-fitting equation but the travel time does not appear to change much in this case compared to the amount of diversion. The maximum change in the travel time is an increase of 7.3%. Since this is rather high, full diversion at the 90 percent loading scenario will have unreasonable effects on the network operations. The next level down (80% 1A, 100% 1B) only has a 5.2% increase in the travel time. This is much closer to 5% but still high. Diverting a lower number of vehicles than this would increase the travel time within reasonable limits. However, it should be noted that the benefits of route diversion on the crash risk are much lower at lower diversion levels.

Travel Time vs. Percent Vehicles Diverted from DP-1A

$$y = 0.1362x^2 + 6.0515x + 23409$$
$$R^2 = 0.9326$$

$$y = 0.0444x^2 - 3.4614x + 23577$$
$$R^2 = 0.2104$$

$$y = 0.1268x^2 - 10.801x + 23563$$
$$R^2 = 0.9413$$

Legend:
- 100% 1B
- 50% 1B
- 0% 1B
- Poly. (0% 1B)
- Poly. (50% 1B)
- Poly. (100% 1B)

Y-axis: Travel Time (VHT)
X-axis: Percetn Vehicles Diverted from DP-1A
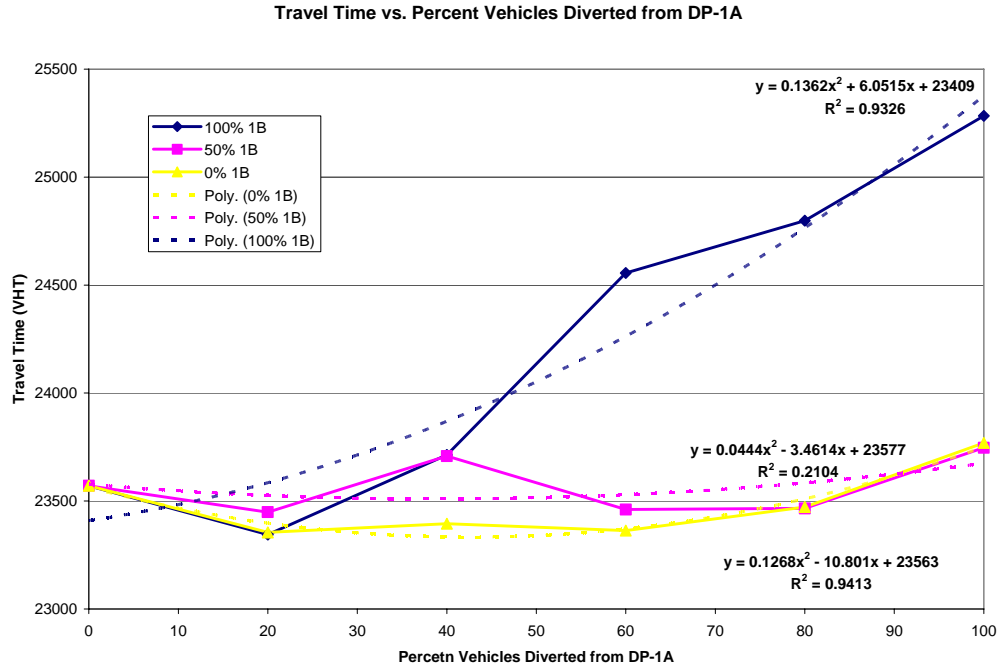
Figure 5-26. Travel Time Plot for Cases 31 to 45

5.2.1.3.2 Re-Entry Ramp Volume

In addition to the increase in the overall network travel time, there is another disadvantage that must be considered when diverting vehicles at such high loading scenarios. The ramp capacity at the on-ramp where vehicles are diverted to must be considered to make sure that the ramp is not oversaturated. At the 60 and 80 percent loading scenarios this is not much of an issue due to the very low levels of congestion. However, during the 90 percent loading scenario this can be quite problematic. For example, when 100 percent of the vehicles are sent to the further re-entry location the flow rate on that ramp increases by more than 900 vehicles / hour. Added to the 875 veh/hr that would normally use the ramp during the 90 percent loading scenario this means that the ramp volume would be increased to almost 1900 veh/hr. At

the 100 percent loading scenario this ramp volume would be even higher at just under 2000 veh/hr. With such high volumes congestion builds up on the on-ramps and spills onto the surface street. Additionally the level of service of the on-ramp will be decreased severely. For the further re-entry location the surface street that is affected is S.R. 50 (Colonial Drive) which is a major arterial roadway throughout Orlando. Even though the overall travel time increase is acceptable, blocking such a major roadway would cause problems on portion of Colonial Drive that are not built on this network. Therefore, route diversion does not look to be a viable option at the 90 percent loading scenario.

5.2.1.4 100 Percent Loading Scenario

The 100 percent loading scenario is analyzed by test cases 46 to 60 as stated in the experimental design. The method of analysis mirrors the previous analysis of similar test runs performed at varying loading levels. As previously seen during the analysis of route diversion at the 90 percent loading scenario, the area of effect of route diversion on the crash risk along the freeway increases as the traffic volume increases. The 100 percent loading scenario is no different as the area of effect is quite large. As can be seen in Figure 5-27, diverting vehicles during such high traffic volumes changes the crash risk as far away from the diversion location (Station 33) as 7 miles upstream (Station 19). The effect can also extend downstream for 7 miles (Station 46) as evidenced in Figure 5-27.

Once again the most likely cause for this large area of effect is the heavy congestion that dominates the loading scenario. During this scenario there are several large queues that envelope the downtown area. When route diversion is applied, the queues still remain but they are either reduced in length or simply move downstream. Therefore, the tail end of the congested area

166

would move downstream as well causing a change in the traffic conditions, and therefore the rear-end crash risk, at only the upstream end of the queuing area. This effect can be seen in Figure 5-27 by noting the large decreases in crash risk from stations 18 to 22 at all diversion levels. When vehicles are diverted further downstream on the freeway – they are effectively kept off of the freeway for a longer period of time – the queue tends to move further downstream and causes an even greater safety benefit in the upstream area. This is evidenced by comparing the 0% 1B (short diversion) and the 100% 1B (long diversion) cases. Note this is also seen in Figures 5-14 and 5-22 for the 80 and 90 percent loading scenarios, respectively. However, in the latter two cases the effect is not as apparent as the 100 percent loading scenario since in this loading scenario the traffic volumes are much higher. Note that downstream of the crash risk reduction areas (stations 18 to 22 for 0% and 50% 1B and stations 18 to 27 for 100% 1B) there is an area of increased rear-end crash risk. This crash risk increase is caused by the speed differential that is created between the free flow areas upstream of the queue and the congested conditions that occur at the tail end of the queue. Upstream of this crash risk increase the traffic flow operates in regime 2 (free flow) conditions. At this location and downstream into the downtown area, the traffic conditions are congested (regime 1). The speed differential of faster moving vehicles approaching the slower moving vehicles in the queue increases the crash risk at the interface between the free flow and queuing conditions.
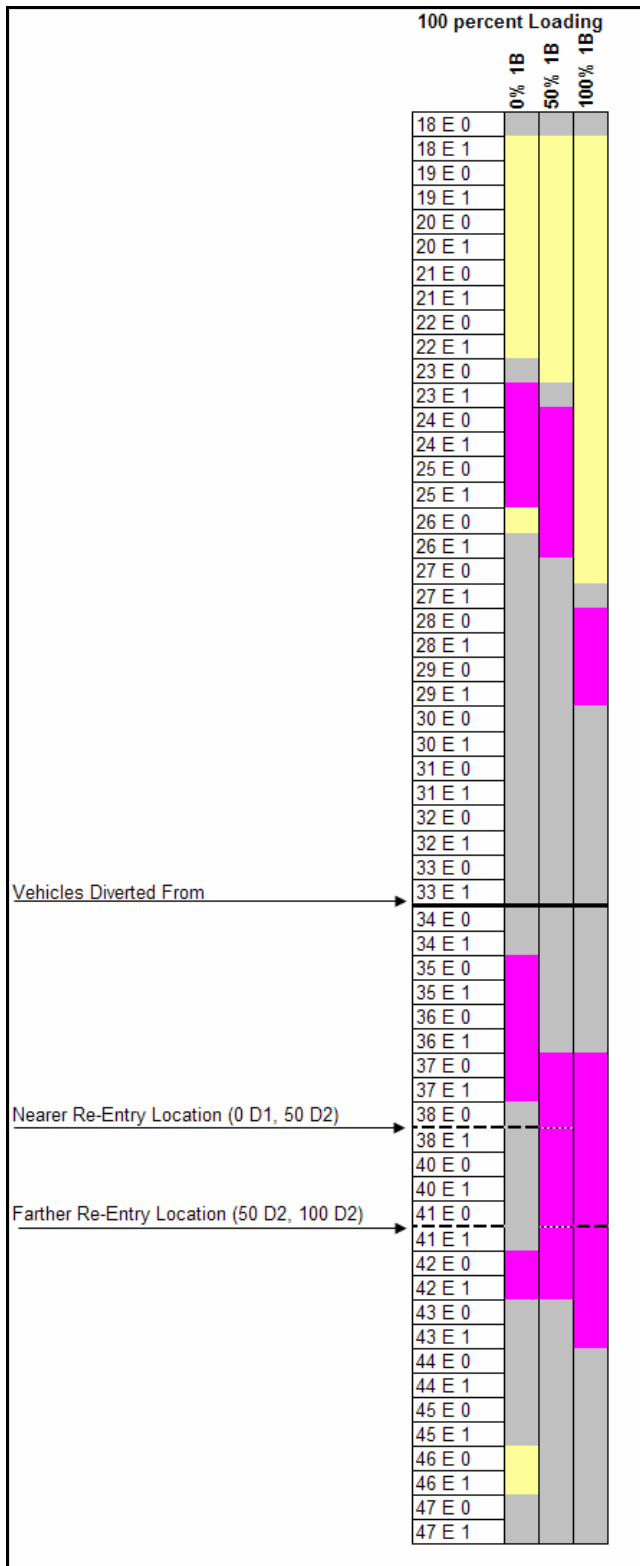
Figure 5-27. Locations Affected by Route Diversion at 100 Percent Loading Scenario

Tables 5-25, 5-26, and 5-27 summarize the change in the crash risk for the test cases 46 to 60. Please note that for the 0% 1B cases there are many areas where the risk changes as opposed to the 3 distinct areas for the other % 1B scenarios. Therefore, the overall average change in the risk over all of these stations is calculated.

Table 5-25. Summary of Average Rear-End Crash Risk Change for Cases 46 to 50

	Test Case ID					
	Base	**Case 46**	**Case 47**	**Case 48**	**Case 49**	**Case 50**
	---	**20% 1A** **0% 1B**	**40% 1A** **0% 1B**	**60% 1A** **0% 1B**	**80% 1A** **0% 1B**	**100% 1A** **0% 1B**
Average Crash Risk (All Stations with Change)	0.466	0.479	0.474	0.482	0.487	0.473
Crash Risk Benefit	---	-0.013	-0.008	-0.015	-0.021	-0.007
T-Statistic (Benefit Significance)	---	1.481	0.965	2.084	2.896	0.563
ORCI	---	-0.318	-0.206	-0.385	-0.523	-0.179

Table 5-26. Summary of Average Rear-End Crash Risk Change for Cases 51 to 55

	Test Case ID					
	Base	**Case 51**	**Case 52**	**Case 53**	**Case 54**	**Case 55**
	---	**20% 1A** **50% 1B**	**40% 1A** **50% 1B**	**60% 1A** **50% 1B**	**80% 1A** **50% 1B**	**100% 1A** **50% 1B**
Average Crash Risk (Stations 19 to 22)	-0.278	-0.331	-0.326	-0.377	-0.452	-0.482
Crash Risk Benefit	---	0.054	0.048	0.099	0.174	0.204
T-Statistic (Benefit Significance)	---	3.051	2.241	5.465	14.261	23.156
Average Crash Risk (Stations 24 to 26)	-0.131	-0.111	-0.105	-0.072	-0.009	0.020
Crash Risk Benefit	---	-0.020	-0.026	-0.059	-0.121	-0.151
T-Statistic (Benefit Significance)	---	1.544	2.016	4.372	10.882	6.405
Average Crash Risk (Stations 37 to 42)	1.102	1.152	1.167	1.177	1.221	1.242
Crash Risk Benefit	---	-0.051	-0.065	-0.075	-0.120	-0.140
T-Statistic (Benefit Significance)	---	3.466	3.094	4.115	7.310	8.276
ORCI	---	-0.198	-0.421	-0.312	-0.531	-0.676

Table 5-27. Summary of Average Rear-End Crash Risk Change for Cases 56 to 60

	Test Case ID					
	Base	**Case 56**	**Case 57**	**Case 58**	**Case 59**	**Case 60**
	---	**20% 1A** **0% 1B**	**40% 1A** **0% 1B**	**60% 1A** **0% 1B**	**80% 1A** **0% 1B**	**100% 1A** **0% 1B**
Average Crash Risk (Stations 19 to 27)	-0.168	-0.167	-0.165	-0.204	-0.278	-0.367
Crash Risk Benefit	---	-0.001	-0.003	0.037	0.110	0.200
T-Statistic (Benefit Significance)	---	0.116	0.339	2.999	7.240	14.235
Average Crash Risk (Stations 28 to 29)	-0.225	-0.206	-0.219	-0.202	-0.151	-0.112
Crash Risk Benefit	---	-0.019	-0.006	-0.023	-0.074	-0.113
T-Statistic (Benefit Significance)	---	1.860	0.519	2.220	5.517	9.601
Average Crash Risk (Stations 37 to 43)	1.137	1.176	1.197	1.229	1.234	1.235
Crash Risk Benefit	---	-0.039	-0.060	-0.092	-0.097	-0.098
T-Statistic (Benefit Significance)	---	2.226	3.936	5.634	5.753	6.379
ORCI	---	-0.558	-0.795	-0.572	0.413	1.763

The first interesting trend that is noticed upon examining Tables 5-25, 5-26, and 5-27 is the fact that the ORCI values are almost all negative. For the previous loading scenarios there were very few negative values which showed that route diversion almost always provided a net safety benefit. However, for the 100 percent loading scenario it appears that route diversion primarily serves to decrease the overall safety of the corridor. Additionally, it does not appear that larger values of % 1A provide a larger value of ORCI as was seen in the previous loading scenarios. Lastly, there is no trend for the values of % 1B and the ORCI. In some cases larger % 1B values increases the crash risk (40% 1A), in other cases the crash risk is decreased (100% 1A). The linear regression equation (Table 5-28) shows that both the % 1A and % 1B variables are statistically insignificant.

171

Table 5-28. Linear Regression Analysis for L in Test Cases 46 to 60 (100 Percent Loading)

Parameter	Estimate	Standard Error	t Value	Pr > |t|
Intercept	-0.89407	0.408276	-2.19	0.049
% 1A	0.007912	0.005456	1.45	0.1727
% 1B	0.003727	0.00378	0.99	0.3436

While the rear-end crash risk is increased due to route diversion at the 100 percent loading level, the lane-change crash risk tends to decrease. Tables 5-29, 5-30, and 5-31 summarize the change in the lane-change risk for cases 46 to 50, 51 to 55, and 56 to 60, respectively. Due to the large number of very small individual areas that are affected by route diversion, the average crash risk is calculated over the affected areas together rather than for specific areas that are affected. The areas that exhibit a change in the lane-change risk due to route diversion are outlined in Figure 5-28.

Table 5-29. Summary of Average Lane-Change Crash Risk Change for Cases 46 to 50

	Test Case ID					
	Base	**Case 46**	**Case 47**	**Case 48**	**Case 49**	**Case 50**
	---	**20% 1A 0% 1B**	**40% 1A 0% 1B**	**60% 1A 0% 1B**	**80% 1A 0% 1B**	**100% 1A 0% 1B**
Average Crash Risk (All Stations with Change)	0.5332	0.5109	0.4769	0.4521	0.3580	0.2695
Crash Risk Benefit	---	0.0224	0.0564	0.0812	0.1753	0.2637
T-Statistic (Benefit Significance)	---	0.8283	2.4508	3.5977	7.4541	10.9271
LCRCI	---	0.4027	1.0147	1.4612	3.1549	4.7468

Table 5-30. Summary of Average Lane-Change Crash Risk Change for Cases 51 to 55

	Test Case ID					
	Base	**Case 51**	**Case 52**	**Case 53**	**Case 54**	**Case 55**
	---	**20% 1A 50% 1B**	**40% 1A 50% 1B**	**60% 1A 50% 1B**	**80% 1A 50% 1B**	**100% 1A 50% 1B**
Average Crash Risk (All Stations with Change)	0.5643	0.5062	0.4961	0.4522	0.3923	0.3490
Crash Risk Benefit	---	0.0581	0.0682	0.1120	0.1720	0.2153
T-Statistic (Benefit Significance)	---	3.1448	3.4135	6.9400	10.8968	12.9103
LCRCI	---	1.5103	1.7742	2.9133	4.4731	5.5983

Table 5-31. Summary of Average Lane-Change Crash Risk Change for Cases 56 to 60

	Test Case ID					
	Base	**Case 56**	**Case 57**	**Case 58**	**Case 59**	**Case 60**
	---	**20% 1A 100% 1B**	**40% 1A 100% 1B**	**60% 1A 100% 1B**	**80% 1A 100% 1B**	**100% 1A 100% 1B**
Average Crash Risk (All Stations with Change)	0.5744	0.5496	0.4969	0.4049	0.3519	0.2975
Crash Risk Benefit	---	0.0248	0.0775	0.1694	0.2225	0.2769
T-Statistic (Benefit Significance)	---	1.4680	5.7177	10.8796	15.2773	19.1712
LCRCI	---	0.7432	2.3237	5.0834	6.6753	8.3067
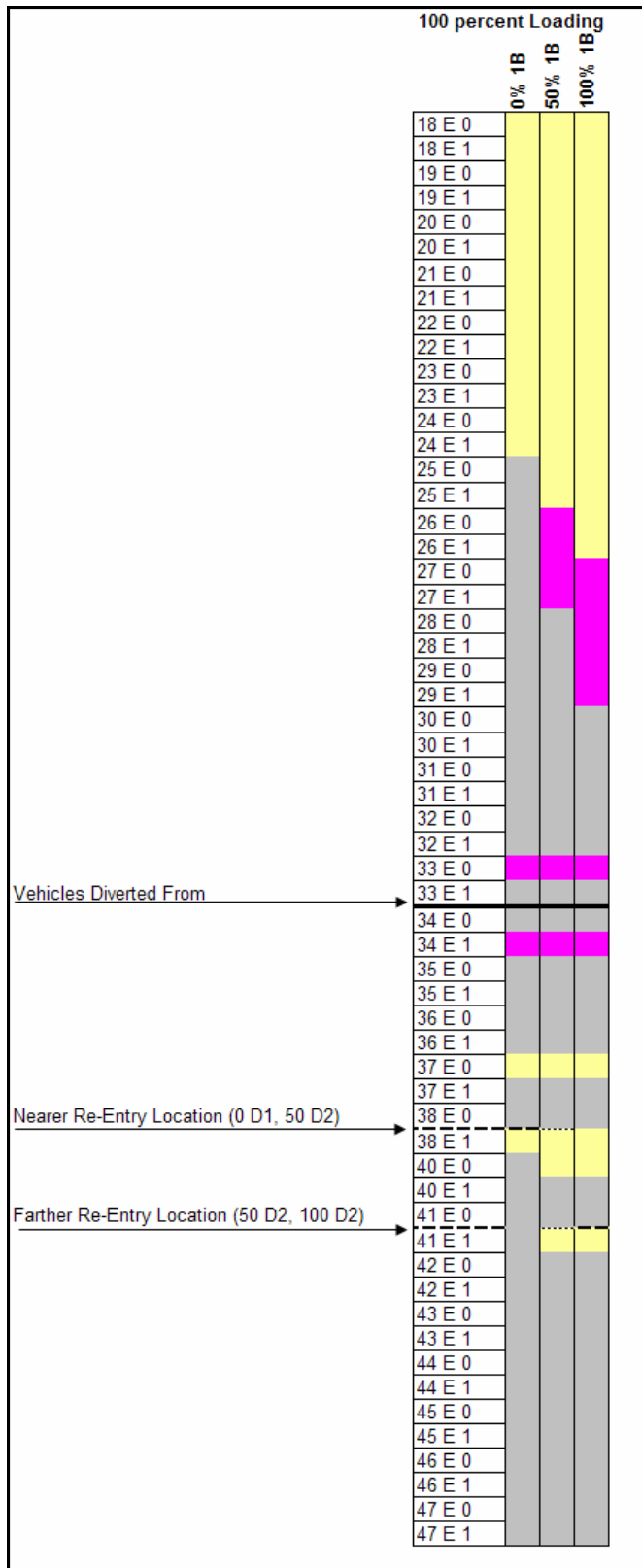
Figure 5-28. Locations Affected by Route Diversion at 100 Percent Loading Scenario (Lane-Change Risk)

174

It is interesting to note that the same trends appear in the lane-change crash risk values at the 100 percent loading scenario that were seen for the other measures for crash risk at lower loading levels. Also interesting is the fact that the LCRCI value shows an improvement in the lane-change crash risk due to route diversion even though the rear-end crash risk worsened. The general trend in the LCRCI versus the diversion is shown in the linear regression model given in Table 5-32.

Table 5-32. Linear Regression Analysis for LCRCI in Test Cases 46 to 60 (100 Percent Loading)

Parameter	Estimate	Standard Error	t Value	Pr > |t|
Intercept	-2.0080	0.5128	-3.92	0.0021
% 1A	0.0686	0.0069	10.02	<.0001
% 1B	0.024704	0.004748	5.20	0.0002

5.2.1.4.1 Travel Time Analysis

The travel time plot for cases 46 to 60 is presented below in Figure 5-29. The travel time during the 0% 1B scenarios do not change very much. Therefore, the low R^2 is not that unreasonable since it can be expected that the travel time would never change much when vehicles are diverted at that level. The other two curves show a much greater change in the travel time due to route diversion and are fit within reasonable limits by a quadratic curve. The maximum travel time seen by the route diversion is 7.2% for the 100 % 1A, 100% 1B case. To reach reasonable limits at the 100% 1B scenario the maximum amount of diversion at % 1A would only be about 40% which provides only a 4% increase in the travel time. For the 50% 1B curve, diverting any amount of vehicles would provide a reasonable travel time for the network with a maximum increase of 4.9%.

Travel Time vs. Percent Vehicles Diverted from DP-1A

$y = -0.1497x^2 + 42.018x + 34693$
$R^2 = 0.9636$

$y = 0.3052x^2 - 14.259x + 34857$
$R^2 = 0.9633$

$y = 0.1155x^2 - 10.159x + 34991$
$R^2 = 0.3826$
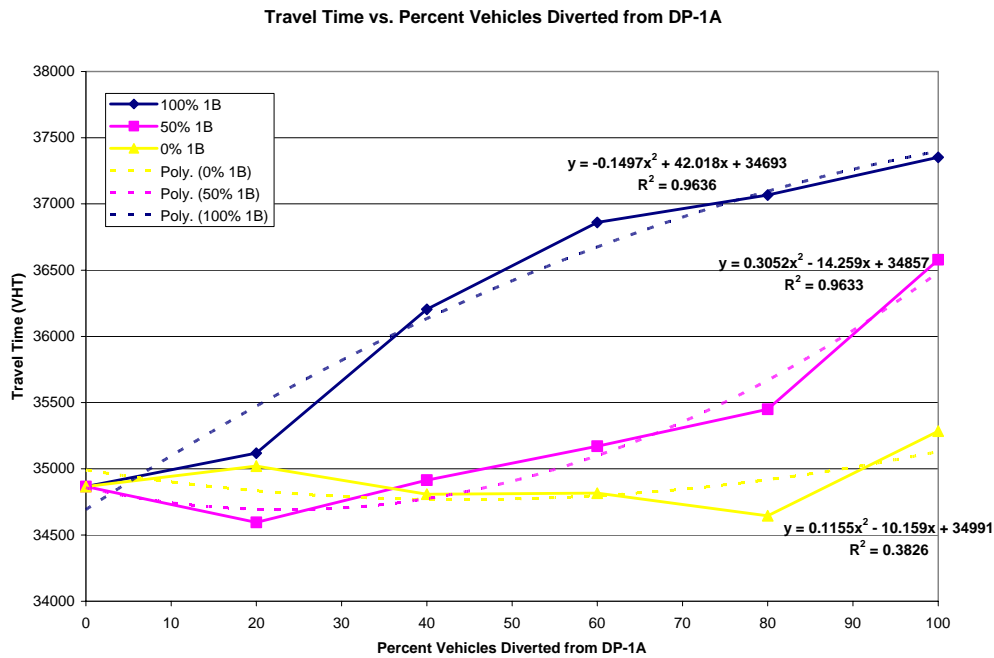
Figure 5-29. Travel Time Plot for Cases 46 to 60

5.2.1.3.2 Re-Entry Ramp Volume

Like the 90 percent loading scenario, diverting vehicles at the 100 percent loading scenario will increase the demand of the downstream on-ramps to levels greater than capacity. For example, when all vehicles are diverted to the furthest re-entry location, a scenario which provides the highest safety benefits – the ramp volume would be increased to 2000 veh/hr. This high ramp volume is unreasonable as it will reduce the level of service on the ramp to F and will also cause major delays and backups on Colonial Drive. Therefore, this cannot be accepted as a realistic strategy.

176

5.2.2 Analysis of Second Diversion Route

As previously mentioned in Section 4.8.2, the second diversion route is short compared to the first. There is only one diversion point for this route (DP 2) and this controls the percentage of vehicles that are diverted. The on-ramp that vehicles are diverted from typically has a low traffic flow rate as well (approximately 350 vehicles / hour) and the vehicles are diverted to the same ramp described as the furthest re-entry location in the previous section. This on-ramp has a typical volume of 970 veh/hr. The short diversion distance, in addition to the low diversion volumes, causes this route to not be as effective at reducing the crash risk along the freeway as the first route. The results of the analysis of the 2nd diversion route are given in the following sections.

5.2.2.1 60 Percent Loading Scenario

Cases 61 to 65 were created to examine the effects of diverting 20 to 100 percent of the vehicles from the South Street ramp using the 2nd diversion route. These test cases are labeled as 20% to 100%, respectively, which indicates the percentage of vehicles diverted for each case. As shown below in Figure 5-30, the rear-end crash risk does not change much during the application of the third diversion route at the 60 percent loading case. This lack of change is also presented in Table 5-33. Note the very small values of the ORCI given in this table.
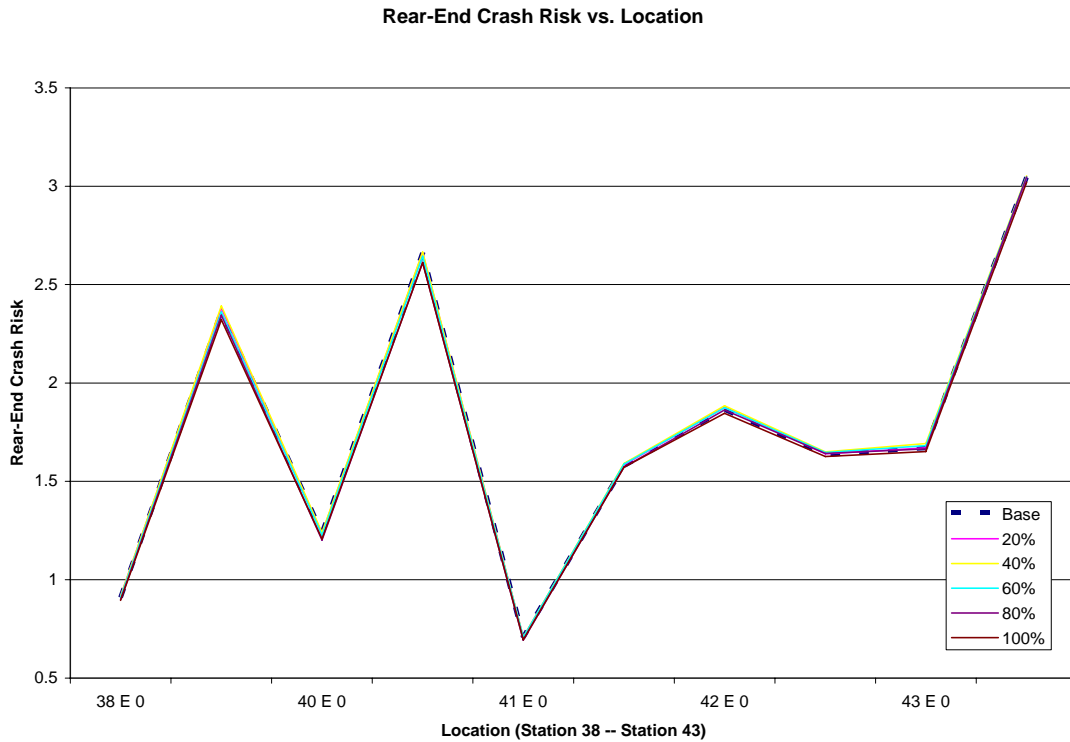
Figure 5-30. Average Rear-End Crash Risk vs. Location for Cases 61 to 65

Table 5-33. Summary of Average Rear-End Crash Risk Change for Cases 61 to 65

	Test Case ID					
	Base	**Case 61**	**Case 62**	**Case 63**	**Case 64**	**Case 65**
	---	**20%**	**40%**	**60%**	**80%**	**100%**
Average Crash Risk (Stations with Difference)	2.195	2.198	2.208	2.192	2.174	2.162
Crash Risk Benefit	---	-0.003	-0.013	0.003	0.021	0.033
T-Statistic (Benefit Significance)	---	0.148	0.902	0.190	1.356	2.422
ORCI	---	-0.014	-0.066	0.016	0.106	0.163

This lack of effect by the second diversion route compared to the first occurs for a few reasons. First, the ramp volumes affected are much different. The South Street ramp that vehicles are diverted from at DP-2 has a much lower volume (about 350 veh/hr) than the Orange Blossom Trail ramp that vehicles are diverted from using DP-1A (about 1020 veh/hr).

Therefore, it is expected that the effects would be much lower since a much smaller volume of traffic flow is being moved. Secondly, in the second diversion route vehicles are only diverted a little less than 1.0 mile downstream. Because this distance is extremely short, the traffic stream may not develop a stable traffic pattern due to the reduced flow rate before the vehicles are reinserted onto the network. Lastly, since this is the 60 percent loading scenario the traffic flow volumes are not very high. Therefore, the effect of the route diversion would be minimized. Note that only at the highest level of loading (case 65 – 100%) was the change in the crash risk significant. Even still, this value is rather small at 0.033 for each of five stations that were affected.

The effect of cases 61 to 65 are almost the same on the lane-change risk as the rear-end risk. Basically, there is almost no change in the lane-change crash risk. This can be seen in the Figure 5-31. For this reason, the LCRCI values are not calculated since no station showed significant change in the crash risk in any of the test cases.

Lane-Change Crash Risk vs. Location
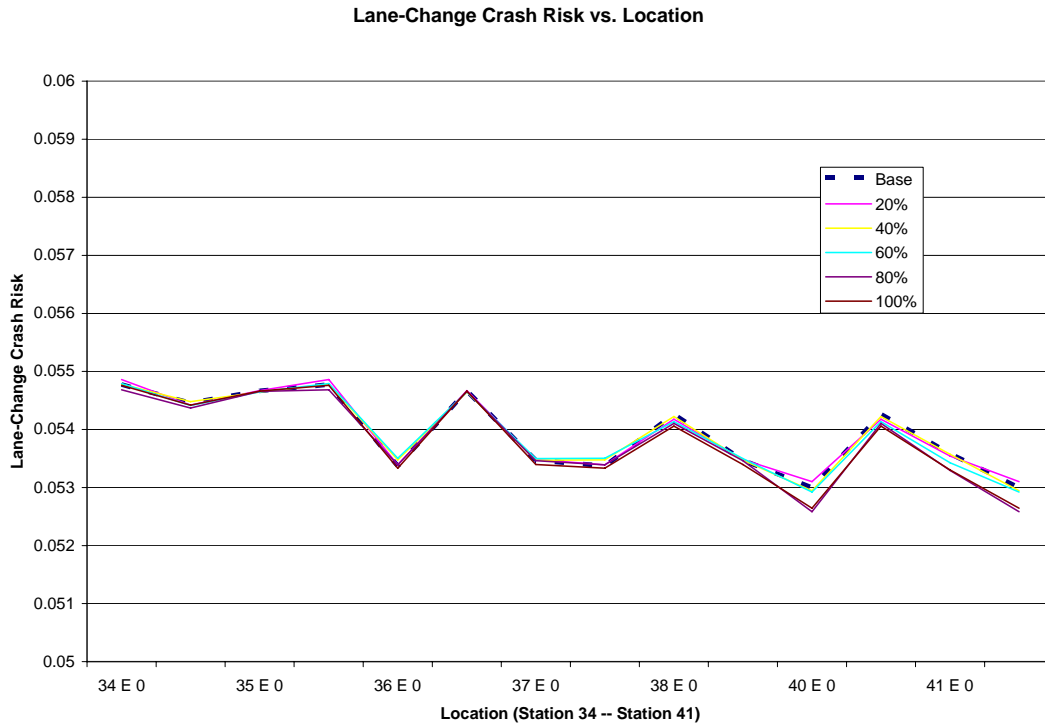
Figure 5-31. Average Lane-Change Crash Risk vs. Location for Cases 61 to 65

5.2.2.2 80 Percent Loading Scenario

The effects of using the shorter diversion route on the rear-end crash risk are not much more apparent during the 80 percent loading scenario than the 60 percent loading scenario. As can be seen in Figure 5-32, all of the curves representing the crash risk at different levels of diversion have about equal rear-end risk values. This is further shown in Table 5-34 where it can be seen that the change in the crash risk is insignificant at all cases and the values of ORCI are very low. Additionally, note that the values do not increase or decrease in sequence but rather they are random. This further shows the ineffectiveness of this shorter route diversion at this loading scenario.

Rear-End Crash Risk vs. Location
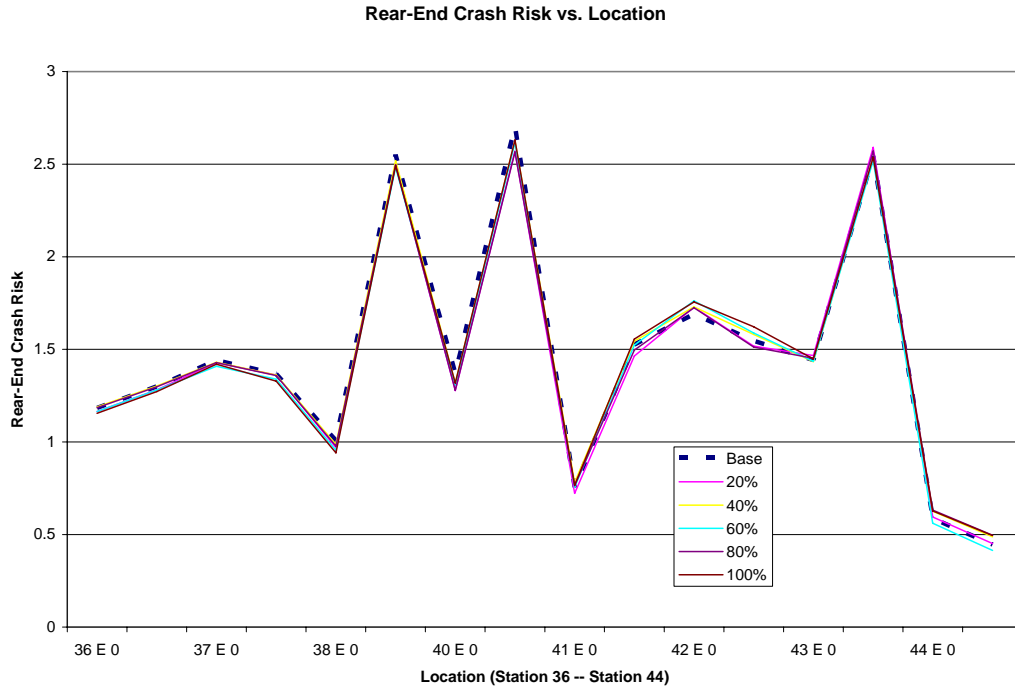
Figure 5-32. Average Rear-End Crash Risk vs. Location for Cases 66 to 70

Table 5-34. Summary of Average Rear-End Crash Risk Change for Cases 66 to 70

	Test Case ID					
	Base	Base 66	Case 67	Case 68	Case 69	Case 70
	---	20%	40%	60%	80%	100%
Average Crash Risk (Stations with Difference)	1.440	1.408	1.439	1.416	1.419	1.432
Crash Risk Benefit	---	0.032	0.002	0.024	0.021	0.008
T-Statistic (Benefit Significance)	---	1.730	0.095	1.310	1.090	0.691
ORCI	---	0.421	0.021	0.318	0.270	0.110

Once again the lane-change crash risk mirrors the rear-end crash risk for these test cases. There is almost no change between any of the five test cases (66 to 70) and the base case for the 80 percent loading case. The LCRCI values have been calculated for each case and are

181

presented in Table 5-35. Please note that the changes in the risk are never statistically significant and all LCRCI values are extremely small.

Table 5-35. Summary of Average Lane-Change Crash Risk Change for Cases 66 to 70

	Test Case ID					
	Base	**Case 61**	**Case 62**	**Case 63**	**Case 64**	**Case 65**
	---	**20%**	**40%**	**60%**	**80%**	**100%**
Average Crash Risk (Stations with Difference)	1.1359	1.1487	1.1327	1.1047	1.1466	1.0778
Crash Risk Benefit	---	-0.0128	0.0033	0.0312	-0.0106	0.0581
T-Statistic (Benefit Significance)	---	0.1893	0.0602	0.5945	0.1594	1.0245
ORCI	---	-0.0767	0.0196	0.1875	-0.0639	0.3487

5.2.2.3 90 Percent Loading Scenario

At the 90 percent loading scenario the cases involving the 2nd diversion route (cases 71 to 75) show much more change in the crash risk than the previous loading scenarios. Multiple stations along the freeway show a change in the crash risk. Figures 5-33 and 5-34 (below) show a plot of the rear-end crash risk vs. location. It is important to note that unlike the cases for the 1st diversion route, which showed change in the crash risk that could be clearly defined into specific sections with lower and higher crash risk, the locations exhibiting change in the rear-end crash risk are not well defined. Most of the stations that show a change have a higher crash risk due to the route diversion. The stations that do show an improvement, Stations 28 and 37, are surrounded by stations which have a much higher crash risk when route diversion is implemented.

182
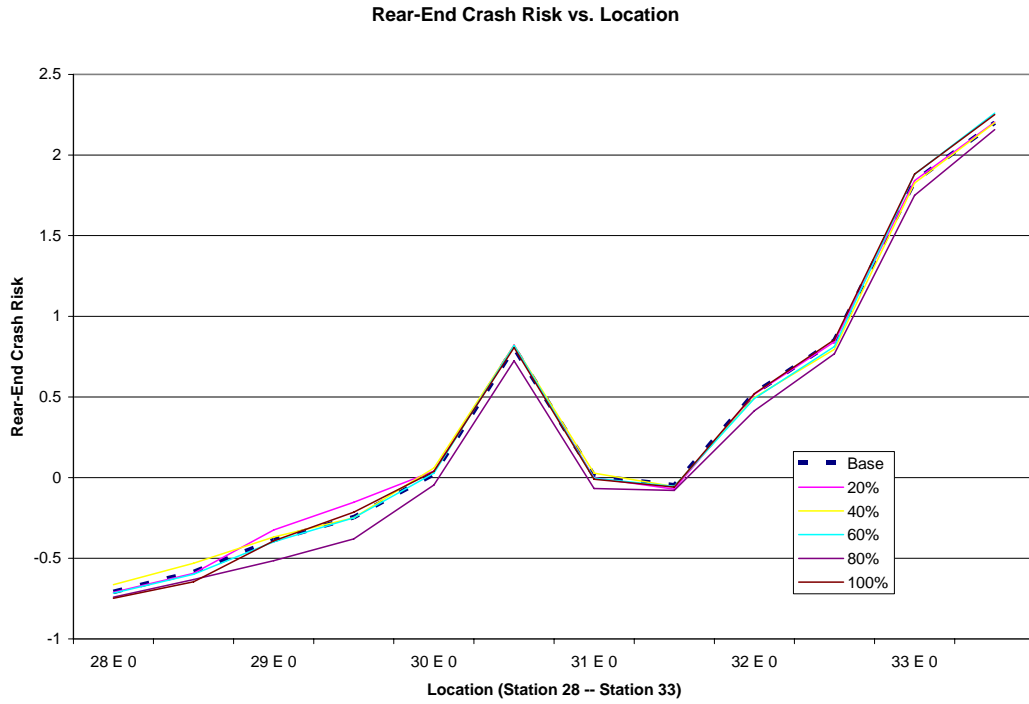
Figure 5-33. Average Rear-End Crash Risk vs. Location for Cases 71 to 75
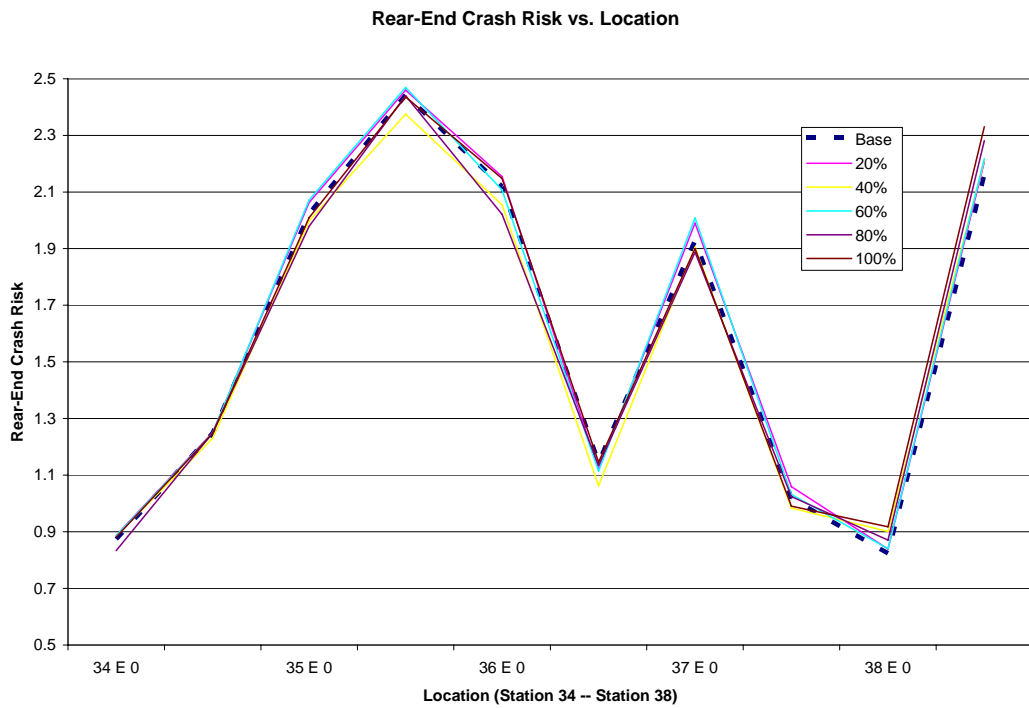
Figure 5-34. Average Rear-End Crash Risk vs. Location for Cases 71 to 75 – 2

183

The tabulated results of the rear-end crash risk for cases 71 to 75 are given in Table 5-36. Almost all values of the ORCI are negative implying that route diversion reduces the rear-end crash safety along the freeway in these cases. The general pattern is increasing values of ORCI until a peak at the 80% diversion case and then dipping back to a negative value.

Table 5-36. Summary of Average Rear-End Crash Risk Change for Cases 71 to 75

	Test Case ID					
	Base	Case 71	Case 72	Case 73	Case 74	Case 75
	---	20%	40%	60%	80%	100%
Average Crash Risk (Stations with Difference)	1.082	1.122	1.116	1.106	1.080	1.115
Crash Risk Benefit	---	-0.040	-0.034	-0.024	0.002	-0.033
T-Statistic (Benefit Significance)	---	2.084	0.797	0.833	0.070	1.427
ORCI	---	-0.556	-0.472	-0.340	0.028	-0.467

Although the lane-change crash risk shows a significant change during these scenarios, all values of the LCRCI are negative as well. This means that route diversion has a negative impact on the lane-change crash risk at all diversion levels. The results are given in Table 5-37 below. Additionally, no location showed a positive benefit in the lane-change risk during these test cases. The effects of route diversion 2 are to increase the lane-change risk significantly.

Table 5-37. Summary of Average Lane-Change Crash Risk Change for Cases 71 to 75

	Test Case ID					
	Base	Case 71	Case 72	Case 73	Case 74	Case 75
	---	20%	40%	60%	80%	100%
Average Crash Risk (Stations with Difference)	0.8391	0.9316	0.9315	0.9235	0.8654	0.9260
Crash Risk Benefit	---	-0.0925	-0.0924	-0.0844	-0.0263	-0.0869
T-Statistic (Benefit Significance)	---	1.9665	1.8845	1.7583	0.5316	1.8559
LCRCI	---	-2.2205	-2.2172	-2.0263	-0.6319	-2.0853

184

5.2.2.4 100 Percent Loading Scenario

At the 100 percent loading scenario the results are about the same. Implementation of the

2nd diversion route causes an increase in the overall rear-end crash risk throughout the network.

This can be seen in Table 5-38. Additionally, much like the 90 percent loading case, the

locations that experience a change in the rear-end crash risk are not well defined along the

network. Because of this and the lack of a general pattern in the ORCI and the amount of

vehicles the 2nd diversion route does not seem to be a reliable option.

Table 5-38. Summary of Average Rear-End Crash Risk Change for Cases 76 to 80

	Test Case ID					
	Base	**Case 76**	**Case 77**	**Case 78**	**Case 79**	**Case 80**
	---	**20%**	**40%**	**60%**	**80%**	**100%**
Average Crash Risk (Stations with Difference)	0.484	0.486	0.488	0.494	0.500	0.497
Crash Risk Benefit	---	-0.001	-0.003	-0.010	-0.016	-0.013
T-Statistic (Benefit Significance)	---	0.214	0.527	0.958	1.984	1.789
ORCI	---	-0.054	-0.153	-0.445	-0.714	-0.589

The lane-change crash also shows very little change due to the 2nd diversion route. The

results are presented in Table 5-39 for inspection.

Table 5-39. Summary of Average Lane-Change Crash Risk Change for Cases 76 to 80

	Test Case ID					
	Base	**Case 76**	**Case 77**	**Case 78**	**Case 79**	**Case 80**
	---	**20%**	**40%**	**60%**	**80%**	**100%**
Average Crash Risk (Stations with Difference)	0.6310	0.6315	0.5999	0.6337	0.6222	0.5797
Crash Risk Benefit	---	-0.0005	0.0311	-0.0027	0.0087	0.0513
T-Statistic (Benefit Significance)	---	0.0230	1.2305	0.1118	0.3301	2.0912
ORCI	---	-0.0082	0.4976	-0.0435	0.1396	0.8203

185

5.2.2 Route Diversion Summary

It is important to note that the specific results found in this study are applicable only to the specific area of the network that is modeled and route diversion implemented. Therefore, the values of the risk change for a particular test case and the linear regression models that were created to compare the ORCI and LCRCI based on the amount of vehicles diverted are specific to Interstate-4 through downtown Orlando for the specific ramps used in this study. Because of this, the regression models created cannot be used to predict the change in the ORCI or LCRCI for other diversion locations. However, the general trends found from these should remain regardless of the location. For example, the trend that the risk decreases at the location where vehicles are diverted from and increases at the location where diverted vehicles are reinserted onto the freeway should hold for any situation. However, the amount of the decrease and increase in the crash risk will depend on the ramp volumes and traffic flow along the freeway location. The conclusions and trends that are found from this study are as follows:

- Route diversion serves to reduce the overall rear-end and lane-change crash risk on the freeway at lower loading levels (up to 90 percent loading) for the first diversion route.

- Route diversion serves to increase the overall rear-end and lane-change crash risk on the freeway at extremely high levels of congestion (100 percent loading) for the first diversion route.

- The length of the freeway that is affected by route diversion increases as the amount of traffic increases along the network.

- At lower levels of congestion, the primary area affected by route diversion is the area between the initial diversion point and the re-entry area.

186

- At higher levels of congestion, route diversion reduces the crash risk at the upstream end of queues that are formed during this loading case. Therefore, the main area affected by route diversion is located much upstream of the area where the route diversion actually occurs. This occurs because when vehicles are diverted the traffic demand is reduced at the middle of a very long queuing section. This reduced flow serves to shorten the length of the queuing section on the tail (upstream) end of the queue by providing more storage space in the middle of the queue that would have been filled by the diverted vehicles. Comparing the base case to the route diversion case, the only difference that is seen is upstream end of the queuing section – in the base case it remains congested while in the diversion case the congested is reduced. This area where the congestion is reduced shows lower values of both the rear-end and lane-change crash risk.

- At lower levels of congestion (60 and 80 percent loading), the reduction in rear-end crash risk increases with the increasing number of vehicles that are diverted and also increase the further away vehicles are diverted to. The reduction in the lane-change crash risk only increases with the number of vehicles that were diverted although there is some evidence which shows that diverting vehicles further away helps to reduce the lane-change crash risk even further.

- At levels of moderate and high congestion (90 and 100 percent loading, respectively), the effects of route diversion are not predictable in nature. Diverting a higher percentage of vehicles may not necessarily reduce the crash risk more.

- At levels of moderate and high congestion (90 and 100 percent loading, respectively), high levels of route diversion causes congestion on the on-ramps that vehicles use to re-

187

enter the freeway. This congestion spills onto the surface streets and blocks a major arterial roadway during the peak traffic periods.

- At lower levels of congestion (60 and 80 percent loading) the increase in travel time that is realized due to route diversion is minimal.

- The travel time increase due to route diversion increases as congestion increases.

- When congestion starts to build up on the network (80 – 100 percent loading), route diversion shows a crash migration effect at the area where the vehicles are diverted to on the network. Therefore, at higher levels of congestion route diversion decreases the crash risk in the upstream areas nearer the diversion location and increases the crash risk at the downstream areas where diverted vehicles re-enter the freeway.

- Diverting vehicles a very small distance along the freeway (less than 1 mile) from an on-ramp with a small traffic volume does not serve to change the crash risk significantly.

Therefore, route diversion should only be applied in off-peak situations (when the mainline traffic flow is un-congested) if the goal of diverting vehicles is to reduce the real-time crash risk along the freeway. Not only do the results show an overall improvement in the crash risk for all diversion levels but the increase in the travel time is relatively small during these low network loading scenarios. However, care must be taken during the 80 percent loading case to ensure the that small area of the freeway that experiences an increase in the crash risk does not already have a high crash risk value. If so, route diversion may serve to make an already high risk area even more risky and cause more crashes. Additionally, vehicles should be diverted from ramps with high inflow volumes and be diverted as far downstream as possible in order to maximize the safety benefits.

188

5.3 Analysis of Ramp Metering

As previously mentioned, the second half of the experimental design was performed to evaluate the effectiveness of ramp metering at reducing the two different crash risk measures along the freeway. The first step in this process was to determine the best ALINEA parameters which are used to compare the ALINEA metering strategy with the Zone metering strategy. Once completed, the different cases performed with the traffic-cycle realization of the Zone algorithm were examined to determine the best cycle length to use. Next the different one-car-per-cycle methods were compared and, finally, the most beneficial strategies from all categories were compared against each other to determine the "best" ramp metering strategy for reducing the crash risk along the network corridor.

The analysis of these test cases is performed in a similar manner as the route diversion test cases. However, there is one important difference that must be mentioned. In general, for route diversion, the area of the freeway that is affected by a particular diversion strategy is constant for varying percentages of vehicles that are diverted. In other words, the area of the freeway that is affected when 100 percent of the vehicles are diverted is about the same as when 40 percent of the vehicles are diverted – the 40 percent diversion case just shows a much smaller change in the crash risk. This is not true for the ramp metering cases, however. When different metering strategies are used, the locations that are affected by ramp metering change. Therefore, when analyzing the ramp metering cases, specific areas of crash risk increase and decrease are not specified. Instead, the network as a whole is examined and all locations that show a change in the crash risk are analyzed together.

5.3.1 Analysis of ALINEA Parameters

5.3.1.1 100 Percent Loading Scenario

The experimental design used to find the best ALINEA parameters is given in Table 4-5 in Section 4.9.1. The ramps metered as part of this subsection of the experimental design are the ramps that make up zone 1 (Figure 4-18). This zone encompasses the 3 ramps immediately upstream of the Interstate-4 / S. R. 408 Interchange. To analyze the changes in the rear-end and lane-change crash risks due to the different ALINEA parameter configurations, the ORCI and LCRCI are used, respectively. As noted previously, these values are calculated from all stations within the network that experience a change in the respective risk value due to the implementation of the ramp metering strategy. The values of the ORCI and LCRCI are given below in Table 5-40 for potion of the experimental design performed at the 100 percent loading scenario. Note in Table 5-40 that each test case is denoted by its respective case number and the ALINEA parameters that the case represents. For example, Case 81 (C 30, O 0.17) represents the case with a 30 second cycle length and a critical occupancy of 0.17.

Table 5-40. Summary of ORCI and LCRCI for Cases 81 to 89

	Test Case ID								
	Case 81	Case 82	Case 83	Case 84	Case 85	Case 86	Case 87	Case 88	Case 89
	C 30 O 0.17	C 30 O 0.20	C 30 O 0.23	C 45 O 0.17	C 45 O 0.20	C 45 O 0.23	C 60 O 0.17	C 60 O 0.20	C 60 O 0.23
# of Stations with RE Risk Change	16	18	15	20	15	17	17	13	9
ORCI	0.0061	-0.4203	-0.2962	-0.2241	-0.1659	-0.5479	-0.3304	-0.3587	-0.3591
# of Stations with LC Risk Change	8	6	6	8	10	10	6	8	4
LCRCI	3.0360	2.6416	2.5904	3.3258	2.2548	2.0591	1.5371	1.1249	1.1040

It is important to note that the ORCI value is negative for all cases except the case with the smallest cycle length (30 seconds) and critical occupancy (0.17). Negative values of the ORCI and LCRCI mean that the rear-end and lane-change crash risk, respectively, are increased in the particular scenario; however, the magnitude of this increase is very small in every case. Therefore, the overall rear-end safety along the network is decreased slightly with the application of ALINEA ramp metering using most of the tested configurations. This slight increase in the crash risk occurs due to the particular ramps that are metered in this scenario – the ramps immediately upstream of the Interstate-4 / S. R. 408 Interchange. Metering these ramps alone does not significantly change the amount of congestion on the freeway since there is a large inflow of vehicles at the Interstate-4 / S. R. 408 Interchange located immediately downstream of this area. In fact the occupancies increases (slightly) which causes a small increase in the rear-end and lane-change crash risk.

Looking at the values of ORCI and LCRCI in Table 5-40 it is also apparent that higher values of these two variables occur during shorter cycle lengths and lower values of the critical occupancy. In other words, crash risk is reduced more on the network with lower values of cycle length and critical occupancy. This is more clearly seen when the ORCI and LCRCI values are averaged across individual levels of a particular value (i.e. ORCI averaged for all cases with a 30 second cycle length compared to ORCI averaged for all cases with a 45 second cycle length). This is presented below in Table 5-41. As shown more clearly in Table 5-41, the values of ORCI and LCRCI increase with shorter cycle lengths and smaller critical occupancies. Therefore, shorter cycle lengths and smaller critical occupancy values provide the best safety results. The smaller critical occupancy values allow the metering algorithm to become more restrictive at lower levels of congestion while the smaller cycle lengths allow smaller platoons of vehicles

onto the network which, in this particular traffic flow condition, results in smaller crash risk values.

Table 5-41. ORCI and LCRCI across different levels of ALINEA Parameters (100 Percent Loading)

	ORCI	LCRCI
O = 0.17	-0.1828	2.6330
O = 0.20	-0.3149	2.0071
O = 0.23	-0.4010	1.9178
C = 30	-0.2368	2.7560
C = 45	-0.3126	2.5466
C = 60	-0.3494	1.2553

A linear regression model was created to help explain the trends between the two ALINEA parameters and the ORCI and LCRCI. These two models are displayed in Tables 5-42 and 5-43, respectively. Since the coefficients of the cycle length and critical occupancy parameters are negative for both of the models, this implies that lower values of these two variables provide better safety benefits. Even though the parameter estimates in the ORCI model are not statistically significant (which probably signifies the lack of a linear relationship rather than the lack of a relationship altogether), the sign of the parameter estimate shows that if it were significant lower cycle lengths would provide greater safety benefits.

Table 5-42. Linear Regression Analysis for ORCI in Test Cases 81 to 89 (100 Percent Loading)

Parameter	Estimate	Standard Error	t Value	Pr > |t|
Intercept	0.5968	0.4080	1.46	0.1939
Cycle	-0.0038	0.0037	-1.01	0.3493
Crit_Occ	-3.6373	1.8491	-1.97	0.0967

Table 5-43. Linear Regression Analysis for LCRCI in Test Cases 81 to 89 (100 Percent Loading)

Parameter	Estimate	Standard Error	t Value	Pr > |t|
Intercept	6.8209	1.2175	5.60	0.0014
Cycle	-0.0500	0.0110	-4.53	0.0040
Crit_Occ	-11.9195	5.517058	-2.16	0.0740

5.3.1.2 90 Percent Loading Scenario

Like the ALINEA runs for the 100 percent loading cases, the values of the ORCI and LCRCI were calculated for cases 90 to 98 which were run at 90 percent loading. These values are represented below in Table 5-44.

Table 5-44. Summary of ORCI and LCRCI for Cases 90 to 98

	Test Case ID								
	Case 90	Case 91	Case 92	Case 93	Case 94	Case 95	Case 96	Case 97	Case 98
	C 30 O 0.17	C 30 O 0.20	C 30 O 0.23	C 45 O 0.17	C 45 O 0.20	C 45 O 0.23	C 60 O 0.17	C 60 O 0.20	C 60 O 0.23
# of Stations with RE Risk Change	16	12	11	16	17	8	14	5	9
ORCI	2.0057	0.8274	0.4980	1.3397	0.8875	0.0695	1.1504	0.2043	0.2055
# of Stations with LC Risk Change	4	2	4	6	0	2	4	6	6
LCRCI	1.3549	0.4174	0.0369	0.6966	0.0000	-0.5846	0.9367	-0.5275	-0.4792

Once again the values of the ORCI and LCRCI found in Table 5-45 have the general trend that they decrease with increasing values of the cycle length and critical occupancy. For the 90 percent loading cases (unlike the 100 percent loading cases), the ORCI and LCRCI values are mostly positive which implies that, in general, the ALINEA strategies serve to reduce both the rear-end and lane-change crash risk. The averages of the two crash risk summary variables across individual levels of a particular variable (presented in Table 5-45) confirm this trend.

Table 5-45. ORCI and LCRCI across different levels of ALINEA Parameters (90 Percent Loading)

	ORCI	LCRCI
O = 0.17	1.4986	0.9961
O = 0.20	0.6397	-0.0367
O = 0.23	0.2577	-0.3423
C = 30	1.1104	0.6031
C = 45	0.7655	0.0373
C = 60	0.5201	-0.0233

The linear regression models for the ORCI and LCRCI shown in Tables 5-46 and 5-47, respectively, confirm the same trends found for the scenarios performed at the 100 percent loading scenario. Please note that all of the parameter estimates are statistically significant in this case which shows that these trends are linear for the 90 percent loading scenarios. The coefficients of the cycle length and critical occupancy parameters are negative (like the 100 percent loading case) for both models. This shows that the overall risk benefit is maximized when lower values of the cycle length and critical occupancy are used for the ALINEA parameters.

Table 5-46. Linear Regression Analysis for ORCI in Test Cases 90 to 98 (90 Percent Loading)

Parameter	Estimate	Standard Error	t Value	Pr > |t|
Intercept	5.8205	0.7525	7.73	0.0002
Cycle	-0.0197	0.0068	-2.88	0.0279
Crit_Occ	-20.6821	3.4100	-6.07	0.0009

Table 5-47. Linear Regression Analysis for LCRCI in Test Cases 90 to 98 (90 Percent Loading)

Parameter	Estimate	Standard Error	t Value	Pr > |t|
Intercept	5.6066	0.9236	6.07	0.0009
Cycle	-0.0209	0.0084	-2.49	0.0469
Crit_Occ	-22.3063	4.185329	-5.33	0.0018

As a result of this portion of the experimental design, the following results are found:

- A lower value of the critical occupancy in the ALINEA algorithm provides the highest safety benefits

- A lower value of the cycle length provides the highest safety benefits when the traffic-cycle realization of ALINEA is applied

Dhindsa (2005) performed a similar study to determine the best values of the cycle length and critical occupancy for the ALINEA algorithm when used to reduce the real-time crash risk on a freeway. In his study, much like this study, Dhindsa showed that a smaller cycle length provides greater safety results when the ALINEA algorithm is implemented. Using a smaller cycle length with this restrictive metering algorithm allows smaller platoons of vehicles to enter the freeway mainline at an increased frequency. Typically, this would serve to increase the risk of a rear-end crash as vehicles merge onto the freeway mainline more frequently. However, when the traffic pattern on the mainline has small gaps between successive vehicles that can accommodate only a few vehicles merging at a time, this situation provides greater safety benefits than when larger platoons of vehicles try to merge into the same small gaps in the mainline traffic. At the particular levels of traffic flows experienced on this network, these smaller platoons cause less turbulence in the traffic flow and effectively reduce the crash risk more than if a larger cycle length is used with the same metering algorithm.

However, Dhindsa found that using a higher value of critical occupancy in the ALINEA algorithm would improve the safety conditions on the freeway; this is contradictory to the results found in this study. To understand which of these values is most appropriate then, it is important to examine the ALINEA algorithm in detail. From Equation 3, using lower value of the critical

occupancy would cause the ALINEA algorithm to restrict the metering rate at lower levels of congestion than if a higher value of the critical occupancy is used. This would essentially allow fewer vehicles onto the network per metering cycle during periods of light congestion which will induce less turbulence on the mainline traffic flow. However, if a higher critical occupancy value is used the meter would not be as restrictive and allow more vehicles onto the network for a given time period. This does not make sense from a safety perspective as this would increase congestion and speed variation. For this reason, the results of this study are used to describe the relationship between the critical occupancy and crash risk.

Therefore, the final outcome of this portion of the experimental design is that the optimal values for the ALINEA algorithm with the traffic-cycle realization are a cycle length of 30 seconds and a critical occupancy of 0.17. These values will be used to compare ALINEA traffic-cycle method with the other ramp metering methods being considered.

5.3.2 Analysis of Zone Strategy with Traffic-Cycle Realization

The experimental design given in Section 4.9.3 describes the other ramp metering test cases that are examined in this study. In order to determine the trends between the rear-end and lane-change crash risk and specific variables in the experimental design, these cases are split into different groups for analysis. The first group that will be looked at are the cases that use the Zone ramp metering algorithm with the traffic cycle realization. These cases are analyzed together in order to determine which cycle length and which metered zone most successfully reduces the two real-time crash risk measures and are reproduced below in Table 5-48. Zone 1 encompasses the area just upstream of the I-4 / S. R. 408 interchange, Zone 2 meters the four

196

ramps just downstream of this interchange, and Zone 3 meters an that is the union of Zones 1 and 2. A schematic drawing of the Zones is shown in Figure 4-18.

Table 5-48. Test Cases Representing Zone Metering Algorithm and Traffic-Cycle Realization

Case Number	Percent Loading	Metered Zone	Algorithm	Cycle Length
99	100	1	Zone	30
100	100	1	Zone	45
101	100	1	Zone	60
105	100	2	Zone	30
106	100	2	Zone	45
107	100	2	Zone	60
111	100	3	Zone	30
112	100	3	Zone	45
113	100	3	Zone	60
117	90	1	Zone	30
118	90	1	Zone	45
119	90	1	Zone	60
123	90	2	Zone	30
124	90	2	Zone	45
125	90	2	Zone	60
129	90	3	Zone	30
130	90	3	Zone	45
131	90	3	Zone	60

The values of the ORCI and LCRCI have been calculated for the cases performed at the 100 percent loading scenario and are presented below in Table 5-49. The cases are denoted in Table 5-49 by the zone that is being metered and the cycle length that is used as well as the corresponding case number from Table 5-48. For example, Case 111 represents the case where zone 3 is metered using a 30 second cycle length. As shown in Table 5-49, the values of the ORCI and LCRI tend to increase for longer cycle lengths which show improved safety conditions as the cycle lengths increases. Metering zone 1 does not appear to yield significant safety benefits as evidenced by the low values of ORCI and LCRCI. In fact, the majority of the cases involving zone 1 have a negative overall safety impact. Metering zone 2 provides better

safety improvements but zone 3 provides the most substantial reduction in both the rear-end and lane-change crash risk. The average value of ORCI for zone 3 is about 6 times as high as the average value of the ORCI for zone 2.

Table 5-49. Summary of ORCI and LCRCI for Zone TC Cases at 100 Percent Loading

	Test Case ID								
	Case 99	Case 100	Case 101	Case 105	Case 106	Case 107	Case 111	Case 112	Case 113
	Z 1 C 30	Z 1 C 45	Z 1 C 60	Z 2 C 30	Z 2 C 45	Z 2 C 60	Z 3 C 30	Z 3 C 45	Z 3 C 60
# of Stations with RE Risk Change	1	2	1	10	21	27	42	45	46
ORCI	-0.0605	-0.0081	0.0657	0.7435	1.5832	1.7290	6.4865	8.9248	8.4413
# of Stations with LC Risk Change	0	6	14	14	14	12	32	36	38
LCRCI	0.0000	-0.6198	-0.9364	1.5090	1.7608	1.8896	7.3917	9.5295	8.7241

The test cases from Table 5-48 performed at the 90 percent loading scenario show similar results. The values of the ORCI and LCRCI are presented below in Table 5-50. The trends found in Table 5-49 are the same found above in Table 5-50. In general, the values of ORCI and LCRCI increase with the cycle length. Additionally, metering zone 1 tends to yield a negative safety impact while metering zones 2 and 3 have a positive safety impact.

Table 5-50. Summary of ORCI and LCRCI for Zone TC Cases at 90 Percent Loading

	Test Case ID								
	Case 117	Case 118	Case 119	Case 123	Case 124	Case 125	Case 129	Case 130	Case 131
	Z 1 C 30	Z 1 C 45	Z 1 C 60	Z 2 C 30	Z 2 C 45	Z 2 C 60	Z 3 C 30	Z 3 C 45	Z 3 C 60
# of Stations with RE Risk Change	8	3	1	17	20	28	25	30	34
ORCI	-0.2957	-0.3318	-0.0881	1.7783	2.3628	3.5568	5.2674	6.7534	7.0750
# of Stations with LC Risk Change	8	8	6	4	4	8	12	16	12
LCRCI	-1.5900	-1.7860	-1.5152	0.9005	0.9776	1.4372	3.7512	4.7700	3.8661

Note that for the runs performed at both the 90 percent and 100 percent loading scenarios the values of the ORCI and LCRCI are correlated with the number of stations that show a rear-end or lane-change crash risk, respectively. This means that greater safety benefits are found when a larger section of the freeway is affected by the ramp metering strategy. Therefore, it makes sense that metering zone 3 would provide the best results since this zone is the largest of the three zones considered in this study; this zone had 7 metered ramps and spanned a length of 4.5 miles. Although zone 1 is almost 2.5 miles long, the reason that large safety benefits are not realized when zone 1 is metered is that there is a bottleneck that occurs in the downstream end of this zone at the Interstate-4 / S. R. 408 Interchange.

The positive values of ORCI and LCRCI when zones 2 and 3 are metered show that net safety benefits are realized for these scenarios. However, looking at the individual loop detector stations shows that while most stations exhibit a decrease in the respective crash risk, at some locations the crash risk is increased significantly. This implies that ramp metering, like route diversion, has the potential to cause crash migration – the reduction of the crash risk at one area combined with the increase in the crash risk at another. Because of this phenomenon the crash risk vs. location is examined to determine the strength of its effects. Figure 5-35 shows a plot of the rear-end crash risk for the test cases that are shown in Table 5-48 for the 100 percent loading case.
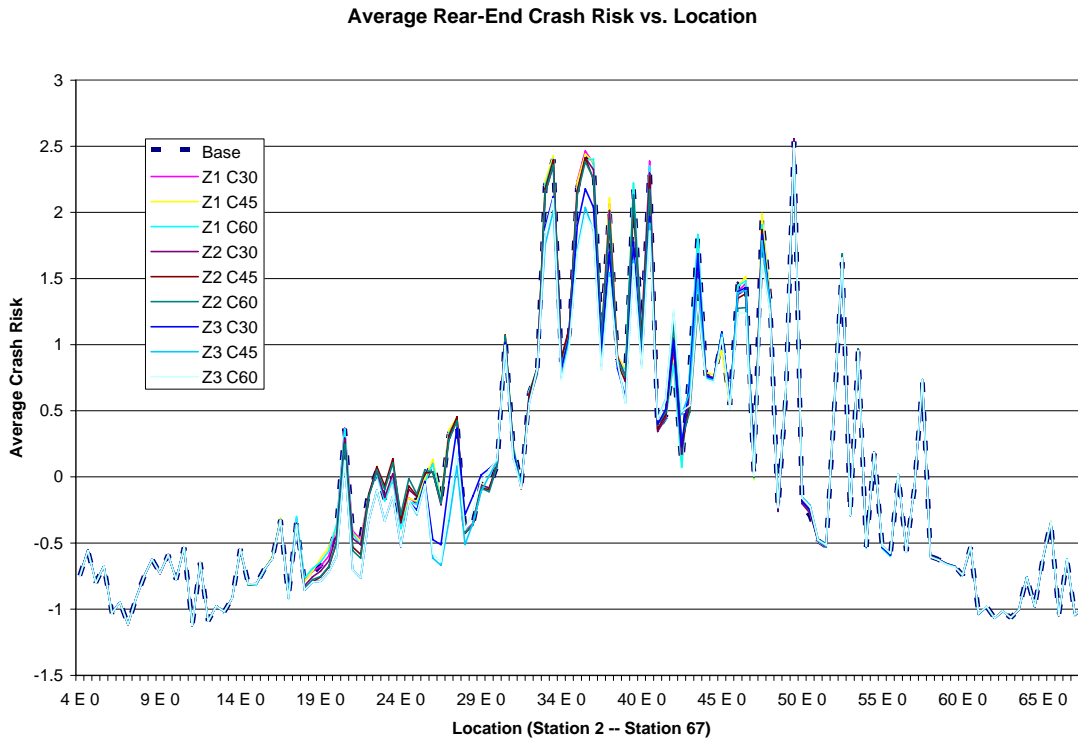
Figure 5-35. Average Rear-End Crash Risk vs. Location for Zone TC Cases at 100 Percent Loading

Figure 5-35 is rather confusing due to the large number of curves representing the different test cases. Additionally, the scale of the plot is relatively large compared to the differences in the crash risk. Zooming in on individual areas of the plot could be done (similar to the route diversion cases) however this would require numerous plots as the area of effect is spread out over multiple stations. Instead, a plot of the difference in the rear-end crash risk for each case compared to the base case vs. location is created for the stations that were affected by ramp metering. These crash difference values are found by subtracting the crash risk at a particular location from the base case to determine the difference. Positive values imply a reduction in the crash risk while negative values show an increase in the crash risk. This plot is shown below in Figure 5-36.

200

Average Rear-End Crash Risk Difference vs. Location
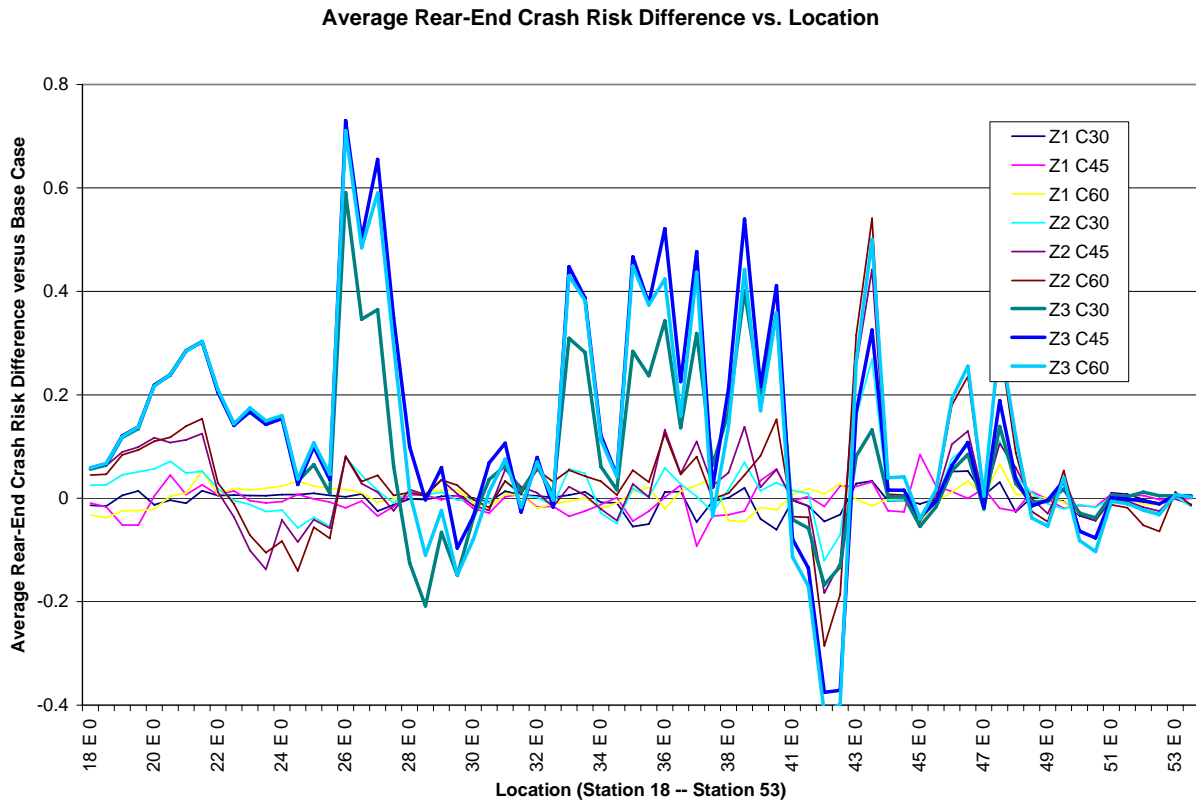
Figure 5-36.   Average Rear-End Crash Risk Difference vs. Location for Zone TC Cases at 100 Percent Loading

From Tables 5-49 and 5-50, the best Zone algorithm, traffic-cycle realization cases are those that metered zone 3. In Figure 5-36, it is clear to see that for these cases the crash risk is increased between Stations 28-30 and 41-42 (denoted by a negative crash risk difference for these locations). These two locations have the largest increases in the crash risk compared to the other, trivial, increases elsewhere. The rear-end crash increase at Stations 28-30 occurs due to the congested conditions that typically persist at these locations during the base case. When ramp metering is implemented the tail of the queue conditions, which typically occurs just upstream of this location, moves downstream near Stations 28-30. This causes slightly more

congestion which increases the crash risk compared to the typical (base) conditions at this location. This movement of congestion throughout the network is the reason that the output of two rear-end crash risk regime models needed to be normalized. Ramp metering causes areas of congestion (regime 1 conditions) to become un-congested (regime 2 conditions) and vice versa. Only by combining the models were the crash risk effects able to be determined.

The crash risk increase at Stations 41-42 occurs for the same reason. Congested conditions from the downtown area move slightly downstream as the traffic volume in the downtown area decreases. This, in turn, increases the congestion around Stations 41-42 which causes increased values of the rear-end crash risk. Although the crash risk increases are rather large in these two areas they are considered allowable for two reasons. The first is that they occur at locations that typically have a low rear-end crash risk value compared to surrounding locations. This can be seen by examining Figure 5-37, below, which shows a plot of the base rear-end crash risk at the 100 percent loading scenario. At Stations 27-28 the average crash risk is 0.0 (which is already low) while at Stations 41-42 the average crash risk is 0.45. Just upstream and downstream of Stations 41-42 the rear-end crash risk value is 2.3 and 1.8, respectively. Therefore, since the crash risk is lower at Stations 41-42 than the surrounding stations, raising it slightly (to 0.65) in order to increase the overall safety of the network seems like a reasonable compromise. The second reason to allow this crash risk increase is that the overall rear-end safety benefit is large and amounts to an average decrease of the rear-end crash risk of about 0.2 per location (34 stations). Increasing the rear-end risk by 0.4 for a small area (just 4 stations) in order to reduce the risk by 0.2 over a much larger area seems reasonable.

Average Rear-End Crash Risk vs. Location
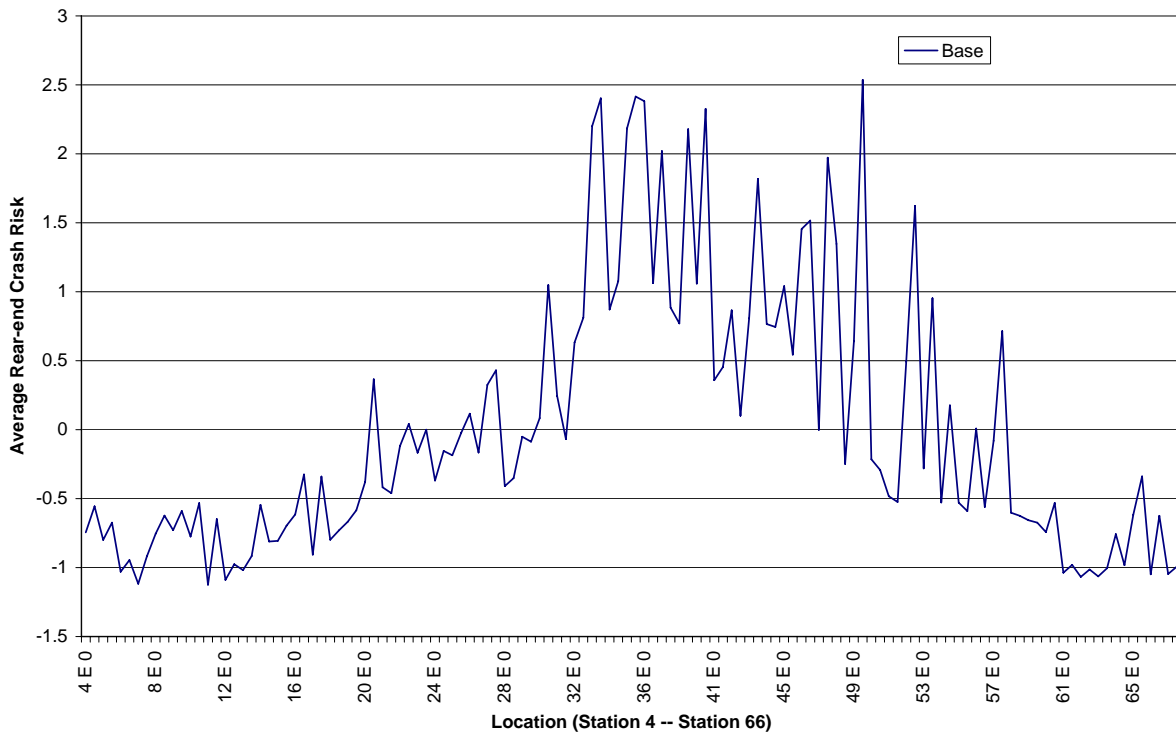
Figure 5-37. Average Rear-End Crash Risk for Base Case at 100 Percent Loading

The plot of the lane-change crash risk difference vs. location is given below in Figure 5-38 for the 100 percent loading scenarios. As shown in Figure 5-38, the best Zone traffic-cycle realization cases (metering zone 3) causes a decrease in the lane-change crash risk at the upstream locations while implementing this method increases the lane-change crash risk slightly between Stations 29 to 43 (which encompasses the downtown area). The decrease in the crash risk is much more substantial than (about 8 times the magnitude of) the increase in the crash risk. As shown in Figure 5-39, the location where the lane-change crash risk is increased due to the Zone ramp metering is an area where the lane-change crash risk is already high along the network corridor. Therefore, care would have to be taken when implementing the ramp

203

metering due to the increase in the lane-change crash risk at a location where it is already high. However, the increase is only about 2% of the original value so it should not have that great of an effect. Metering zones 1 or 2 does not cause this increase in the crash risk at Stations 29 to 43 but the lane-change safety benefit provided by these scenarios is minimal.
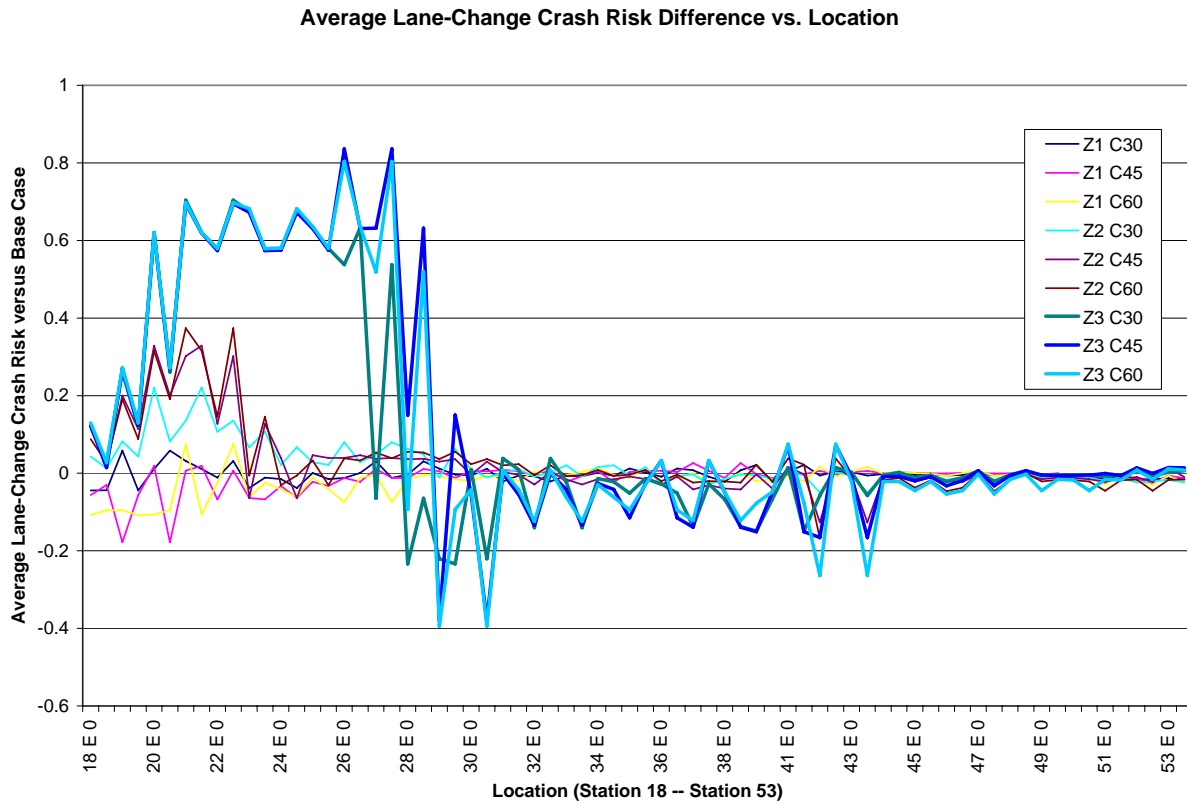
Figure 5-38. Average Lane-Change Crash Risk Difference vs. Location for Zone TC Cases at 100 Percent Loading

Average Lane-Change Crash Risk vs. Location

Figure 5-39. Average Lane-Change Crash Risk for Base Case at 100 Percent Loading

For the cases performed at the 90 percent loading scenario, the results are similar. Figure 5-40 shows the difference in the rear-end crash risk while Figure 5-41 shows the difference in the lane-change crash risk for the various test cases.

Average Rear-End Crash Risk Difference vs. Location
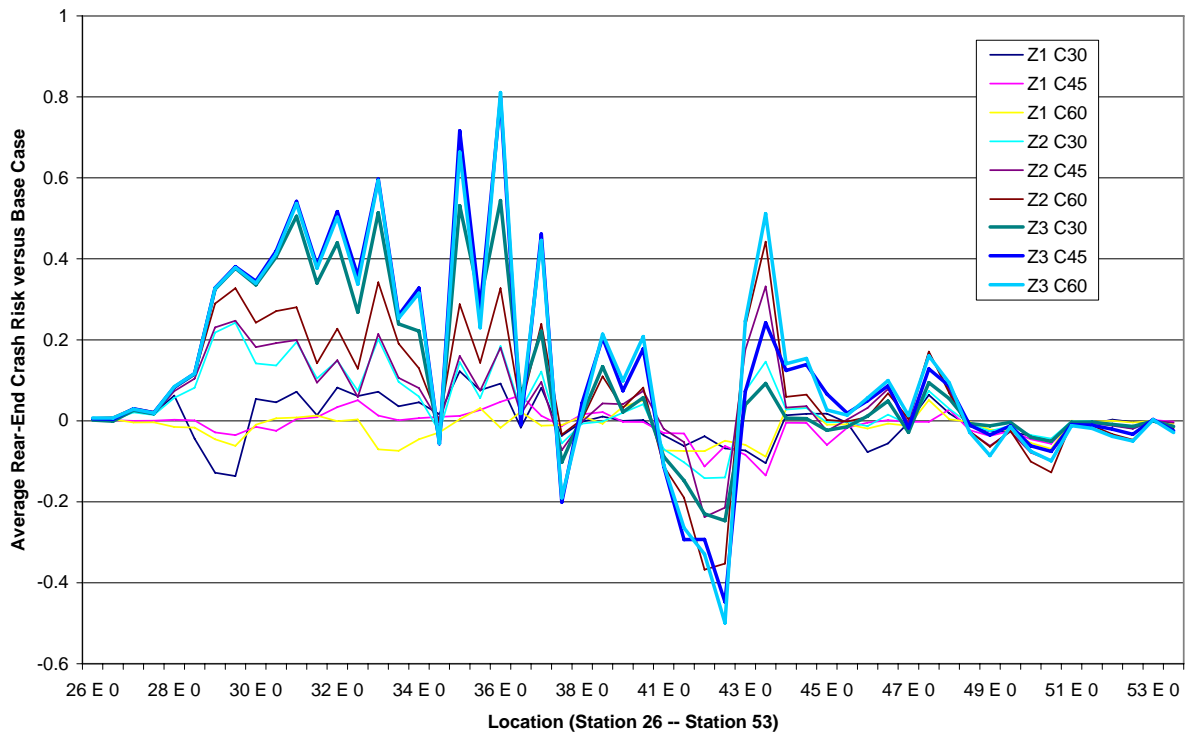
Figure 5-40. Average Rear-End Crash Risk Difference vs. Location for Zone TC Cases at 90 Percent Loading

Average Lane-Change Crash Risk Difference vs. Location

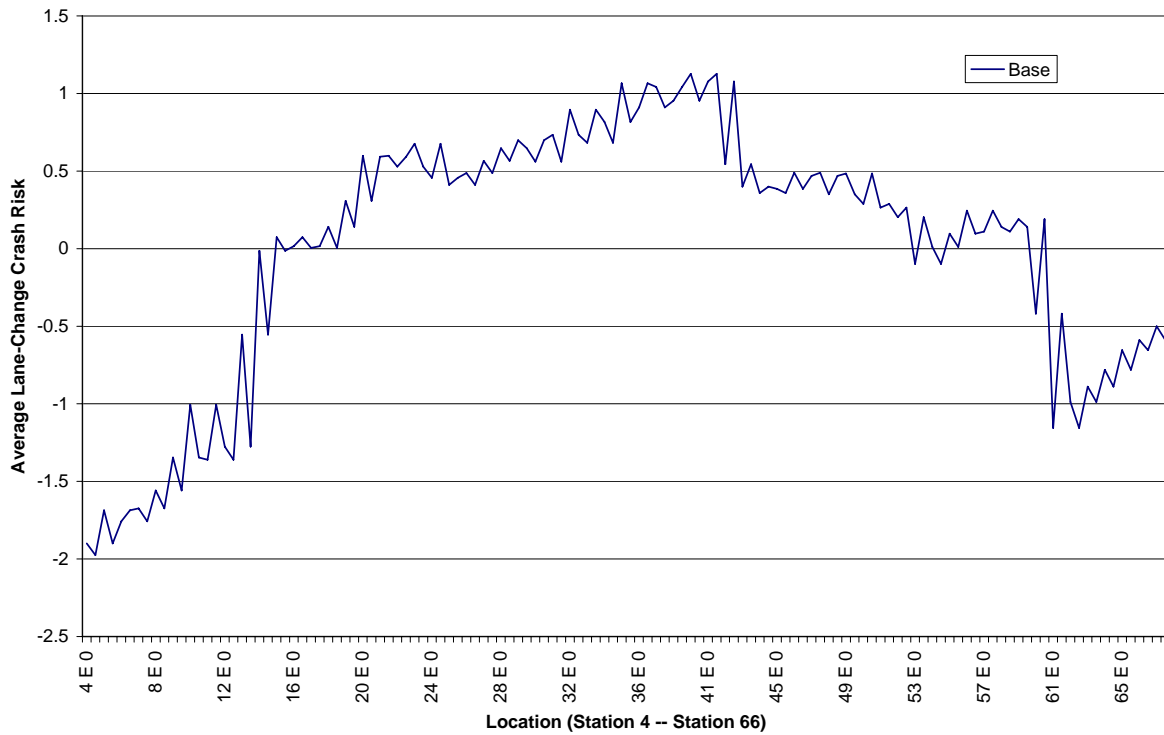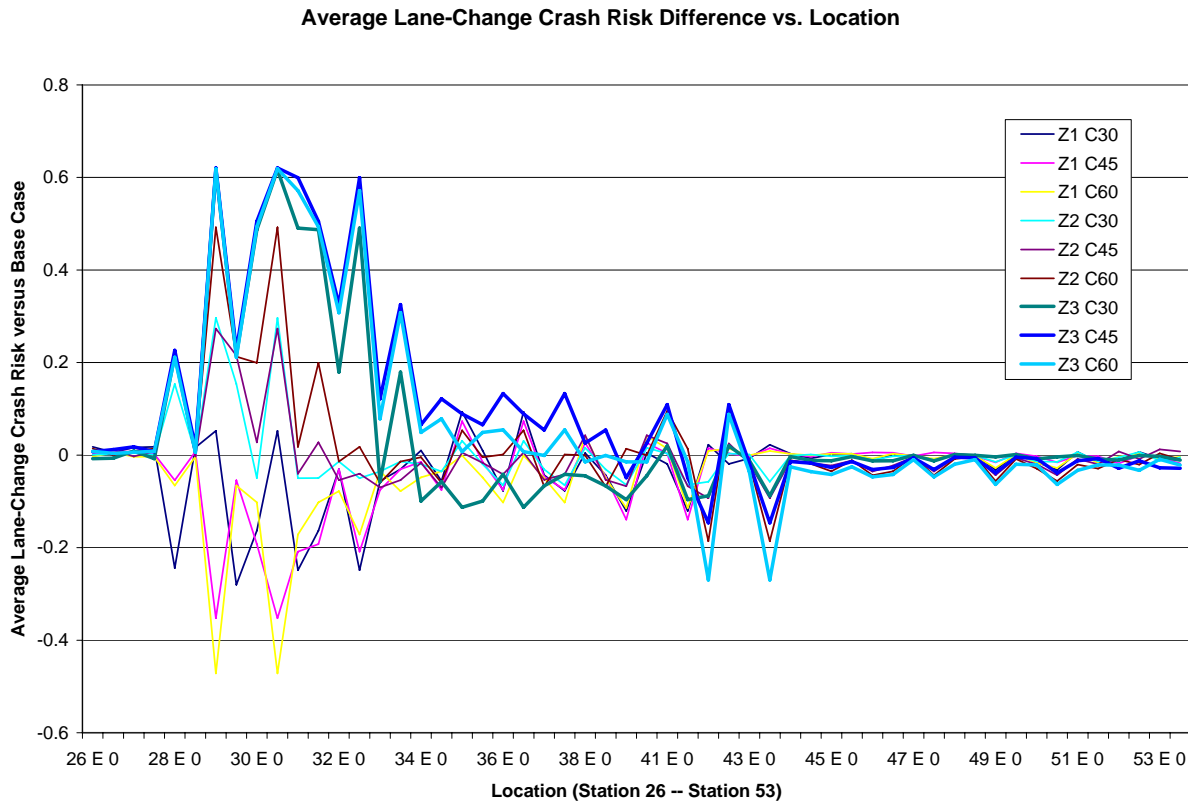**Figure 5-41. Average Lane-Change Crash Risk Difference vs. Location for Zone TC Cases at 90 Percent Loading**

The plot of the rear-end crash risk difference shows that for the best zone ramp metering case the crash risk is only increased at Stations 41 to 42. Once again this is just an isolated instance and the base crash risk at this location is already lower than the surrounding stations so the small crash risk increase can be overlooked for the greater crash risk decrease. Figure 5-41 shows that at the 90 percent loading scenario the lane-change crash risk also increased for just a small area of the freeway as compared to the 100 percent loading scenarios. Therefore, this section shows that the best case involving the Zone algorithm with the traffic-cycle realization is to meter zone 3 using a 60 second cycle length. Although this method causes some crash migration effects, the locations that experience high levels of rear-end crash risk migration are

207

areas with traditionally low rear-end crash risk values. The effects of the lane-change crash risk migration is small compared to the overall reduction in the lane-change crash risk and can therefore be tolerated in order to reduce the overall lane-change crash risk across the network.

5.3.3 Analysis of One-Car-Per-Cycle Realization Strategies

The previous two sections examined both the ALINEA and Zone algorithm when used with the traffic-cycle realization. The next group of ramp metering cases that are examined are those cases that implement the one-car-per-cycle realization as opposed to the traffic-cycle realization. The specific cases from the experimental design that are analyzed in this group are displayed below in Table 5-51.

Table 5-51. Test Cases Representing One-Car-Per-Cycle Realization of Zone and ALINEA

Case Number	Percent Loading	Metered Zone	Algorithm	Cycle Length
103	100	1	Zone	OCPC
104	100	1	ALINEA	OCPC
109	100	2	Zone	OCPC
110	100	2	ALINEA	OCPC
115	100	3	Zone	OCPC
116	100	3	ALINEA	OCPC
121	90	1	Zone	OCPC
122	90	1	ALINEA	OCPC
127	90	2	Zone	OCPC
128	90	2	ALINEA	OCPC
133	90	3	Zone	OCPC
134	90	3	ALINEA	OCPC

The values of ORCI and LCRCI have been calculated for both the 100 percent loading scenarios and the 90 percent loading scenarios and are presented below in Tables 5-52 and 5-53, respectively. The tables reference the test case numbers presented above in Table 5-51 as well as describes the cases by the metering type and traffic realization. For example, case 104 (Z 1

ALINEA OCPC) represents using the ALINEA algorithm to meter the ramps that comprise zone 1 while implementing the one-car-per-cycle (or OCPC) realization.

Table 5-52. Summary of ORCI and LCRCI for OCPC Cases at 100 Percent Loading

	Test Case ID					
	Case 103	Case 104	Case 109	Case 110	Case 115	Case 116
	Z 1 OCPC	Z 1 ALINEA OCPC	Z 2 OCPC	Z 2 ALINEA OCPC	Z 3 OCPC	Z 3 ALINEA OCPC
# of Stations with RE Risk Change	5	7	0	36	3	39
ORCI	0.1578	0.0883	0.0000	5.2296	0.1139	7.2222
# of Stations with LC Risk Change	0	8	4	26	0	34
LCRCI	0.0000	1.5736	-0.4676	8.1495	0.0000	12.0102

Table 5-53. Summary of ORCI and LCRCI for OCPC Cases at 90 Percent Loading

	Test Case ID					
	Case 121	Case 122	Case 127	Case 128	Case 133	Case 134
	Z 1 OCPC	Z 1 ALINEA OCPC	Z 2 OCPC	Z 2 ALINEA OCPC	Z 3 OCPC	Z 3 ALINEA OCPC
# of Stations with RE Risk Change	1	5	3	34	6	37
ORCI	-0.0719	0.0029	-0.4136	5.8677	-0.7912	5.7074
# of Stations with LC Risk Change	6	2	2	20	6	22
LCRCI	-1.5124	-0.5614	-0.7378	6.6130	-1.9127	8.3968

For each of the crash risk performance measures (ORCI and LCRCI) almost every test case using the ALINEA algorithm with the one-car-per-cycle realization outperforms using the Zone Algorithm with the one-car-per-cycle-realization. This is expected based on the previous findings. In the experimental design to determine the best ALINEA parameters, the safety along the freeway corridor increased as the cycle length decreased. This shows that when using ALINEA, allowing smaller platoons of vehicles onto the freeway more frequently provides the

best results. Therefore, it would make sense that the one-car-per-cycle realization would provide good safety results since this method allows only a single vehicle to enter the freeway at an increased frequency. Similarly, the previous section showed that using a longer cycle length improves the ability of the Zone algorithm to decrease the two crash risk values. Therefore, implementing the one-car-per-cycle realization, which uses the shortest cycle lengths, goes against this trend and, therefore, does not perform well.

Additionally, ALINEA is more restrictive than the Zone algorithm at higher levels of congestion. As seen in Equation 5, the Zone algorithm includes a term that accounts for the spare capacity of the zone. This spare capacity is found by examining all mainline loop detectors within the zone, not just those near entrance ramps. Therefore, if congestion is increased near the ramps that are being metered but the detectors still show a relatively low traffic density the Zone algorithm will allow more vehicles into the network to fill this spare capacity. The ALINEA algorithm does not consider the spare capacity and would therefore be more restrictive. This will lead to a reduction in the safety measures of effectiveness (ORCI and LCRCI) for the Zone algorithm as allowing more vehicles into the network would increase the crash risk. When this is combined with the one-car-per-cycle realization, at some ramps vehicles enter the freeway almost as soon as they arrive at the ramp. Therefore, the Zone algorithm with one-car-per-cycle methodology shows no great difference between the metering and non-metering case.

Figures 5-42 and 5-43 below show the differences in the rear-end and lane-change crash risk vs. location, respectively, for the cases run at 100 percent loading.

Figure 5-42. Average Rear-End Crash Risk Difference vs. Location for OCPC Cases at 100 Percent Loading

Average Lane-Change Crash Risk Difference vs. Location

Figure 5-43. Average Lane-Change Crash Risk Difference vs. Location for OCPC Cases at 100 Percent Loading

Once again Figures 5-42 and 5-43 show that ramp metering causes a crash migration effect when the best ALINEA OCPC case (metering zone 3) is implemented. However, as evidenced by the positive values of ORCI and LCRCI for the one-car-per-cycle realization performed with the ALINEA algorithm, the overall effect of the ALINEA cases is a reduction in the crash risk through the network corridor. The rear-end crash risk is increased in a localized area and caused primarily by the creation of a new bottleneck area just downstream of the downtown area. The lane-change crash risk increases throughout the downtown area (Stations 32 to 40) but this increase is rather trivial compared to the crash risk decrease that is noted.

Similar plots are created for the 90 percent loading scenarios and are presented below in Figures 5-44 and 5-45. The same trends exist for metering at the 90 percent loading case. Any metering performed at zone 1 does little to reduce the crash risk significantly. Additionally, metering any zone using the Zone algorithm and one-car-per-cycle realization does not affect the crash risk substantially. The increase in the rear-end crash risk caused by the ALINEA strategies occurs near Stations 41 to 43 which is traditionally a low rear-end crash risk region. For the lane-change crash risk, implementing the ALINEA ramp metering strategy at the 90 percent loading scenario does not show any evidence of crash migration.

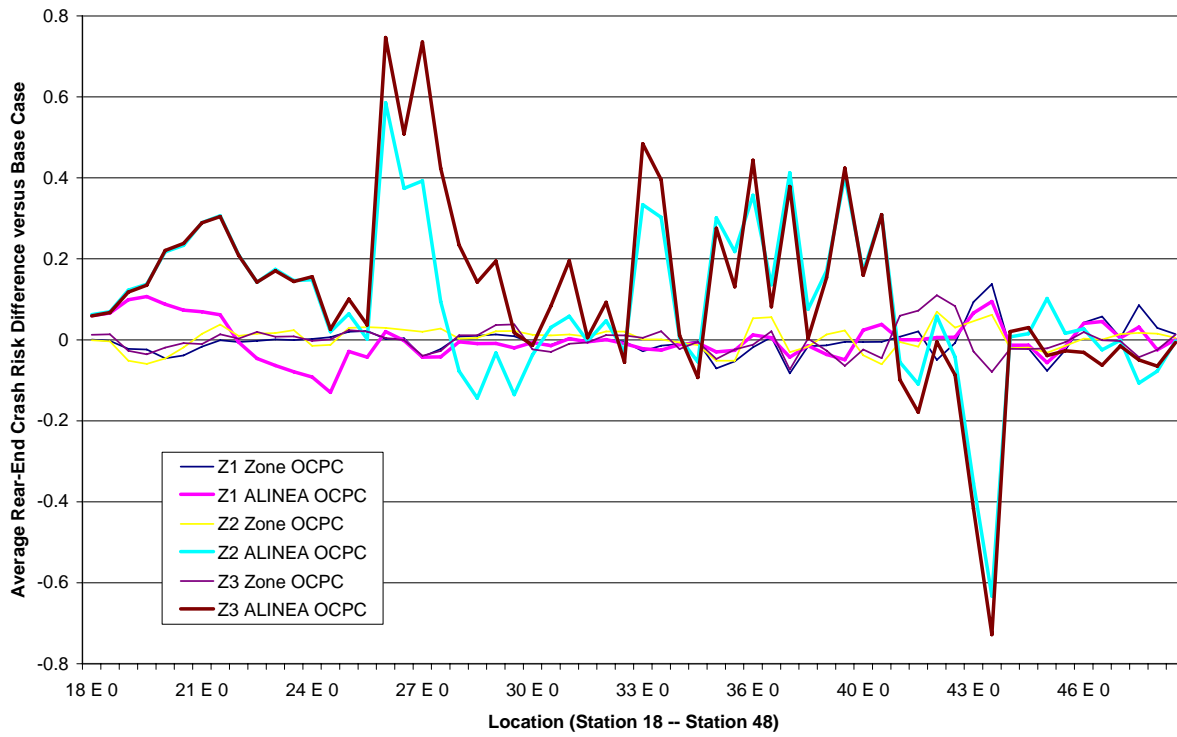**Average Rear-End Crash Risk Difference vs. Location**
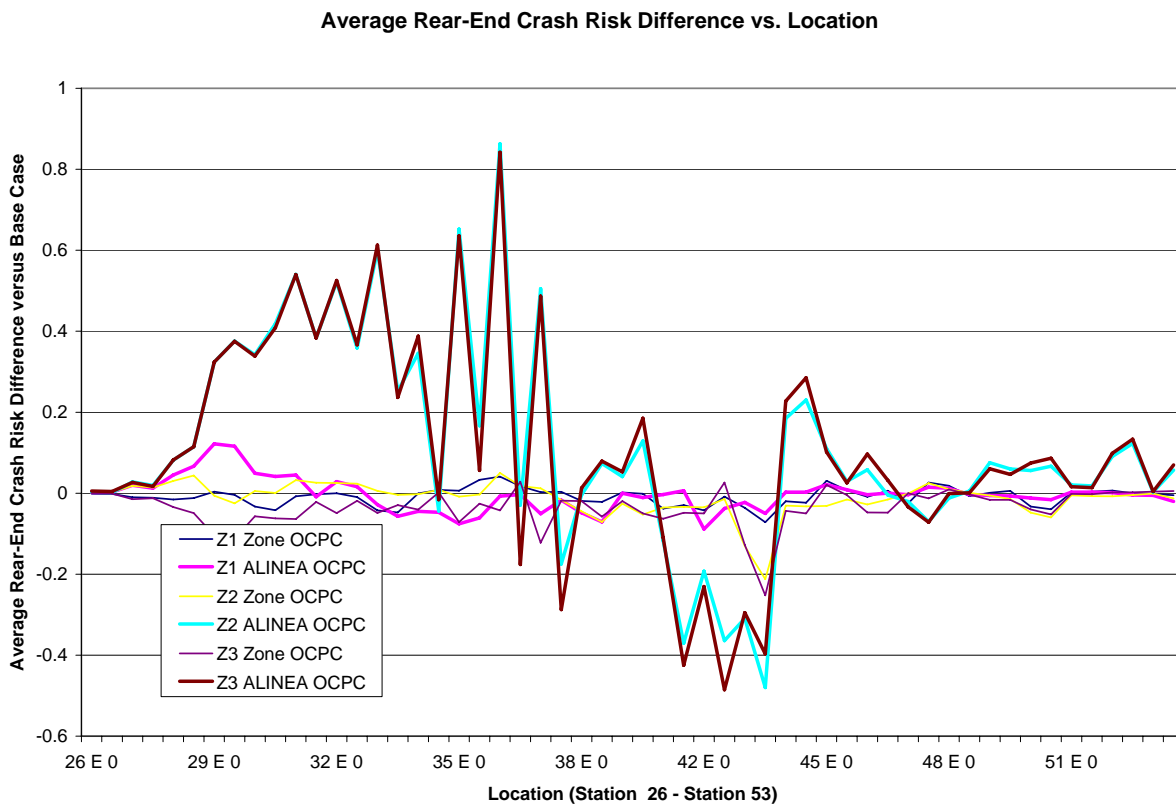
Figure 5-44. Average Rear-End Crash Risk Difference vs. Location for OCPC Cases at 90 Percent Loading

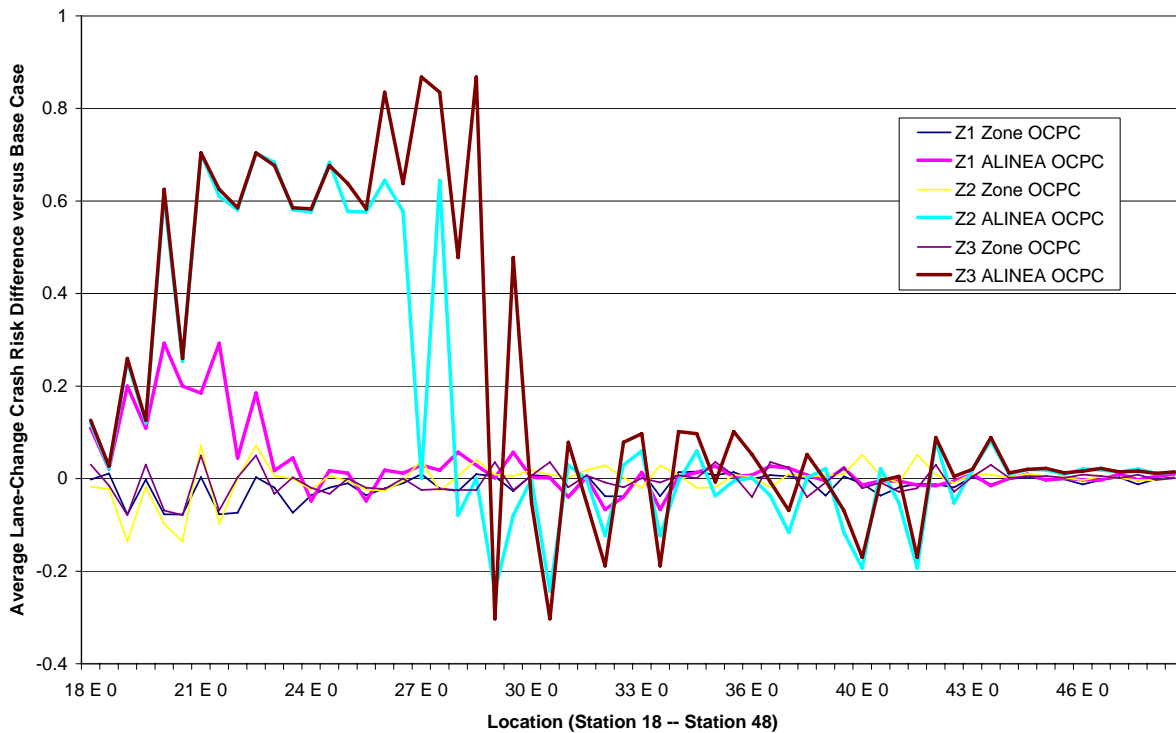**Average Lane-Change Crash Risk Difference vs. Location**
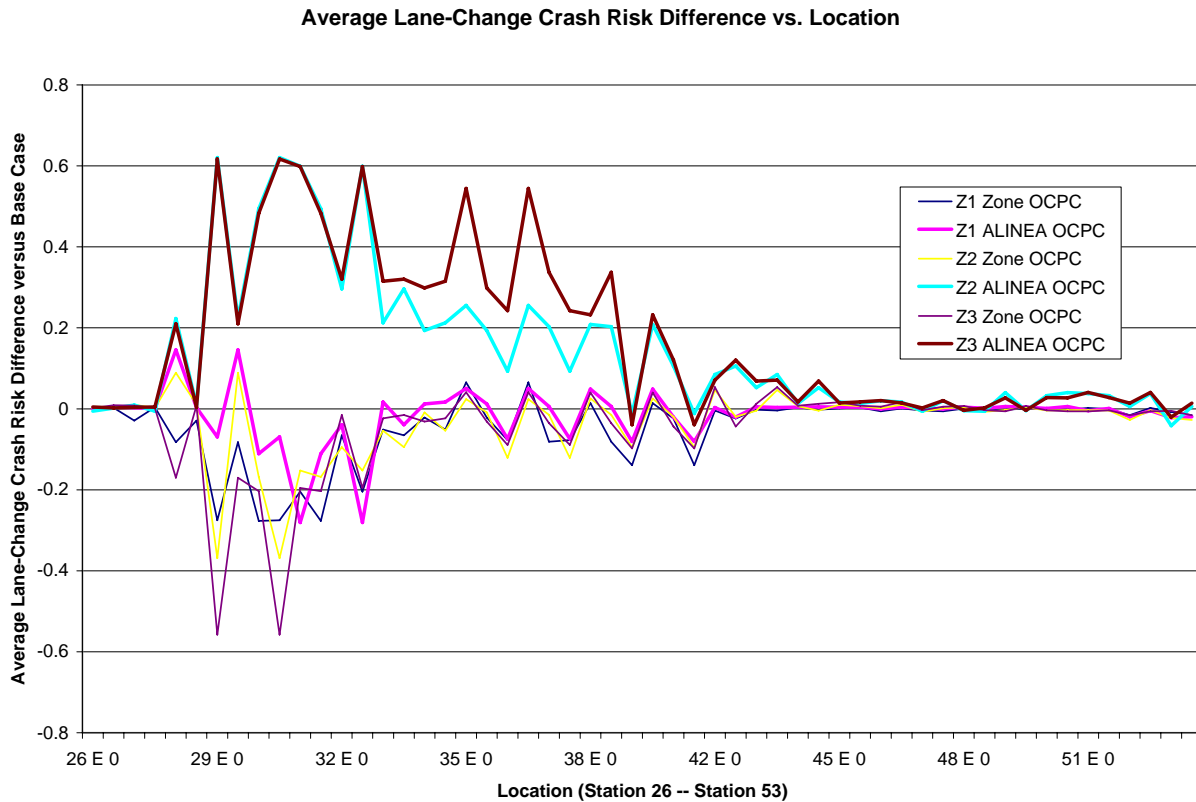
Figure 5-45. Average Lane-Change Crash Risk Difference vs. Location for OCPC Cases at 90 Percent Loading

Therefore, this section shows that when the one-car-per-cycle realization method is applied to the ramp metering algorithms that are being considered, ALINEA outperforms the Zone algorithm at reducing both the rear-end and lane-change crash risk. Also, the trends in this section show that metering zone 1 with either the ALINEA or Zone algorithm shows very minimal, though existent, crash risk benefits compared to metering zones 2 or 3.

5.3.4 Determining the Final "Best" Ramp Metering Strategy

The purpose of the previous sections was to compare similar ramp metering strategies to determine the best implementation methods for these strategies. For example, Section 5.3.1

214

found that the best implementation of the ALINEA algorithm with the traffic-cycle realization is to use a small cycle length of 30 seconds and a critical occupancy of 0.17 (found from the experimental design given in Table 4-5). Section 5.3.2 found that when the Zone algorithm is used with the traffic-cycle realization a longer cycle length is needed (60 seconds) to provide the best safety results. Section 5.3.3 showed that the one-car-per-cycle implementation method with the Zone algorithm causes negligible safety benefits while the one-car-per-cycle implementation of the ALINEA algorithm significantly decreases both crash risk measures. In all cases, metering zones 2 and 3 provided the best safety results. Previous results have shown that metering zone 1 (using any method) causes a negligible change in the crash risk on the network compared to metering the other two zones. This occurs because zone 1 is located immediately upstream of the bottleneck that occurs at the Interstate-4 / S. R. 408 Interchange. Therefore, zone 1 scenarios will be excluded from the comparison in this section in order to reduce the complexity of this analysis. However, these strategies now need to be compared against each other to determine which metering strategy provides the best overall crash risk change in the downtown portion of Interstate-4.

Table 5-54 shows the remaining test cases at the 100 percent loading level as well as the summarized ORCI and LCRCI values. The test cases are denoted with the same nomenclature that has been used in previous sections. A similar table is presented in Table 5-55 for the test cases run at the 90 percent loading scenario. Note that in these tables the strategies that use the traffic-cycle realization are denoted with the abbreviation TC while the one-car-per-cycle abbreviation used is OCPC.

Table 5-54. Summary of ORCI and LCRCI for Best Ramp Metering Cases at 100 Percent Loading

	Test Case ID					
	Case 107	**Case 108**	**Case 110**	**Case 113**	**Case 114**	**Case 116**
	Z 2 Zone TC	**Z 2 ALINEA TC**	**Z 2 ALINEA OCPC**	**Z 3 Zone TC**	**Z 3 ALINEA TC**	**Z 3 ALINEA OCPC**
# of Stations with RE Risk Change	27	37	39	46	48	42
ORCI	1.7290	9.9240	5.4254	8.4413	12.7085	7.1622
# of Stations with LC Risk Change	20	40	34	48	40	44
LCRCI	1.9229	10.4808	8.1703	8.2556	15.5739	12.1375

Table 5-55. Summary of ORCI and LCRCI for Best Ramp Metering Cases at 90 Percent Loading

	Test Case ID					
	Case 125	**Case 126**	**Case 128**	**Case 131**	**Case 132**	**Case 134**
	Z 2 Zone TC	**Z 2 ALINEA TC**	**Z 2 ALINEA OCPC**	**Z 3 Zone TC**	**Z 3 ALINEA TC**	**Z 3 ALINEA OCPC**
# of Stations with RE Risk Change	28	37	32	35	41	34
ORCI	3.5568	5.0898	5.8645	6.9996	5.9780	5.6343
# of Stations with LC Risk Change	18	30	28	24	32	28
LCRCI	1.3670	10.3241	7.2852	4.1848	11.1706	8.9160

From Table 5-54, comparing the values of the ORCI and LCRCI shows that the best ramp metering combination at the 100 percent loading scenario is using the ALINEA strategy with the traffic-cycle realization. From Table 5-55, the best metering combination at the 90 percent loading scenario is not so clear. The ALINEA TC method provides the highest LCRCI values as well as the second highest ORCI for each metered zone. However, the other cases have a higher values of ORCI which shows they are better at reducing the rear-end crash risk. Therefore, no judgment about the best case at the 90 percent loading scenario could be made until the effects of crash migration are considered.

To examine for possible crash migration issues of this best ramp metering strategy a plot of the rear-end crash risk difference and lane-change crash risk difference vs. location is produced. These plots are presented in Figures 5-46 and 5-47, respectively, for the 100 percent loading scenario.
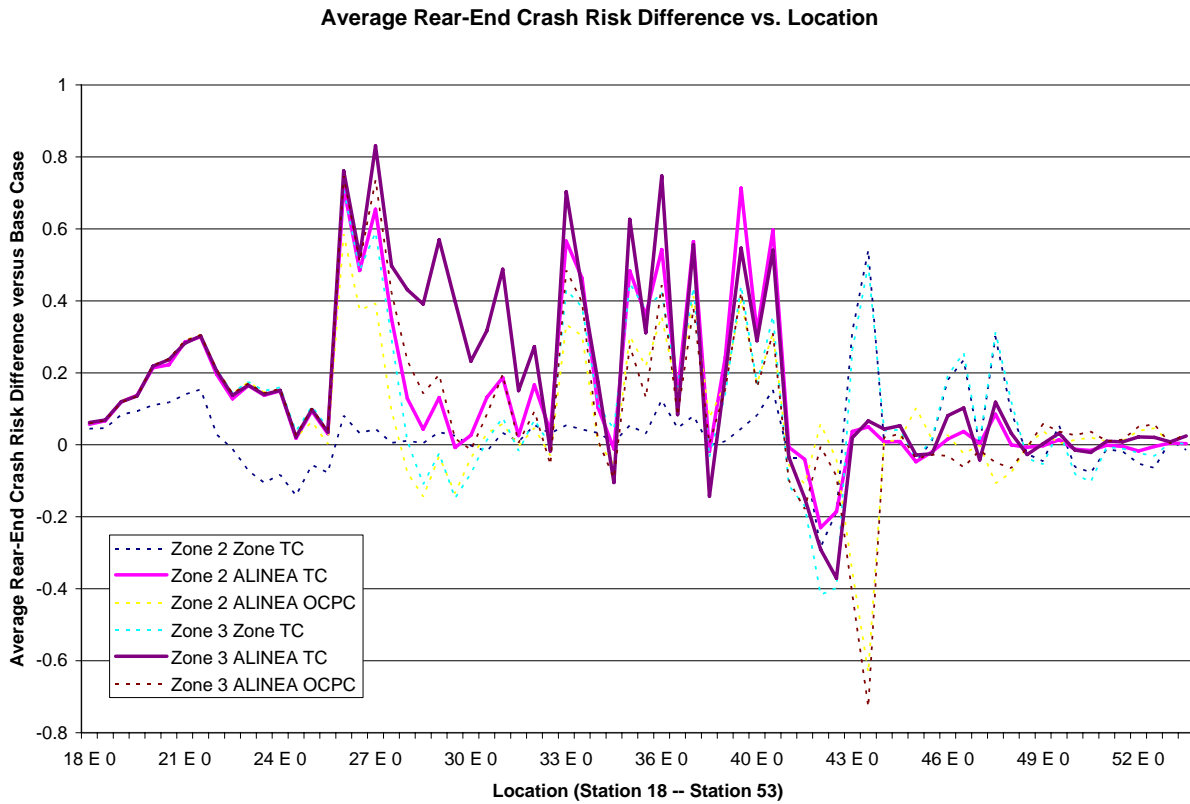

Figure 5-46. Average Rear-End Crash Risk Difference vs. Location for Best Cases at 100 Percent Loading

Average Lane-Change Crash Risk Difference vs. Location

Figure 5-47. Average Lane-Change Crash Risk Difference vs. Location for Best Cases at 100 Percent Loading

As shown in Figure 5-46, the rear-end crash migration is minimal for the ALINEA traffic-cycle strategy compared with the other well-performing metering scenarios. The crash risk only increases significantly only for the area between Stations 41 and 42. This risk increase is much less than a similar increase experienced by other strategies. The lane-change crash risk increases slightly between stations 28 and 43 but this increase is very small in magnitude and does not compare to the crash risk decrease realized just upstream.

Similar plots are created for runs performed at the 90 percent loading scenario. These plots are produced below in Figures 5-48 and 5-49. From Figure 5-48 it is seen that using the ALINEA strategy with the traffic-cycle realization causes a crash risk increase from stations 37

to 43. Although the magnitude of the increase is small from Stations 37 to 40, between Stations 41 to 43 this crash risk increase is substantial. The other metering strategies show a similar crash risk increase at Stations 41 to 43 but not to the magnitude that is realized with the ALINEA TC method. However, for the lane-change crash risk (presented in Figure 5-49) the ALINEA TC method causes greater crash risk decreases and less crash migration.
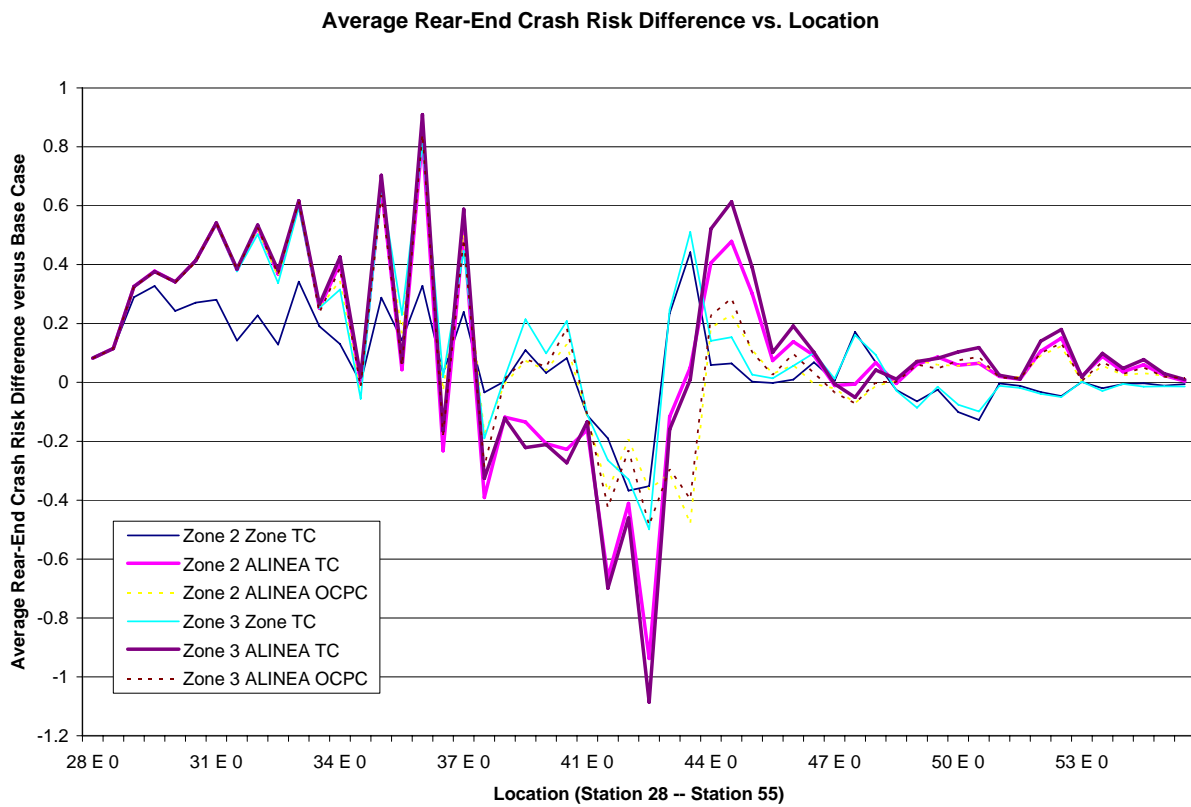
Figure 5-48. Average Rear-End Crash Risk Difference vs. Location for Best Cases at 90 Percent Loading

Average Lane-Change Crash Risk Difference vs. Location
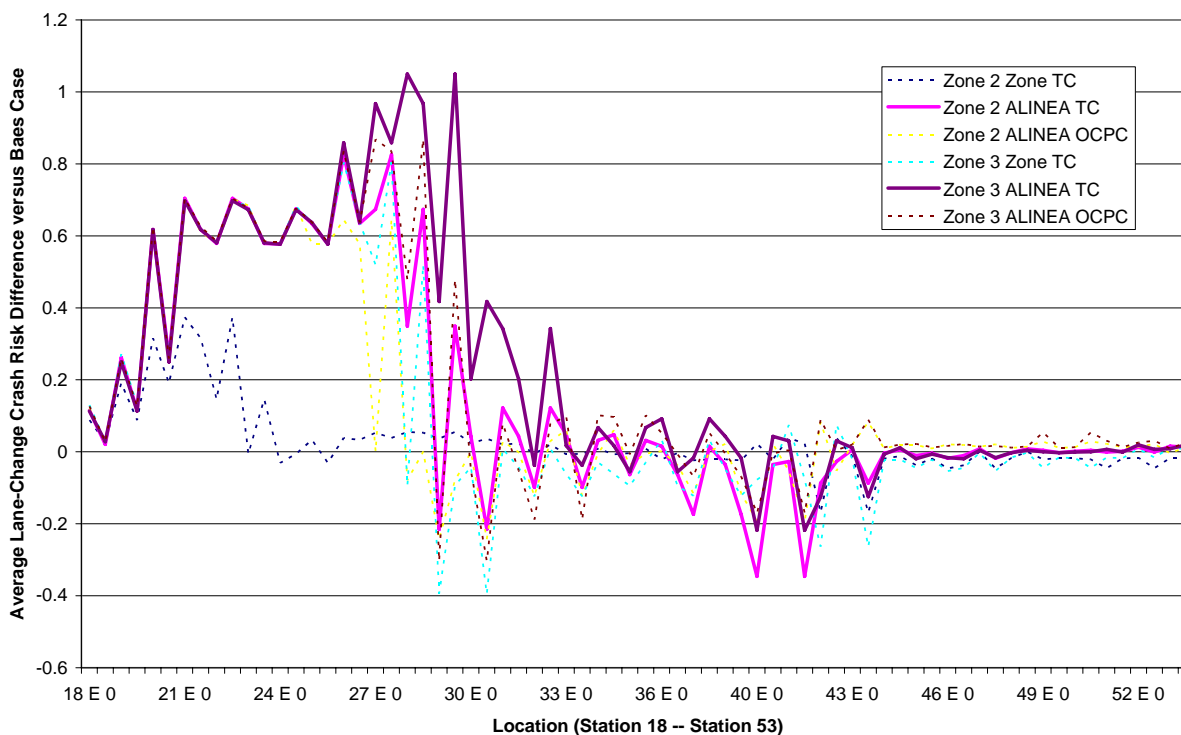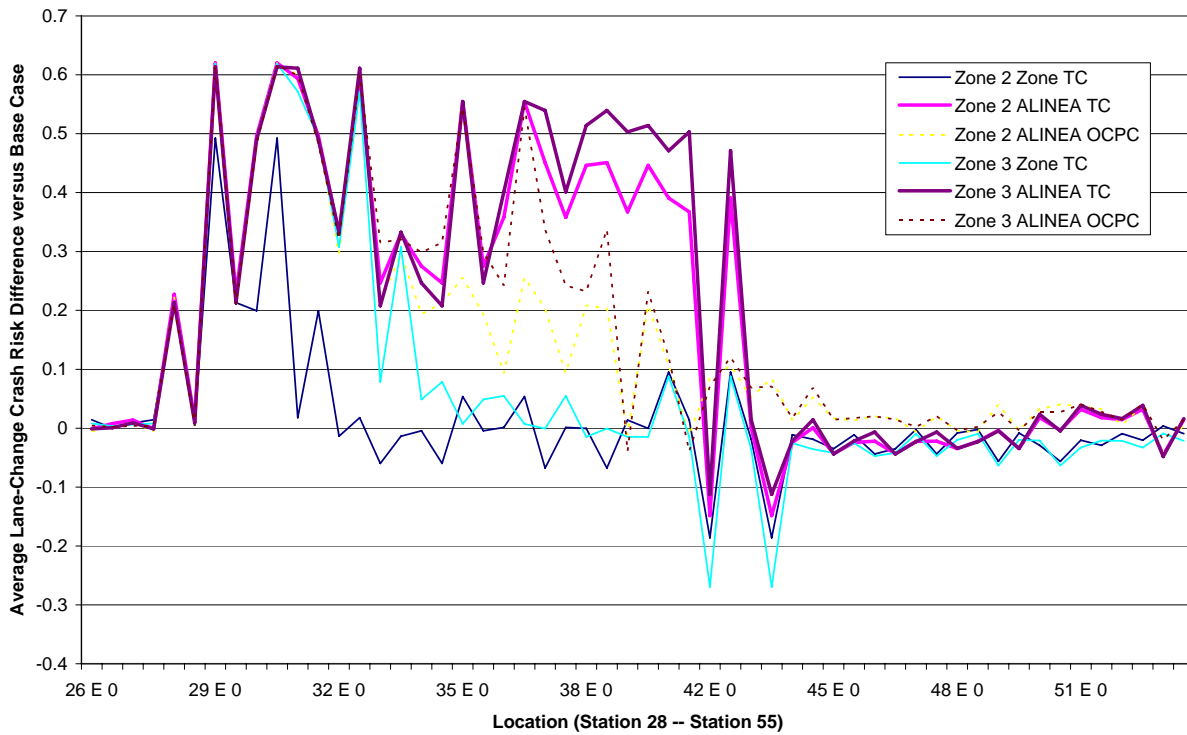

Figure 5-49. Average Lane-Change Crash Risk Difference vs. Location for Best Cases at 90 Percent Loading

Therefore, at the 90 percent loading scenario, there is significant rear-end crash risk migration caused by the best ALINEA traffic-cycle strategy. In fact, the largest increase in the rear-end crash risk (1.08 at Station 42 E 1) is greater than the largest decrease in the rear-end crash risk (0.91 at Station 36 E 0). This amount of crash migration has never occurred in any of the scenarios presented before and should not be considered as reasonable. The next best strategy appears to be using the ALINEA strategy with the one-car-per-cycle realization as evidenced by the high values of ORCI and LCRCI in Table 5-55. The crash migration that occurs for this scenario is much less than the ALINEA traffic-cycle strategy and it provides reasonable safety benefits.

220

5.3.5 Travel Time Analysis

While ramp metering has a positive effect on the rear-end and lane-change crash risk along the Interstate-4 corridor there is the potential that delaying vehicles on the on-ramps will have negative impacts on the operational capabilities of the network. In order to account for this fact the total network travel time was calculated for each of the scenarios performed and compared. The network travel time for all runs performed in this portion of the experimental design is given below in Table 5-56. The average travel time considered for this table was the overall network travel time which included both the decreased travel time on the mainline freeway and the increased travel times of vehicles delayed at the metered on-ramps.

Table 5-56. Travel Time Summary for Ramp Metering Scenarios

Case Number	Percent Loading	Metered Zone	Algorithm	Cycle Length	Average Travel Time Increase
99	100	1	Zone	30	0.77%
100	100	1	Zone	45	1.18%
101	100	1	Zone	60	1.57%
102	100	1	ALINEA	BEST	-0.84%
103	100	1	Zone	OCPC	-0.22%
104	100	1	ALINEA	OCPC	0.35%
105	100	2	Zone	30	1.42%
106	100	2	Zone	45	0.20%
107	100	2	Zone	60	1.49%
108	100	2	ALINEA	BEST	-0.37%
109	100	2	Zone	OCPC	0.84%
110	100	2	ALINEA	OCPC	3.35%
111	100	3	Zone	30	-1.42%
112	100	3	Zone	45	-1.92%
113	100	3	Zone	60	-1.69%
114	100	3	ALINEA	BEST	-1.87%
115	100	3	Zone	OCPC	0.63%
116	100	3	ALINEA	OCPC	3.17%
117	90	1	Zone	30	-1.44%
118	90	1	Zone	45	-1.02%
119	90	1	Zone	60	-0.35%
120	90	1	ALINEA	BEST	0.01%
121	90	1	Zone	OCPC	-1.14%
122	90	1	ALINEA	OCPC	0.04%
123	90	2	Zone	30	-0.60%
124	90	2	Zone	45	-0.35%
125	90	2	Zone	60	-1.71%
126	90	2	ALINEA	BEST	4.61%
127	90	2	Zone	OCPC	-1.04%
128	90	2	ALINEA	OCPC	10.23%
129	90	3	Zone	30	0.96%
130	90	3	Zone	45	1.77%
131	90	3	Zone	60	-0.28%
132	90	3	ALINEA	BEST	5.35%
133	90	3	Zone	OCPC	0.68%
134	90	3	ALINEA	OCPC	9.41%

From Table 5-56 it can be seen that the overall network travel times for the Zone algorithm are smaller than the network travel times that are experienced when the ALINEA metering algorithm is used. The coordination of the Zone metering algorithm, which increases the metering rate at one ramp to compensate for reduced flows at other on-ramps, helps to decrease the average delay for all vehicles on the on-ramps. This, in turn, reduces the average travel time along the entire network. Similar travel time decreases have been realized in other studies that used the Zone metering algorithm to improve traffic operations (Stephanedes, 1994). When ALINEA is used the metering rate at one ramp is defined only by the conditions of the nearest downstream loop detector. Therefore, a large queue of vehicles can be formed at one ramp while another ramp operates at near free-flow due to the lack of demand. This causes the network travel time to be much higher than when the Zone algorithm is used. Additionally, as the cycle length increases for each metering algorithm the average network travel time decreases. This shows that using the traffic-cycle realization outperforms the one-car-per-cycle realization from a traffic operations perspective as well as a traffic safety perspective.

As noted in Table 5-56, the strategy that was found to be the most beneficial during the 100 percent loading scenario (ALINEA with traffic-cycle realization) also provided a decrease in the average travel time along the network. When zone 2 is metered, this travel time decrease was about 0.4% of the overall network travel time while there was a 1.9% decrease when zone 3 was metered. Therefore, this strategy provides both safety and operational benefits. The best metering strategy at the 90 percent loading strategy (ALINEA with one-car-per-cycle realization) did not have reasonable travel time changes. When this strategy is used the average network travel time is increased by 10%. Such a large travel time increase is unrealistic to impose on drivers in the field and, therefore, this scenario cannot be considered as a practical metering

alternative. Using the ALINEA algorithm with traffic-cycle realization also has increased travel times of about 5%. Combined with the high levels of crash migration shown in Section 5.3.4 and this strategy is not a viable alternative. Therefore, the next best strategy, using the Zone algorithm with the traffic-cycle realization, should be used. This method provides good safety benefits as seen in Section 5.3.4 and serves to help decrease the average network travel time (1.7% decrease for zone 2 and 0.3% decrease for zone 3). As shown in Figures 5-48 and 5-49, this method also does not induce high levels of crash migration. Therefore, this strategy should be used in the downtown area at moderate levels of congestion (90 percent loading).

5.3.6 Metering Ramps over the Entire Network Corridor

5.3.6.1 100 Percent Loading Scenario

As previously determined, the best ramp metering strategy at the 100 percent loading scenario is to employ the ALINEA metering algorithm with the traffic-cycle realization (30 second cycle length). In the previous sections, the safety effects of ramp metering were only examined when the ramps in the downtown portion of the Interstate-4 freeway were metered. However, ramp metering is not necessarily constrained to this area like route diversion is (since ramp metering does not depend on the availability of practical diversion routes). Therefore, in order to reduce the rear-end and lane-change crash risk over the entire freeway area it is possible to implement ramp metering at all on-ramps within the network corridor.

The ALINEA algorithm with the traffic-cycle realization and 30 second cycle length was applied to the on-ramps within the network on the eastbound direction of Interstate-4. Summary statistics comparing the network wide implementation of ramp metering with the

224

implementation in the downtown area only is given in Table 5-57. As shown in this table, both the rear-end and lane-change safety are clearly increased with the network wide metering implementation which is evidenced by the increased values of ORCI and LCRCI.

Table 5-57. Summary of Network-Wide Ramp Metering Strategies at 100 Percent Loading

	Test Case	
	Whole Network	Downtown Portion
# of Stations with RE Risk Change	68	48
ORCI	17.3678	12.7085
# of Stations with LC Risk Change	73	40
LCRCI	24.3552	15.5739

The increase in the ORCI and LCRCI is about 34% and 56%, respectively, when the all the ramps in the network corridor are metered compared to when just the ramps in the downtown region are metered. However, the number of ramps that are metered in the network wide implementation is about triple the number of ramps that are metered in the downtown implementation. This implies that the safety increase is not proportionally related to the number of ramps metered. A plot of the average rear-end and lane-change crash risk difference is shown below in Figures 5-50 and 5-51, respectively.

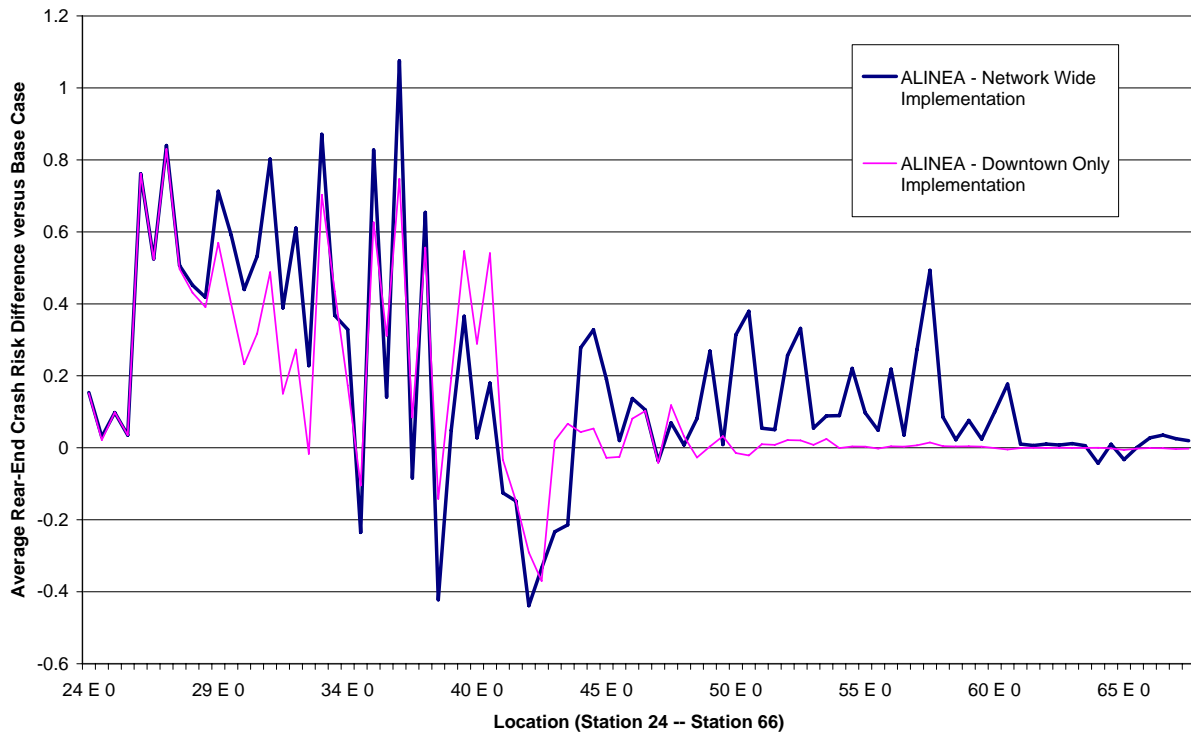**Average Rear-End Crash Risk Difference vs. Location**

Figure 5-50. Average Rear-End Crash Risk Difference vs. Location for Network-Wide Cases at 100 Percent Loading

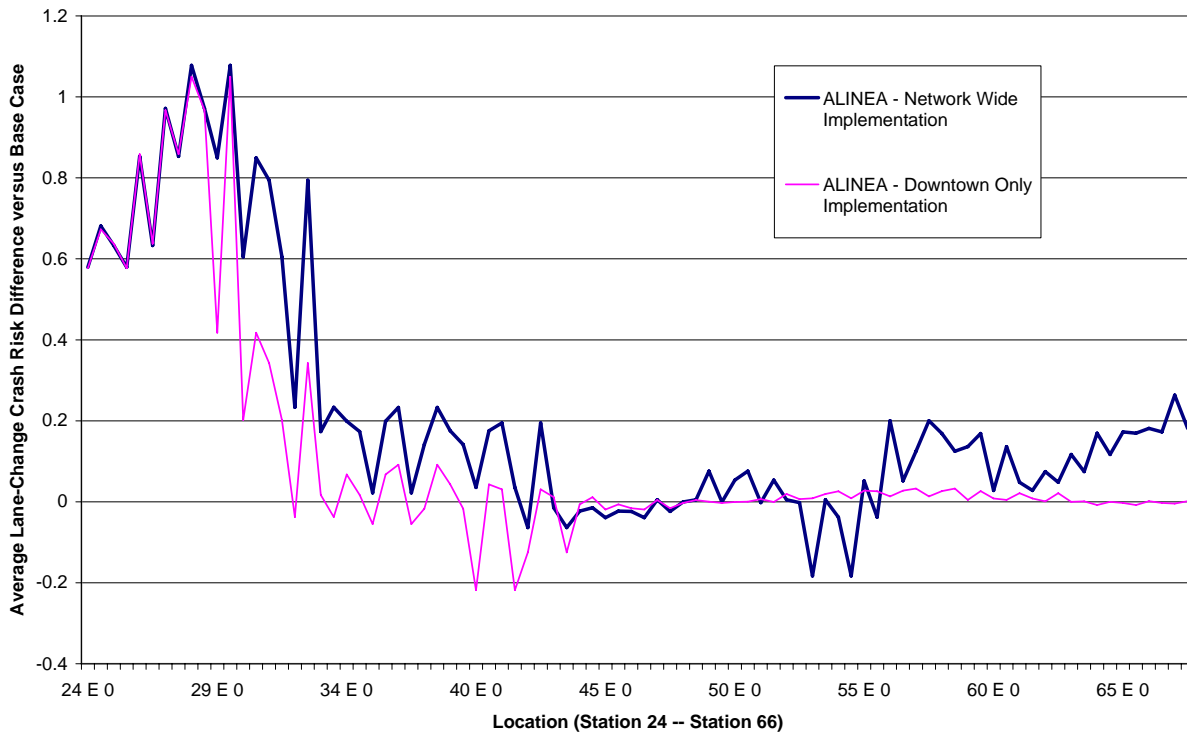**Average Lane-Change Crash Risk Difference vs. Location**

Figure 5-51. Average Lane-Change Crash Risk Difference vs. Location for Network-Wide Cases at 100 Percent Loading

As shown in Figures 5-50 and 5-51, at most locations the crash risk difference is greater for the network wide implementation than the downtown only implementation. This shows that the safety is improved when all of the ramps along Interstate-4 are metered as compared to when just the ramps in the downtown area are metered. What is interesting to note, however, is that the additional crash risk changes (both rear-end and lane-change) caused by the network wide implementation are only realized in the downtown area and downstream of this area (Stations 29 to 66). Stations 4 to 28 do not show a significant difference in the respective crash risk values between the network wide implementation and the downtown only implementation. One of the reasons for this is that the crash risk values in this upstream area are already low. These low

crash risk values are caused by the lower traffic volumes and higher speeds that occur in this area compared to other areas along the network. Additionally, the ramps in this area of the network are spaced further apart than the ramps in the downtown portion and just north of downtown. Therefore, when ramps are metered the effect isn't as magnified as when multiple, closer ramps are metered in succession in other areas of the network.

Looking at the real-time crash risk vs. time, it can be seen that this reduction in the crash risk occurs during the majority of the simulation run-time. This is shown in Figures 5-52 and 5-53 and confirms that the rear-end and lane-change crash risk, respectively, are reduced in real-time for most time periods when ramp metering is implemented. The time periods that show an increase in the crash risk have only a very small increase that can be deemed insignificant. Therefore, it is confirmed that at the 100 percent loading scenario implementing the ALINEA algorithm with the traffic-cycle realization throughout the entire network provides a better real-time safety benefit than by just metering the downtown ramps.
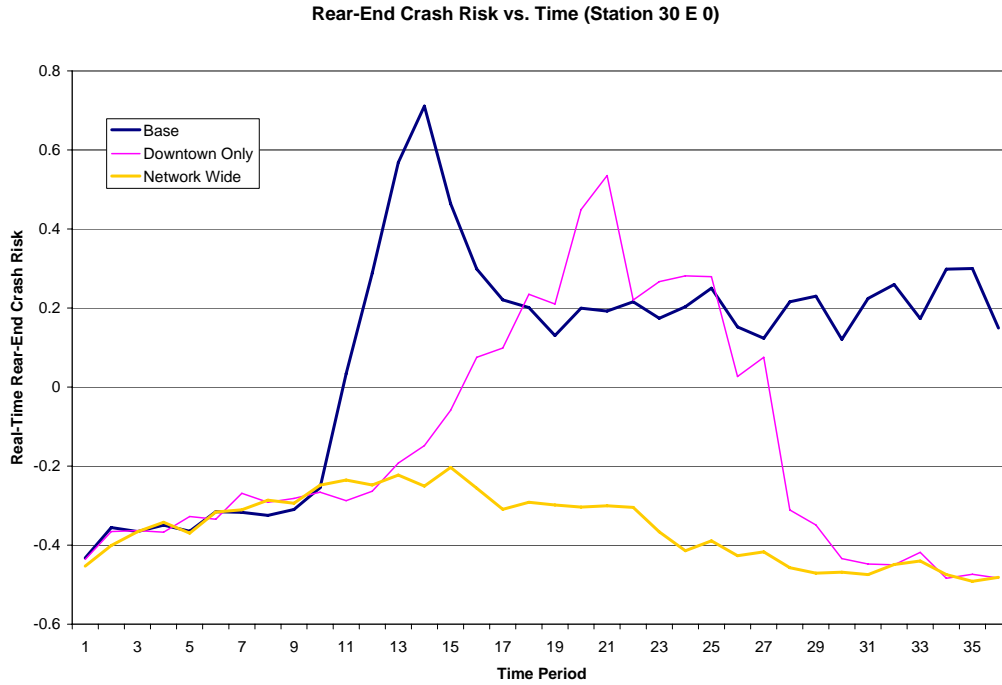
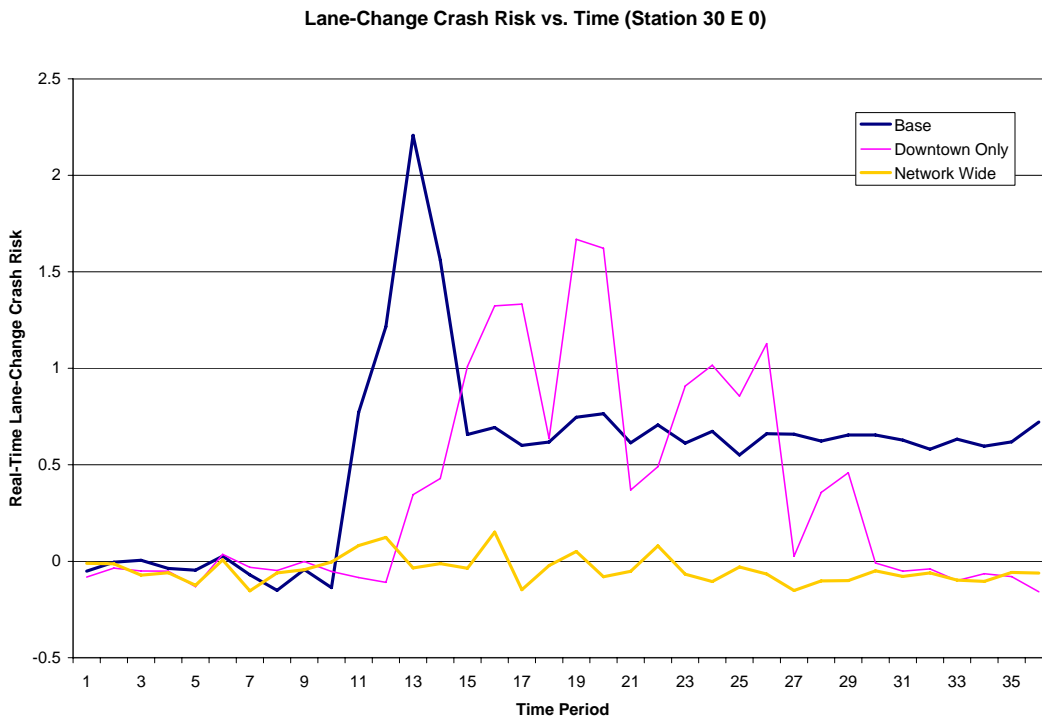**Figure 5-52. Plot of Rear-End Crash Risk vs. Time for Station 30 E 0 at 100 Percent Loading**

Figure 5-53. Plot of Lane-Change Crash Risk vs. Time for Station 30 E 0 at 100 Percent Loading

229

Additionally, implementing the ALINEA traffic-cycle strategy over the entire network serves to reduce the overall network travel time by 5%. When compared to the 2% reduction in travel time that is realized when ALINEA is implemented in the downtown area only, this means that implementing ALINEA network-wide provides both additional operational and safety benefits.

5.3.6.2 90 Percent Loading Scenario

In order to reduce the crash risk across the entire network at the 90 percent loading scenario, the best metering algorithm needs to be implemented in both the downtown and non-downtown regions throughout the network. However, unlike the 100 percent loading scenario, the 90 percent loading scenario did not have a clear-cut best algorithm. The ALINEA algorithm with a 30 second cycle length provided an excellent lane-change crash risk reduction and was the second best strategy at reducing the rear-end crash risk (as evidenced in Table 5-55). However, this strategy had very large crash migration effects that increased the crash risk greatly at some locations and even caused unreasonable travel time increases. The Zone algorithm with a 60 second cycle length had better rear-end crash risk reduction but also a less substantial lane-change crash risk benefit.

For this reason, Zone method was selected as the best and should be implemented throughout the network. However, because the ALINEA was ruled out in the downtown area mainly due to crash migration, there is the possibility that if implemented network-wide the effects of crash migration would be lessened and ALINEA would yield the best safety results. Therefore, both methods were tested throughout the entire network to determine the best

230

network-wide metering case at the 90 percent loading scenario. Additionally, a combination of Zone in the downtown area and ALINEA in the non-downtown areas was tested to see if the safety could be improved while minimizing the effects of crash migration. A numerical summary of the results is presented below in Table 5-58.

Table 5-58. Summary of Network-Wide Ramp Metering Strategies at 100 Percent Loading

	Test Case			
	Zone Downtown Only	**Zone Entire Network**	**Zone Downtown, ALINEA Elsewhere**	**ALINEA Entire Network**
# of Stations with RE Risk Change	35	49	49	55
ORCI	6.9996	8.2178	9.0507	8.6979
# of Stations with LC Risk Change	24	77	63	63
LCRCI	4.1848	9.8322	11.5249	14.4103

From these results, it appears that applying the combination of Zone and ALINEA provides the best rear-end crash risk results while implementing the ALINEA algorithm alone throughout the network corridor improves the lane-change crash risk safety the most. In order to determine which strategy is the best overall strategy, the plot of the crash risk differences need to be examined to discover potential crash migration issues. The plots for the rear-end and lane-change crash risk differences are given below in Figures 5-54 and 5-55, respectively.

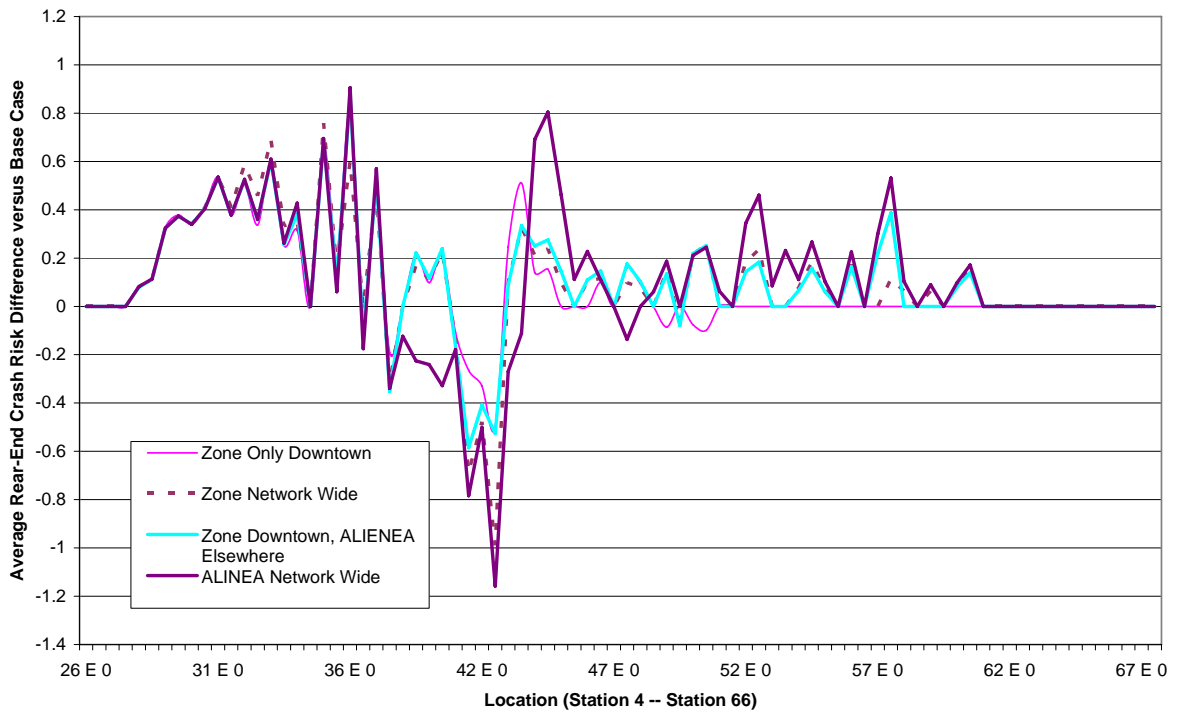**Average Rear-End Crash Risk Difference vs. Location**

Figure 5-54. Average Rear-End Crash Risk Difference vs. Location for Network-Wide Cases at 90 Percent Loading
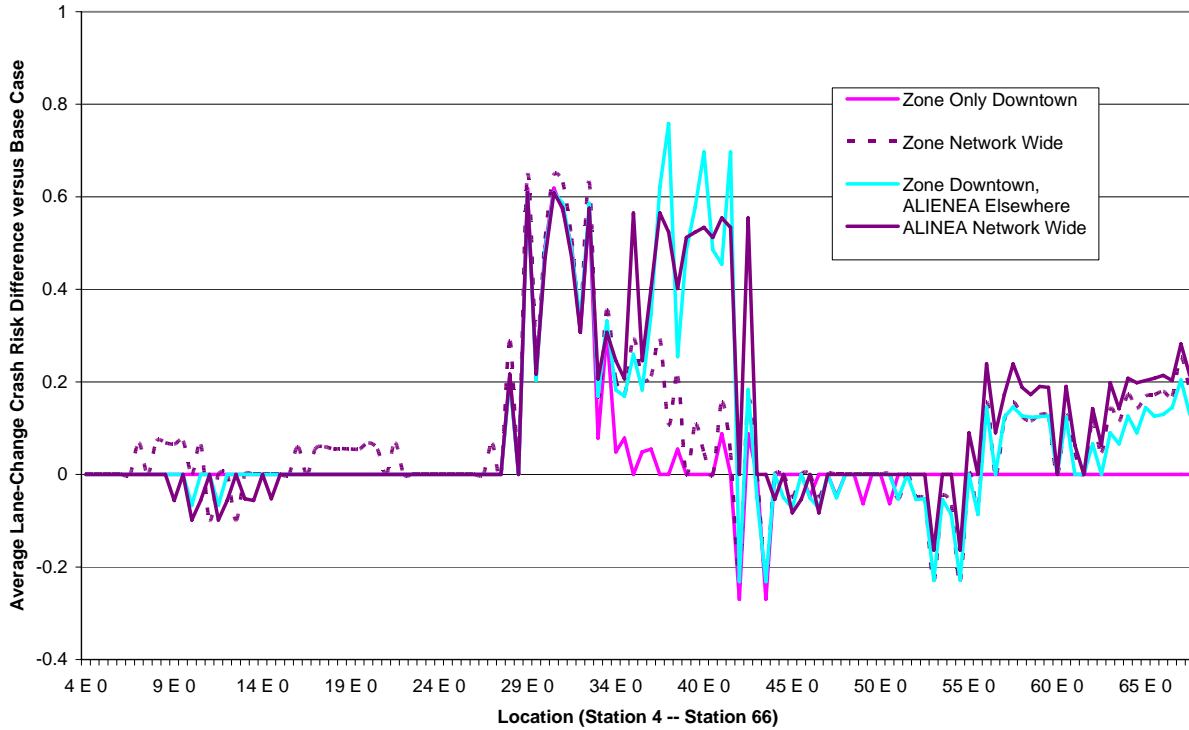
Figure 5-55. Average Lane-Change Crash Risk Difference vs. Location for Network-Wide Cases at 90 Percent Loading

Figure 5-54 shows that when the Zone and ALINEA algorithms are both implemented network-wide the effects of crash migration increase significantly at Stations 41 to 42. However, the combination of Zone and ALINEA, with the Zone algorithm implemented in the downtown areas and the ALINEA algorithm implemented in the non-downtown areas, decreases the effects of the crash migration to levels similar to the downtown only implementation of ramp metering. Figure 5-55, which shows the lane-change crash risk difference, shows that the effects of crash migration are about equal for each of the network-wide ramp metering implementations. Therefore, based on the reduced crash migration effects as well as the high ORCI and LCRCI

233

values, the best network-wide ramp metering strategy is determined to be the combination of Zone and ALINEA. Similar to the 100 percent loading scenarios, changes in the rear-end crash risk are mainly seen between Stations 28 through 62 even when all the ramps are metered. Although there are some lane-change crash risk changes upstream of this area (Stations 6 to 24) these differences are extremely small in magnitude and could be ignored.

Considering the change in the overall network travel time verifies the results of the best metering scenario. The overall network travel time is increased 3% when ALINEA is implemented network-wide. However, both the ALINEA and Zone combination as well as the Zone network-wide implementation yield a decrease in the overall network travel time of about 3%. Compared to the 0.5% reduction that is seen when just the Zone algorithm is implemented downtown, this shows that metering ramps throughout the entire corridor provides additional operational and safety benefits. Since the safety benefits are slightly higher for the Zone and ALINEA combination, this strategy is determined to be the best strategy at the 90 percent loading scenario.

5.4 Ramp Metering Summary

The general conclusions from the ramp metering portion of the experimental design are as follows:

- The implementation of ramp metering helps to reduce both the overall rear-end and lane-change crash risk across the network corridor.

- The implementation of ramp metering also causes crash risk migration. Although the extent of the crash migration is not large compared to the overall crash benefit (the increase in the crash risk is much smaller than the decrease in the crash risk) it must still

234

be noted. The area at which the crash risk is increased is usually an area that operated at mild levels of congestion in the base case and became congested due to the implementation of ramp metering. In most cases the migration effect was rather negligible due to already low crash risk values at that location. However, in some cases the increase was significant and, therefore, care must be taken before ramp metering can be implemented in that area.

- When using the ALINEA algorithm with the traffic-cycle realization, a lower critical occupancy (0.17) and shorter cycle length (30 seconds) performs the best at reducing the crash risk.

- When using the Zone ramp metering algorithm along with the traffic-cycle realization, a longer cycle length (60 seconds) provides the best results from a safety perspective.

- Using the one-car-per-cycle traffic realization method does not perform as well at reducing the rear-end and lane-change crash risk as using the traffic-cycle realization in the manner mentioned previously.

- The best ramp metering strategy at heavy congestion (100 percent loading) is to use the ALINEA algorithm with the traffic-cycle realization. The reason for this is that the ALINEA algorithm is more restrictive than the Zone algorithm during periods of heavy congestion. This occurs because the ALINEA algorithm does not account for spare capacity of the freeway to store vehicles like the Zone algorithm does (Equation 5). Therefore, as long as the detectors associated with on-ramps show congestion the meters will all operate at the minimum rates even if there is spare capacity within the metered section. Allowing less vehicles onto the network will greatly reduce the overall crash risk on the network. When this method is applied to all the ramps in the network, not just

the ones in the downtown area, the crash risk values and total network travel time are reduced even further.

- The best ramp metering strategy at lower levels of congestion (90 percent loading) is to use the Zone algorithm with the traffic-cycle realization. This occurs because the ALINEA algorithm causes unacceptable levels of crash migration during this loading scenario. However, neglecting to consider effects of crash migration, the ALINEA traffic-cycle algorithm also provides the good safety benefits at the 90 percent loading scenario. When ramp metering is applied to the entire network corridor at the 90 percent loading case, the best metering strategy is to employ the Zone algorithm in the downtown area and the ALINEA algorithm elsewhere. This provides a reduction in the two crash risk measures as well as the total network travel time.

- Of the three different zones that were metered (Zone 1, 2, and 3) the best results were found when Zone 3 was metered. This zone was the largest zone which encompassed the other two zones in their entirety and spanned the entire length of the downtown area of Interstate-4. Based on the results of this study, larger crash risk decreases are seen when a longer portion of the freeway is metered.

- When a large interchange (such as the I-4 / S. R. 408 Interchange) is present, metering the area just downstream of this interchange (Zone 2) provides much better safety benefits than metering the area just upstream (Zone 1).

CHAPTER 6. CONCLUSIONS

This study has examined the potential of route diversion and ramp metering to be used as a real-time crash prevention technique. The objective of this study was to assess whether or not each of these ITS strategies would reduce the real-time rear-end and lane-change crash risk along an urban freeway and identify the most effective implementation methods and situations to employ them. To do this, Interstate-4 through Orlando, Florida was simulated in the PARAMICS micro-simulation program. Various implementations of route diversion and ramp metering were applied to the network and the crash risk values compared to determine the best cases. Multiple network loading scenarios were considered (60%, 80%, 90%, and 100%) to examine the effectiveness of the ITS measures at different levels of congestion. Additionally, the effect of the strategies on the network travel time was considered to ensure that the ITS strategies did not sacrifice operational capabilities of the traffic network in an attempt to improve the safety conditions.

The study found that route diversion successfully reduces both the rear-end and lane-change crash risk at periods of low traffic volumes (realized at the 60% and 80% network loading scenarios). In general, the further vehicles are diverted away from the initial diversion location, the more the crash risk values are reduced. Diverting more vehicles from a particular on-ramp increases the safety benefit. Therefore, vehicles should be diverted from on-ramps with higher demand volumes in order to maximize the safety benefits. At higher loading levels, although the crash risk is decreased at the diversion area, it is significantly increased at the location of the freeway that diverted vehicles re-enter the traffic stream. In order to minimize this crash migration effect, vehicles should be diverted to locations with lower real-time crash

237

risk values. In general, when vehicles are diverted during times of extreme congestion (100% loading) the overall safety benefit is an increase in the crash risk along the freeway.

Ramp metering is found to be beneficial at the higher loading scenarios (90% and 100% loading). Since the ramp metering algorithms are only activated when the freeway is congested, implementing ramp metering at the lower loading scenarios does not change the crash risk significantly along the network corridor. As found in this study, when the ramps in the downtown Orlando area are metered the best safety benefits during the 100% loading scenario is realized when the uncoordinated ALINEA metering algorithm is used. This occurs because ALINEA is generally more restrictive than the coordinated strategy tested – the Zone algorithm. At the 90% loading scenario, ALINEA causes large amount of crash migration downstream of the downtown area. Therefore, the coordinated Zone algorithm is preferred as it reduces the crash migration effects significantly. In both cases, the traffic-cycle realization of ramp metering yields significantly higher safety results than implementing the algorithms on a one-car-per-cycle basis.

When ramp metering is applied to the entire network, as opposed to just the extremely congested downtown areas, the crash risk values are shown to decrease for a longer section of the freeway. At the 100% loading scenario, applying ALINEA to all the ramps within the study area increases the overall safety benefits realized. At the 90% loading scenario, applying the Zone algorithm in the downtown areas and the ALINEA algorithm in the non-downtown areas serves to decrease the overall crash risk for the freeway corridor and reduces the crash risk for a longer section of the freeway. Also found in this study is the fact that ALINEA yields the best safety results when a shorter cycle length of 30 seconds is used while the best benefits from the Zone algorithm are realized when a longer, 60 second, cycle length is applied.

238

6.1 Recommendations for Further Research

This research clearly shows the benefits of both route diversion and ramp metering on the real-time rear-end and lane-change crash risk on a typical urban freeway. However, there are several ways in which this research could be expanded. First, the transferability of this work needs to be examined. Route diversion and ramp metering should be tested on other freeways in different locations to ensure that the trends found in the results of this study hold for other regions as well. This will involve recalibrating the risk models that were used in this study using loop data taken from other freeways as the models used in this study are unique to Interstate-4. Once new models are created, the freeways used to calibrate the models should be simulated and the various route diversion and ramp metering strategies tested to confirm the trends found in this study. The transferability of the route diversion results could also be extended to this same freeway corridor by modeling the effects of other diversion routes through downtown Orlando. These routes would have to be feasible for drivers to use but would confirm that the general trends from this study are applicable to other diversions. Note that it is expected that the general trends from these results will hold on other freeways – mainly that more diverting vehicles further away and at lower loading scenarios will improve the safety conditions on the freeway. However, the exact results will not be transferable due to the uniqueness of geometry and ramp conditions on each freeway. Additionally, with the ramp metering strategies it is expected that the general trends of metering more ramps and using the more restrictive algorithm (ALINEA) at higher loading conditions improves the safety conditions will hold true. The exact results, however, depend on different factors that define the uniqueness of each freeway.

Another way in which this research could be extended is to test the route diversion and ramp metering strategies in the field. While the micro-simulation gives researchers an idea of what should be expected when these strategies are implemented, it is possible that drivers will react to the strategies in a way that cannot be simulated. Therefore, the scenarios that show improved safety results could be implemented in the field to confirm that this is truly the case. Note that the strategies that show negative safety impacts should not be implemented in the field until there is evidence that they will not increase the crash risk. Only by field implementation will this be truly known.

Finally, combinations of route diversion and ramp metering could be tested. Previous studies by Dilmore (2004) and Dhindsa (2006) have shown that variable speed limits have potential for safety benefits. Therefore, combinations of these three ITS strategies could be examined to see if they will enhance the risk reducing potential of each strategy.

APPENDIX: ROUTE DIVERSION AND RAMP METERING CODE

```
static int diversion1 = 80;
static int diversion2 = 0;
static int diversion3 = 0;
static int diversion4 = 0;
static int diversion5 = 0;
int count1 = 0;
int count2 = 0;
int count3 = 0;
int count4 = 0;
int count5 = 0;
int  qpo_RTM_decision(LINK* link, VEHICLE* vehicle)
{
 if (qpg_VHC_origin(vehicle) == 25 || qpg_VHC_origin(vehicle) == 82 || qpg_VHC_origin(vehicle) == 35)
 {
  if (link == qpg_NET_linkByIndex(1414) && qpg_VHC_origin(vehicle) == 25 &&
(qpg_VHC_destination(vehicle) >= 39 && qpg_VHC_destination(vehicle) <= 58))
  {
   if (rand()%100 < diversion1)
   {
    count1++;
    qps_GUI_printf("Diversion 1 %i\n", count1);
    return 2;
   }
   else return 0;
  }
  else if (link == qpg_NET_linkByIndex(1209) && qpg_VHC_origin(vehicle) == 25 &&
(qpg_VHC_destination(vehicle) >= 39 && qpg_VHC_destination(vehicle) <= 58))
  {
   if (rand()%100 < diversion2 && (qpg_VHC_destination(vehicle) < 123))
   {
    count2++;
    qps_GUI_printf("Diversion 2 %i\n", count2);
    return 2;
   }
   else return 0;
  }
  else if (link == qpg_NET_linkByIndex(1132) && qpg_VHC_origin(vehicle) == 82 &&
(qpg_VHC_destination(vehicle) == 3 || (qpg_VHC_destination(vehicle) >= 96 && qpg_VHC_destination(vehicle)
<= 121)))
  {
   if (rand()%100 < diversion3)
   {
    count3++;
    qps_GUI_printf("Diversion 3 %i\n", count3);
    return 2;
   }
   else return 0;
  }
  else if (link == qpg_NET_linkByIndex(1248) && qpg_VHC_origin(vehicle) == 82 &&
(qpg_VHC_destination(vehicle) == 3 || (qpg_VHC_destination(vehicle) >= 96 && qpg_VHC_destination(vehicle)
```

```
<= 121)))
  {
  if (rand()%100 < diversion4)
   {
   count4++;
   qps_GUI_printf("Diversion 4 %i\n", count4);
   return 3;
   }
  else return 0;;
  }
  else if (link == qpg_NET_linkByIndex(1329) && qpg_VHC_origin(vehicle) == 35 &&
(qpg_VHC_destination(vehicle) >= 39 && qpg_VHC_destination(vehicle) <= 58))
  {
  if (rand()%100 < diversion5)
   {
   count5++;
   qps_GUI_printf("Diversion 5 %i\n", count5);
   return 1;
   }
  else return 0;
  }
  else return 0;
 }
 else return 0;
}
```

Sample of "Phases" File used for ALINEA Ramp Metering

use plan 1
 on node 811 phase 1
 with loops
  Detector68 lane 1
  Detector68 lane 2
  Detector68 lane 3

 with parameters
30 ##1 cycle length
0.17 ##2 critical occupancy
10.5 ##3 minimum green
27 ##4 maximum green
0 ##5
0 ##6
0 ##7
0 ##8
0 ##9
0 ##10
0 ##11
0 ##12
0 ##13
0 ##14
1 ##15
0 ##16
27 ##17

Sample of "Plans" File used for ALINEA Ramp Metering

```
plan count 1

plan 1 definition
loops 3
parameters 17

if (init)  { fixed; }
if (parameter[15] < 2 * parameter[1])

{

parameter[5] = occupancy[1] running;
parameter[6] = occupancy[2] running;
parameter[7] = occupancy[3] running;


if (parameter[5] > 0.5) {parameter[5] = 0.5;}
if (parameter[6] > 0.5) {parameter[6] = 0.5;}
if (parameter[7] > 0.5) {parameter[7] = 0.5;}

parameter[11] = parameter[11] + parameter[5];
parameter[12] = parameter[12] + parameter[6];
parameter[13] = parameter[13] + parameter[7];

parameter[15] = parameter[15] + 1;
green2=parameter [16];
green3=parameter [16];

}

else

{

parameter[14] = (parameter[11] + parameter[12] + parameter[13]) / (3 * parameter[1]);
if (parameter[14] > 1) {parameter[14] = 1;}

parameter[8] = parameter[5];
parameter[9] = parameter[6];
parameter[10] = parameter[7];

report parameter[14];


parameter[15] = 1;
parameter[8] = 0; parameter[9] = 0; parameter[10] = 0; parameter[11] = 0; parameter[12] = 0; parameter[13] = 0;

parameter[16] = parameter[17] + parameter[1] / 730 * 70 * (parameter[2] - parameter[14]);
```

```
report parameter[16];

     if ( parameter [16] < parameter [3] )
        {
    parameter [16] = parameter [3];

        }
 if ( parameter [16] > parameter [4] )
        {
    parameter [16] = parameter [4] ;

        }

green2=parameter [16];
green3=parameter [16];

report parameter[16];

parameter[17] = parameter[16];


}
```

```c
#include <stdlib.h>
#include <stdio.h>
#include <string.h>
#include <math.h>
#include <limits.h>

#include "programmer.h"
#include "plugin_p.h"

static int deteccount[15];
static int deteccountold[15];
static int detecflow[15];
static float smoothedflow[15];
static float smoothedflowold[15];
static float averagespeed[15];

static int oncount[9];
static int oncountold[9];
static int onflow[9];
static float onsmoothedflow[9];
static float onsmoothedflowold[9];

static int offcount[11];
static int offcountold[11];
static int offflow[11];
static float offsmoothedflow[11];
static float offsmoothedflowold[11];

static float proprate[9];

static float M;
static float rate[9];
static float minrate[9];

static int cycle = 30;    // change me!!!




DETECTOR* det1;
NODE* n[9];
LINK* deteclink[15];
float density[15];

void zone1();
void zone2();
void zone3();

void qpx_NET_postOpen(void)
```

```
{
int i;


qps_GUI_printf("API: Ramp Metering\n");

qps_GUI_printf("%s\n",qpg_DTC_name(qpg_NET_detectorByIndex(64)));

n[0] = qpg_NET_nodeByIndex(765);
n[1] = qpg_NET_nodeByIndex(758);
n[2] = qpg_NET_nodeByIndex(759);
n[4] = qpg_NET_nodeByIndex(188);
n[5] = qpg_NET_nodeByIndex(460);
n[6] = qpg_NET_nodeByIndex(761);
n[7] = qpg_NET_nodeByIndex(199);
n[8] = qpg_NET_nodeByIndex(202);


qps_SIG_action(n[0], 1, 2, API_ACTION_MAXIMUM_GREEN, API_ACTIONMODE_SET, cycle);
qps_SIG_action(n[0], 1, 2, API_ACTION_MINIMUM_GREEN, API_ACTIONMODE_SET, 0);
qps_SIG_action(n[0], 2, 1, API_ACTION_MAXIMUM_GREEN, API_ACTIONMODE_SET, cycle);
qps_SIG_action(n[0], 2, 1, API_ACTION_MINIMUM_GREEN, API_ACTIONMODE_SET, 0);

qps_SIG_action(n[1], 1, 2, API_ACTION_MAXIMUM_GREEN, API_ACTIONMODE_SET, cycle);
qps_SIG_action(n[1], 1, 2, API_ACTION_MINIMUM_GREEN, API_ACTIONMODE_SET, 0);
qps_SIG_action(n[1], 2, 1, API_ACTION_MAXIMUM_GREEN, API_ACTIONMODE_SET, cycle);
qps_SIG_action(n[1], 2, 1, API_ACTION_MINIMUM_GREEN, API_ACTIONMODE_SET, 0);

qps_SIG_action(n[2], 1, 2, API_ACTION_MAXIMUM_GREEN, API_ACTIONMODE_SET, cycle);
qps_SIG_action(n[2], 1, 2, API_ACTION_MINIMUM_GREEN, API_ACTIONMODE_SET, 0);
qps_SIG_action(n[2], 2, 1, API_ACTION_MAXIMUM_GREEN, API_ACTIONMODE_SET, cycle);
qps_SIG_action(n[2], 2, 1, API_ACTION_MINIMUM_GREEN, API_ACTIONMODE_SET, 0);

qps_SIG_action(n[4], 1, 2, API_ACTION_MAXIMUM_GREEN, API_ACTIONMODE_SET, cycle);
qps_SIG_action(n[4], 1, 2, API_ACTION_MINIMUM_GREEN, API_ACTIONMODE_SET, 0);
qps_SIG_action(n[4], 2, 1, API_ACTION_MAXIMUM_GREEN, API_ACTIONMODE_SET, cycle);
qps_SIG_action(n[4], 2, 1, API_ACTION_MINIMUM_GREEN, API_ACTIONMODE_SET, 0);

qps_SIG_action(n[5], 1, 2, API_ACTION_MAXIMUM_GREEN, API_ACTIONMODE_SET, cycle);
qps_SIG_action(n[5], 1, 2, API_ACTION_MINIMUM_GREEN, API_ACTIONMODE_SET, 0);
qps_SIG_action(n[5], 2, 1, API_ACTION_MAXIMUM_GREEN, API_ACTIONMODE_SET, cycle);
qps_SIG_action(n[5], 2, 1, API_ACTION_MINIMUM_GREEN, API_ACTIONMODE_SET, 0);

qps_SIG_action(n[6], 1, 2, API_ACTION_MAXIMUM_GREEN, API_ACTIONMODE_SET, cycle);
qps_SIG_action(n[6], 1, 2, API_ACTION_MINIMUM_GREEN, API_ACTIONMODE_SET, 0);
qps_SIG_action(n[6], 2, 1, API_ACTION_MAXIMUM_GREEN, API_ACTIONMODE_SET, cycle);
qps_SIG_action(n[6], 2, 1, API_ACTION_MINIMUM_GREEN, API_ACTIONMODE_SET, 0);

qps_SIG_action(n[7], 1, 2, API_ACTION_MAXIMUM_GREEN, API_ACTIONMODE_SET, cycle);
qps_SIG_action(n[7], 1, 2, API_ACTION_MINIMUM_GREEN, API_ACTIONMODE_SET, 0);
qps_SIG_action(n[7], 2, 1, API_ACTION_MAXIMUM_GREEN, API_ACTIONMODE_SET, cycle);
qps_SIG_action(n[7], 2, 1, API_ACTION_MINIMUM_GREEN, API_ACTIONMODE_SET, 0);

qps_SIG_action(n[8], 1, 2, API_ACTION_MAXIMUM_GREEN, API_ACTIONMODE_SET, cycle);
```

```
qps_SIG_action(n[8], 1, 2, API_ACTION_MINIMUM_GREEN, API_ACTIONMODE_SET, 0);
qps_SIG_action(n[8], 2, 1, API_ACTION_MAXIMUM_GREEN, API_ACTIONMODE_SET, cycle);
qps_SIG_action(n[8], 2, 1, API_ACTION_MINIMUM_GREEN, API_ACTIONMODE_SET, 0);



for (i = 0; i < 15; i++)
{
 deteccount[i] = 0;
 deteccountold[i] = 0;
 detecflow[i] = 0;
 smoothedflowold[i] = 0;
 smoothedflow[i] = 0;

 oncount[i] = 0;
 oncountold[i] = 0;
 onflow[i] = 0;
 onsmoothedflow[i] = 0;
 onsmoothedflowold[i] = 0;

 offcount[i] = 0;
 offcountold[i]=0;
 offflow[i]=0;
 offsmoothedflow[i]=0;
 offsmoothedflowold[i]=0;

 deteclink[i] = qpg_DTC_link(qpg_NET_detectorByIndex(i*2 + 62));

 density[i] = 0;

}

rate[0] = 2000;
rate[1] = 2000;
rate[2] = 2000;
rate[4] = 2000;
rate[5] = 2000;
rate[6] = 2000;
rate[7] = 2000;
rate[8] = 2000;


minrate[0] = 670;
minrate[1] = 188;
minrate[2] = 222;
minrate[4] = 301;
minrate[5] = 540;
minrate[6] = 295;
minrate[7] = 455;

}

void qpx_NET_timeStep(void)
```

```
{
 int i;
 int g;
 float meterrate;


 if ((double)qpg_CFG_simulationTime() - (float)floor((double)qpg_CFG_simulationTime())>0.0)
 return;

 if ((int)qpg_CFG_simulationTime() % cycle == 1)
 {
 if (rate[0] < 1900)
 {
  meterrate = rate[0] * cycle / 1900;
  qps_SIG_action(n[0], 1, 2, API_ACTION_CURRENT_GREEN, API_ACTIONMODE_SET, (int)meterrate);
  qps_GUI_printf("SIGNAL ACTIVATED 0 %f %f %f %i\n", qpg_CFG_simulationTime(), rate[0],
onsmoothedflow[0],  (int)meterrate);

 }
 else
 {
 meterrate = cycle;
 qps_SIG_action(n[0], 1, 2, API_ACTION_CURRENT_GREEN, API_ACTIONMODE_SET, (int)meterrate);
 }

 if (rate[1] < 1900)
 {
  meterrate = rate[1] * cycle / 1900;
  qps_SIG_action(n[1], 1, 2, API_ACTION_CURRENT_GREEN, API_ACTIONMODE_SET, (int)meterrate);
  qps_GUI_printf("SIGNAL ACTIVATED 1 %f %f %f %i\n", qpg_CFG_simulationTime(), rate[1],
onsmoothedflow[1],  (int)meterrate);
 }
 else
 {
 meterrate = cycle;
 qps_SIG_action(n[1], 1, 2, API_ACTION_CURRENT_GREEN, API_ACTIONMODE_SET, (int)meterrate);
 }

 if (rate[2] < 1900)
 {
  meterrate = rate[2] * cycle / 1900;
  qps_SIG_action(n[2], 1, 2, API_ACTION_CURRENT_GREEN, API_ACTIONMODE_SET, (int)meterrate);
  qps_GUI_printf("SIGNAL ACTIVATED 2 %f %f %f %i\n", qpg_CFG_simulationTime(), rate[2],
onsmoothedflow[2],  (int)meterrate);
 }
 else
 {
 meterrate = cycle;
 qps_SIG_action(n[2], 1, 2, API_ACTION_CURRENT_GREEN, API_ACTIONMODE_SET, (int)meterrate);
 }

 if (rate[4] < 1900)
 {
  meterrate = rate[4] * cycle / 1900;
```

```
  qps_SIG_action(n[4], 1, 2, API_ACTION_CURRENT_GREEN, API_ACTIONMODE_SET, (int)meterrate);
  qps_GUI_printf("SIGNAL ACTIVATED 4 %f %f %f %i\n", qpg_CFG_simulationTime(), rate[4],
onsmoothedflow[4],  (int)meterrate);
 }
 else
 {
  meterrate = cycle;
  qps_SIG_action(n[4], 1, 2, API_ACTION_CURRENT_GREEN, API_ACTIONMODE_SET, (int)meterrate);
 }

 if (rate[5] < 1900)
 {
  meterrate = rate[5] * cycle / 1900;
  qps_SIG_action(n[5], 1, 2, API_ACTION_CURRENT_GREEN, API_ACTIONMODE_SET, (int)meterrate);
  qps_GUI_printf("SIGNAL ACTIVATED 5 %f %f %f %i\n", qpg_CFG_simulationTime(), rate[5],
onsmoothedflow[5],  (int)meterrate);
 }
 else
 {
  meterrate = cycle;
  qps_SIG_action(n[5], 1, 2, API_ACTION_CURRENT_GREEN, API_ACTIONMODE_SET, (int)meterrate);
 }

 if (rate[6] < 1900)
 {
  meterrate = rate[6] * cycle / 1900;
  qps_SIG_action(n[6], 1, 2, API_ACTION_CURRENT_GREEN, API_ACTIONMODE_SET, (int)meterrate);
  qps_GUI_printf("SIGNAL ACTIVATED 6 %f %f %f %i\n", qpg_CFG_simulationTime(), rate[6],
onsmoothedflow[6],  (int)meterrate);
 }
 else
 {
  meterrate = cycle;
  qps_SIG_action(n[6], 1, 2, API_ACTION_CURRENT_GREEN, API_ACTIONMODE_SET, (int)meterrate);
 }

 if (rate[7] < 1900)
 {
  meterrate = rate[7] * cycle / 1900;
  qps_SIG_action(n[7], 1, 2, API_ACTION_CURRENT_GREEN, API_ACTIONMODE_SET, (int)meterrate);
  qps_GUI_printf("SIGNAL ACTIVATED 7 %f %f %f %i\n", qpg_CFG_simulationTime(), rate[7],
onsmoothedflow[7],  (int)meterrate);
 }
 else
 {
  meterrate = cycle;
  qps_SIG_action(n[7], 1, 2, API_ACTION_CURRENT_GREEN, API_ACTIONMODE_SET, (int)meterrate);
 }

 if (rate[8] < 1900)
 {
  meterrate = rate[8] * cycle / 1900;
  qps_SIG_action(n[8], 1, 2, API_ACTION_CURRENT_GREEN, API_ACTIONMODE_SET, (int)meterrate);
```

251

```
   qps_GUI_printf("SIGNAL ACTIVATED 8 %f %f %f %i\n", qpg_CFG_simulationTime(), rate[8],
onsmoothedflow[8],  (int)meterrate);
  }
  else
  {
  meterrate = cycle;
  qps_SIG_action(n[8], 1, 2, API_ACTION_CURRENT_GREEN, API_ACTIONMODE_SET, (int)meterrate);
  }

 }

 if ((int)qpg_CFG_simulationTime() % 30 == 0)
 {


  for (i=0; i<15; i++)
  {
  smoothedflowold[i] = smoothedflow[i];
  deteccountold[i] = deteccount[i];
  deteccount[i] = qpg_DTI_count(i*2+62, 1, 0) + qpg_DTI_count(i*2+62, 2, 0) + qpg_DTI_count(i*2+62, 3, 0);
  detecflow[i] = deteccount[i] - deteccountold[i];
  g = detecflow[i] * 120;
  smoothedflow[i] = (g - smoothedflowold[i])*0.15 + smoothedflowold[i];

  density[i] = 5280 * ((qpg_DTI_occupancy(i*2+62,1,APILOOP_SMOOTHED) +
qpg_DTI_occupancy(i*2+62,2,APILOOP_SMOOTHED) +
qpg_DTI_occupancy(i*2+62,3,APILOOP_SMOOTHED)) / 3 / 300 * detecflow[i]) / 14;

//   qps_GUI_printf("%f %f %f\n", qpg_DTI_occupancy(i*2+62,1,APILOOP_SMOOTHED), density[i]);

  averagespeed[i] = (qpg_DTI_speed(i*2+62,1,APILOOP_SMOOTHED) +
qpg_DTI_speed(i*2+62,2,APILOOP_SMOOTHED) + qpg_DTI_speed(i*2+62,3,APILOOP_SMOOTHED)
)*2.2369 / 3;
  }

  for (i=0; i < 9; i++)
  {
  onsmoothedflowold[i] = onsmoothedflow[i];
  oncountold[i] = oncount[i];
  oncount[i] = qpg_DTI_count(i+135,1,0);
  onflow[i] = oncount[i] - oncountold[i];
  g = onflow[i] * 120;
  onsmoothedflow[i] = (g - onsmoothedflowold[i]) * .15 + onsmoothedflow[i];


  }

  for (i=0; i < 11; i++)
  {
  offsmoothedflowold[i] = offsmoothedflow[i];
  offcountold[i] = offcount[i];
  offcount[i] = qpg_DTI_count(i+144,1,0);
  offflow[i] = offcount[i] - offcountold[i];
```

```
    g = offflow[i] * 120;
    offsmoothedflow[i] = (g - offsmoothedflowold[i]) * .15 + offsmoothedflow[i];
   }

// qps_GUI_printf("%i %f %f \n", offflow[3], offsmoothedflowold[3], offsmoothedflow[3]);

 }


 if ((int)qpg_CFG_simulationTime() % cycle == 0)
 {

// CHANGE THIS zone1() zone2() zone3()  also change CYCLE variable

  zone1();


 }
}

[0] * M / (onsmoothedflow[0] + onsmoothedflow[1]);
 rate[1] = M - rate[0];

 if (rate[0] < minrate[0])
 {
  rate[0] = minrate[0];
 }
 if (rate[1] < minrate[1])
 {
  rate[1] = minrate[1];
 }
}

void zone24()
{
 float maxdens;
 float minspeed;
 float S;

 if (max(density[5], max(density[4], density[3])) < 32)
 {
  maxdens = max(density[5], max(density[4], density[3]));
  minspeed = min(averagespeed[5], min(averagespeed[4], averagespeed[3]));

  S = (32 - maxdens)*(minspeed*3);
 }
 else
 {
  S = 0;
 }

 M = 1800 + 2100 + 2100 + offsmoothedflow[4] + offsmoothedflow[3] + S - smoothedflow[3] -
 onsmoothedflow[3];
```

```c
rate[2] = M;

if (rate[2] < minrate[2])
{
 rate[2] = minrate[2];
}
}


void zone61()
{
 float maxdens;
 float minspeed;
 float S;
 float demand;

 if(max(density[0], max(density[1], max(density[2], max(density[3], max(density[4], density[5]))))) < 32)
 {
  maxdens = max(density[0], max(density[1], max(density[2], max(density[3], max(density[4], density[5])))));
  minspeed = min(averagespeed[0], min(averagespeed[1], min(averagespeed[2], min(averagespeed[3],
min(averagespeed[4], averagespeed[5])))));

  S = (32 - maxdens) * (minspeed * 3);
 }
 else
 {
  S = 0;
 }

 M = 6000 + offsmoothedflow[4] + offsmoothedflow[3] + offsmoothedflow[2] + offsmoothedflow[1] +
offsmoothedflow[0] + S - smoothedflow[0] - onsmoothedflow[3];

 qps_GUI_printf("%f %f %f ", -1*smoothedflow[0], S, M);

 demand = onsmoothedflow[0] + onsmoothedflow[1] + onsmoothedflow[2];

 rate[0] = onsmoothedflow[0] * M / demand;
 rate[1] = onsmoothedflow[1] * M / demand;
 rate[2] = onsmoothedflow[2] * M / demand;

 if (rate[0] < minrate[0])
  rate[0] = minrate[0];
 if (rate[1] < minrate[1])
  rate[1] = minrate[1];
 if (rate[2] < minrate[2])
  rate[2] = minrate[2];

 qps_GUI_printf("%f %f %f\n", rate[0], rate[1], rate[2]);

}

void zone62()
{
 float maxdens;
```

```
float minspeed;
float S;
float demand;


if(max(density[10], max(density[9], max(density[8], max(density[7], max(density[6], density[5])))))) < 32)
{
 maxdens = max(density[10], max(density[9], max(density[8], max(density[7], max(density[6], density[5])))));
 minspeed = min(averagespeed[10], min(averagespeed[9], min(averagespeed[8], min(averagespeed[7],
min(averagespeed[6], averagespeed[5])))));

 S = (32 - maxdens) * (minspeed * 3);
}
else
{
 S = 0;
}

M = 6000 + offsmoothedflow[5] + offsmoothedflow[6] + offsmoothedflow[7] + S - smoothedflow[5];

qps_GUI_printf("%f %f %f ", -1*smoothedflow[5], S, M);

demand = onsmoothedflow[4] + onsmoothedflow[5] + onsmoothedflow[6] + onsmoothedflow[7];

rate[4] = onsmoothedflow[4] * M / demand;
rate[5] = onsmoothedflow[5] * M / demand;
rate[6] = onsmoothedflow[6] * M / demand;
rate[7] = onsmoothedflow[7] * M / demand;

if (rate[4] < minrate[4])
 rate[4] = minrate[4];
if (rate[5] < minrate[5])
 rate[5] = minrate[5];
if (rate[6] < minrate[6])
 rate[6] = minrate[6];
if (rate[7] < minrate[7])
 rate[7] = minrate[7];

qps_GUI_printf("%f %f %f %f\n", rate[4], rate[5], rate[6], rate[7]);

}

void zone63()
{
float maxdens;
float minspeed;
float S;


if(max(density[10], max(density[11], max(density[12], max(density[13], density[14])))) < 32)
{
 maxdens = max(density[10], max(density[11], max(density[12], max(density[13], density[14]))));
 minspeed = min(averagespeed[10], min(averagespeed[11], min(averagespeed[12], min(averagespeed[13],
averagespeed[14],))));
```

```c
    S = (32 - maxdens) * (minspeed * 3);
  }
else
{
 S = 0;
  }

M = 6000 + offsmoothedflow[8] + offsmoothedflow[9] + offsmoothedflow[10] + S - smoothedflow[10];

qps_GUI_printf("%f %f %f ", -1*smoothedflow[10], S, M);

rate[8] = M;


if (rate[8] < minrate[8])
 rate[8] = minrate[8];


qps_GUI_printf("%f\n", rate[8]);

}

void largezone()
{
 float maxdens;
 float minspeed;
 float S;
 float demand;


 if(max(density[14], max(density[13], max(density[12], max(density[11], max(density[10], max(density[9],
max(density[8], max(density[7], max(density[6], max(density[5], max(density[4], max(density[3], max(density[2],
max(density[1], density[0])))))))))))))) < 32)
 {
  maxdens = max(density[0], max(density[1], max(density[2], max(density[3], max(density[4], max(density[5],
max(density[6], density[7]))))))));
  maxdens = max(maxdens, max(density[13], max(density[8], max(density[9], max(density[10], max(density[11],
max(density[12], density[14]))))))));

  minspeed = min(averagespeed[0], min(averagespeed[1], min(averagespeed[2], min(averagespeed[3],
min(averagespeed[4], min(averagespeed[5], min(averagespeed[6], averagespeed[7]))))))));
  minspeed = min(minspeed, min(averagespeed[13], min(averagespeed[8], min(averagespeed[9],
min(averagespeed[10], min(averagespeed[11], min(averagespeed[12], averagespeed[14]))))))));


  S = (32 - maxdens) * (minspeed * 3);
  }
else
{
 S = 0;
  }
```

```
 M = 6000 + offsmoothedflow[0] + offsmoothedflow[1] + offsmoothedflow[2] + offsmoothedflow[3] +
offsmoothedflow[4] + offsmoothedflow[5] + offsmoothedflow[6] + offsmoothedflow[7] + offsmoothedflow[8] +
offsmoothedflow[9] + offsmoothedflow[10] + S - smoothedflow[0];

 qps_GUI_printf("%f %f %f ", -1*smoothedflow[0], S, M);

 demand = onsmoothedflow[0] + onsmoothedflow[1] + onsmoothedflow[2] + onsmoothedflow[3] +
onsmoothedflow[4] + onsmoothedflow[5] + onsmoothedflow[6] + onsmoothedflow[7] + onsmoothedflow[8];

 rate[0] = onsmoothedflow[0] * M / demand;
 rate[1] = onsmoothedflow[1] * M / demand;
 rate[2] = onsmoothedflow[2] * M / demand;
 rate[3] = onsmoothedflow[3] * M / demand;
 rate[4] = onsmoothedflow[4] * M / demand;
 rate[5] = onsmoothedflow[5] * M / demand;
 rate[6] = onsmoothedflow[6] * M / demand;
 rate[7] = onsmoothedflow[7] * M / demand;
 rate[8] = onsmoothedflow[8] * M / demand;


 if (rate[0] < minrate[0])
  rate[0] = minrate[0];
 if (rate[1] < minrate[1])
  rate[1] = minrate[1];
 if (rate[2] < minrate[2])
  rate[2] = minrate[2];
 if (rate[3] < minrate[3])
  rate[3] = minrate[3];
 if (rate[4] < minrate[4])
  rate[4] = minrate[4];
 if (rate[5] < minrate[5])
  rate[5] = minrate[5];
 if (rate[6] < minrate[6])
  rate[6] = minrate[6];
 if (rate[7] < minrate[7])
  rate[7] = minrate[7];
 if (rate[8] < minrate[8])
  rate[8] = minrate[8];

 qps_GUI_printf("%f %f %f %f %f %f %f %f %f\n", rate[0], rate[1], rate[2], rate[3] , rate[4], rate[5], rate[6], rate[7]
, rate[8]);

}
*/

void zone1()
{
 float maxdens;
 float minspeed;
 float S;
 float demand;

 if(max(density[0], max(density[1], max(density[2], max(density[3], max(density[4], density[5]))))) < 32)
 {
```

```
  maxdens = max(density[0], max(density[1], max(density[2], max(density[3], max(density[4], density[5]))))));
  minspeed = min(averagespeed[0], min(averagespeed[1], min(averagespeed[2], min(averagespeed[3],
min(averagespeed[4], averagespeed[5]))))));

 S = (32 - maxdens) * (minspeed * 3);
 }
 else
 {
 S = 0;
 }

 M = 6000 + offsmoothedflow[4] + offsmoothedflow[3] + offsmoothedflow[2] + offsmoothedflow[1] +
offsmoothedflow[0] + S - smoothedflow[0] - onsmoothedflow[3];

 qps_GUI_printf("%f %f %f  ", -1*smoothedflow[0], S, M);

 demand = onsmoothedflow[0] + onsmoothedflow[1] + onsmoothedflow[2];

 rate[0] = onsmoothedflow[0] * M / demand;
 rate[1] = onsmoothedflow[1] * M / demand;
 rate[2] = onsmoothedflow[2] * M / demand;

 if (rate[0] < minrate[0])
  rate[0] = minrate[0];
 if (rate[1] < minrate[1])
  rate[1] = minrate[1];
 if (rate[2] < minrate[2])
  rate[2] = minrate[2];

 qps_GUI_printf("%f %f %f\n", rate[0], rate[1], rate[2]);

 }

 void zone2()
 {
 float maxdens;
 float minspeed;
 float S;
 float demand;

 if(max(density[4], max(density[5], max(density[6], max(density[7], max(density[8], max(density[9],
density[10]))))))) < 32)
 {
  maxdens = max(density[4], max(density[5], max(density[6], max(density[7], max(density[8], max(density[9],
density[10])))))));
  minspeed = min(averagespeed[4], min(averagespeed[5], min(averagespeed[6], min(averagespeed[7],
min(averagespeed[8], min(averagespeed[9], averagespeed[10])))))));

 S = (32 - maxdens) * (minspeed * 3);
 }
 else
 {
 S = 0;
 }
```

```
    M = 6000 + offsmoothedflow[4] + offsmoothedflow[5] + offsmoothedflow[6] + offsmoothedflow[7] + S -
smoothedflow[4];

    qps_GUI_printf("%f %f %f  ", -1*smoothedflow[0], S, M);

    demand = onsmoothedflow[4] + onsmoothedflow[5] + onsmoothedflow[6] + onsmoothedflow[7];

    rate[4] = onsmoothedflow[4] * M / demand;
    rate[5] = onsmoothedflow[5] * M / demand;
    rate[6] = onsmoothedflow[6] * M / demand;
    rate[7] = onsmoothedflow[7] * M / demand;

    if (rate[4] < minrate[4])
     rate[4] = minrate[4];
    if (rate[5] < minrate[5])
     rate[5] = minrate[5];
    if (rate[6] < minrate[6])
     rate[6] = minrate[6];
    if (rate[7] < minrate[7])
     rate[7] = minrate[7];

    qps_GUI_printf("%f %f %f % f\n", rate[4], rate[5], rate[6], rate[7]);
}

void zone3()
{
 float maxdens;
 float minspeed;
 float S;
 float demand;

 if(max(density[10], max(density[9], max(density[8], max(density[7], max(density[6], max(density[5],
max(density[4], max(density[3], max(density[2], max(density[1], density[0]))))))))))) < 32)
 {
  maxdens = max(density[0], max(density[1], max(density[2], max(density[3], max(density[4], max(density[5],
max(density[6], density[7]))))))));
  maxdens = max(maxdens, max(density[8], max(density[9], density[10])));

  minspeed = min(averagespeed[0], min(averagespeed[1], min(averagespeed[2], min(averagespeed[3],
min(averagespeed[4], min(averagespeed[5], min(averagespeed[6], averagespeed[7]))))))));
  minspeed = min(minspeed, min(averagespeed[8], min(averagespeed[9], averagespeed[10])));


 S = (32 - maxdens) * (minspeed * 3);
 }
 else
 {
 S = 0;
 }

 M = 6000 + offsmoothedflow[0] + offsmoothedflow[1] + offsmoothedflow[2] + offsmoothedflow[3] +
offsmoothedflow[4] + offsmoothedflow[5] + offsmoothedflow[6] + offsmoothedflow[7] + S - smoothedflow[0];
```

```
qps_GUI_printf("%f %f %f ", -1*smoothedflow[0], S, M);

demand = onsmoothedflow[0] + onsmoothedflow[1] + onsmoothedflow[2] + onsmoothedflow[3] +
onsmoothedflow[4] + onsmoothedflow[5] + onsmoothedflow[6] + onsmoothedflow[7];

rate[0] = onsmoothedflow[0] * M / demand;
rate[1] = onsmoothedflow[1] * M / demand;
rate[2] = onsmoothedflow[2] * M / demand;
rate[3] = onsmoothedflow[3] * M / demand;
rate[4] = onsmoothedflow[4] * M / demand;
rate[5] = onsmoothedflow[5] * M / demand;
rate[6] = onsmoothedflow[6] * M / demand;
rate[7] = onsmoothedflow[7] * M / demand;


if (rate[0] < minrate[0])
 rate[0] = minrate[0];
if (rate[1] < minrate[1])
 rate[1] = minrate[1];
if (rate[2] < minrate[2])
 rate[2] = minrate[2];
if (rate[3] < minrate[3])
 rate[3] = minrate[3];
if (rate[4] < minrate[4])
 rate[4] = minrate[4];
if (rate[5] < minrate[5])
 rate[5] = minrate[5];
if (rate[6] < minrate[6])
 rate[6] = minrate[6];
if (rate[7] < minrate[7])
 rate[7] = minrate[7];

qps_GUI_printf("%f %f %f %f %f %f %f %f \n", rate[0], rate[1], rate[2], rate[3] , rate[4], rate[5], rate[6], rate[7]);
}
```

LIST OF REFERENCES

Abdel-Aty, M. and Abdalla, F. "Modeling Driver's Diversion from Normal Routes Under ATIS Using Generalized Estimating Equations and Binomial Probit Link Function." Transportation, Vol. 31 No. 3, 327-348, 2004.

Abdel-Aty M. and Dhindsa A. "Coordinated use of Variable Speed Limits and Ramp Metering for Improving Traffic Safety on Congested Freeways." Preprint No. TRB 07-0008, 86th Annual Meeting of the Transportation Research Board, January 2007.

Abdel-Aty, M., Dilmore, J., and Dhindsa, A. "Evaluation of Variable Speed Limits for Real-Time Freeway Safety Improvement." Accident Analysis and Prevention No. 38, 335-345, March 2006.

Abdel-Aty, M., Uddin, N., and Pande, A. "Split Models for Predicting Multi-Vehicle Crashes during High-Speed and Low-Speed Operating Conditions on Freeways." Transportation Research Record No. 1908, 51-58, 2005.

Abdel-Aty, M., Uddin, N., Pande, A., Abdalla, M., Hsia, L. "Predicting Freeway Crashes from Loop Detector Data by Matched Case-Control Logistic Regression." Transportation Research Record No. 1897, 88-95, 2004.

Abdel-Aty, M., Vaughn, K., Kitamura, R., and Jovanis, P. "Impact of ATIS on Drivers' Decisions and Route Choice: A Literature Review." PATH, University of California, Berkeley, UCB-ITS-PRR-93-11.

Abdulhai, B., Sheu, J., and Recker, W. "Simulation of ITS on the Irvine FOT Area Using Paramics 1.5 Scalable Microscopic Simulator – Phase 1: Model Calibration and Validation." California PATH Research Report UCB-ITS-PRR-99-12, 1999.

Abdullahi, B., Shalaby, A., Lee, J., and Georgi, A. "Microsimulation Modeling and Impact Assessment of Streetcar Transit Priority Options: the Toronto Experience," Presented at the Transportation Research Board 81st Annual Meeting, Washington, DC, 2002.

Bertini, R., Lindgren, R., and Tantiyanugulchai, S. "Application of PARAMICS Simulation at a Diamond Interchange." Portland State University, Transportation Research Group, Research Report PSU-CE-TRG-02-02, April 2002.

Bohenberger, K. and May, A. "Advanced Coordinated Traffic Responsive Ramp Metering Strategies." PATH, University of California, Berkeley, UCB-ITS-PWP-99-19, November 1999.

Boxill, S. and Yu, L. "An Evaluation of Traffic Simulation Models for Supporting ITS Development." Center for Transportation Training and Research, Texas Southern University, October 2000.

Cambridge Systematics. "Twin Cities Ramp Meter Evaluation Phase II – Interim Ramp Meter Strategy." Report Prepared for Minnesota DOT, November 2001.

Chu, L., Liu, H, and Recker, W. "Using Microscopic Simulation to Evaluate Potential Intelligent Transportation System Strategies Under Non-Recurrent Congestion." Transportation Research Record No. 1886, 76-84, 2004.

Chu, L., Liu, X., Recker, W., and Hague, S. "A Calibration Procedure for Microscopic Traffic Simulation." Transportation Research Board, 82nd Annual Meeting, Washington, D.C, 2003.

Dhindsa, A. "Evaluating Ramp Metering and Variable Speed Limits to Reduce Crash Potential on Congested Freeways using Micro-Simulation." Master's Thesis, University of Central Florida, Orlando, 2005.

Dilmore, J. "Implementation Strategies for Real-time Traffic Safety Improvements on Urban
Freeways." Master's Thesis, University of Central Florida, Orlando, 2005.

Drummond, K., Hoel, L., and Miller, J. "Using Simulation to Predict Safety and Operational
Impacts of Increasing Traffic Signal Density." Transportation Research Record No.
1784, 100-107, 2002.

Federal Highway Administration. "Interstate Trivia." U. S. Department of Transportation,
http://www.fhwa.dot.gov/programadmin/interstate.html, Accessed October 2006.

Florida Department of Transportation, "Florida Traffic Information (FTI) CD", 2003.

Gardes,Y., May, A., Dahlgren, J., and Skabardonis, A. "Freeway Calibration and Application of
the PARAMICS Model." Transportation Research Board 81st Annual Meeting.
Washington, D. C., January 2002.

Hall, R. "Traveler Route Choice: Travel Time Implications of Improved Information and
Adaptive Decisions." Transportation Research A, 17, 201-214.

Hasan, M., Jha, M., and Ben-Akiva, M. "Evaluation of Ramp Control Algorithms Using
Microscopic Traffic Simulation." Transportation Research C, Vol. 10, 229-256, 2002.

Jin, W. and Zhang, M. "Evaluation of On-Ramp Control Algorithms." PATH University of
California, Davis, UCB-ITS-PWP-2001-14, April 2001.

Koble, H., Adams, T., Samant, V. "Control Strategies in Response to Freeway Incidents."
Report No. FHWA/RD-80/005, Federal Highway Administration, Washington, D. C.,
1980.

Korve Engineers, Inc. "State Route 242 Widening Project." Operations Analysis Report to
Contra Costa Transportation Authority, 1996.

Lee, C., Hellinga, B., and Ozbay, K. "Quantifying the Effects of Ramp Metering on Freeway Safety." Accident Analysis and Prevention No. 28, 279-288, 2006.

Lee, C., Hellinga, B., and Saccomanno, F. "Assessing Safety Benefits of Variable Speed Limits." Transportation Research Record No. 1897, 183-190, 2004.

Lee, C., Hellinga, B., and Saccomanno, F. "Real-Time Crash Prediction Model for Application to Crash Prevention in Freeway Traffic." Transportation Research Record No. 1840, 67-77, 2003.

Levinson, D., Zhang, L., Das, S., and Sheikh, A. "Evaluating Ramp Meters: Evidence From the Twin Cities Ramp Meter Shut-Off." Presented at the Transportation Research Board 81st Annual Meeting, Washington, D.C., 2002

Lieberman, E. and Rathi, A., "Traffic simulation." in Traffic Flow Theory, Gartner and Messer, eds., Oak Ridge National Laboratory, http://www.cta.ornl.gov/cta/research/trb/tft.html, 1997.

Mahmassani, H. and Jayakrishnan, R. "System Performance and User Response Under Real-Time Information in a Congested Traffic Corridor." Transportation Research 25A, 293-307, 1991.

Masher, D., Ross, D., Wong, P., Tuan, P., Zeidler, and Peracek, S. "Guidelines for Design and Operating of Ramp Control Systems." Report of Stanford Research Institute, Menid Park, California, 1975.

Masinick, J. and Teng, H. "An Analysis on the Impact of Rubbernecking on Urban Freeway Traffic." Research Report No. UVACTS-15-0-62, University of Virginia, August, 2004.

Oh, C., Oh, J., Ritchie, S., and Chang, M. "Real-time Estimation of Freeway Accident Likelihood" Transportation Research Board 80th Annual Meeting, Washington, D.C., 2001.

Oh, H. and Sisiopiku, V. "A modified ALINEA ramp metering model." Presented at the Transportation Research Board 80th Annual Meeting, Washington, D.C., 2001.

Oh, J. and Jayakrishnan, R. "Emergence of Private Advanced Traveler Information System Providers and Their Effect on Traffic Network Performance." Transportation Research Record No. 1783, 167-177, 2002.

Oketch, T. and Carrick, M. "Calibration and Validation of a Micro-simulation Model in Network Analysis." Presented at the Transportation Research Board 84th Annual Meeting, Washington, D. C., 2005.

Pande, A. and Abdel-Aty, M. "A Comprehensive Analysis of the Relationship Between Real-Time Traffic Surveillance Data and Rear-End Crashes on Freeways." Forthcoming in the Journal of the Transportation Research Board, Accepted November 2005.

Pande, A. and Abdel-Aty, M. "Assessment of Freeway Traffic Parameters Leading to Lane-Change Related Collisions." Forthcoming in the Accident Analysis and Prevention, Accepted March 2006.

Pande, A., Abdel-Aty, M., and Hsia L. "Spatio-Temporal Variation of Risk Preceding Crash Occurrence on Freeways." Transportation Research Record No. 1908, 26-36, 2005.

Papageorgiou, M. and Kotsialos, A. "Freeway Ramp Metering: An Overview." IEEE Transactions on Intelligent Transportation Systems, Vol. 3, No. 4, December 2002.

Papageorgiou, M., Hadj Salem, H., and Blosseville, J. "ALINEA: A Local Feedback Control Law for On-Ramp Metering." Transportation Research Record No. 1320, 58-64, 1991.

Papageorgiou, M., Hadj Salem, H., and MIddleham, F. "ALINEA Local Ramp Metering: Summary of Field Results." Transportation Research Record No. 1603, 90-98, 1997.

Park, B. and S. Yadlapati, "Development and Testing of Variable Speed Limit Logics at Work Zones Using Simulation," Presented at the Transportation Research Board 82nd Annual Meeting, Washington, D.C., 2003.

Quadstone Limited, "PARAMICS Modeler Version 4.1 Reference Manual." Edinburgh, U.K., 2002.

Research and Innovative Technology Admisitration, Bureau of Transportation Statistics. "National Transportation Statistics – 2005." Research and Innovative Technology Administration, Bureau of Transportation Statistics, December 2005.

Roess, R., Prassas, E., McShane, W. Traffic Engineering. Prentice Hall, Third Edition, October 2003.

Shah, V., Wunderlich, K., Toppen, A., Larkin, J. "Potential of Advanced Traveler Information System to Reduce Travel Disutility: Assessment in Washington, D. C., Region." Transportation Research Record No. 1826, 7-15, 2003.

Shaw, J. and Nam, D. "Micro-Simulation: Freeway System Operational Assessment and Project Selection in Southeastern Wisconsin: Expanding the Vision." Presented at the Transportation Research Board 81st Annual Meeting, Washington, D.C., 2002.

Smaragdis, E. and Papageorgiou, M. "A Series of New Local Ramp Metering Strategies." Transportation Research Record No. 1856, 74-86, 2003.

Stephanedas, Y. and Chang, K. "Optimal Control of Freeway Corridors." ASCE Journal of Transportation Engineering, 119, 4, 504-514, 1993.

Stephanedes, Y. "Implementation of On-Line Zone Control Strategies for Optimal Ramp Metering in the Minneapolis Ring Road." In the Proceedings of the 7th International Conference on Road Traffic and Control, April 1994.

Stewart, P. "M8 PARAMICS Ramp Metering Assessment." Executive Summary Form, Scottish Executive Development Department, www.scotland.gov.uk/library3/transport/m8paramics.pdf (accessed on February 20, 2004)

Trapp, R., "Microscopic Traffic Flow Modeling of Large Urban Networks –Approach and Techniques at the Example of the City of Cologne," Presented at the Transportation Research Board 81st Annual Meeting, Washington, DC, 2002.

Wisconsin DOT. "Freeway System Operational Assessment - PARAMICS Calibration and Validation Guidelines (Draft), Technical Report I-33." Wisconsin DOT, District 2, 2002.

Yang, Q. and Koutsopoulos, H. "A Microscopic Traffic Simulator for Evaluation of Dynamic Traffic Management Systems." Transportation Research C 4(3), 113-129, 1996.

Zhang, M., Kim, T., Nie, X., Jin, W., Chu, L., and Recker, W. "Evaluation of On-Ramp Control Algorithms." California PATH Research Report, UCB ITS PRR 2001 36, 2001.